

# JOURNAL OF FACADE DESIGN & ENGINEERING

VOLUME 11 / NUMBER 2 / 2023

## **SPECIAL ISSUE**

MULTIFUNCTIONAL FAÇADES  
FOR RENOVATION THROUGH  
INDUSTRIALIZATION

EDITORS IN CHIEF

**ULRICH KNAACK & THALEIA KONSTANTINO**

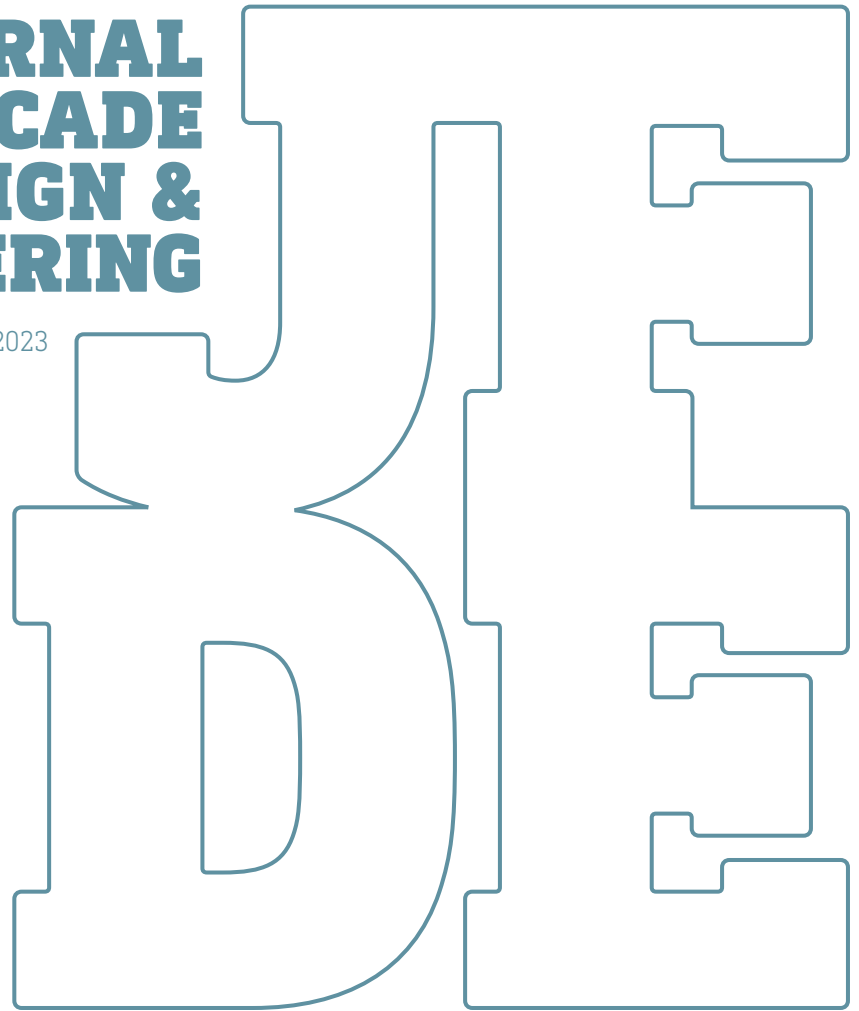
GUEST EDITORS

**PROF. EMER. MARIA FOUNTI, DR. STEFANO AVESANI,  
DR. PERU ELGUEZABAL ESNARRIZAGA**

SUPPORTED BY THE EUROPEAN FACADE NETWORK

**JOURNAL  
OF FACADE  
DESIGN &  
ENGINEERING**

VOLUME 11 / NUMBER 2 / 2023



**SPECIAL ISSUE**

MULTIFUNCTIONAL FAÇADES  
FOR RENOVATION THROUGH  
INDUSTRIALIZATION

EDITORS IN CHIEF

**ULRICH KNAACK & THALEIA KONSTANTINO**

GUEST EDITORS

**PROF. EMER. MARIA FOUNTI, DR. STEFANO AVESANI,  
DR. PERU ELGUEZABAL ESNARRIZAGA**

SUPPORTED BY THE EUROPEAN FACADE NETWORK

## JFDE Journal of Facade Design and Engineering

JFDE presents new research results and new proven practice of the field of facade design and engineering. The goal is to improve building technologies, as well as process management and architectural design. JFDE is a valuable resource for professionals and academics involved in the design and engineering of building envelopes, including the following disciplines:

- Architecture
- Building Engineering
- Structural design
- Climate design
- Building Services Engineering
- Building Physics
- Design Management
- Facility Management

JFDE is directed at the scientific community, but it will also feature papers that focus on the dissemination of science into practice and industrial innovations. In this way, readers explore the interaction between scientific developments, technical considerations and management issues.

### Publisher

Stichting OpenAccess, Rotterdam

### Owner

TU Delft / Faculty of Architecture and the Built Environment  
Julianalaan 134, 2628 BL Delft, The Netherlands

### Contact

Alessandra Luna Navarro  
editors@jfde.eu  
<https://jfde.eu/>

### Policies

**Peer Review Process** – The papers published in JFDE are double-blind peer reviewed.

**Open Access** – JFDE provides immediate Open Access (OA) to its content on the principle that making research freely available to the public supports a greater global exchange of knowledge.

Licensed under a Creative Commons Attribution 4.0 International License (CC BY 4.0).

**Indexation** – JFDE is indexed in the Directory of Open Access Journals (DOAJ), Google Scholar, Inspec IET and Scopus.

**Publication Ethics** – Editors, authors and publisher adopt the guidelines, codes to conduct and best practices developed by the Committee on Publication Ethics (COPE).

**Copyright Notice** – Author(s) hold their copyright without restrictions.

### Cover image

ENSNARE modular façade system combining RIVENTI's and ONYX's technologies. Image courtesy of Nuria Jorge.

### Design & layout & proofreading

**Design** – Sirene Ontwerpers, Amsterdam

**Layout & Open Access** – Stichting OpenAccess, Rotterdam

**Proof-reading** – Usch Engelmann, Rotterdam

ISSN 2213-302X (Print)  
ISSN 2213-3038 (Online)  
ISBN 978-90-833861-4-0

### Editorial board

#### Editors in Chief

Ulrich Knaack  
Thaleia Konstantinou  
*Delft University of Technology, The Netherlands*

#### Editors

Alessandra Luna Navarro  
Tatiana Armijos Moya  
*Delft University of Technology, The Netherlands*

#### Editorial Board

Alejandro Prieto Hoces, *Universidad Diego Portales, Escuela de Arquitectura, Chile* // Daniel Aelenei, *Universidade Nova de Lisboa, Lisbon, Portugal* // Enrico de Angelis, *Polytechnico Milano, Milan, Italy* // Julen Astudillo, *TECNALIA Research & Innovation, San Sebastian, Spain* // Carlo Battisti, *IDM Südtirol - Alto Adige, Italy* // Anne Beim, *Royal Danish Academy of Fine Arts, Copenhagen, Denmark, Denmark* // Jan Belis, *Ghent University, Belgium* // Jan Cremers, *Hochschule für Technik Stuttgart (HFT), Germany* // Andy van den Dobbelsteen, *Delft University of Technology, Delft, the Netherlands* // Paul Donnelly, *Washington University, St. Louis, USA* // Chris Geurts, *TNO, Delft, Netherlands* // Mikkel K. Kragh, *University of Southern Denmark, Odense, Denmark* // Klaus Kreher, *Lucerne University of Applied Sciences and Art, Lucerne, Switzerland* // Bert Lieverse, *Association of the Dutch Façade Industry, Nieuwegein, The Netherlands* // Steve Lo, *University of Bath, Bath, United Kingdom* // Andreas Luible, *Lucerne University of Applied Sciences and Art, Lucerne, Switzerland* // Enrico Sergio Mazzucchelli, *Politecnico di Milano ABC Department, Italy* // David Metcalfe, *Centre for Window and Cladding Technology, United Kingdom* // Mauro Overend, *University of Cambridge, Cambridge, United Kingdom* // Uta Pottgiesser, *Delft University of Technology, Architecture and the Built Environment, Netherlands* // Josemi Rico-Martinez, *University of the Basque Country, Donostia- San Sebastian, Spain* // Paolo Rigone, *UNICMI, Milan, Italy* // Holger Strauss, *Innobuild GmbH, Berlin, Germany* // Jens Schneider, *University of Darmstadt, Darmstadt, Germany* // Holger Techen, *University of Applied Sciences Frankfurt, Frankfurt, Germany* // Nil Turkeri, *Istanbul Technical University, Istanbul, Turkey* // Claudio Vásquez Zaldívar, *Pontificia Universidad Católica de Chile, Santiago, Chile* // Aslihan Ünlü Tavit, *Istanbul Technical University, Istanbul, Turkey* // Stephen Wittkopf, *Lucerne University of Applied Sciences and Art, Lucerne, Switzerland*

#### Submissions

All manuscripts and any supplementary material should be submitted to the Editorial Office (editors@jfde.eu), through the Open Journal System (OJS) at the following link: <https://jfde.eu/>

#### Author Guidelines

Detailed guidelines concerning the preparation and submission of manuscripts can be found at the following link: <https://jfde.eu/index.php/jfde/about/submissions>

# Contents

- 001 **Definition and design of a prefabricated and modular façade system to incorporate solar harvesting technologies**  
Izaskun Alvarez-Alava, Peru Elguezabal, Nuria Jorge, Tatiana Armijos-Moya, Thaleia Konstantinou
- 029 **SmartWall**  
Emmanouil Katsigiannis, Petros Gerogiannis, Ioannis A. Atsonios, Aris Manolitsis, Maria Founti
- 051 **Plasmochromic Modules for Smart Windows: Design, Manufacturing and Solar Control Strategies**  
Mirco Riganti, Julia Olive, Francesco Isaia, Michele Manca
- 071 **Implementation of a multifunctional Plug-and-Play façade using a set-based design approach**  
David Masip Vilà, Grazia Marrone, Irene Rafols Ribas
- 097 **Off-site prefabricated hybrid façade systems**  
Ioannis A. Atsonios, Emmanouil Katsigiannis, Andrianos Koklas, Dionysis Kolaitis, Maria Founti, Charalampos Mouzakis, Constantinos Tsoutis, Daniel Adamovský, Jaume Colom, Daniel Philippen, Alberto Diego
- 123 **Automation process in data collection for representing façades in building models as part of the renovation process**  
Kepa Iturralde, Asier Mediavilla, Peru Elguezabal
- 145 **Comparative cost analysis of traditional and industrialised deep retrofit scenarios for a residential building**  
Martino Gubert, Jamal Abdul Ngoyaro, Miren Juaristi Gutierrez, Riccardo Pinotti, Davide Brandolini, Stefano Avesani
- 169 **Assessing the circular re-design of prefabricated building envelope elements for carbon neutral renovation**  
Ivar J.B. Bergmans, Silu Bhochhibhoya, Johannes A.W.H. Van Oorschot
- 197 **Energy-saving potential of thermochromic coatings in transparent building envelope components**  
Matthias Fahland, Jolanta Szelwicka, Wiebke Langgemach



# MULTIFUNCTIONAL FAÇADES FOR RENOVATION THROUGH INDUSTRIALIZATION

**Maria Founti<sup>1</sup>, Stefano Avesani<sup>2</sup>, Peru Elguezabal Esnarrizaga<sup>3</sup> (Eds.)**

- 1 Laboratory of Heterogeneous Mixtures and Combustion Systems, School of Mechanical Engineering, National Technical University of Athens, Zografou, Greece.
- 2 Eurac research, Institute for Renewable Energy, Energy Efficiency Buildings – Building envelope technologies team, Bolzano, Italy
- 3 TECNALIA, Basque Research and Technology Alliance (BRTA), Spain

## Editorial

*In the pursuit of a sustainable future, and as the global community strives to reduce carbon emissions and combat climate change, the renovation of existing buildings stands as a pivotal challenge.*

*Industrialized, multifunctional, prefabricated façade components can offer an efficient, effective, and reliable approach able to boost buildings' deep renovation. By off-site manufacturing in controlled environments, we harness efficiency, precision, and sustainability as well as a quality level that onsite is not possible to achieve. Prefabricated façade elements can be carefully designed, and hence directly manufactured, with all needed details on insulation, airtightness, and thermal performance to enhance the energy efficiency of the building. The versatility of prefabricated components also lends itself to innovative design solutions thanks to the extensive use of digital tools, overcoming the old pre-concept of prefabrication as lack of design freedom. Architects and engineers are presented with a canvas of possibilities, enabling the integration of renewable energy systems, advanced insulation materials, and cutting-edge technologies. Thanks to modular and scalable approaches a wide range of alternatives can be provided, still under an industrialized concept. This flexibility allows for tailored solutions that align with the unique characteristics of each building and its surroundings, a key feature to assure high market penetration in the renovation market.*

*However, research and innovations are still needed for the development of multifunctional envelope solutions coupling passive and active technologies for deep renovation, that are sufficiently flexible and customizable, encompassing advances in ICT, digitalization, automation, and robotics and that can address significant market segments in EU for deep renovation reaching Near Zero-Energy Building (NZEB) standards, while being competitive for a recognized set of added values.*

*This Special Issue compiles results of EU H2020 funded projects working on the development of multifunctional envelope solutions for deep renovation of buildings. The projects have a common and aligned objective to develop and demonstrate plug & build smart components, including insulation materials, heating and cooling elements, ventilation, smart windows, energy production, solar harvesting, and storage with necessary connecting and controlling parts to be integrated in a prefabricated envelope system. They highlight that plug & build solutions are suitable for mass production by industry for buildings undergoing deep renovation to NZEB standards. They also underline that the development and implementation of digital based technologies can boost the application of such industrialized concepts. The following projects have offered contributions and support in the preparation of the Special Issue (in alphabetical order):*

- *DRIVE0* (<https://www.drive0.eu/>), that aims to enhance a consumer centered circular renovation process.
- *ENSNARE* (<https://www.ensnare.eu/>), that develops modular adaptable components and a set of digital tools and a digital platform to support and accelerate the renovation process;
- *INFINITE* (<https://infinitebuildingrenovation.eu/>), that develops five all-in-one industrialized envelope kits coupling industrialization and digitalization for deep renovation of residential buildings;

- PLURAL (<https://www.plural-renovation.eu/concept>), that develops a palette of versatile, adaptable, scalable, off-site prefabricated plug-and-play kits that account for user needs and integrate various renewable energy technologies together with digital tools to support decision making;
- StepUP (<https://www.stepup-project.eu/>) that aims to make decarbonisation of existing buildings a reliable, attractive investment by developing solutions and technologies for the uptake of deep energy renovation processes;
- Switch2Save (<https://switch2save.eu/>), that develops lightweight Insulating Glass Units (IGUs) suitable for large windows and glass façades integrating electrochromic (EC) and thermochromic (TC) windows with optimized maximum energy saving potential.

*The selected articles cover a variety of technology developments and system /kit assessment topics. They address the design of prefabricated opaque and transparent façade systems to incorporate renewable technologies using a range of materials, manufacturing, implementation, and experimental performance assessment towards nZEB. They also present innovative approaches in data collection for representing façades into building models, comparative cost analysis of traditional and industrialized deep retrofit scenarios for a residential building and holistic assessment methods for off-site prefabricated hybrid façade systems.*

*The presented innovative, affordable, ready-to-go, all-in-one façade systems are intended mostly for deep renovation of residential and office buildings, in some cases without the removal of the existing envelope. They address the energy and comfort needs of building users, creating a high-quality environment opening new horizons for the transformation of renovation practices. For this transformation to reach its full potential, collaboration and knowledge-sharing are imperative. We invite architects, engineers, manufacturers, and policymakers to profit from the new ideas presented in the Special Issue aiming to help them to refine and implement best and innovative practices.*

*In conclusion, we believe that the results and lessons-learned presented in this Special Issue can act as an inspiration for further industrialization of prefabricated all-in-one façade components, setting a first science-demonstrated basis of robust methods and technologies. The innovative solutions set the stage for a paradigm shift in building renovation practices. Embracing the all-in-one technologies and approaches presented in this Special Issue can not only accelerate our progress towards a sustainable future but also paves the way for a more resilient and prosperous society.*

*As guest editors, we would like to thank the authors and reviewers for their contributions and support in this Special Issue. Finally, the constructive comments and continuous support of the JFDE Editors Thaleia Konstantinou and Tatiana Armijos Moya are gratefully acknowledged.*

**Maria Founti, Prof. Emer.** NTUA, Director Lab. Heterogenous Mixtures and Combustion Systems, Coordinator of the PLURAL project

**Dr. Stefano Avesani,** Leader of the Team on Building Envelope Technologies, Senior Researcher, Eurac Research, coordinator of the INFINITE project

**Dr. Peru Elguezabal Esnarrizaga,** Senior Researcher, TECNALIA Research & Innovation, Energy, Climate Change and Urban Transition Unit, coordinator of the ENSNARE project

# Definition and design of a prefabricated and modular façade system to incorporate solar harvesting technologies

**Izaskun Alvarez-Alava<sup>1\*</sup>, Peru Elguezabal<sup>1,2</sup>, Nuria Jorge<sup>3</sup>, Tatiana Armijos-Moya<sup>4</sup>, Thaleia Konstantinou<sup>4</sup>**

\* Corresponding author, [izaskun.alvarez@tecnalia.com](mailto:izaskun.alvarez@tecnalia.com)

1 TECNALIA, Basque Research and Technology Alliance (BRTA), Spain

2 University of the Basque Country UPV/EHU, Department of Electrical Engineering, Spain

3 Riventi Fachadas Estructurales S.L., Spain

4 TU Delft, Faculty of Architecture and the Built Environment, Department of Architectural Engineering + Technology, Netherlands

## Abstract

*The current research presents the design and development of a prefabricated modular façade solution for renovating residential buildings. The system is conceived as an industrialised solution that incorporates solar harvesting technologies, contributing to reducing energy consumption by employing an “active façade” concept.*

*One of the main challenges was to achieve a highly flexible solution both in terms of geometry and enabling the incorporation of different solar-capturing devices (photovoltaic, thermal, and hybrid). Therefore, to be able to provide alternative customised configurations that can be fitted to various building renovation scenarios. Guided by the requirements and specifications, the design was defined after an iterative process, concluding with a final system design validated and adopted as viable for the intended purpose.*

*A dimensional study for interconnecting all the technologies composing the system was carried out. Potential alternative configurations were assessed under the modularity and versatility perspective, resulting in a set of alternative combinations that better fit the established requirements. Complementarily, the system also integrates an active window solution a component that incorporates an autonomous energy recovery system through ventilation.*

*The main outcome is explicated in a highly versatile modular façade system, which gives existing buildings the possibility to achieve Nearly Zero Energy Building requirements.*

## Keywords

*multifunctional prefabricated façade, industrialisation, renewable integration, façade renovation*

## DOI

<http://doi.org/10.47982/jfde.2023.2.T1>

# 1 INTRODUCTION

## 1.1 CONTEXT

The existing building stock plays a vital role in the energy transition and achieving carbon neutrality in the built environment, accounting for nearly 40% of energy consumption in Europe (Tsemekidi-Tzeiranaki et al., 2020). The European Union's building stock comprises over 220 million units, with approximately 85% built before 2001. It is projected that 85-95% of the current buildings will still be standing in 2050 (European Commission, 2020). In line with this, the Energy Performance of Buildings Directive (EPBD) mandates that all existing buildings must be converted into zero-emission buildings by 2050. Deep renovation, with savings of at least 60% of the current energy consumption, is needed to achieve the decarbonisation goals and additional benefits, job creation, and elimination of energy poverty. Presently, around 75% of the building stock is energy inefficient, and only about 1% undergoes renovation annually, with deep renovation only in 0.2% of the building stock per year (European Commission, 2020).

Recognising this challenge, the European Commission launched the Renovation Wave in 2020 as part of the European Green Deal. This initiative includes an action plan outlining specific regulatory, financial, and supportive measures to promote building renovation and double the current rate of annual energy renovation by 2030 while encouraging comprehensive renovation (European Commission, 2019, 2020). The "fit for 55" package also recognises buildings as one of the key sectors to cut down emissions and supports the renovation and the increase of the renewable energy sources application (European Commission, 2021).

---

Given the urgency, the EU must prioritise strategies that improve energy efficiency, reduce carbon emissions, and promote sustainability throughout a building's lifespan (European Commission, 2023).

---

Consequently, stakeholders such as policymakers, social housing corporations, institutional real estate owners, financial organisations, and end-users are increasingly focusing on the potential of renovating the existing building stock to achieve energy-neutral standards. To accomplish this, it is crucial to enhance the process of building renovation by increasing both the rate and depth of renovation (Artola, Rademaekers, Williams, & Yearwood, 2016; Economidou et al., 2011; Jensen, Maslesa, Berg, & Thuesen, 2018).

Currently, the annual renovation rate of the building stock varies between 0.4% and 1.2% across EU Member States, falling short of meeting emission targets (Broers, Vasseur, Kemp, Abujidi, & Vroon, 2019; European Commission, 2020). To align with policy objectives, this rate needs to increase to approximately 2.5-3% of the housing stock per year (Sandberg et al., 2016; Wilson, Pettifor, & Chrysochoidis, 2018). Additionally, most improvements in residential buildings are limited to basic maintenance and shallow renovation, necessitating broader and deeper energy renovation measures. While shallow renovation, such as standard thermal wall insulation and insulated glazed components, offers lower initial costs, it fails to provide a sufficient return on investment in financial terms (Filippidou, Nieboer, & Visscher, 2016; Semprini, Gulli, & Ferrante, 2017).

Furthermore, in response to the energy crisis, the issue can be addressed by incorporating renewable energy sources (RES) into the building structure. This can be achieved by utilising specific installation methods within a modular framework, resulting in the creation of a multifunctional façade module (MFM). In this scenario, the innovative building façade serves various purposes, such as providing protection, harnessing energy, and converting it into usable forms (Li & Chen, 2022).

## 1.2 SOA IN ENERGY RETROFITTING THROUGH THE FAÇADE

Deep renovation interventions are based on applying different technologies to buildings, considering façades, roofs, windows, heat and cooling production, ventilation or renewables (Streicher et al., 2020; Moran et al., 2020). When combining such technologies, alternative packages can be compiled to achieve different impact levels after the intervention, typically considering an upgrade of the envelope.

To increase energy performance, ventilated façades are widely used in renovation (Colinart et al., 2019; De Gracia et al., 2013). This system increases the thermal resistance to heat flow of the existing wall by means of adding thermal insulation (*Gagliano & Aneli, 2020*). This results in a reduction of the energy demand, mainly for heating during cold periods of the year. The systems usually comprise the elements substructure, insulation, waterproof membrane, and cladding panels. It is a dry solution, which is installed on an existing wall by fully assembling all the elements on-site, and some experiences with prefabrication variations have also been considered in the past (Avesani et al., 2020).

However, the evolution of envelope systems is moving towards increasingly industrialised solutions (Wasim et al. 2020; Ferdous et al. 2019; Navaratnam et al. 2019; *D'Oca et al. 2018*), manufactured off-site under controlled conditions by specialised workers. This approach provides the opportunity to incorporate energy-related technologies into the envelope components (Van Roosmalen, Herrmann, & Kumar, 2021). Industrialisation gives more reliability to guarantee higher product quality and minimises on-site activities, where uncertainty about the correct execution grows exponentially. At the same time, the interest in prefabricated solutions is currently growing due to the lack of specialised labour in the construction sector.

Modular curtain walling is also an increasingly widespread example of industrialised envelope systems but is applied mostly for new buildings rather than for renovation activities. These solutions are made up of modules formed by a self-supporting frame that contains the different layers together with the elements of the enclosure. These modules are manufactured entirely in the factory, and the on-site intervention is limited to the positioning and fixing of the modules on the building. Many of the performance requirements for these systems are guaranteed through standardised tests in approved laboratories. However, modular solutions have so far not penetrated the retrofitting market to any significant extent. Mainly because a solution flexible enough to adapt to the built environment has not been achieved and because they are substantially more expensive than other in-situ assembly systems, theoretically offering similar performance. It is common for curtain walling systems to be conceived as a new-build solution, so their application to the built environment is not obvious.

A relevant aspect that ventilated façades and curtain walling have in common is the widespread use of aluminium profiles as a framing element. Its strength, lightness, and durability against external agents make it an ideal material for this use. Different aluminium alloys provide alternative profiles with different properties, while the possibility to recycle this material indefinitely also contributes to reducing construction waste. On the other hand, the production of aluminium from raw materials requires a rather high amount of energy (Efthymiou, Cöcen, & Ermolli, 2010).

In the most innovative areas, new envelope systems with integrated renewables are being developed to meet the EU's decarbonisation targets for the building stock (Du, Huang & Jones, 2019; D'Oca et al., 2018). Many of these developments (Bonato et al., 2019) are part of solutions conceived under a modular concept which considers the integration of solar technologies for use inside the building (Elguezabal & Arregi, 2018). Nevertheless, although there have been some research approaches towards solutions for the decarbonisation of the building stock in recent years (Van Roosmalen, Herrmann, & Kumar, 2021; Streicher et al., 2020; Navaratnam et al., 2019; Du, Huang & Jones, 2019; D'Oca et al. 2018), it has become apparent that these experiences are not yet sufficiently developed in aspects such as the industrialisation of the system, flexibility in terms of modularity, interchangeability and customisation of solar collection technologies to provide an ad-hoc response to the demands of each building and the accessibility for maintenance and replacement that these active envelope systems may require.

In this context, a need has been identified to develop new façade systems for the retrofitting sector that integrate solar capture technologies. These solutions will reduce the building's fossil energy consumption and are conceived from a prefabricated and industrialised perspective under a systemic approach, aiming to minimise on-site operations and offer maximum performance guarantees.

The purpose of this paper is to explain the process followed for the definition and design of prefabricated and modular façade systems to incorporate solar and renewable technologies. It is a modular and industrialised façade system capable of integrating different solar collection technologies under different configurations, enabling the possibility to meet different needs for alternative buildings. The designed active façade gets a new functionality, namely solar harvesting, enabling this component to be employed in multiple ways in conventional solar systems in residential buildings. The large-scale objective is to achieve a solution that meets the decarbonisation needs of the building stock to achieve the EU's 2050 targets. The main defining characteristics of this system are:

- Versatility in terms of construction and energy. It is a system aimed at the refurbishment sector, adaptable to different building scenarios. It offers the integration of different technologies for collecting solar energy depending on the specific energy needs. These components are also interchangeable, using a plug-and-play mechanical fixing system.
- Integration of the service network of the solar technology in the same modular solution. From a modular perspective, the system contemplates the possibility of interconnecting the solar panels between modules, generating the necessary network on the same façade plane, making it fully accessible for installation and maintenance.
- Modular design under the premises of industrialisation to achieve a system that offers guarantees in terms of anticipating the expected performance, especially in this case where it is not only necessary to guarantee the functionalities as a construction product but also as a renewable energy collector element, functionally active throughout its useful life.

## 2 METHODOLOGY

The methodology carried out to achieve a solution with the aforementioned characteristics can be summarised as follows:

- A Definition of the industrialised façade panel design concept
- The main premises to define the conceptual design of the system are: (1) to develop an industrialised system, (2) to conceive it for implementation in the envelope refurbishment sector, and (3) to integrate different solar collecting technologies. Taking these conditions into account, the concept design of the developed system has been based on the characteristics of ventilated façade systems, which are solutions mechanically fixed on an existing wall and modular curtain walling solutions that have a high degree of industrialisation.
- B Analysis and definition of the dimensional and technical specifications to be considered in the design phase of the façade system:
- To have great flexibility to be adapted to the wide range of construction typologies that constitute the European building stock. Parameters such as distance between floors, distance between windows and dimensions, overhangs and irregularities, etc., have been considered. An analysis of the dimensional limitations imposed by the transport of the façade modules has also been carried out.
  - To have the appropriate versatility from the energy point of view so that the façade system can integrate different solar collecting technologies that meet the specific demand of each building. The modularity and restrictions of each solar technology and alternative combinations have been considered for their integration into a façade module, fulfilling the specifications defined in the previous point. Likewise, the integration of active windows with a heat recovery system has also been considered. This provides the façade system with an energy-efficient solution for the opening elements.
  - To ensure that the infrastructure associated with solar technologies is fully accessible for connection and maintenance during all phases of the façade system's operational life and decommissioning. To this end, a specific space has been defined within the modular system, named access zone. Its dimensions are variable depending on the needs of the technologies integrated into the façade system.
- C Analysis and definition of the regulatory requirements that the façade system must comply with the Construction Product perspective (EU Parliament, 2011). As there is no specific standard for this innovative system, the essential characteristics (performance) that will be required of this system have been defined based on the following product standards:
- EAD 090062-00-0404: Kits for external claddings mechanically fixed (EOTA, 2018)
  - EN 13830: Curtain walling. Product standard (CEN, 2020)
  - EN 50583: Photovoltaics in buildings

The selection of the first standard as a reference for the design is based on the premise of developing an envelope solution oriented towards the renovation sector; thus, it will be installed and fixed on an existing wall. Likewise, as a priority objective, it is established that this solution should have a high degree of industrialisation so that on-site activities are reduced as much as possible. Hence, the product standard for curtain walling is set as the second reference standard. Finally, the standard

that contemplates the integration of photovoltaic technology in buildings has been considered, as the façade system comprises, among others, this solar energy collection technology.

- D Detailed definition of the façade system based on the established requirements and specifications and design principles towards an industrialised solution (Lessing, 2006; Viana, Tommelein, & Formoso, 2017). Modularity of the technologies, the connection and interchangeability through plug-and-play systems have been part of the design guidelines.
- E Evaluation of the performance of the façade system as a Construction Product. The most critical performances have been selected. These performances are those with the highest level of uncertainty, and the verification of these is made either by simulations, during the design phase, or laboratory tests once the detailed design has been defined. The manufacture of full-scale prototypes for laboratory tests has also allowed to validate the production and assembly process, as well as the suitability of the different elements composing the complete façade. The achievement of each of the evaluation phases has led to an iterative review of the construction design.

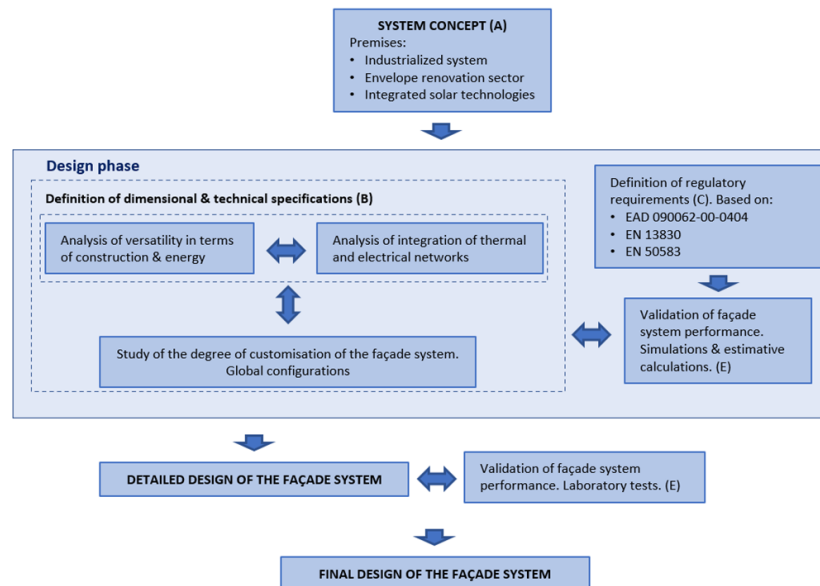


FIG. 1 Methodology followed for the development of the innovative façade system.

### 3 RESULTS

#### 3.1 DESCRIPTION OF THE SYSTEM

This initial section in Chapter 3 provides a general description of the façade system developed with its main characteristics. Sections 3.2, 3.3, and 3.4 describe each of the system's components and the research conducted to define them.

The modular system consists of two independent layers: the inner layer and the outer layer. These layers are joined together through a mechanical fastening system.

The developed façade system has significant similarities with ventilated façades, as it is defined as a solution mechanically fixed to a supporting wall, but also with curtain walls as the system is conceived as a fully modular concept. From the energy performance perspective, it provides improved thermal insulation to the façade as well as the generation of energy (electrical and thermal) thanks to the solar collecting technologies incorporated. The flexibility of the modular system allows the external active skin to be customised according to the different energy requirements of each building. An aluminium supporting mesh gives the system the required modularity and flexibility.

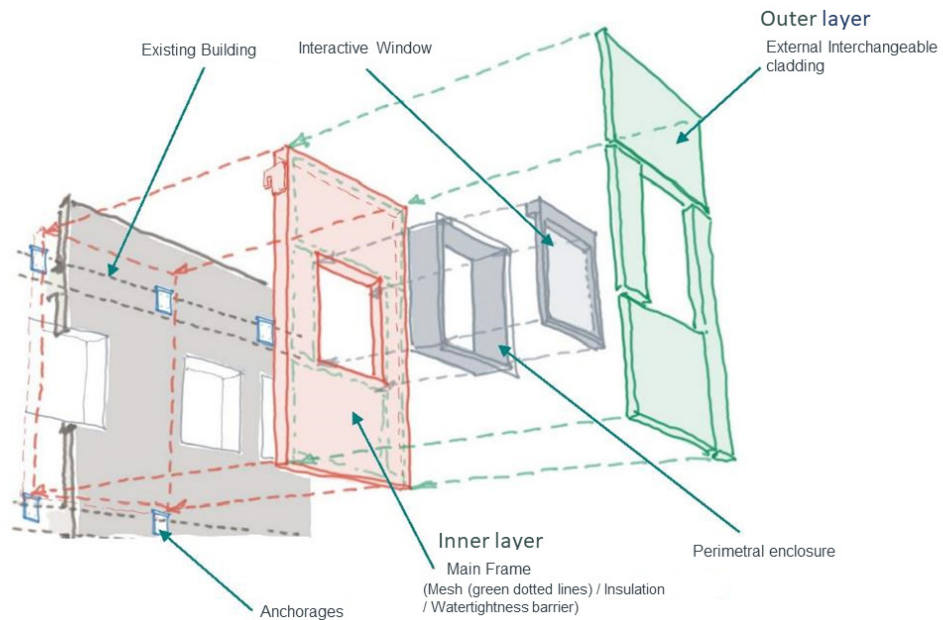


FIG. 2 Modular façade system concept.

The inner layer covers structural, thermal insulation, air and watertightness. The outer layer incorporates different solar harvesting technologies and the access zones through which the infrastructure associated with these technologies runs on the façade plane.

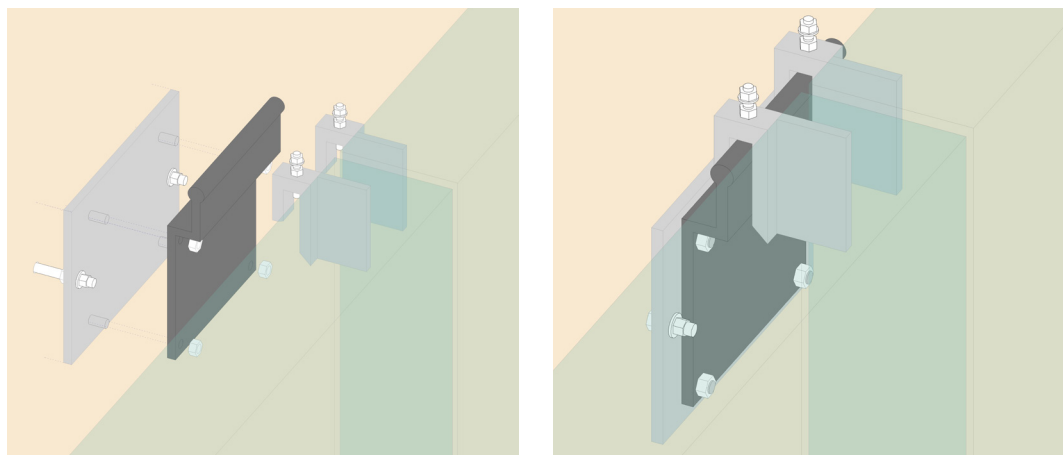


FIG. 3 Anchoring system designed by ENAR. Exploded view (left). Assembly (right)

The inner layer consists of a structural aluminium main frame containing thermal insulation and a breathable membrane. The membrane defines the watertight plane of the system. Constructively, the mainframe works as a modular tongue and groove curtain wall system. The anchoring system consists of a set of two support plates fixed to the slab of the building and two hanging elements at the top of the mainframe. This concept is similar to those used for anchoring modular curtain wall solutions.

One of the plates (grey in FIG 3.) is fixed to the slab of the building, and the other plate, which is placed in the front (black in FIG 3.), allows the adjustment in the perpendicular direction of the façade. The top hanging elements are placed on the outer plate. The position of the modules is adjusted by means of the levelling screws located on the hanging elements. This assembly has three degrees of freedom, allowing the façade module to be positioned and adjusted in all three axes. This design involves a bottom-up assembly process that allows access to the anchoring elements during the installation process. Finally, on the back of the mainframe, covering the whole surface, a continuous low-density insulation layer is deployed. This insulation layer absorbs the vertical misalignment of the existing wall and fills in the space generated between the modules and the façade. This element is an essential component of the modular façade system to guarantee that no air cavity is generated between the module and the existing façade.

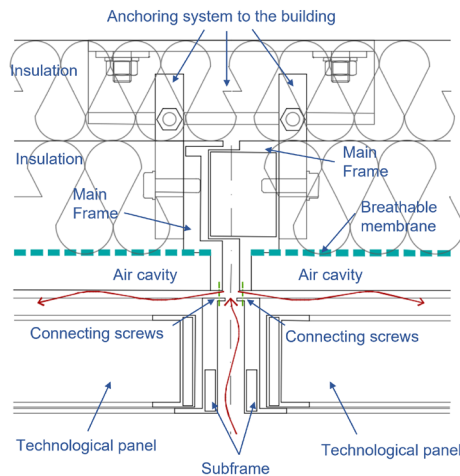


FIG. 4 Schematic horizontal section of the modular façade system. The red arrows indicate the air path from the outside into the air cavity through the perimetral joint between the subframe and the mainframe.

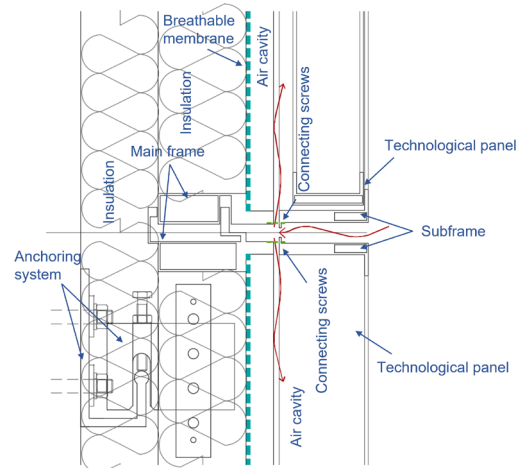


FIG. 5 Schematic vertical section of the modular façade system. The red arrows indicate the air path from the outside into the air cavity through the perimetral joint between the subframe and the mainframe.

The outer layer is composed of different solar collecting technologies combined with the access zones in which the energetic network associated with these active elements is arranged. Technological panels are formed, integrating every solar technology in a subframe. These technological panels are fixed to the mainframe with a mechanical plug & play connection. A screw is mechanically fixed every 30 centimetres to a specifically designed channel that is located in the mainframe. These fixings are placed around the entire perimeter of the technology panel and can be removed and replaced multiple times. This fixing system makes it easy to replace the panels independently in case the panel is broken or damaged. It turns this outer layer into an easily interchangeable enclosure, while the mainframe does not require to be replaced. Moreover, the connection system between the internal and external layers generates a perimetral opened joint that allows the ventilation of the air cavity between the two layers. This guarantees the

correct hygrothermal behaviour of the façade and, at the same time, benefits the efficiency of the photovoltaic technologies. From a constructive point of view, this configuration can be integrated into cladding systems that are mechanically fixed to a supporting wall, such as ventilated façade systems.

The main features of each of the active technologies that are integrated into the outer layer can be summarised as follows:

- Thermal solar panel for thermal energy generation. It captures solar energy through an aluminium absorber and transfers the energy to a hydraulic circuit.
- Photovoltaic panels with aluminium and synthetic stone substrates to transform irradiation into electricity, an energy that is then distributed through electric circuits.
- Hybrid panel for the generation of thermal and electrical energy. It combines photovoltaic and solar thermal technologies.

The connection between the technology panels and the layout of the infrastructure in the façade plane requires an accessible space next to the solar technologies. The solution to this need is solved through the so-called access zones that are also located in the exterior layer; a chamber that is generated as part of that layer. They follow the same aesthetics and fixing system as the technological panels and have a phenolic panel cladding as closure. They are fully registrable, generating a continuous track to interconnect the technological panels and can be arranged vertically or horizontally depending on the configuration of the technological layer and the energy networks required depending on the case. Access to the infrastructure for maintenance throughout its service life is possible thanks to the hinge system incorporated in the cladding of the access zones, allowing the cladding to be opened 180°.

Finally, the façade system responds to the glazing elements of the buildings by incorporating active windows with an intelligent ventilation and heat recovery system. This component substantially improves the management of the building's ventilation from the perspective of comfort and energy efficiency. An autonomous control system manages air renewal considering the results of the monitoring of the indoor conditions. The active window is located in the same plane as the insulation layer of the system to guarantee its continuity.

Therefore, this industrialised envelope system allows a fast and accessible connection between all its components in all phases of its service life and even during the decommissioning phase. Since the façade system is installed from the outside very quickly, the impact on the building's activity is very low or even negligible. It is designed to allow for the replacement of the outer layer panels for maintenance purposes. The system also ensures a high degree of flexibility to be adapted to different building typologies that are present in the building stock, guaranteeing fast and efficient manufacturing and installation processes. The system allows the combination of different solar harvesting technologies, aiming to incorporate a significant number of interconnected active panels and, therefore, enabling the adoption of large-scale renewable energy solutions as part of façade energy refurbishment interventions.

## 3.2 ANALYSIS OF CONSTRUCTION AND ENERGY VERSATILITY

In the design phase, the first analysis focused on the dimensional definition of the façade modules and their flexibility in both width and height. Afterwards, the solar technologies were analysed to define a wide variety of interchangeable technological panels, taking into account optimum energy performance.

### 3.2.1 Architectural modularity of the façade system

The developed modular façade system is designed to be adaptable to a broad typology of existing buildings. The general dimensions (width and height) of the façade module have been defined considering the following aspects:

- Constructive characteristics of the residential building stock. The distance between floors in the building stock varies greatly. Residential buildings less than 40 years old have distances of 2.75 m between axes. However, older buildings have greater distances between 3 and 3.2 m in height. Windows also vary greatly in size, but a width of 0.70 m to 1.10 m can be taken as a reference for single-leave windows, and double-leave windows range from 1 m to 1.6 m. The height is usually between 1.30 m and 1.70 m.
- Maximum weight allowed of the module on the existing structure. The self-weight of the modular façade, as well as the wind load on the façade, will be transmitted directly to the floor slabs of the building as point loads through the anchoring system between the façade module and the existing wall. Therefore, the permissible maximum weight of the modules will depend on the load-bearing capacity of the building structure. This parameter must be verified in each project. However, as a design parameter, a target of 100 kg/m<sup>2</sup> has been established for the modular façade. It is higher than conventional curtain walls, whose weight is around 40-70 kg/m<sup>2</sup>. Regarding the load limitation of the auxiliary means required in the installation phase, conventional cranes have a peak load limitation of 2000 kg.
- Optimisation of transport to avoid exorbitant costs (MITMA, 2023). The standard dimensions of the trucks have been considered to establish the modularity of the system.

After analysing these aspects, a 2.2x3.40 m module was defined as the maximum size that would adequately cover the established main requirements of flexibility, lightness, easy transport, and installation. On the other hand, the total thickness of the modular system is variable and adaptable. The inner layer and the outer layer have an established thickness of 133 mm and 103 mm, respectively. The perimetral opened joint between them is 4 mm thick. However, the insulation layer behind the mainframe has a variable thickness, depending on the case. This dimension will be defined taking into account the lack of vertical alignment of the existing façade and the cavity generated between the module and the existing wall that needs to be filled with insulation. At least 40 mm of insulation will be needed. Therefore, the total thickness of the modular system will be at least 280 mm.

### 3.2.2 Technological panel modularity

A fundamental aspect to be analysed during the design of the modular system is the dimensional flexibility of the technological panels to be integrated into the outer layer. To this end, the requirements and limitations of each of the technologies and the restrictions imposed by their integration have been identified. Based on this study, a technology database has been created, offering all the possibilities for technological panels and their different combinations within a façade module.

Common requirements for all the technologies have also been established:

- The maximum weight of the technological panels is set at 50 kg (INSST, 2011). This condition is imposed to facilitate the handling by two operators during the assembly phase of the façade in the workshop manufacturing process and to facilitate maintenance and replacement processes during their lifetime.
- All the technologies are integrated into an aluminium subframe. The subframe, combined with the technologies, forms the technological panel. This subframe is mechanically fixed to the mainframe of the inner layer. This allows the standardisation of the connection between the two layers, regardless of the technologies selected for the outer layer. The geometry of the subframe allows a quick and removable connection to the main frame.

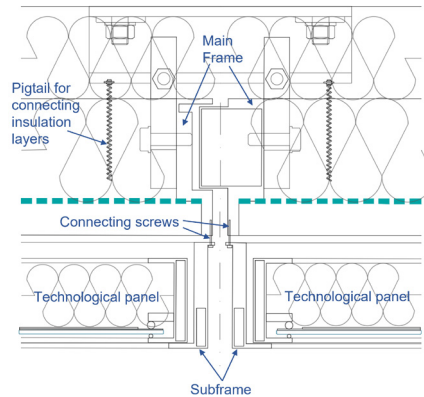


FIG. 6 Schematic horizontal section of the connection between the technological panels and the mainframe via the subframe.

The analysis and results on the modularity obtained for each technology are summarised below: solar thermal (ST), photovoltaic (PV), and hybrid technology (PVT).

#### Solar Thermal panel (ST)

The ST technology consists of an external glass, an aluminium absorber with integrated hydraulic channels, an airtight air chamber between these two elements, and rock wool insulation on the back of the absorber. One inlet and one outlet hydraulic pipe to interconnect multiple ST panels are also part of these panels. An aluminium frame closes all the elements so that this assembly is integrated into the subframe. The limiting element to determine the size of the ST panel is the geometry of the absorber. The dimensions of this collector have been established considering the following conditions:

- The manufacturing process of the absorber limits the maximum dimensions of the collector to 510x1660 mm.
- This collector, which is also the basis of the hybrid panel (PVT), must have compatible dimensions to be able to attach the photovoltaic technology with an adequate distribution of cells. In other words, the absorber must be valid both for ST and for PVT technologies.
- Offer at least three configuration alternatives that can be installed vertically and horizontally.

As a balanced solution meeting all these requirements, an absorber of 485x1660 mm was selected.

The image below shows the modularity exercise carried out for ST. The combination of one, two or three absorbers (ST1, ST23, and ST34) offers the possibility of positioning the panels vertically (V) or horizontally (H). The hydraulic connections are arranged on the side (L) or in the upper area (U). A single absorber solar thermal panel is also feasible.

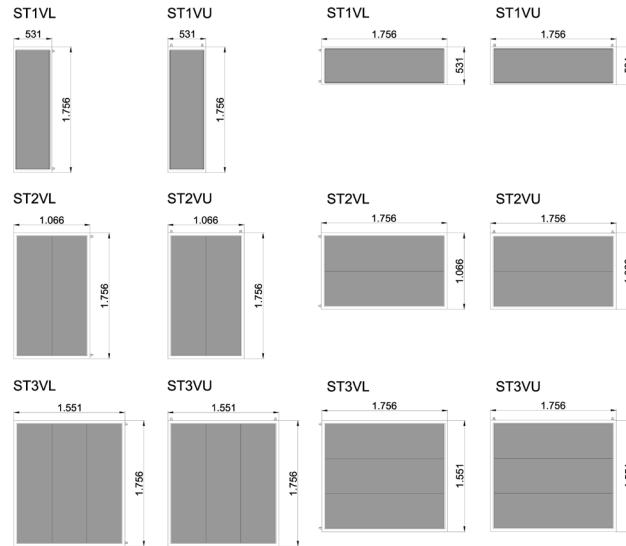


FIG. 7 Modularity analysis of solar thermal technology.

The following table shows the dimensions of the technological panel in all its combinations.

TABLE 1 Modularity of solar thermal panel (ST)

TECHNOLOGY	CODE NAME	ST PANEL DIMENSION	ST PANEL DIMENSION
		(width) [mm]	(height) [mm]
ST PANELS	ST1VL	571	1756
	ST1VU	531	1796
	ST1HL	1796	531
	ST1HU	1756	571
	ST2VL	1106	1756
	ST2VU	1066	1796
	ST2HL	1796	1086
	ST2HU	1756	1126
	ST3VL	1591	1756
	ST3VU	1551	1796
	ST3HL	1796	1551
	ST3HU	1756	1591
	ST4VL	2076	1756
	ST4VU	2036	1796
	ST4HL	1796	2056
	ST4HU	1756	2096

### Hybrid panel (PVT)

This technology incorporates the same absorber as the ST panel. A photovoltaic panel is attached to the front surface of the absorber, while an insulation layer is adhered to the back. The hybrid technological panel is generated once these components are integrated into the subframe.

The density of cells in PVT panels is dependent on the number of absorbers. For example, a PVT panel with one absorber can accommodate 20 photovoltaic cells, but a PVT panel with two absorbers integrates up to 60 cells.

Under the same conditions as in the case of ST panels, an analogous modularity study is carried out for hybrid technology, obtaining 32 types of PVT panels. These panels contain 1, 2, 3 or 4 absorbers. The data is included in Table 7 in the Appendix.



FIG. 8 Prototype of ST panel combining RIVENTI's and KAMEL's technologies.

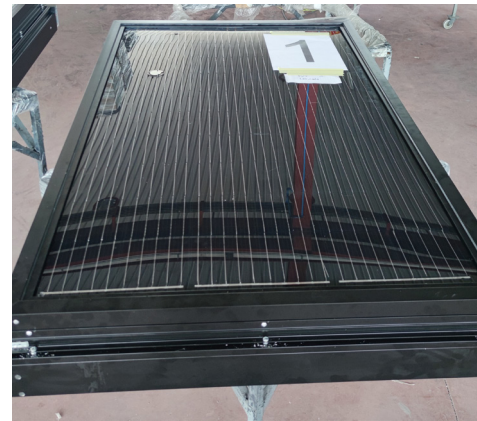


FIG. 9 PVT panel, scaled prototype, combining RIVENTI's, TECNALIA's, ONYX's and KAMEL's technologies.

### Photovoltaic panels (PV) with different substrates

The modular façade can accommodate two types of substrates for the lamination of photovoltaic technology; aluminium (PV+AL) and synthetic stone panel (PV+SS). As for the rest of the technologies, these are integrated into the subframe, generating the photovoltaic technological panel. The requirements that have guided the analysis and dimensional design of the photovoltaic panels are:

- Standard supply dimensions of the aluminium and synthetic stone panel are adopted as baseline.
- Limit the waste of substrate generated in the production process to less than 15%.
- Achieve dimensions compatible with ST and PVT technologies to facilitate the combination of all three technologies in the same façade module. This is achieved when the dimension of one side of the PV technology matches the dimension of one side of the ST and PVT technologies.
- Offer a variable density of cells in such a way that the substrate is visible to a greater or lesser extent. Both aluminium and synthetic stone have an aesthetic value, and the visibility of the substrate affects the design of the envelope. The possibility of generating panels with variable cell density provides a great variety of alternatives from an aesthetic point of view.

The dimensions of the optimised panels are available in Table 8 in the Appendix. The figure below shows the different phases of the study.

Cells number	Power (W)	% view of substrate	Cells number	Power (W)	% view of substrate	Cells number	Power (W)	% view of substrate	Cells number	Power (W)	% view of substrate
24	118	20 %	18	88	40 %	20	98	33 %	15	74	50 %

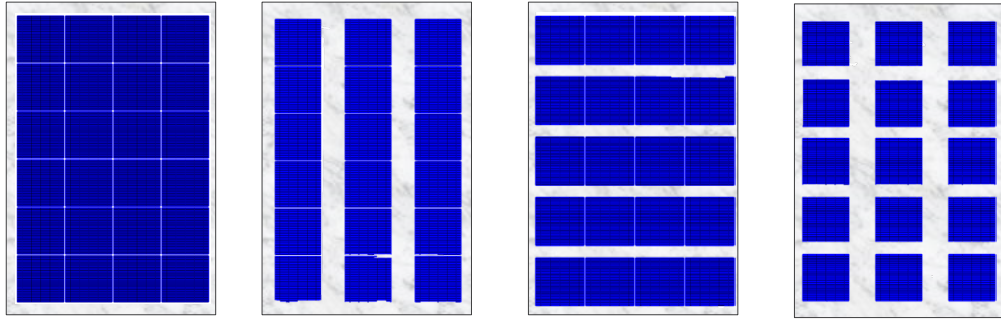


FIG. 10 Study on different cell densities in a 1060x710 mm PV+SS panel. This exercise was carried out for all the dimensions considered. Source: ONYX.

The following table shows the dimensions of PV+AL and PV+SS that are compatible with PVT and ST technologies. This means that they can be easily combined in the same façade module. These dimensions are indicated in bold.

TABLE 2 Dimensions of PV+AL and PV+SS technological panels compatible with PVT and ST technologies.

TECHNOLOGY	PV PANEL DIMENSION	
	(width) [mm]	(height) [mm]
PV+AL	1106	756
	571	766
	571	1476
	756	1591
PV+SS	1106	756
	571	766
	1106	1476
	571	1476
	756	1591

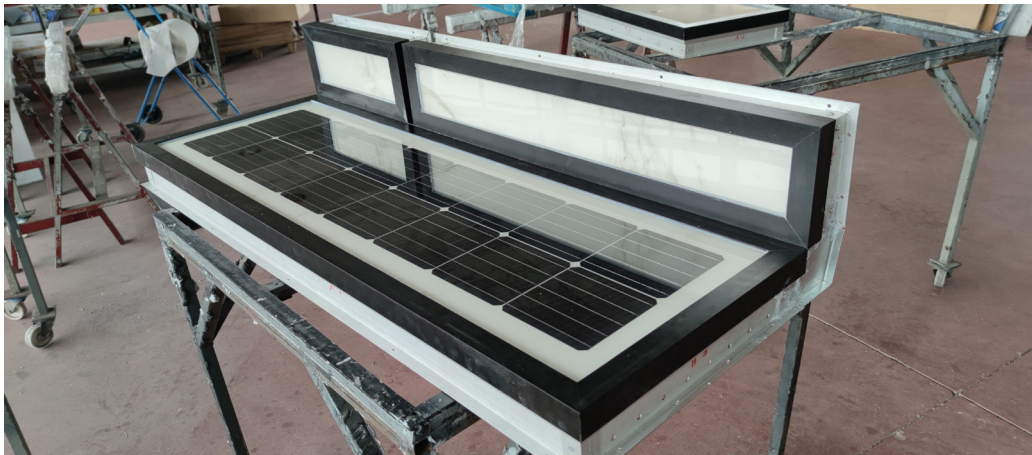


FIG. 11 PV+SS panel, scaled prototype, combining RIVENTI's and ONYX's technologies.

### 3.2.3 Active window

The active window incorporates an intelligent decentralised ventilation system with heat recovery integrating a heat exchanger that takes benefit of the thermal differences between the supply and exhaust air. The air renewal control is activated according to a series of parameters monitored inside the room, mainly humidity, CO<sub>2</sub>, and temperature.

From a constructive point of view, the active window is fixed to the mainframe of the inner layer. This element is positioned aligned with the waterproof membrane and the insulation layer to guarantee the airtightness, watertightness, and correct thermal behaviour of the assembly. The interface between the window and the outer layer of the façade system is solved through the subframe profile. The ventilation box is integrated into the lintel and includes a thermal bridge break that is aligned with the one for the window. The back of the ventilation box must be accessible from inside the building to ensure proper air renewal and to facilitate possible maintenance works. Likewise, the wiring required for the power supply of the ventilation system and for the control system is in an area accessible from inside the building.

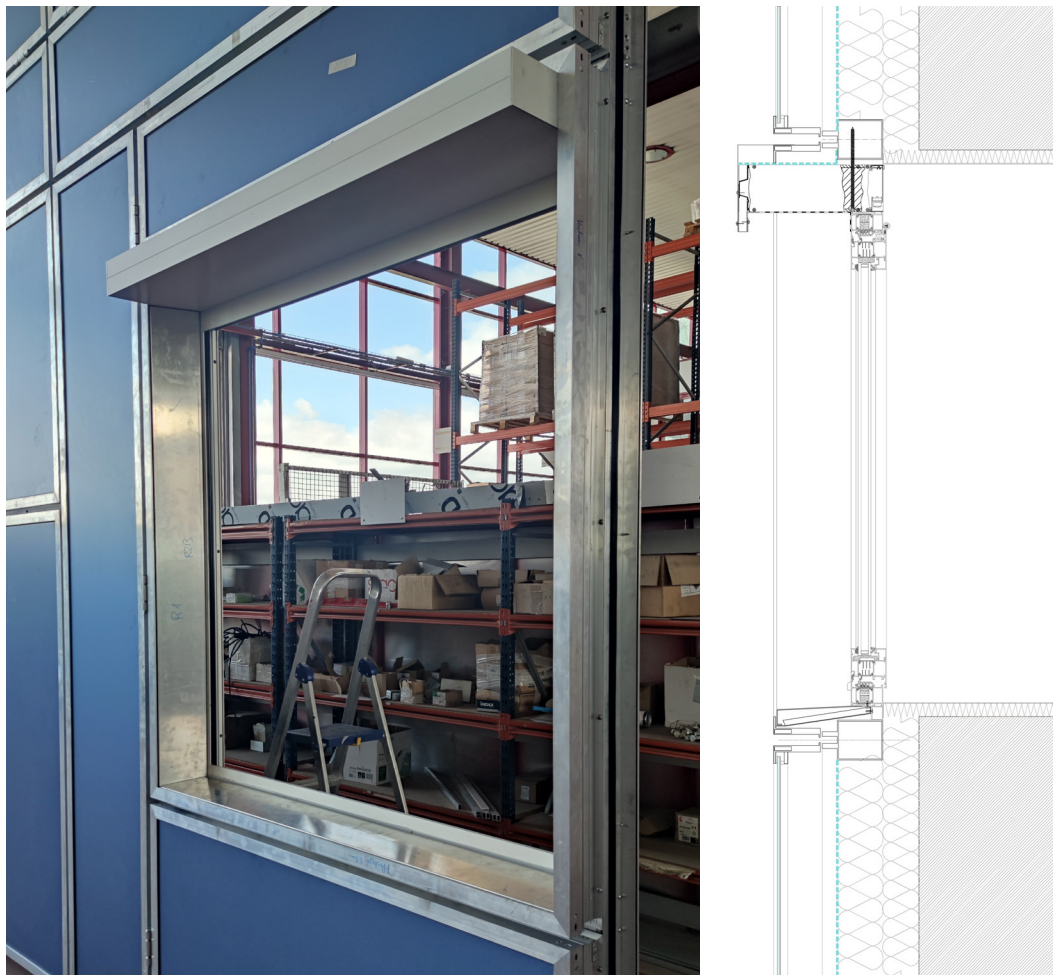


FIG. 12 Integration of the active window in a full-scale prototype of the façade system, combining RIVENTI's and TRESPA's technologies (left). Vertical section (right).

To avoid problems of interferences between the aerator box and the existing façade in the on-site installation phase, some minimum distances between these elements must be considered. Specifically, 10 mm separation between the rear face of the aerator and the existing façade and 20 mm to the horizontal plane of the existing window opening. Thus, the position of the ventilation system in the façade module must be verified in each project according to the characteristics of each building.

All these distances allow the absorption of small deviations in the dimensions of the window opening as well as the incorporation of the finishing elements in the transition area between the new window and the old window for renovations that involve removing the old window. This area is covered with aluminium composite perimeter elements that are installed once the modular façade system that incorporates the new window is in place.

### 3.3 ANALYSIS OF INTEGRATION OF THE ELECTRICAL AND THERMAL NETWORKS IN THE MODULAR FAÇADE SYSTEM

Another innovative aspect of the façade system is the integration of a specific space to interconnect the solar technologies from different modules and to generate an infrastructure network, hydraulic and electrical, on the façade plane that is fully accessible for installation and maintenance.

The layout of the access zones on the façade is defined according to the integrated solar technologies and the connection between them. The access zones must ensure a continuous network on the exterior layer of the façade system. For this purpose, they can be positioned horizontally and vertically.

The access zones are configured by a phenolic panel as a cladding layer, the subframe common to all the technologies of the outer layer of the façade system and a hinge system that allows a 180° opening of the cladding. This opening guarantees full access to the space destined to integrate the installation network.



FIG. 13 Full-scale prototype, combining RIVENTI's and ONYX's technologies. 3 access zones can be seen at the top of the sample. The central access zone is opened, and the lateral ones are closed.

The minimum dimensions of the access zones are defined by the space required by all the components of the integrated network. The hydraulic network requires more space than the electrical one. Valves, air purges, elbows, etc., are elements that must necessarily be placed in these spaces. Therefore, the minimum width in the case of vertical access zones will be 300 mm if the panels with solar thermal technology are located on the same side of the access zone and 400 mm if

they are on both sides of the access zone. In the case of horizontal access zones, these are connected to the solar thermal technologies located below them to ensure proper hydraulic operation. Given this premise, the minimum height required for horizontal access zones is 300 mm. In addition, to define these minimum dimensions, the requirements for supporting elements for piping and electrical wiring have also been considered.

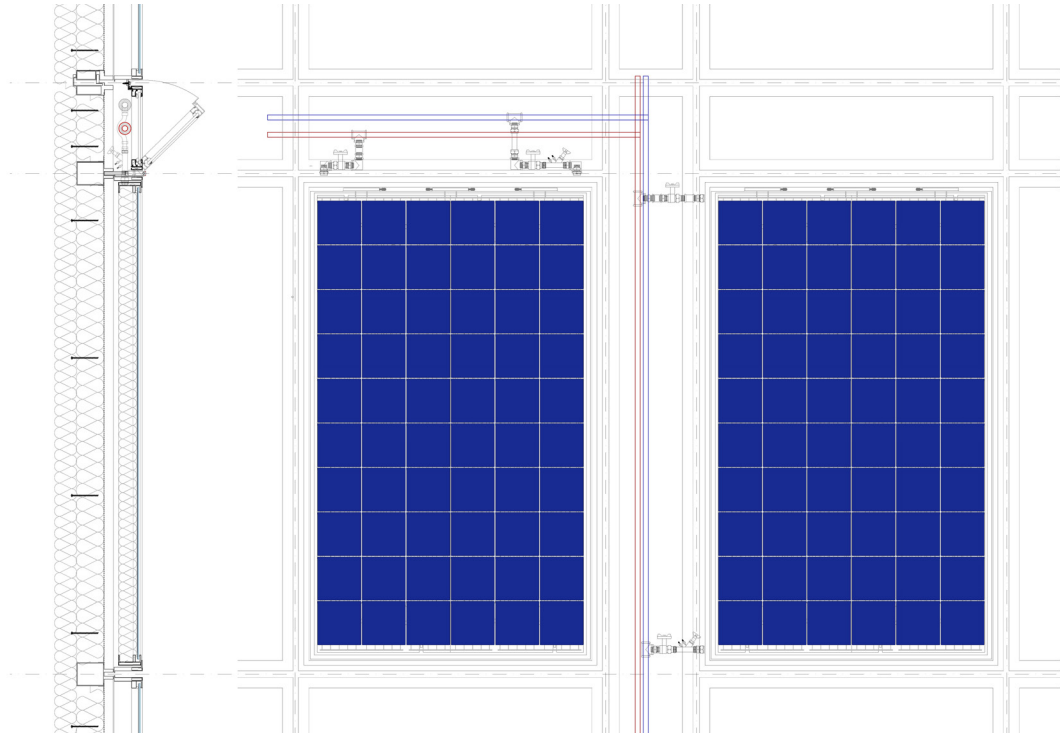


FIG. 14 Distribution of hydraulic infrastructure, connecting PVT panels in vertical and horizontal access zones. Elevation view (right) and vertical section (left).

The access zone can be sized to include services that run along the façade of the building before the renovation, such as drainpipes, gas pipes or cables, also making them accessible. This might require a slight adaptation of their tracks to place them into the outer layer of the modular system.

### 3.4 GLOBAL CONFIGURATION OF THE MODULAR FAÇADE SYSTEM

The modular façade tends to be configured using large modules. The larger the modules, the cheaper they are to manufacture and the quicker the installation of the complete façade system on the building will be. However, it is possible to manufacture smaller modules to suit the needs of every building. Each module can have multiple configurations depending on the type of panels placed on the outer layer and their relative position in the module. The ST and PVT panels are the most limiting ones from a dimensional perspective, as their sizes are fixed by the number of absorbers that they comprise.

Based on the results obtained in the modularity analyses described in the previous sections, the possible combinations of technological panels that a façade module can offer are studied.

Initially, the number of ST or PVT panels was quantified by combining the number of absorbers per panel, their orientation (vertical or horizontal), and the position of the connections (top, right-hand side and left-hand side) with the general network in the access zone (horizontal or vertical). As a result of this analysis, 48 panel alternatives for ST and PVT were obtained.

TABLE 3 ST and PVT combinations depending on the number of absorbers, their orientation and the connection with the access zone.

ABSORBER'S POSITION	N° ABSORBERS Access zones	1		2		3		4	
		PVT	ST	PVT	ST	PVT	ST	PVT	ST
VERTICAL	LATERAL left or right	PVT1VL <sub>L</sub> PVT1VL <sub>R</sub>	ST1VL <sub>L</sub> ST1VL <sub>R</sub>	PVT2VL <sub>L</sub> PVT2VL <sub>R</sub>	ST2VL <sub>L</sub> ST2VL <sub>R</sub>	PVT3VL <sub>L</sub> PVT3VL <sub>R</sub>	ST3VL <sub>L</sub> ST3VL <sub>R</sub>	PVT4VL <sub>L</sub> PVT4VL <sub>R</sub>	ST4VL <sub>L</sub> ST4VL <sub>R</sub>
	UPPER	PVT1VU	ST1VU	PVT2VU	ST2VU	PVT3VU	ST3VU	PVT4VU	ST4VU
HORIZONTAL	LATERAL left or right	PVT1HL <sub>L</sub> PVT1HL <sub>R</sub>	ST1HL <sub>L</sub> ST1HL <sub>R</sub>	PVT2HL <sub>L</sub> PVT2HL <sub>R</sub>	ST2HL <sub>L</sub> ST2HL <sub>R</sub>	PVT3HL <sub>L</sub> PVT3HL <sub>R</sub>	ST3HL <sub>L</sub> ST3HL <sub>R</sub>	PVT4HL <sub>L</sub> PVT4HL <sub>R</sub>	ST4HL <sub>L</sub> ST4HL <sub>R</sub>
	UPPER	PVT1HU	ST1HU	PVT2HU	ST2HU	PVT3HU	ST3HU	PVT4HU	ST4HU

Secondly, the relative position of these panels within the module has been considered. The module is divided into upper zone (U), middle zone (I), and lower zone (L). This iteration results in 48 possible configurations for the module, considering ST and PVT panels with 1, 2, 3 or 4 absorbers.

TABLE 4 Alternative combinations depending on the type of PVT or ST panels (number of absorbers, 2, 3 and 4), their orientation and the positioning of the active panel inside the module.

COMBINATIONS	N° ABSORBERS		
	2	3	4
HAAZ Horizontal absorbers + access zone	HAAZ2U	HAAZ3U	HAAZ4U
	HAAZ2I	HAAZ3I	HAAZ4I
	HAAZ2L	HAAZ3L	HAAZ4L
VAAZ Vertical absorbers + access zone	VAAZ2U	VAAZ3U	VAAZ4U
	VAAZ2I	VAAZ3I	VAAZ4I
	VAAZ2L	VAAZ3L	VAAZ4L
HVAZ Horizontal absorbers + vertical access zone	HVAZ2U	HVAZ3U	HVAZ4U
	HVAZ2I	HVAZ3I	HVAZ4I
	HVAZ2L	HVAZ3L	HVAZ4L
VHAZ Vertical absorbers + horizontal access zone	VHAZ2U	VHAZ3U	VHAZ4U
	VHAZ2I	VHAZ3I	VHAZ4I
	VHAZ2L	VHAZ3L	VHAZ4L

As an example, nine possible module configurations are graphically presented below. In this case, the access zone is horizontal with a vertical PVT panel with 2, 3, and 4 absorbers. The white areas are photovoltaic technology, PV+Al or PV+SS.

## VERTICAL ABSORBERS AND HORIZONTAL ACCESS ZONE (VHAZ)

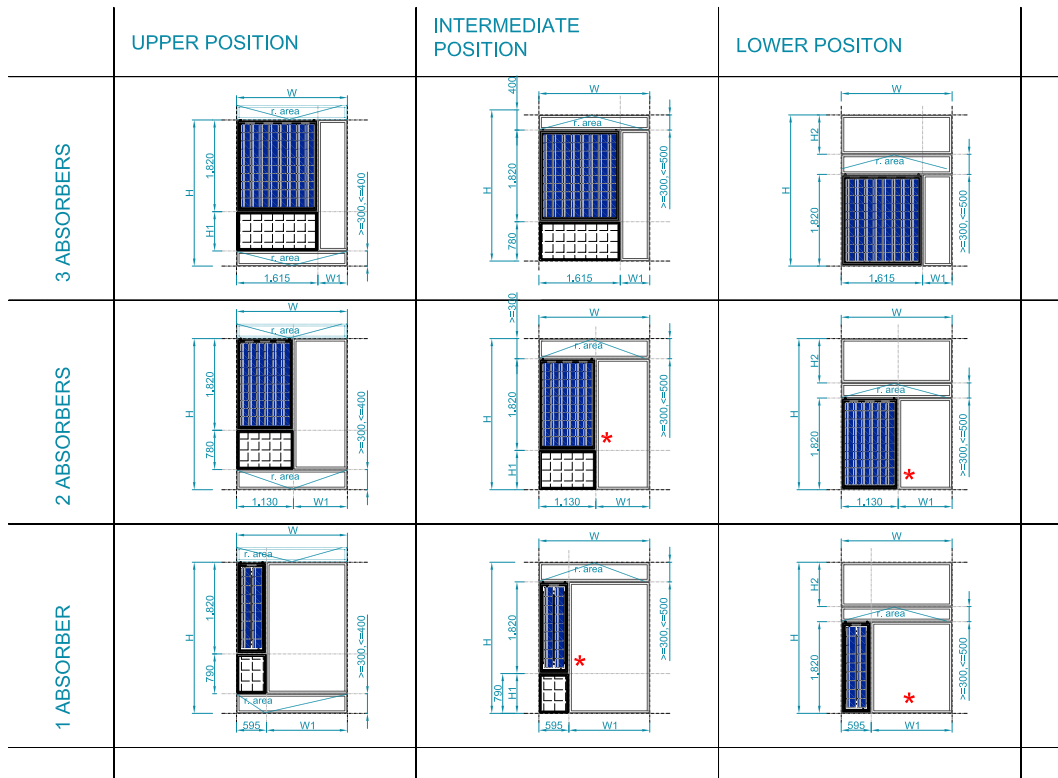


FIG. 15 Graphical representation of nine possible configurations when the access zone is placed horizontally and when the absorber is in the vertical direction (VHAZ)

Finally, after thoroughly defining the system design, all possible combinations of technological panels have been analysed, and an assessment was conducted to quantify the system's weight. Firstly, the weight per square metre of the different components that comprise the modular façade was calculated. This information is presented in the following table.

TABLE 5 Weight values per surface area of the components of the modular façade system.

Layer	Components	Kg/m <sup>2</sup>
Inner	Aluminium profiles	20
	Insulation panels	
	Waterproof Membrane	
Outer	Access zone	18
	ST	32
	PVT	43
	PV+Al	26
	PV+SS	30

Therefore, the weight range per square metre of the modular system varies between 38 and 63 kg/m<sup>2</sup>.

A representative module of 1.13x3.32 m configured by a PVT panel with two absorbers (1.13x1.82 m), a PV+Al (1.13x1 m), and an access zone (1.13x0.5 m) would reach a total weight of 203 kg.

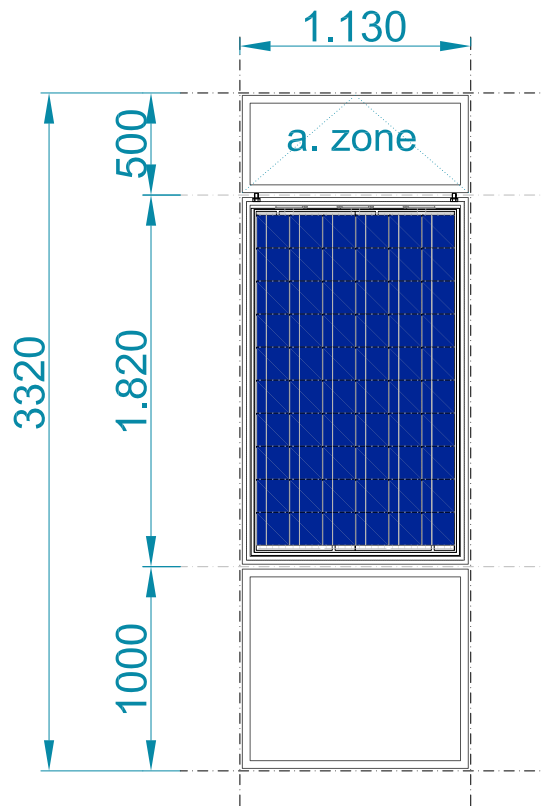


FIG. 16 Representative module

### 3.5 VALIDATION OF SYSTEM PERFORMANCE

As indicated in the Methodology section, reference standards for evaluating the system performance are EAD 090062-00-0404, EN 13830, and EN 50583. As the inner layer is assimilated to a modular curtain wall solution, the assessment of the essential characteristics related to this element will be carried out under Product Standard EN 13830. However, the exterior layer is assimilated in many aspects as an external cladding mechanically fixed, and for that reason, the essential characteristics associated with this element will be evaluated under the standard EAD 090062-00-0404. EN 50583 standard for the assessment of photovoltaic panels as construction products, when installed on buildings, compiles, among others, the above two references depending on whether the photovoltaic technology is integrated into a façade system or is part of the cladding of the building and mechanically fixed to a supporting wall.

The following table shows the priority essential characteristics identified for the new façade system as well as their target value. The reference standards considered to define the target value are also indicated.

These are the main requirements considered critical for the design and validation phase of the innovative façade system. In later development stages towards the commercialisation of the solution, an analysis of other additional requirements may be necessary depending on the application scenario. This is the case of seismic behaviour, a parameter that has not been evaluated yet but that could imply some adaptation of the system to comply with such requirements.

TABLE 6 Priority essential characteristics of new façade system.

No	Essential characteristic	Assessment method	Type of expression of product performance	Target value
<b>Basic Works Requirement 2: Safety in case of fire</b>				
1	Reaction to fire	SBI TEST EN 13501-1, based on EAD	Class	<sup>(1)</sup> B-s3, d0 (required class) B-s2, d0 (desired class)
<b>Basic Works Requirement 4: Safety and accessibility in use</b>				
2	Wind load resistance	Simulations	Level	<sup>(2)</sup> Qw = 2-3 kN/m <sup>2</sup>
3	Weight resistance	Simulation, based on EN 13830	Level	
<b>Basic Works Requirement 6: Energy economy and heat retention</b>				
4	Thermal resistance	Simulation	Level	<sup>(3)</sup> 0.2 W/m <sup>2</sup> ·K (Overall value of the façade)
<b>Durability</b>				
5	Hygrothermal behaviour	Analysis	Description	Not applicable

Two typologies of analysis have been considered for assessing compliance with the priority essential characteristics:

- Validation through simulations and/or estimative calculation. These are related to structural, thermal and hygrothermal performance.
- Validation through tests. This affects mainly the protection against fire performance. Ensuring that the façade system meets the regulatory requirements for fire performance is essential to validate the developed solution.

The evaluation of structural, thermal, and hygrothermal performance was carried out during the design phase. These analyses have allowed us to define in detail the sections of the profiles, the layers of the system, their characteristics and their relative position. As a result of the verification of these essential characteristics together with the modularity exercise described, the detailed solution of the façade system was defined.

Then, the fire reaction was validated through a laboratory test once the design phase was completed. The heterogeneity of the system, configured by the connection of numerous elements, layers and materials, implied a significant uncertainty in this respect.

1 Depending on the building type, the height, and the EU Member State, fire safety requirements vary. The preliminary fire reaction classification of B-s2, d0 should be aimed for, though other classifications such as the B-s3, d0 are valid for façades in many Member States. In the case of the Spanish standard, CTE DB-SI, the maximum classification required is B-s3, d0, for façade elements that occupy more than 10% of the surface area in buildings with a height of more than 18 metres. This class is also required for insulation systems located in ventilated air chambers in buildings with a height of less than 28 metres.

2 Ref Standard CTE DB SE AE. Section 3.3. (CTE DB-SE-AE, 2009)

3 Ref Standard CTE DB HE. (CTE DB-HE, 2022)

## REACTION TO FIRE – SBI TEST

This test evaluates the potential contribution of a product to the development of a fire under a fire situation, simulating a single burning item in a room corner near that product. In the specific case of the new façade system, the outer technological layer, including all the fixing systems, was tested. One test per each of the five technologies considered for these panels was performed, obtaining a preliminary fire reaction classification:

- 1 phenolic sample representing the access zones of the system
- 1 thermal solar sample (ST)
- 1 hybrid sample (PVT)
- 1 photovoltaic sample with aluminium substrate (PV+AL)
- 1 photovoltaic sample with synthetic stone substrate (PV+SS)

The configuration and the dimensions are detailed in the figure below.

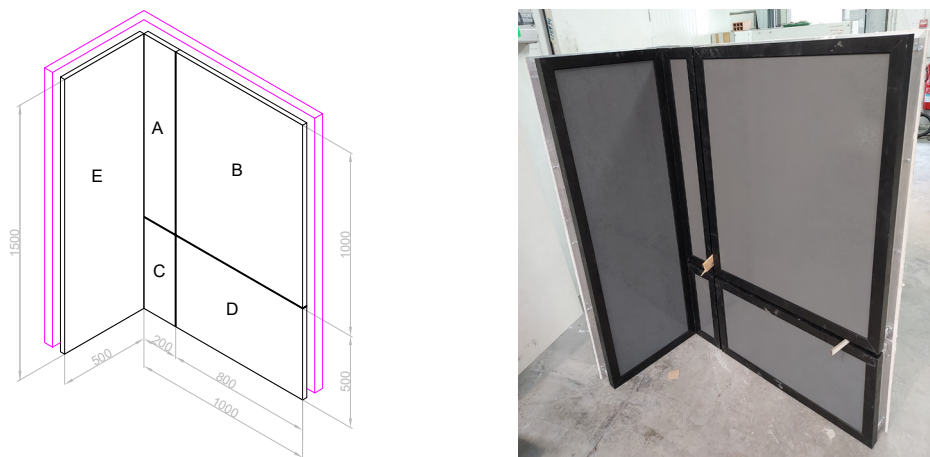


FIG. 17 Configuration and dimensions of the SBI test sample (left). Phenolic sample combining RIVENTI's and TRESPA's technologies (right)

The same result was achieved for all five tests—pictures are included below—concluding with a preliminary reaction to fire classification of B-s1,d0.



FIG. 18 a: sample of ST panels (without selective coating), b: PVT panels sample, c: PV+SS sample, d: PV+AL sample and e: phenolic panels sample. RIVENTI's, TECNALIA's, ONYX's, KAMEL's and TRESPA's technologies were adopted.

## 4 DISCUSSION AND CONCLUSIONS

This paper presents the development process of a prefabricated modular system for renovating residential buildings. The system consists of an industrialised solution that incorporates solar harvesting technologies. One of the main challenges was to achieve a highly flexible solution both in terms of geometry and to enable the incorporation of different solar-capturing devices. The ultimate goal was to achieve a façade system for the renovation sector that is constructively adaptable to a wide range of residential buildings and that provides renewable solar energy, thermal or electrical, depending on the demand of the building. This solution offers existing buildings the possibility to fulfil Nearly Zero Energy Buildings requirements.

The following conclusions have been drawn from the process of developing this modular façade system.

- From a constructive flexibility and architectural adaptability perspective, the solution is adaptable to any distribution and size of windows in the building, whether regular or irregular. However, this system is more suitable for flat façades than for those with balconies. The thickness of the modular façade system is significant, therefore reducing the useful surface area of these elements. Its design allows different thermal insulation levels to be met, as the thickness of the insulation layer is adaptable. Ensuring contact between the insulation layer of the modular system and the existing wall of the building was identified as a complex challenge in the design phase due to the multiple irregular alignments on the vertical plane that commonly appear in buildings. The mainframe of the modular system cannot be adapted to these irregularities. Therefore, to avoid generating an air gap between the façade module and the existing wall, a layer of low-density insulation covering the whole surface was incorporated on the back of the mainframe. As a consequence, this insulation layer limits the contact of the aluminium mainframe with the existing wall, limiting the thermal bridges just to the specific area of the anchorages.
- In terms of the ability to customise the outer layer of the façade system from an energy point of view, offering the possibility to combine different solar technologies. The method that allows obtaining the maximum variety of sizes and combinations has been identified: 1) to analyse the dimensional flexibility of each technology considering aspects such as: size restrictions and % waste limitations at the manufacturing phase of the technological panels and 2) to define the potential sizes of the technological panels (façade element) of the most constraining technology. The energy efficiency of those integrated technologies and the handling during the assembly in the workshop (off-site) needs to be considered, 3) to identify which panel sizes of the technologies with greater dimensional flexibility are compatible with the previous ones, taking into account the energetic performance, 4) to compose all the combinations of panels in the façade module incorporating the access zones. During this study phase, ST and PVT panels with four absorbers were discarded due to the difficulty of handling them, given their dimensions and weight. The maximum dimensions of the PV+Al panels have been limited to 1300x1060 mm due to the restrictions of the lamination process of the photovoltaic cells on the substrate. The maximum surface area of the PV+SS panels has been restricted to 1.7 m<sup>2</sup> not to exceed the maximum weight for their manipulation.
- From the performance point of view. The results of the reaction to the fire test predict a B-s1,d0 classification, higher than the target value established. This highlights the potential of the façade system developed as a solution for the renovation market.

In conclusion, a prefabricated and modular façade solution with the integration of solar technologies to meet the decarbonisation objectives of the EU building stock was developed. The objective of versatility from the constructive and energetic aspect has been achieved in such a way that this system not only adapts to the physiognomy of existing buildings but also to their energy demands.

However, future research is planned in the area of fire performance and propagation assessment of the system in order to ensure that this façade solution can meet the highest regulatory requirements currently applied in certain countries, such as the United Kingdom. Although it is not yet mandatory in many EU countries for façade systems to be certified for their fire performance concerning the spread through the façade, this performance is essential to ensure the safety of users, especially in high-rise buildings.

#### ACKNOWLEDGMENTS

---

The authors would like to thank all those companies and researchers participating in the ENSNARE project for their strong involvement. Especially the contributions from RIVENTI, ENAR, ONYX, KAMEL and TRESPA are gratefully appreciated for the research described in this paper.

#### FUNDING

---

This project has received funding from the European Union's Horizon 2020 research and innovation programme under grant agreement No 958445. This publication reflects only the author's views and the Commission is not responsible for any use that may be made of the information it contains.

## References

---

- Artola, I., Rademaekers, K., Williams, R., & Yearwood, J. (2016). *Boosting Building Renovation: What Potential and Value for Europe? Study*. European Parliament.
- Avesani, S., Andaloro, A., Ilardi, S., Orlandi, M., Terletti, S., & Fedrizzi, R. (2020). Development of an Off-site Prefabricated Rainscreen Façade System for Building Energy Retrofitting. *Journal of Façade Design and Engineering*, 8(2), 39–58. <https://doi.org/10.7480/jfde.2020.2.4830>
- Bonato, P., Fedrizzi, R., D'Antoni, M., Meir, M., (editors) (2019). *State-of-the-art and SWOT analysis of building integrated solar envelope systems*: IEA SHC Task 46, Deliverables A1 and A2. Retrieved from <https://task56.iea-shc.org/publications>
- Broers, W., Vasseur, V., Kemp, R., Abujidi, N., & Vroon, Z. (2019). Decided or divided? An empirical analysis of the decision-making process of Dutch homeowners for energy renovation measures. *Energy Research & Social Science*, 58, 101284.
- CEN - European Committee for Standardization, (2020). EN 13830:2015+A1:2020, Curtain walling – Product standard
- CEN - European Committee for Standardization, (2016). EN 50583: Photovoltaics in buildings
- Colinart, T., Bendouma, M., & Glouannec, P. (2019). Building renovation with prefabricated ventilated façade element: A case study. *Energy and Buildings*. <https://doi.org/10.1016/j.enbuild.2019.01.033>
- CTE DB-HE - Technical building code, basic document *Energy Saving*, Spanish government (2022). <https://www.codigotecnico.org/DocumentosCTE/AhorroEnergia.html>
- CTE DB-SE-AE- Technical building code, basic document *Loads on the buildings*, Spanish government (2009). <https://www.codigotecnico.org/DocumentosCTE/SeguridadEstructural.html>
- DIRECTIVE. (2018/844/EU). *on the energy performance of building*. Brussels: THE EUROPEAN PARLIAMENT AND OF THE COUNCIL Retrieved from <http://data.europa.eu/eli/dir/2018/844/oj>
- DIRECTIVE. (P9\_TA(2023)0068). *on the energy performance of building (recast)*. Brussels: THE EUROPEAN PARLIAMENT AND OF THE COUNCIL Retrieved from [https://www.europarl.europa.eu/doceo/document/TA-9-2023-0068\\_EN.html#title1](https://www.europarl.europa.eu/doceo/document/TA-9-2023-0068_EN.html#title1)
- de Gracia, A., Castell, A., Navarro, L., Oró, E., & Cabeza, L. F. (2013). Numerical modelling of ventilated façades: A review. *Renewable and Sustainable Energy Reviews*, 22, 539–549. <https://doi.org/10.1016/j.rser.2013.02.029>
- D'Oca, S., Ferrante, A., Ferrer, C., Perneti, R., Gralka, A., Sebastian, R., & Op 't Veld, P. (2018). Technical, Financial, and Social Barriers and Challenges in Deep Building Renovation: Integration of Lessons Learned from the H2020 Cluster Projects. *Buildings*, 8(12), 174. <https://doi.org/10.3390/buildings8120174>
- Du, H., Huang, P., & Jones, P. (2019). Modular façade retrofit with renewable energy technologies: The definition and current status in Europe. *Energy and Buildings*, 205, 109543. <https://doi.org/10.1016/j.enbuild.2019.109543>
- Economidou, M., Atanasiu, B., Despret, C., Maio, J., Nolte, I., Rapf, O., . . . Strong, D. (2011). Europe's Buildings Under the Microscope: 2011. *Buildings Performance Institute Europe (BPIE)*.
- Elguezabal, P., & Arregi, B. (2018). An analysis of the potential of envelope-integrated solar heating and cooling technologies for reducing energy consumption in European climates. *Journal of Façade Design and Engineering*, 6(2), 085–094. <https://doi.org/10.7480/jfde.2018.2.2102>
- Efthymiou, E., Cöcen, O. N., & Ermolli, S. R. (2010). Sustainable aluminium systems. *Sustainability*, 2(9), 3100–3109. <https://doi.org/10.3390/su2093100>
- EOTA – European Organisation for Technical Assessment. (2018), EAD 090062-00-0404: Kits for external claddings mechanically fixed. Retrieved from <https://www.eota.eu/eads>
- European Commission. (2019). *The European Green Deal*. Brussels Retrieved from [https://ec.europa.eu/info/sites/info/files/european-green-deal-communication\\_en.pdf](https://ec.europa.eu/info/sites/info/files/european-green-deal-communication_en.pdf)
- European Commission. (2020). *A Renovation Wave for Europe - greening our buildings, creating jobs, improving lives*. Brussels Retrieved from [https://energy.ec.europa.eu/system/files/2020-10/eu\\_renovation\\_wave\\_strategy\\_0.pdf](https://energy.ec.europa.eu/system/files/2020-10/eu_renovation_wave_strategy_0.pdf)
- European Commission. (2021). 'Fit for 55': delivering the EU's 2030 Climate Target on the way to climate neutrality. Brussels Retrieved from <https://eur-lex.europa.eu/legal-content/EN/TXT/PDF/?uri=CELEX:52021DC0550>

- Ferdous, W., Bai, Y., Ngo, T. D., Manalo, A., & Mendis, P. (2019). New advancements, challenges and opportunities of multi-storey modular buildings – A state-of-the-art review. *Engineering Structures* (Vol. 183, pp. 883–893). Elsevier Ltd. <https://doi.org/10.1016/j.engstruct.2019.01.061>
- Filippidou, F., Nieboer, N., & Visscher, H. (2016). Energy efficiency measures implemented in the Dutch non-profit housing sector. *Energy and Buildings*, 132, 107–116.
- Gagliano, A., & Aneli, S. (2020). Analysis of the energy performance of an Opaque Ventilated Façade under winter and summer weather conditions. *Solar Energy*, 205, 531–544. <https://doi.org/10.1016/j.solener.2020.05.078>
- INSST - Ministry of Labour and Immigration, Government of Spain. Manual handling of loads. Technical guideline of National Institute of Health and Safety at Work (2011). 27a8b126-a827-4edd-aa4c-7c0ca0a86cda (insst.es)
- Jensen, P. A., Maslesa, E., Berg, J. B., & Thuesen, C. (2018). 10 questions concerning sustainable building renovation. *Building and Environment*, 143, 130–137.
- Lessing, J. (2006). Industrialized House-Building: Concept and processes, Licentiate thesis. Lund: Lund University. Retrieved from [https://www.lth.se/fileadmin/projekteringsmetodik/publications/Lessing\\_lic-webb.pdf](https://www.lth.se/fileadmin/projekteringsmetodik/publications/Lessing_lic-webb.pdf)
- Li, Y., & Chen, L. (2022). Investigation of European modular façade system utilizing renewable energy. *International Journal of Low-Carbon Technologies*, 17, 279–299.
- Mitma - Ministry of Transport, Mobility and Agenda of the Government of Spain (2023). Inspection and safety in overland transport. Weights and dimensions. Esquema Longitud - Vehículos rígidos, Tren de carreteras, Vehículos articulados, Trenes de carretera de transporte de vehículos | Ministerio de Transportes, Movilidad y Agenda Urbana (mitma.gob.es)
- Moran, P., O'Connell, J., & Goggins, J. (2020). Sustainable energy efficiency retrofits as residential buildings move towards nearly zero energy building (NZEB) standards. *Energy and Buildings*, 211. <https://doi.org/10.1016/j.enbuild.2020.109816>
- Sandberg, N. H., Sartori, I., Heidrich, O., Dawson, R., Dascalaki, E., Dimitriou, S., . . . Završ, M. Š. (2016). Dynamic building stock modelling: Application to 11 European countries to support the energy efficiency and retrofit ambitions of the EU. *Energy and Buildings*, 132, 26–38.
- Navaratnam, S., Ngo, T., Gunawardena, T., & Henderson, D. (2019). Performance review of prefabricated building systems and future research in Australia. *Buildings*, Vol. 9, Issue 2. MDPI AG. <https://doi.org/10.3390/buildings9020038>
- REGULATION (EU) No 305/2011 of the European Parliament and of the Council of 9 March 2011 laying down harmonized conditions for the marketing of construction products and repealing Council Directive 89/106/EEC Text with EEA relevance. Retrieved from: <https://eur-lex.europa.eu/legal-content/EN/TXT/?uri=CELEX:32011R0305>
- Semprini, G., Gulli, R., & Ferrante, A. (2017). Deep regeneration vs shallow renovation to achieve nearly Zero Energy in existing buildings: Energy saving and economic impact of design solutions in the housing stock of Bologna. *Energy and Buildings*, 156, 327–342.
- Streicher, K. N., Mennel, S., Chambers, J., Parra, D., & Patel, M. K. (2020). Cost-effectiveness of large-scale deep energy retrofit packages for residential buildings under different economic assessment approaches. *Energy and Buildings*, 215. <https://doi.org/10.1016/j.enbuild.2020.109870>
- Tsemekidi-Tzeiranaki, S., Bertoldi, P., Paci, D., Castellazzi, L., Serrenho, T., Economidou, M., & Zangheri, P. (2020). *Energy consumption and energy efficiency trends in the EU-28, 2000-2018*. EUR 30328 EN, Publications Office of the European Union, Luxembourg, ISBN 978-92-76-21074-0, doi: 10.2760/847849. Retrieved from: <https://publications.jrc.ec.europa.eu/repository/handle/JRC120681>
- Van Roosmalen, M., Herrmann, A., & Kumar, A. (2021). A review of prefabricated self-sufficient façades with integrated decentralized HVAC and renewable energy generation and storage. *Energy and Buildings* (248). Elsevier Ltd. <https://doi.org/10.1016/j.enbuild.2021.111107>
- Viana, D., Tommelein, I., & Formoso, C. (2017). Using Modularity to Reduce Complexity of Industrialized Building Systems for Mass Customization. *Energies*, 10(10), 1622. <https://doi.org/10.3390/en10101622>
- Wasim, M., Han, T. M., Huang, H., Madiyev, M., & Ngo, T. D. (2020). An approach for sustainable, cost-effective and optimised material design for the prefabricated non-structural components of residential buildings. *Journal of Building Engineering*, 32. <https://doi.org/10.1016/j.jobbe.2020.101474>
- Wilson, C., Pettifor, H., & Chryssochoidis, G. (2018). Quantitative modelling of why and how homeowners decide to renovate energy efficiently. *Applied energy*, 212, 1333–1344.

TABLE 7 Sizing measures for hybrid panel (PVT)

TECHNOLOGY	CODE NAME	ST PANEL DIMENSION	ST PANEL DIMENSION
		(width) [mm]	(height) [mm]
PVT PANELS	PVT2VL	1106	1756
	PVT2VU	1066	1796
	PVT2HL	1796	1086
	PVT2HU	1756	1126
	PVT3VL	1591	1756
	PVT3VU	1551	1796
	PVT3HL	1796	1551
	PVT3HU	1756	1591
	PVT4VL	2076	1756
	PVT4VU	2036	1796
	PVT4HL	1796	2056
	PVT4HU	1756	2096

TABLE 8 Dimensional analysis of PV+SS. Panels that exceed 50kg are indicated in green. Source: Onyx solar.

	PV PANEL	PV PANEL	PV PANEL
	width [mm]	height [mm]	weight [kg]
Optimized substrate	2600	1000	78
	3200	1440	138
	1060	710	15
	1420	1060	30
	1420	1420	80.7
	1420	790	22
	1590	710	23
	710	710	10
Optimized PV	1700	1000	34
	1475	480	14
	1650	850	28



# SmartWall

Towards residential nZEB with off-site prefabricated hybrid façade systems using a variety of materials

**Emmanouil Katsigiannis<sup>1\*</sup>, Petros Gerogiannis<sup>1</sup>, Ioannis A. Atsonios<sup>1</sup>, Aris Manolitsis<sup>1</sup>, Maria Founti<sup>1</sup>**

\* Corresponding author: makatstuc@gmail.com

<sup>1</sup> Laboratory of Heterogeneous Mixtures and Combustion Systems, School of Mechanical Engineering, National Technical University of Athens, Zografou, Greece.

## Abstract

*Following the need of urban areas to maintain the existing building stock and simultaneously upgrade the overall energy performance, the renovation down-to-nZEB state has already become a necessity. In this regard, a vast range of prefabricated solutions have been developed lately. The main objective of such solutions would be not only to constitute an effective system to tackle building energy consumption but also to be versatile in terms of implementation and economic viability. In this regard, an adaptable off-site prefabricated envelope solution with an embodied HVAC system called "SmartWall" has been developed. The SmartWall can minimise thermal losses through the well-insulated envelope while, at the same time, its integrated HVAC system efficiently maintains indoor thermal comfort conditions. This study examines the virtual implementation of the SmartWall as a "Plug-n-Play" renovation solution to reach the nZEB state of a typical apartment in a multi-family residence in Athens. The analysis considers two SmartWall alternatives using conventional and eco-friendly materials. The results indicate a reduction of 88% in primary energy consumption without affecting thermal comfort conditions and highlighting that the nZEB state can be ensured if the SmartWall application is enhanced with photovoltaic modules.*

## Keywords

*nZEB renovation, prefabricated wall, all-in-one façade kit, integrated HVAC component, TRNSYS simulation*

## DOI

<http://doi.org/10.47982/jfde.2023.2.T2>

# 1 INTRODUCTION

In the realm of building renovation, the demand for efficient and cost-effective solutions has led to the emergence of innovative retrofitting methods. One such method gaining significant traction is the utilisation of prefabricated façade systems (Rovers et al., 2018). These systems offer a transformative approach to renovating existing buildings by providing a range of benefits, including improved energy efficiency, reduced construction time and cost, enhanced aesthetics, and minimised disturbance to occupants. Prefabricated façade systems encompass a wide array of modular components and panels that are manufactured off-site and then assembled on the building's façade in order to thermally enhance the envelope and upgrade the HVAC systems towards nearly Zero Energy Building (nZEB) state (Sandberg, Orskaug, & Andersson, 2016). The advantages and applications of prefabricated façade systems shed light on how they are revolutionising the landscape of building renovation and revitalisation projects (Evola, Costanzo, Urso, Tardo, & Margani, 2022). By leveraging the potential of these systems, building owners and developers can achieve remarkable outcomes in terms of both performance and aesthetics while streamlining the renovation process.

Efficient, integrated HVAC systems and renewable energy sources (RES) are necessary for achieving the nZEB state through deep renovation schemes (Attia et al., 2017; Fiorentini, Cooper, & Ma, 2015). Passive and heat recovery systems, smart windows, adaptive control systems, and nano-enabled coatings must also be fully utilised towards the energy balance and optimisation of multifunctional wall panels. The integration of HVAC systems into multifunctional façades is a crucial technology that has been studied and developed by several EU-funded projects. These projects aim to determine the feasibility and technical suitability of integrating various components such as heat pumps, convectors, ventilation units, heat recovery systems, RES, thermoelectric components, and smart control systems (D'Oca et al., 2018).

A range of such innovative building solutions have been explored and developed within the frame of EU-funded projects to enhance energy efficiency and performance.

- MORE-CONNECT involves a prefabricated roof module that incorporates heating units and integrated renewable energy sources.
- E2VENT project focuses on an adaptive ventilated façade with smart heat recovery and thermal energy storage. It utilises phase change materials.
- 4rinEU explores an externally added prefabricated timber façade with integrated ventilation and solar thermal panel.
- iNSpire project integrates a micro heat pump with heat recovery into a prefabricated timber frame wall panel.
- P2ENDURE involves a Plug-and-Play combination of multifunctional wall panels with smart windows and a prefabricated HVAC system.

Other projects include a prefabricated wall panel with an embedded duct system for heat recovery in domestic hot water distribution, a thermoelectric system that integrates radiant cooling and PV technologies in the building envelope, attached or integrated photovoltaics and solar thermal systems for electricity and hot water production, and thermal active insulation that reduces heat losses and complements the heating system. In more detail, the project MORE-CONNECT has developed roof modules that integrate renewable energy sources and combined heating units. The initial models were put to use in Heerlen, the Netherlands. As part of this initiative, prototypes of Dutch dwellings built in the 1960s were retrofitted with prefabricated modular roofs. These

roofs include integrated combined heating units (convectors) with decentralised demand and CO<sub>2</sub>-controlled mechanical ventilation units with heat recovery. The roofs also have 40 m<sup>2</sup> PV panels corresponding to 6.4 kWp. To minimise the disturbance for occupants during maintenance or parts replacement, a fully prefabricated installation box containing an air-to-air heat pump, boiler, mechanical exhaust fan, and PV converters was placed on the roof.

Moreover, E2VENT provided energy-efficient ventilated façades that can adapt and exchange heat for significant energy savings through an innovative adaptive ventilated façade system (FIG 1). This system includes a Smart Modular Heat Recovery Unit (SMHRU) for air renewal that recovers heat from extracted air using a double heat exchanger, ensuring indoor air quality while limiting energy losses. Additionally, the system includes a Latent Heat Thermal Energy Storage (LHTES) based on phase change materials that provides a heat storage system for heating and cooling peak saving. The system has a smart management feature that controls it on a real-time basis, targeting optimal performance, including sensors, communication with existing systems, and prediction of weather patterns. Finally, the system has an efficient anchoring system that limits thermal bridges.

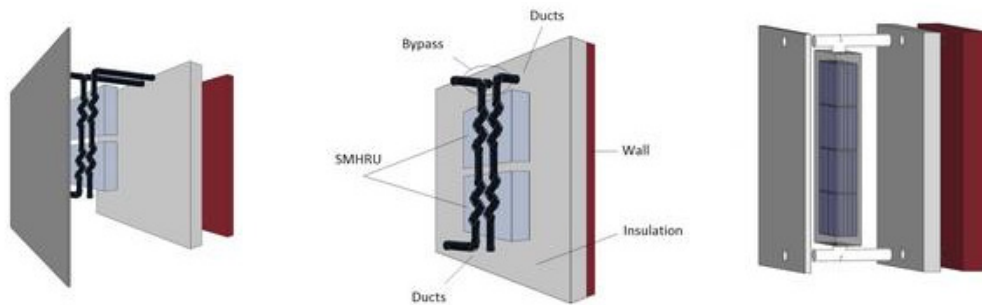


FIG. 1 E2vent system (left), Smart Modular Heat Recovery Unit (SMHRU, middle) and Latent Heat Thermal Energy Storage (LHTES, right)

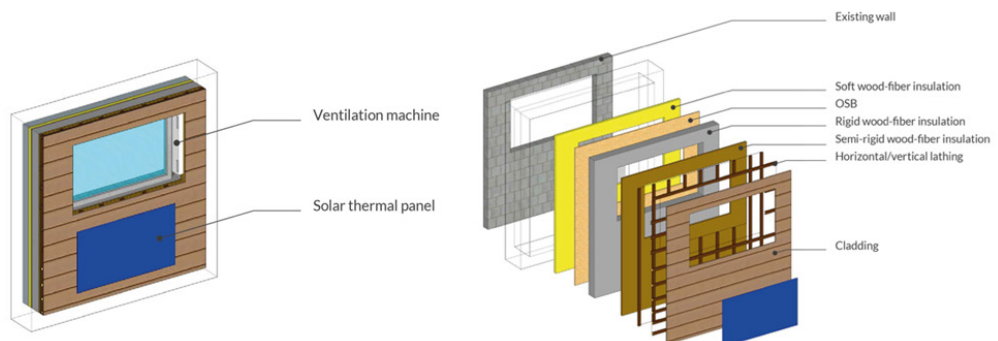


FIG. 2 Prefabricated timber-based façade module – 4rinEU project

The 4rinEU project developed a timber-based prefabricated multifunctional façade, which does not replace the existing façade but is added externally to improve performance and expand the number of functions of the existing envelope. The technology involves a prefabricated timber façade module that integrates various components such as new windows, a decentralised ventilation device, and a solar thermal panel. The integration of such components allows for the direct installation of devices during envelope renovation, increasing the building's energy performance and improving user comfort (see FIG 2).

A timber façade-integrated prefabricated system has been developed as part of the iNSpire project. This system includes a kit consisting of a wooden frame envelope module that incorporates ducts and an air-to-heat pump. During the prefabrication stage, pipes, ducts, and wires for domestic water, heating, ventilation, electricity, and solar energy generation are integrated into the timber frame façade elements. A micro heat pump is added to the exhaust of the Mechanical Ventilation with Heat Recovery (MVHR) unit (see FIG 3), and the condenser is added to the supply air, utilising the remaining heat for active heating. Acoustic silencers are also included in advance, and air outlets and inlets can be integrated through the prefabricated window reveals. Unlike previous projects that applied prefabricated timber envelope retrofit solutions, this concept attempted to incorporate heat recovery ventilation systems despite the potential installation's impact on occupied flats (Ochs, Siegele, Dermentzis, & Feist, 2015).

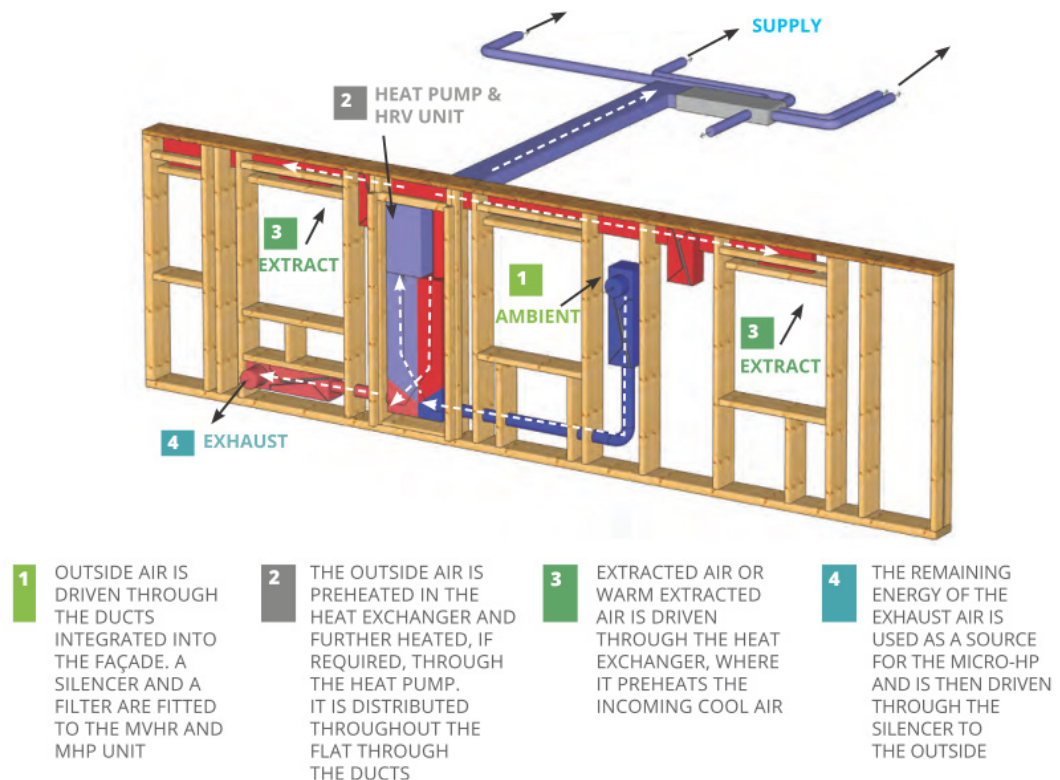


FIG. 3 Prefabricated MHVR wall system with integrated micro heat pump and ventilation unit with heat recovery

Furthermore, P2ENDURE has developed an advanced Plug-and-Play (PnP) solution that combines multifunctional wall panels, smart windows, and prefabricated HVAC systems. The integration of 180° rotating windows with double positioning Low-E glass reduces thermal radiation in the summer and minimises heat dispersion from the interior during the winter. These windows not only promote natural ventilation but also seamlessly integrate with cutting-edge home automation solutions, offering high energy efficiency, improved indoor climate, and enhanced security features. The PnP HVAC assembly comprises an air-heat pump, domestic hot water (DHW) storage capacity, mechanical ventilation system, expansion barrel, and control systems. It can be equipped with a split-engine option consisting of two cores, one for energy conversion and storage and the other for ventilation and heating/cooling. The application of smart connectors significantly reduces on-site installation time for pipe and duct connections. Additional thermal technologies leverage a compact seasonal

storage system based on innovative high-density materials capable of supplying heating, cooling, and domestic hot water (DHW) using up to 100% RES (Piaia, Turillazzi, Longo, Boeri, & Giulio, 2019). The system design integrates various components and utilises enhanced thermo-chemical materials, which have undergone rigorous testing and evaluation through field trials, including prototypes tailored for three distinct climate zones.

Last but not least, in terms of integrating smart solutions, several projects (BERTIM<sup>1</sup>, E2vent<sup>2</sup>, iNSPiRe<sup>3</sup>, RetroKit<sup>4</sup>) have included the design and development of building monitoring systems. These systems enable user interaction, operational control, and communication with sensors and hardware. Real-time intelligent management systems and control strategies have been implemented to optimise building performance and ensure the availability of detailed building supervision information. Recognising the potential of ICT-based innovations, such as smart control systems, the European Commission acknowledges their significant contribution to deep renovation initiatives. These – and many more – EU-funded projects not only focus on smart building controls but also on effectively translating captured building data into user-friendly information and establishing effective communication channels with end-users.

As a continuation of the aforementioned retrofitting solutions, an all-in-one façade component called “SmartWall” has been developed. This prefabricated kit consists of high thermal performance materials and incorporates an HVAC distribution system, aiming to reduce thermal losses through the envelope as well as increase the heating and cooling systems’ efficiency (Katsigiannis et al., 2022). In the current work, the application of SmartWall is assessed as a renovation solution in a poorly insulated multi-family pilot building in Athens, Greece. Two versions or two different alternatives of design materials are examined with respect to the energy performance of the renovated building without affecting the indoor thermal comfort conditions. The building in the initial state (existing) and in the two SmartWall renovation scenarios are fully simulated using TRNSYS software. The effectiveness of such a renovation solution, as well as the potential for the building to reach the nZEB state – with a single retrofitting intervention – is explored.

## 2 SMARTWALL SYSTEM OVERVIEW

The SmartWall is a multifunctional wall assembly that incorporates several technologies, such as fully prefabricated masonry with either metal or timber-based frame and various insulation materials, a slim-type fan coil for heating and cooling, and high-performance windows. This system can be installed on an existing envelope either on the exterior as a façade wall or on the interior when space or aesthetic considerations are at stake. Photovoltaic panels can be mounted on vertical external surfaces for power generation (see FIG 4). Alternatively, photovoltaic (PV) panels can be installed on the roof in case the building geometry features balconies or volumes that create shadows. It is applicable to any climate in Europe, yet it is especially effective in climates with

---

1 <http://www.bertim.eu/>

2 <http://www.e2vent.eu/> (2015-2018)

3 [www.inspirefp7.eu/](http://www.inspirefp7.eu/)

4 <http://www.retrokitproject.eu/>

significant cooling demands. The SmartWall is constructed as a modular Plug-and-Play panel that contains flexible piping and electrical wiring connections, enabling it to accommodate existing or new heating/cooling systems and electrical services (switches, plugs, etc.) and reducing on-site installation time.

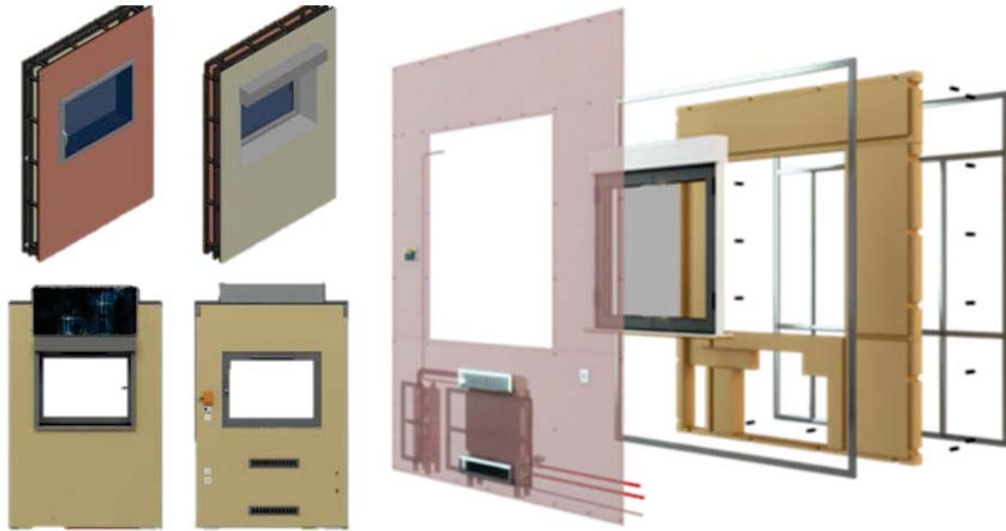


FIG. 4 SmartWall internal and external view - with and without installed PV (left), SmartWall layer overview (right)

The SmartWall, as a versatile modular façade panel, can be adapted to any dimension up to 4 m in height and can be decorated with any finishing material. The dimensions of a SmartWall panel, in case of a real implementation, depend on several parameters such as the building geometry limitations, the integrated commercial components, i.e., the common size of the wall boards (interior/exterior) and/or the slim-type fan coil dimensions. Depending on which side of the external wall the SmartWall panel is installed (interior or exterior), the selection of the appropriate finishing layers may differ.

For more peculiar structural elements such as bulges and balconies, where SmartWall cannot be fitted, the thermal performance is not affected. Existing thermal bridges, in such cases, are neither minimised nor increased. In most cases, utilising a well-insulated façade with high-performance Low-E windows and incorporating an efficient HVAC system allows the upgrade of a renovated building to nZEB status. Additionally, the incorporated smart systems, such as a human-centric HVAC control system and smart window blinds, provide an optimal balance between visual and thermal comfort.

The layout of the SmartWall HVAC systems is illustrated in the overview provided in FIG 5. A low-temperature air-to-water heat pump is used to supply the terminals inside the SmartWall panel for both heating and cooling. Inside each room, the conditioned air is distributed by the integrated slim-type Fan Coil Unit (FCU) utilising water as the heat transfer medium (FIG 5). The FCU is a device that combines a pipe coil where the water flows and a fan that blows air heated or cooled from the coil before it goes into the room. Such FCUs are used to be fed with low to medium water temperature

for heating, meaning 45 - 55 °C, whereas the respective temperature range needed for cooling in order to provide their nominal capacity values is 7-12°C. For a general application, the domestic hot water is also supplied by the same heat pump. In addition to the heat pump's operation for hot water production, solar panels can be utilised. And a PV system with panels is used for renewable electricity production. Inside the SmartWall panel, a dedicated control system is installed, which is responsible for operating the SmartWall and eventually regulating indoor conditions by using acquired data from fan coil operation, temperature, relative humidity and air quality sensors, fire protection system, etc.

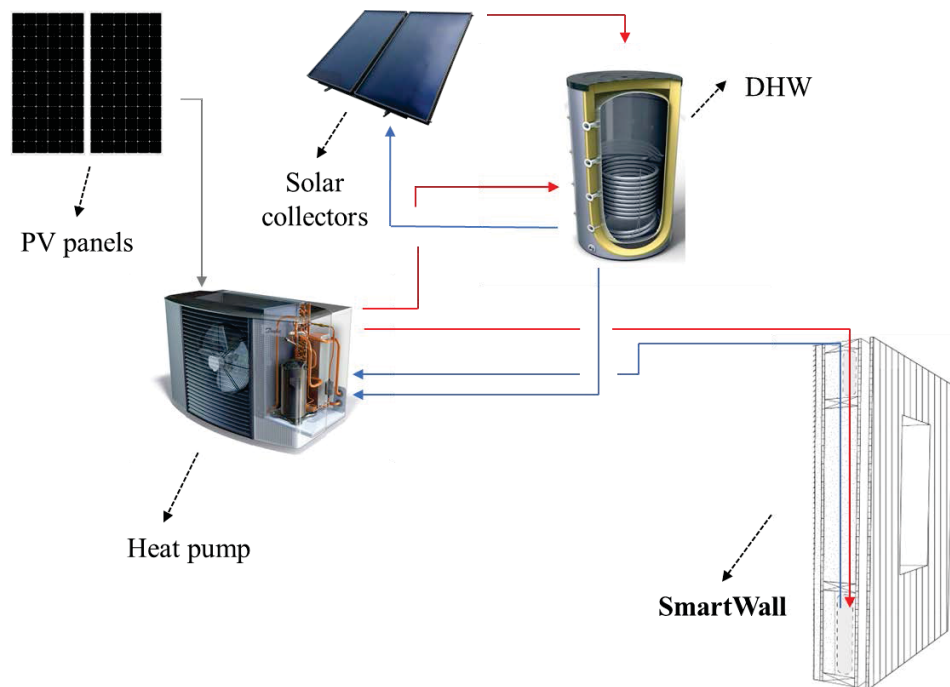


FIG. 5 SmartWall auxiliary system overview – Power (PV), heating (heat pump and solar collectors) and cooling (heat pump) generation

The current study examines two different SmartWall alternatives depending on the design materials used for construction. All materials are commercial materials, and their characteristics are available from the manufacturers. Three basic design components differentiate each type; the frame, the material used for insulation and the finishing boards.

## 2.1 METAL-BASED SMARTWALL

Regarding the metal version of SmartWall, the wall materials are anchored on two frames made by Hollow Rectangular Section (HRS) structural steel members with section dimensions of 50x30 mm and a thickness of 1.8 mm. Spacers made by the heat breaker structure are placed in the fixing points to ensure movement treatment, except for the bottom side, where the spacers are made from the HRS frame, for structural reasons. The use of this type of SmartWall is identical for high-risk seismic areas. Regarding thermal performance-related materials, a mineral wool layer of 160 mm thickness is used as a main insulator, while a mineral wool layer with aluminium foil of 30 mm thickness covers the side between the existing envelope and the added wall panel.

Additionally, a 20 mm thick VIP panel is incorporated in the rear side of the HVAC systems to create a thermally homogenous surface with similar thermal resistance. Last but not least, a 12.5 mm thick gypsum board constitutes the internal side of SmartWall coated with a multifunctional layer. In the case that the SmartWall is externally applied, a cement board is used instead. The inventory of the materials used for the SmartWall construction as well as their thermal properties, are presented in TABLE 1. The final thermal transmittance (U-value) of the SmartWall panel, including the HVAC systems of the FCU, is 0.25 W/m<sup>2</sup>K.

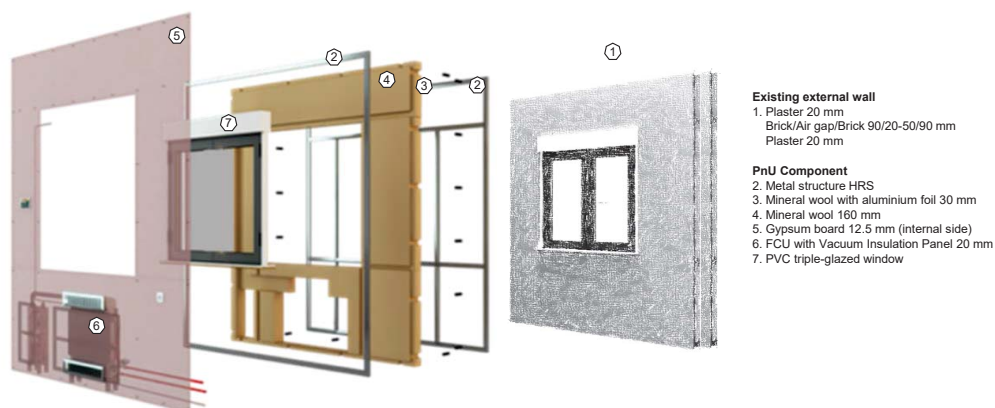


FIG. 6 Metal frame SmartWall panel - layer configuration

TABLE 1 Thermal properties of SmartWall incorporated materials

SmartWall alternative	SmartWall material	Thickness	Thermal conductivity	Density	Specific Heat Capacity
		mm	W/mK	kg/m <sup>3</sup>	J/kgK
<b>Metal-based</b>	Steel	-	60.5	7854	434
	Gypsum board	12.5	0.20	680	980
	Mineral wool	160	0.035	28	1030
	Air cavity	-	0.167	1.2	1000
	Vacuum Insulation Panel (VIP)	20	0.0075 <sup>5</sup>	195	800
<b>Timber-based</b>	Timber frame and studs	-	0.13	650	1200
	Weatherboard	20	0.13	570	2100
	Wood-fiber board	60	0.048	270	2100
	Wood-fiber blow-in insulation	100	0.038	30	2100
	Oriented Strand Board (OSB)	22	0.13	595	1700
	Softwood fibre insulation	60	0.036	60	2100
<b>Both alternatives</b>	Window glass	40	0.056 <sup>6</sup>	-	-
	Window frame	100	0.14 <sup>7</sup>	-	-

- 5 Taking into account the edge effect
- 6 the resulting U-value of glass is  $U_g=1.40\text{W}/(\text{m}^2\text{K})$
- 7 the resulting U-value of frame is  $U_f=1.40\text{W}/(\text{m}^2\text{K})$

## 2.2 TIMBER-BASED SMARTWALL

This SmartWall version, in addition to the first above-mentioned type, consists of more eco-friendly materials, meaning materials with lower embodied energy. The frame is made of two lightweight timber-based frames interconnected by horizontal supports of the same material and several anchoring points together with some fixings needed to secure the interconnection with the existing masonry. Wood fibre blow-in and softwood are used for the insulation layers, while OSB (Oriented Strand Board) and weatherboards are combined with a ventilated layer to complete the wall assembly, as presented in FIG 7. The final U-value of the SmartWall panel, including the mechanical parts of the FCU, is 0.188 W/m<sup>2</sup>K.

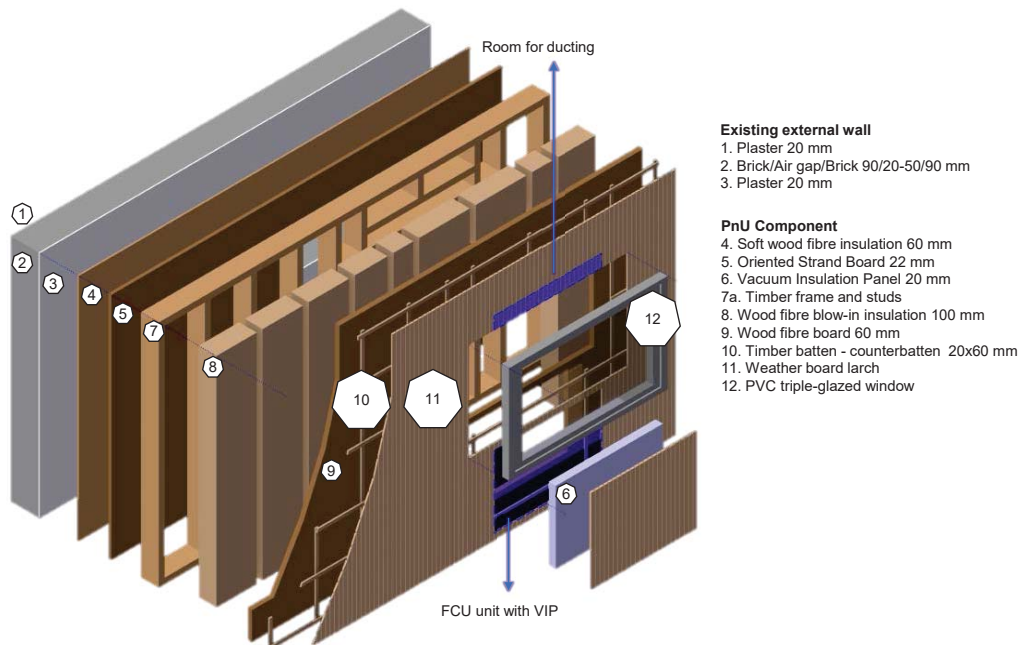


FIG. 7 Timber frame SmartWall panel – layer configuration

## 3 METHODOLOGY

The SmartWall application is examined as a renovation solution on a typical storey of a detached multi-family building in Greece. The retrofitting scenarios are assessed in terms of energy performance and thermal comfort conditions with the two aforementioned SmartWall types. As a reference case, the existing state of the building has been considered. The energy performance is examined based on the heat losses through the envelope (heating demand), the efficiency of the installed heating and cooling system (energy consumption for HVAC), and the contribution of the renewables (PV production vs energy consumption). The indoor conditions are examined in terms of ensuring thermal comfort regardless of the installed HVAC system.

It should be mentioned at this point that the differentiation of each examined renovation scenario refers to the design and the materials used for the wall assembly. The incorporated systems of the retrofitted state for heating, cooling and DHW are identical for both cases examined.

The calculation of the final U-value has been conducted via COMSOL Multiphysics software – in compliance with ISO 10211:2007 – taking into account all thermal bridges that occurred from integrating the mechanical equipment into the SmartWall. Moreover, adjusted U-values have been considered for the wall parts that include windows, doors or other openings. The thermal behaviour of the external wall with the metal-framed SmartWall is characterised by an overall U-value of  $0.25 \text{ W/m}^2\text{K}$ , whereas the corresponding U-value for the timber-based SmartWall is  $0.178 \text{ W/m}^2\text{K}$ .

### 3.1 CASE STUDY DESCRIPTION

The case study where the SmartWall solution is implemented is a typical floor of a multi-family building located in a southern suburb of Attica (Voula), Greece, constructed in 1971. The building is detached (see FIG 8) with a total floor area of  $881.57 \text{ m}^2$  distributed into four levels. The renovated area is the first floor that corresponds to  $222 \text{ m}^2$  with a continuous 3-side balcony of circa  $78 \text{ m}^2$ . The examined storey consists of two apartments (A1 and A2) and an unconditioned adjacent staircase area.

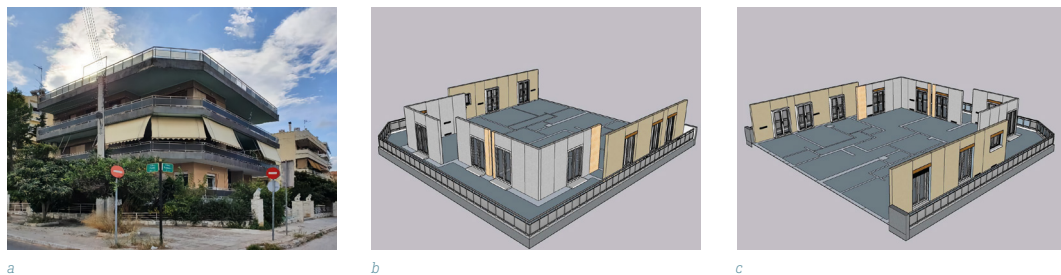


FIG. 8 Greek pilot building (a) – Isometric views of SmartWall application on 1<sup>st</sup> floor (b & c)

Main construction details include a structural frame for all floors, brick masonry with cement rendering or plaster finish, with exterior acrylic paint, and without a thermal insulation layer. The external walls constitute a surface of approximately  $151 \text{ m}^2$  with a 23.4% window-to-wall ratio. The U-value of the uninsulated existing external wall based on the Greek regulation is 2.44. The corresponding U-value for the horizontal building elements is 3.05 for the roof and  $2 \text{ W/m}^2\text{K}$  for the floor/ceiling surfaces. The thermal performance of the external wall for the existing and the two renovated states with the corresponding SmartWall types are presented in TABLE 2. U-values for the examined renovated states are calculated taking into account the existing wall layers and all potential thermal bridges from integrated parts (FCU and openings), normalised based on each SmartWall type area.

TABLE 2 Thermal transmittance of external wall

	Existing state	SmartWall – Metal frame	SmartWall – Timber frame
Total thickness mm	200-230	410-440	502-532
U-value W/m <sup>2</sup> K	2.44 <sup>9</sup>	0.25 <sup>10</sup>	0.18 <sup>11</sup>

The existing state of the building includes electric radiators of 2 kW in each conditioned zone and split-type air heat pump units for cooling with SEER of 1.7. Additionally, it is only naturally ventilated mainly during periods when the outdoor temperature is favourable. Infiltration from openings is determined considering 9.8 m<sup>3</sup>/(h·m<sup>2</sup>) and 12.5 m<sup>3</sup>/(h·m<sup>2</sup>) for doors and windows, respectively. Greek regulation proposes a typical fresh air change rate for residences equal to 15 m<sup>3</sup>/h·per occupant or 0.75 m<sup>3</sup>/h·per m<sup>2</sup> of conditioned area.

### 3.2 TRNSYS IMPLEMENTATION

The building is geometrically defined in Sketchup and imported into TRNBuild (see FIG 9). Weather conditions used for the simulation process are provided from the TRNSYS library (file “GR-Athinai-167140” of the meteonorm database). The renovated area has been divided into 17 thermal zones, as illustrated in FIG 10. From these, nine zones contain conditioning systems for heating and cooling, in which the SmartWall panels with embedded FCUs are installed. The ground floor, the semi-basement, and the 2<sup>nd</sup> floor of the building are also included in the model. However, it is assumed that horizontal surfaces adjacent to the renovated floor are adiabatic.

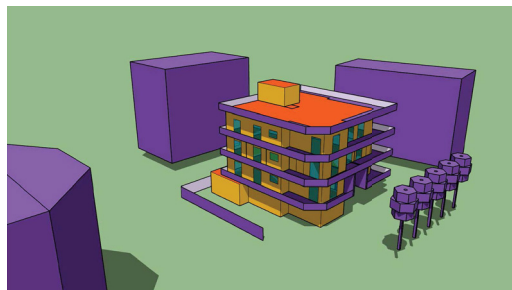


FIG. 9 Building 3D model

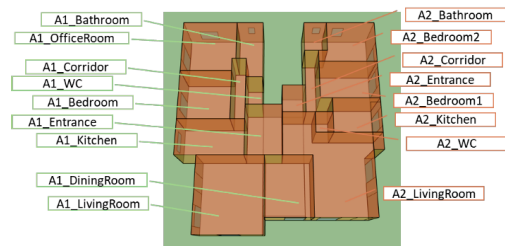


FIG. 10 Assigned thermal zones of the renovated floor

The SmartWall components and their supply systems are defined and simulated via TRNSYS studio. The software’s extensive libraries provide a wide range of components, and its dynamic energy analysis accurately models the transient behaviour of HVAC systems. The main components of the model, as well as their functionality presented, are developed in three main segments with respect to the active systems (FIG 11).

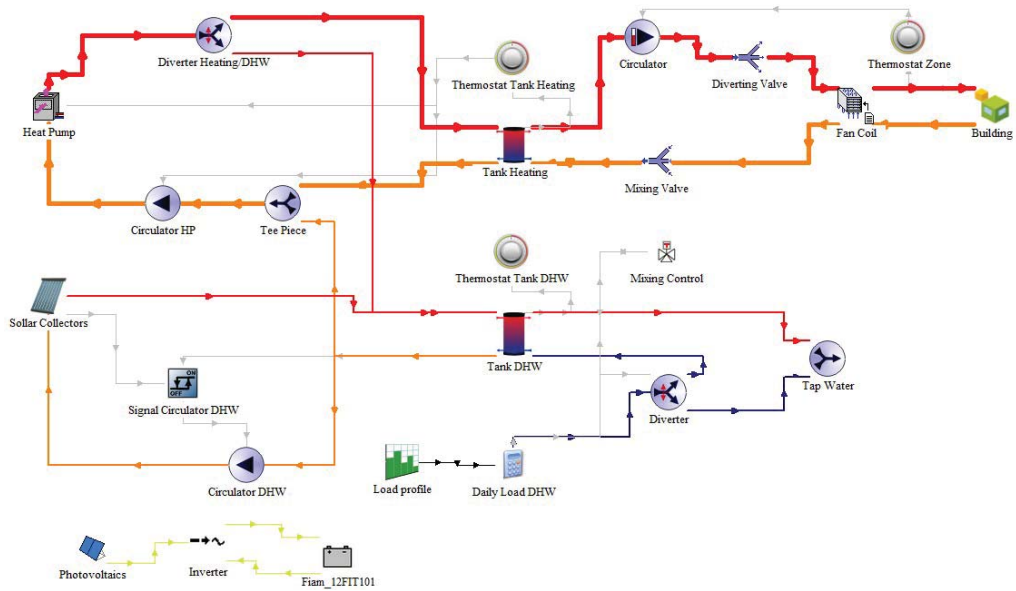


FIG. 11 Overview of simplified TRNSYS model of SmartWall support system

The building unit (type56) encompasses various parameters and regulations related to the building, including its geometry (FIG 9.), operational aspects (occupancy, heating schedules, regimes, etc.), and thermal characteristics of its elements (walls, roof, floor, windows, etc.).

Inside each zone, the distribution is facilitated by a fan coil unit and its corresponding thermostat. Each thermal zone is assigned a variable-speed 2-pipe fan coil with a rated capacity of 2.18 kW for heating. This fan coil unit acts as the terminal device responsible for supplying conditioned air to the zone in accordance with the control signal from the thermostat.

An air-to-water heat pump is used to condition the circulating water that reaches the fan coils. One heat pump is assigned for each apartment. This heat pump, which is an inverter-compressor, low-temperature system with a rated capacity of 9.37 kW for heating and 9.00 kW for cooling, serves as the main source for heating/cooling water for space conditioning and DHW. It maintains the water inside the tanks at different temperature ranges throughout the year, ensuring energy and environmental efficiency. In order to facilitate the simultaneous operation of space heating/cooling and DHW production, a separate tank is assigned for each circuit (DHW, space conditioning).

The supply water is conditioned by the heat pump and stored in a dedicated tank (100 L buffer for each apartment) before being circulated to the fan coil. This arrangement connects the heat pump to the load side, enabling its use for both space heating or cooling, while also improving its operation by minimising frequent start-stops.

A similar storage tank (150 L for each apartment) is utilised for DHW, receiving hot water from both solar collectors and the heat pump. It provides hot water to the building's taps based on a dynamic load profile. The DHW system includes a solar collector component, which utilises incidence angle modifiers (IAMs) to heat water specifically for DHW purposes. A small pump circulates the fluid, considering the temperature difference between the collector and the tank. When the hot water from the solar collector is insufficient, the heat pump for space heating is activated. The control strategy for DHW combines a forced hourly profile with thermostatic control of the water temperature in the

tank. The stored water temperature is regulated at different set points throughout the year, with a total of 2.5 hours of heating distributed during the day.

In terms of power generation, a photovoltaic (PV) array component is included in the model. This component can simulate different types of PV panels, such as monocrystalline, polycrystalline, or thin-film, and incorporates a maximum power point tracker (MPPT). Ten high-performance PV modules (21% efficiency) are connected, covering a total installed area of 20 m<sup>2</sup>. A sequence of batteries and an inverter are also incorporated for power storage and transformation, respectively, converting the DC power generated by the PV panels into AC power required by most household devices. The power is either consumed by the load or fed back to the grid if there is an excess. The assumed interaction with the utility follows a hybrid net-metering regime, where any excess power produced is directed to the national grid and subtracted from later electrical consumption.

The existing state of the examined two-apartment floor is also developed via TRNSYS. Apart from the aforementioned building component (type56), the regimes include a separate electrical radiator for heating and a split-type A/C unit for cooling. A hot water circuit with a 3 kW electric heater supplies both apartments with DHW via a buffer tank of 200 L. The set-up of the system is illustrated in FIG 12.

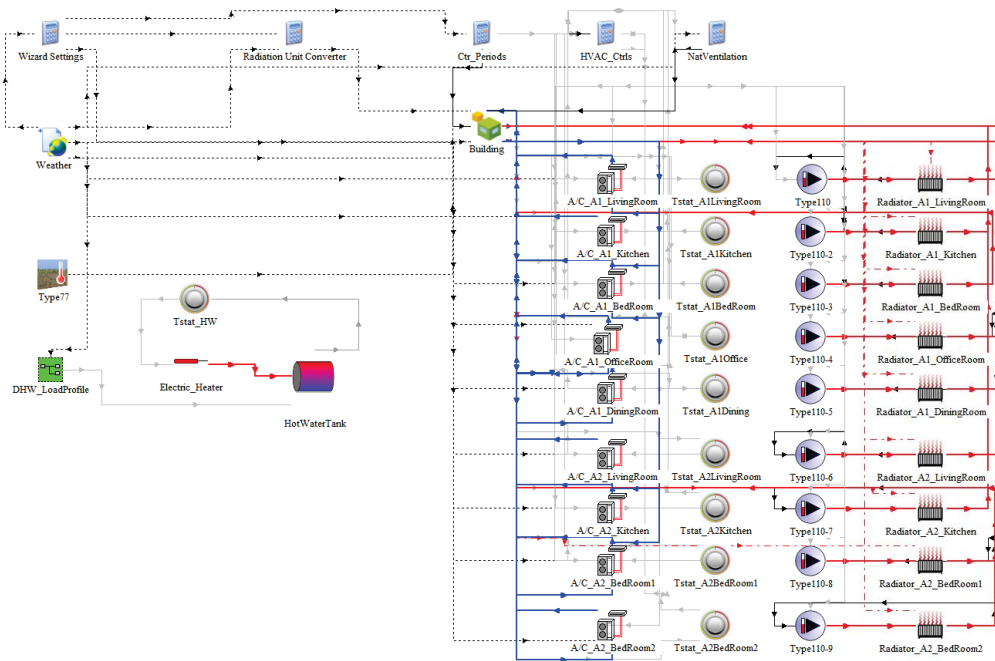


FIG. 12 Overview of TRNSYS model for the heating and cooling system of the existing state

According to Greek regulations for residences, the building operates 18 hours per day and 365 days annually. The internal gains due to occupants, electrical equipment and lighting are considered dynamically based on hourly profiles proposed by ASHRAE (90.1) and (Mitra, Steinmetz, Chu, & Cetin, 2020), as presented in FIG 13.



FIG. 13 Hourly profiles for occupancy, equipment and lighting

The simulations were conducted for a one-year period with a 10-minute timestep, considering a preparatory month to avoid side effects from initial values. Other simulation assumptions and boundary conditions regarding the building and its operation are summarised in TABLE 3.

TABLE 3 Operational characteristics of the pilot building

<b>Occupancy</b>	5 P/100 m <sup>2</sup> of floor area	<b>DHW consumption</b>	50 L/(day·P)
<b>Ventilation/ Infiltration</b>	15 m <sup>3</sup> /(h·P)	<b>Heating setpoint</b>	20° C
	0.75 m <sup>3</sup> /(h·m <sup>2</sup> )	<b>Cooling setpoint</b>	26° C
<b>Electrical equipment</b>	2 W/m <sup>2</sup>		
	6.4 W/m <sup>2</sup>		

### 3.3 KPIS DEFINITION

Specific Key Performance Indicators (KPIs) have been selected in order to better comprehend and assess the impact of the SmartWall application as a retrofitting solution. The area of interest is restricted to the energy performance with reference to the thermal comfort conditions. The energy KPIs used are the primary energy, the renewable energy ratio, and the thermal energy demand. For thermal comfort, the Predicted Mean Vote (PMV) has been taken into account.

The primary energy consumption ( $PE_c$ ), besides being a major metric within the Energy Performance of Buildings Directive (EPBD – Directive 2010/31/EU), is one of the most crucial KPIs regarding the energy assessment of building renovation scenarios. For the residential sector, this indicator concerns the total energy that is consumed annually for heating, cooling, ventilation, and domestic hot water. The primary energy can be normalised per unit floor area [kWh/m<sup>2</sup>/yr] and defined by the following equation:

$$PE_c = \frac{\sum(f_p \times E_{del})}{A_b} \quad 1$$

where,  $PE_c$  is the primary energy consumption in [kWh/m<sup>2</sup>/yr] and is the sum of delivered energy in [kWh/yr], with being the primary energy factor and the delivered energy. It is calculated as the balance of the delivered energy required to meet the energy demands of considered end-uses of the building (heating, cooling, ventilation, DHW), and  $A_b$  is the total area of the building in [m<sup>2</sup>]. A derivation of the appropriate energy performance indicators is necessary because of the potential different fuel sources, i.e. thermal and electrical energy consumption. In the examined case, the primary energy factor is 2.5 for electricity consumed and 2 for the subtracted amount of energy that is exported to the grid (the on-site produced electricity from PVs has a primary energy factor equal to 1), based on prEN 15603.

The Renewable Energy Ratio (RER) is defined as the ratio of the energy from Renewable Energy Systems (RES) and the energy consumption of the building or the apartment over a period of time. It can be determined for thermal needs (heating and cooling) and electricity needs as a whole or separated. The energy from the renewable sources can be calculated by the difference between the total energy consumption and the non-renewable energy of the considered energy flow carrying renewable energy (thermal solar, photovoltaics, heat pumps).

The function describes the renewable energy ratio is:

$$RER = \frac{E_{p,ren}}{E_{p,tot}} \quad 2$$

where,  $E_{p,ren}$  is the renewable primary energy and  $E_{p,tot}$  is the total primary energy use.

Thermal energy demand  $TE_d$  refers to the energy delivered in each conditioned zone in order to maintain the desirable temperature conditions, and it is directly linked with the building's thermal losses. It is calculated as the sum of heating and cooling energy demands.

Last but not least, Predicted Mean Vote (PMV) is the index for the thermal comfort assessment before and after the renovation. According to ASHRAE standard 55 – 2013 and EN ISO 7730, the comfort zone is defined by the combination of six major variables of thermal comfort, indoor thermal environmental factors and personal factors, that produce acceptable thermal environment conditions for the majority of the occupants within a space (Gilani, Khan, & Pao, 2015). Normally, PMV (see equation [3]) is calculated based on four measurable parameters quantities (air velocity, air temperature, mean radiant temperature, and relative humidity) and three assumed parameters (clothing, metabolic rate, and effective mechanical power) (Arakawa Martins, Soebarto, & Williamson, 2022).

$$PMV = (0.303 \exp - 0.0336 M + 0.028) \times \{ (M - W) - 3.5 \times 10 - 3 [5733 - 6.99 (M - W) - p_a] - 0.42 (M - 58.5) - 1.7 \times 10 - 5 \times M (5867 - p_a) - 0.0014M (34 - t_a) - 3.96 \times 10 - 8 f_{cl} [(t_{cl} + 273) 4 - (t_r + 273) 4] - f_{cl} \times h_c (t_{cl} - t_a) \} \quad 3$$

where, M- the metabolic rate ( $W/m^2$ ) of the body surface area

W- the effective mechanical power ( $W/m^2$ )

$I_{cl}$  – Thermal resistance of clothing ( $m^2K/W$ )

$f_{cl}$  – is the clothing surface area factor

$t_a$  – is the air temperature ( $^{\circ}C$ )

$t_r$  – is the mean radiant temperature ( $^{\circ}C$ )

$v_{ar}$  – is the relative air velocity ( $m/s$ )

$p_a$  – is the water vapour partial pressure (Pa)

$h_c$  – is the convective heat transfer coefficient [ $W/(m^2K)$ ]

$t_{cl}$  – clothing surface temperature ( $^{\circ}C$ ).

In the examined model, the required assumptions for the calculation of PMV are summarised in TABLE 4.

TABLE 4 Assumptions for PMV calculation

Metabolic rate	1.2 met
Effective mechanical power	0
Rel. air velocity	0.1 m/s
Clothing factor (winter/summer)	1/0.5

Based on PMV calculations, the thermal discomfort index has also been determined, meaning the percentage of the aggregated period of time that the PMV exceeds 0.5 (too hot) or falls below -0.5 (too cold) within the simulation period.

## 4 RESULTS

Based on the simulations conducted at the building level, FIG 14 provides a visual representation of how SmartWall's passive characteristics contribute to minimising heat losses through the envelope. The required thermal energy to counterbalance the losses ( $TE_d$ ) is equal to 131.4 kWh/m<sup>2</sup> for the existing state, 37.9 kWh/m<sup>2</sup> for the renovation scenario with metal framed SmartWall and 36.9 kWh/m<sup>2</sup> for the timber-based. A demand reduction of 71% is observed for the metal and 72% for the timber SmartWall despite the difference in the U-values (0.25 W/m<sup>2</sup>K for metal framed SmartWall and 0.13 W/m<sup>2</sup>K for the timber-based SmartWall). The impact on the heating needs is clearly more effective compared to the reduction in cooling demand due to the significant solar and internal gains that are not significantly reduced after the renovation. Nevertheless, it can be highlighted that the implementation of SmartWall panels as a renovation solution overall enhances the thermal performance of the building envelope and improves the efficiency of the heating and cooling systems.

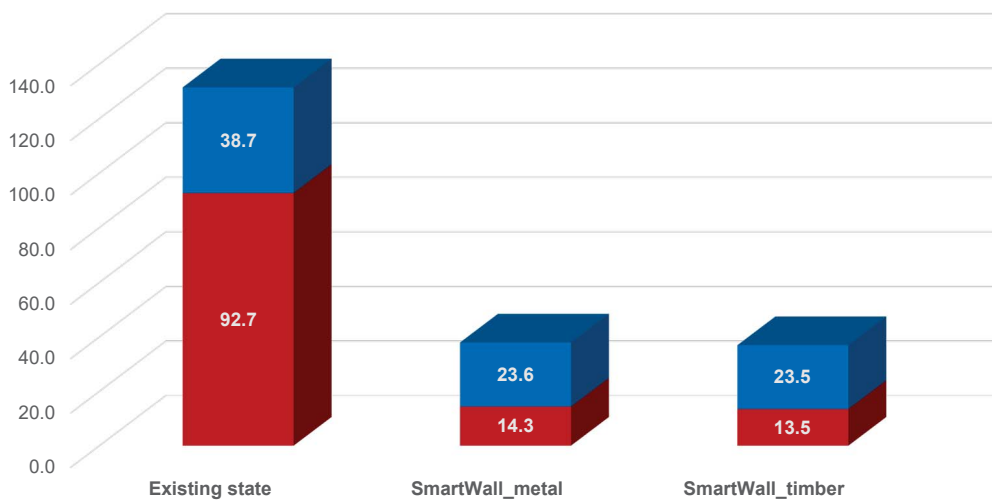


FIG. 14 Heating and cooling demand for the existing state and the two renovated envelopes

FIG 15 presents the Primary Energy consumption ( $PE_c$ ) for heating, cooling, and DHW, comparing the existing state with the application of two SmartWall alternatives. The reduction of the energy consumption is similarly substantial for both SmartWall designs – approximately 65.5 and 64 kWh/m<sup>2</sup> for the metal and timber-based SmartWall – reaching 80% (without the contribution of PV). As illustrated in FIG 15, the primary energy reduction can reach 88% when the SmartWall is combined with 20 m<sup>2</sup> PV panels. The contribution of RES (Renewable Energy Ratio – RER) in both renovation cases is 36% – since the installed systems are identical and the consumption is not significantly different. Of the 36% of RES, the solar thermal system for DHW is responsible for 15%, whereas the remaining 21% refers to PV production.

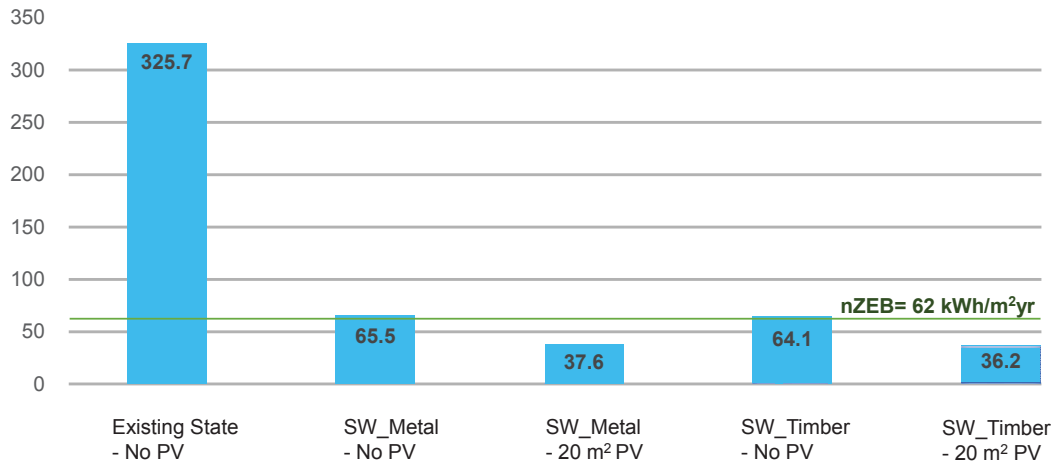


FIG. 15 Primary Energy consumption for existing and renovated state (with and without installed PV) in kWh/m<sup>2</sup>/yr

The limit of the examined building to reach nZEB, based on national building regulation (KENAK), is 62 kWh/m<sup>2</sup>. It can be observed that the nZEB state is feasible in all examined renovated cases with incorporated PV panels. The SmartWall application without installed PV marginally fail to reach the nZEB limitation. On the other hand, it is worth mentioning that the timber-frame SmartWall application presents a similar performance towards the nZEB state compared to the metal-frame alternative.

Focusing on the renovation solution provided, FIG 16 demonstrates the energy profile of the simulated storey using a metal-framed SmartWall. Energy also refers to electrical equipment and lighting consumption, as well as the PV production (with negative values) throughout the simulated year. 65% of the total required electricity of examined apartments refers to heat pump consumption, from which 24% accounts for heating, 28% for cooling and 13% for DHW. The rest of the end-use refers to electrical and lighting equipment (34%) and auxiliary systems (1%) (fan coils, circulation pumps, etc.). Power production from installed PV is significant throughout the year, while the total amount of self-consumed (62%) and exported to the grid (38%) electricity sufficiently counterbalances the total consumption during the months with high solar potential. Similar results are provided for the timber-framed SmartWall.

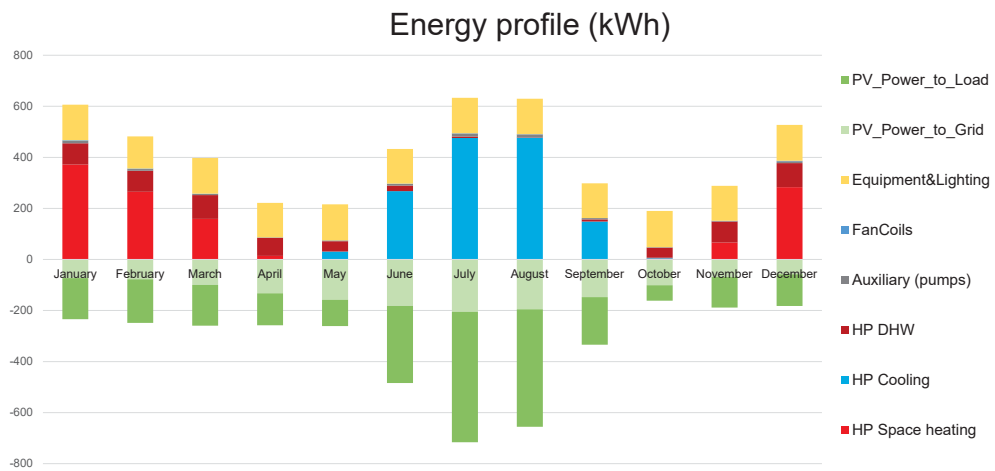


FIG. 16 Energy profile of renovated state for pilot building - SmartWall with metal frame

As far as thermal comfort is concerned, two box-plot figures (FIG 17 and FIG 18) illustrate the PMV deviation in the monitored zones. The highlighted (with cyan colour) thermal zones correspond to the conditioned zones, whereas the rest refer to other auxiliary rooms (WC, corridors, etc.) without any installed heating or cooling system. The red line of each column depicts the median PMV value in each zone, while the top and bottom edges of each box visually represent the upper and lower quartiles, respectively (the upper quartile corresponds to the 0.75 quantile and the lower quartile corresponds to the 0.25 quantile). The lines (whiskers) that extend above and below each box connecting the minimum with the maximum value represent a much less dense data range.

In the existing state of the pilot building, all conditioned zones present median PMV values near zero, indicating satisfactory thermal comfort levels for the occupants. The vast majority of values are within the comfort zone. The discomfort index is 9.14%, meaning that in less than 10% of the simulated period, thermal conditions were outside the acceptable PMV levels (less than -0.5 or higher than 0.5).

Similarly to the existing state, the renovated scenarios present satisfactory thermal comfort levels for the conditioned zones. In specific, the SmartWall-conditioned rooms present smaller deviations (box heights) within the comfort levels, indicating a slightly more acceptable indoor environment compared to the existing state. The thermal discomfort index is calculated below 5% for both renovation scenarios, meaning 3.9% and 4.2% for the metal and the timber-based SmartWall, respectively.

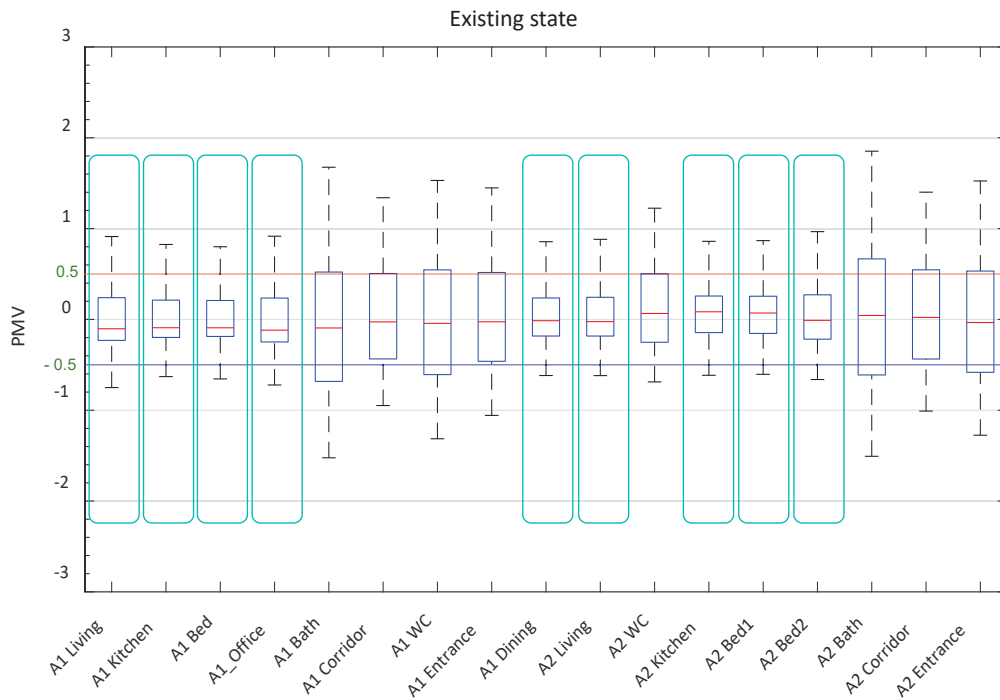


FIG. 17 Thermal comfort deviation - Existing state

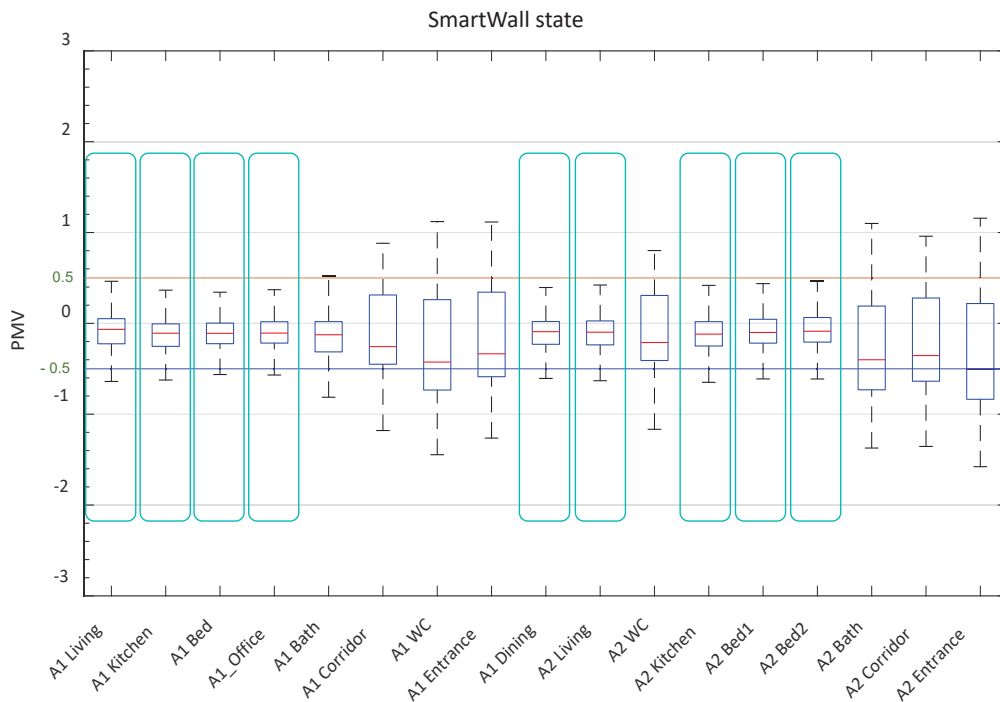


FIG. 18 Thermal comfort deviation - Renovated state

## 5 DISCUSSION – CONCLUSIONS

The present work examined the deep retrofitting solution of SmartWall – a multifunctional prefabricated façade panel with integrated HVAC components. Two different SmartWall designs incorporating conventional (metal frame, mineral wool, gypsum board, etc.) or more environmentally friendly (timber frame, OSB, wood fibre blow-in insulation, etc.) materials are considered renovation scenarios for a storey of a multi-family building located in Attica, Greece. The energy performance of the renovated floor was assessed, taking into account the indoor thermal comfort conditions. The outcome of the evaluation is summarised in the following highlights.

- SmartWall application achieved a simultaneous upgrade in both the building envelope – by reducing heat losses – and the efficiency of HVAC systems.
- The demands for heating and cooling presented a reduction of 71% after the renovation with SmartWall compared to the existing (poorly insulated) state.
- Timber-based type, despite the lower U-value, proved to be marginally more efficient in terms of thermal performance since its application resulted in a higher reduction of thermal energy demand in the examined case.
- A similar SmartWall application in Berlin with a thicker insulation layer (240 mm) is presented in (Katsigiannis et al., 2022), highlighting a heat loss reduction of 77%. This indicates the effectiveness of such façade upgrades in diverse climates with varying heating intensities.
- nZEB state can be achieved with both SmartWall alternatives with incorporated PV considering the limits of national building regulation. Excluding the PV installation, the renovation marginally fails to reach the nZEB state.
- Thermal comfort conditions are within the acceptable levels for all examined cases. However, the thermal discomfort index, which corresponds to the occupancy hours outside the acceptable range, presented an improvement by ca. 5% in the renovated scenarios compared to the existing state.

## References

---

- Arakawa Martins, L., Soebarto, V., & Williamson, T. (2022, January 1). A systematic review of personal thermal comfort models. *Building and Environment*. Elsevier Ltd. <https://doi.org/10.1016/j.buildenv.2021.108502>
- Attia, S., Eleftheriou, P., Xeni, F., Morlot, R., Ménézo, C., Kostopoulos, V., ... Hidalgo-Betanzos, J. M. (2017). Overview and future challenges of nearly zero energy buildings (nZEB) design in Southern Europe. *Energy and Buildings*, 155, 439–458. <https://doi.org/10.1016/j.enbuild.2017.09.043>
- D'Oca, S., Ferrante, A., Ferrer, C., Perneti, R., Gralka, A., Sebastian, R., & Veld, P. op t. (2018). Technical, financial, and social barriers and challenges in deep building renovation: Integration of lessons learned from the H2020 cluster projects. *Buildings*, 8(12). <https://doi.org/10.3390/buildings8120174>
- Evola, G., Costanzo, V., Urso, A., Tardo, C., & Margani, G. (2022). Energy performance of a prefabricated timber-based retrofit solution applied to a pilot building in Southern Europe. *Building and Environment*, 222. <https://doi.org/10.1016/j.buildenv.2022.109442>
- Fiorentini, M., Cooper, P., & Ma, Z. (2015). Development and optimization of an innovative HVAC system with integrated PVT and PCM thermal storage for a net-zero energy retrofitted house. *Energy and Buildings*, 94, 21–32. <https://doi.org/10.1016/j.enbuild.2015.02.018>
- Gilani, S. I. U. H., Khan, M. H., & Pao, W. (2015). Thermal Comfort Analysis of PMV Model Prediction in Air Conditioned and Naturally Ventilated Buildings. In *Energy Procedia* (Vol. 75, pp. 1373–1379). Elsevier Ltd. <https://doi.org/10.1016/j.egypro.2015.07.218>
- Katsigiannis, E., Gerogiannis, P. A., Atsonios, I., Bonou, A., Mandilaras, I., Georgi, A., ... Founti, M. (2022). Energy assessment of a residential building renovated with a novel prefabricated envelope integrating HVAC components. In *IOP Conference Series: Earth and Environmental Science* (Vol. 1078). Institute of Physics. <https://doi.org/10.1088/1755-1315/1078/1/012130>
- Mitra, D., Steinmetz, N., Chu, Y., & Cetin, K. S. (2020). Typical occupancy profiles and behaviors in residential buildings in the United States. *Energy and Buildings*, 210. <https://doi.org/10.1016/j.enbuild.2019.109713>
- Ochs, F., Siegele, D., Dermentzis, G., & Feist, W. (2015). Modelling, testing and optimization of a MVHR combined with a small-scale speed controlled exhaust air heat pump. *Building Simulation Applications, 2015-Febru*, 83–91.
- Piaia, E., Turillazzi, B., Longo, D., Boeri, A., & Giulio, R. Di. (2019, November 29). Plug-and-Play and innovative process technologies (Mapping/ Modelling/Making/ Monitoring) in deep renovation interventions. *TECHNE*. Firenze University Press. <https://doi.org/10.13128/techne-7533>
- Rovers, R., Zikmund, A., Lupišek, A., Borodinecs, A., Novák, E., Matoušková, E., ... Ott, W. (2018). *A Guide Into Renovation Package Concepts for Mass Retrofit of Different Types of Buildings With Prefabricated Elements for (n)ZEB Performance*. Retrieved from <http://www.more-connect.eu/wp-content/uploads/2018/12/A-GUIDE-INTO-RENOVATION-PACKAGE-CONCEPTS-FOR-MASS-RETROFIT-OF-DIFFERENT-TYPES-OF-BUILDINGS-WITH-PREFABRICATED-ELEMENTS-FOR-NZEB-PERFORMANCE.pdf>
- Sandberg, K., Orskaug, T., & Andersson, A. (2016). Prefabricated Wood Elements for Sustainable Renovation of Residential Building Façades. In *Energy Procedia* (Vol. 96, pp. 756–767). Elsevier Ltd. <https://doi.org/10.1016/j.egypro.2016.09.138>



# Plasmochromic Modules for Smart Windows: Design, Manufacturing and Solar Control Strategies

**Mirco Riganti<sup>1</sup>, Julia Olive<sup>1</sup>, Francesco Isaia<sup>2</sup>, Michele Manca<sup>1</sup>**

\* Corresponding author, mmanca@leitat.org

1 LEITAT Technological Center, Terrassa, Barcelona, Spain

2 Eurac research, Institute for Renewable Energy, Energy Efficiency Buildings – Building envelope technologies, Bolzano, Italy

## Abstract

*Active glazing components, which can dynamically regulate incoming solar radiation, are particularly interesting, as they simultaneously impact multiple aspects, such as thermal and visual comfort and overall energy consumption. Near-infrared EC windows (also referred to as “plasmochromic”) enable selective spectral control of the incoming solar radiation and efficiently respond to ever-changing lighting, heating and cooling requirements. They allow to selectively filter a large amount of near-infrared solar radiation passing through the window, thus blocking solar heat gain during hot summer days and letting it permeate over sunny winter days whilst independently regulating the amount of daylight. This article delves into the core attributes of such glazing systems, showcasing recent advancements in their design and fabrication. By evaluating key metrics like luminous transmittance ( $T_{LUM}$ ), solar transmittance ( $T_{sol}$ ), and total solar heat gain coefficient (g-value), the paper presents a preliminary performance assessment of smart glazing employing this technology. Furthermore, the authors prospect the importance of implementing appropriate control strategies for these systems to fully exploit their potential in reducing energy consumption while maximising comfort.*

## Keywords

*solar control, EC windows, plasmochromic devices, energy efficient glazing*

## DOI

<http://doi.org/10.47982/jfde.2023.2.T3>

# 1 INTRODUCTION

The building sector, accounting for approximately 20% of global primary energy consumption, is projected to see significant growth due to population increase and rising living standards (Cao, Dai, & Liu, 2016). The energy requirements for heating, cooling, and lighting are primary contributors to this consumption. Smart glazing systems have emerged as a pivotal technology to enhance energy efficiency and cost savings.

The “window of the future” is envisioned to transition from a vulnerable point in building design to a multifunctional unit with adaptable properties. These windows should seamlessly integrate into a building’s climate control and lighting systems (Favoino & Overend, 2015). Active glazing components, which can modulate solar radiation, are especially appealing. However, current EC windows cannot selectively filter thermal radiation without impacting luminous transmittance.

In contrast, “plasmochromic” (PLSMC) devices, using transparent plasmonic semiconducting nanocrystals as active EC layers, offer a solution to these limitations (Li, Niklasso, & Granqvist, 2012). These materials, allowing for fine-tuning their optical properties, have been developed and implemented by various research groups (Cao, Zhang, Zhang, & Lee, 2018; Garcia et al., 2011; Tsuboi, Nakamura, & Kobayashi, 2016; Xu et al., 2018). This technology enables the creation of intelligent building skins that can dynamically adjust to external and internal conditions, integrating with an “Internet of Things” (IoT) platform for optimised control.

Our recent research has unveiled the unique solar control features of these systems in the near-infrared (NIR) region that can, in principle, enable an independent modulation of the optical transmittance of a smart window in two distinct spectral ranges, namely VIS and NIR ranges (Barawi et al., 2018; Cots et al., 2021). A PLSMC glazing system, as illustrated in Fig. 1, is laminated on the interior side of the exterior glass. In its open circuit potential (OCP), or “warm state”, the device allows both VIS and NIR radiation into the building. When a low/moderate negative bias is applied, it selectively blocks NIR radiation while maintaining VIS transparency, referred to as the “cold state.” At higher negative potentials, incoming radiation is filtered across the solar spectrum, creating a “dark state” that combines full NIR radiation extinction with intense blue colouring.

The primary aim of this paper is to delve into the design, production, and implementation of plasmochromic modules in smart windows. The article also strives to assess the advanced solar control capabilities these modules offer and to present an analysis of control strategies to optimise their performance. Finally, through comparative analysis, the intention is to position plasmochromic modules against the backdrop of existing shading technologies, highlighting their distinctive advantages.

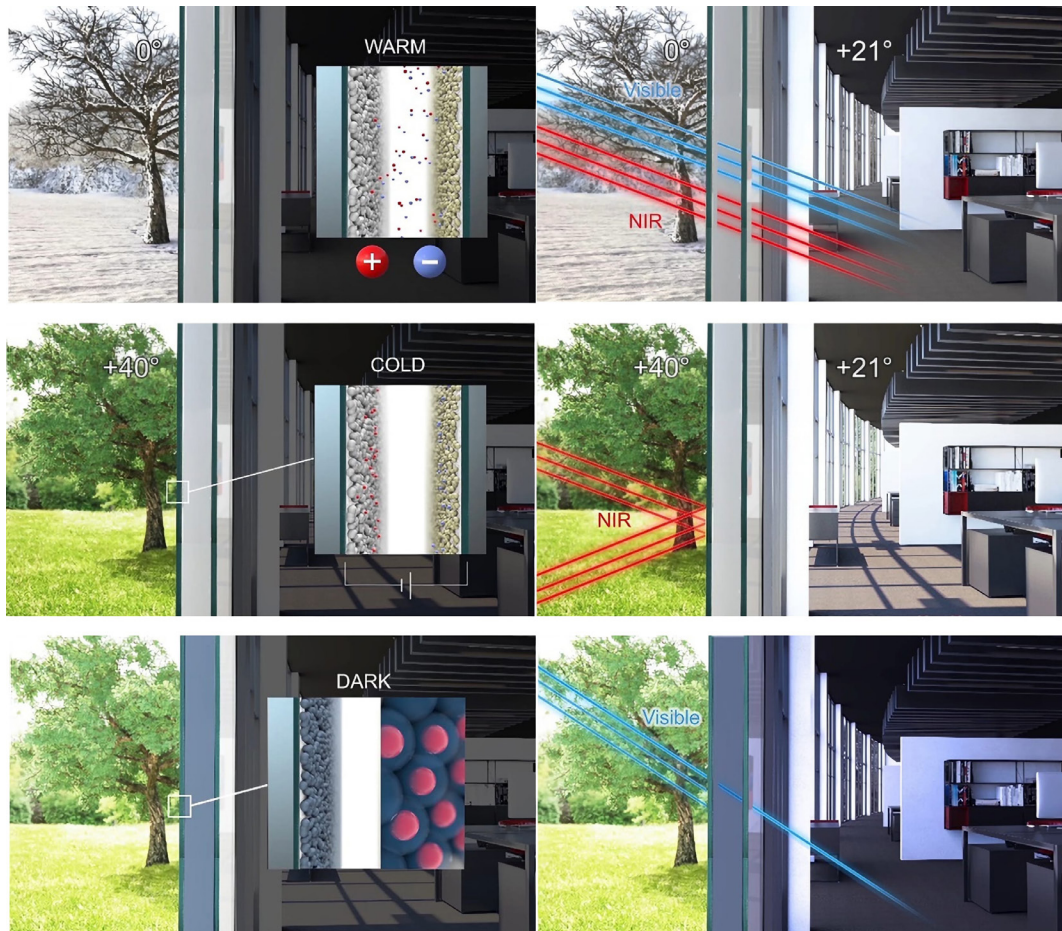


FIG. 1 Functioning schematic of a PLSMC glazing system. (a) In winter, the system allows NIR solar radiation to pass through, acting as a proactive heating mechanism. (b) During mid-season/summer, it can selectively filter out incoming thermal radiation in response to daily changes in sunlight orientation and intensity, blocking up to 95% of NIR radiation, thereby acting as a proactive cooling system. (c) The system also enables independent control of visible sunlight to reduce glare and ensure optimal visual comfort.

## 2 RESEARCH FRAMEWORK AND METHODOLOGY

This investigation focuses on the capabilities of near-infrared electrochromic or plasmochromic windows to dynamically control incoming solar radiation, emphasising their impact on thermal and visual comfort as well as energy consumption. Our research integrates a blend of experimental procedures with computational modelling to not only gauge the PLSMC modules' efficacy under diverse environmental stimuli but also to estimate their influence on the energy performance and internal environment of buildings.

The study unfolds across several methodically organised stages:

- 1 Design and Prototyping:
  - a Development of PLSMC modules initiated with the formulation of specialised inks conducive to a scalable roll-to-roll manufacturing process, optimising aspects such as viscosity and environmental impact of solvents and additives.
  - b Prototypes were then crafted, integrating nanostructured coatings into glazing units while ensuring compatibility with large-scale production and end-use applications.
- 2 Characterisation and Performance Analysis:
  - a Detailed assessment of the optical and thermal properties of the PLSMC modules, examining their performance spectrum across various activation states.
  - b The modules underwent rigorous testing to ascertain key performance metrics, including solar transmittance and luminous transmittance.
- 3 Computational Simulation and Control Strategy Development:
  - a Empirical data from the initial phases were translated into simulation models to predict the behaviour of buildings outfitted with PLSMC smart windows.
  - b Investigation into advanced control algorithms, including Rule-Based Control (RBC) strategies, aimed to optimise the automatic regulation of smart EC glazing systems.
- 4 Integration and Evaluation in Building Context:
  - a Synthesis of the experimental and simulation data facilitated the exploration of PLSMC modules within the context of building integration, considering factors like solar load modulation and visible light transmission.
  - b Comparative analyses were conducted to juxtapose the performance of PLSMC technologies against conventional glazing systems, underscoring the advantages of PLSMC in energy efficiency and occupant comfort.

## 2.1 PLSMC MODULE DEVELOPMENT AND PROTOTYPING

A pivotal issue in the viable industrialisation of this technology consists in the implementation of an “easily-up-scalable” manufacturing process based on roll-to-roll deposition of engineered PLSMC inks. Formulation of the inks includes optimisation of the viscosity, concentration, and environmental impact of solvents and additives. Another key aspect refers to the development of free-standing ion conductive membranes (namely free-standing electrolyte foils) suitable to be laminated at an industrial scale. In general, optimising the architecture and the fabrication procedure of PLSMC modules for large areas remains a major challenge.

PLSMC modules are based on the sandwich-like structure illustrated in Fig. 2. This structure comprises a transparent conductive oxide (TCO) deposited onto a first glass plate, an active PLSMC electrode, a solid ion conductor, a counter-electrode, and another layer of TCO deposited onto a second glass plate.

The manufacturing process consists of four crucial steps, some of which are shown in Fig. 3:

- 1 Ink deposition on transparent conductive glass through serigraphy methodology (both PLSMC and counter electrode inks). In-line drying at 180°C through IR radiation.
- 2 Thermal sintering of the as-deposited films at 450°C.
- 3 Gel electrolyte deposition.
- 4 PLSMC module lamination.

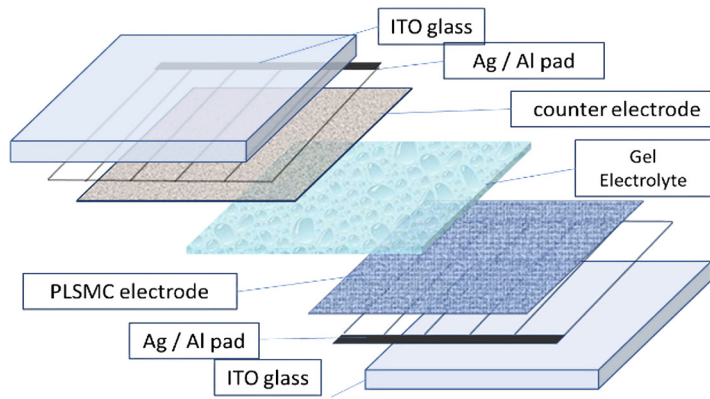


FIG. 2 Schematic illustration of the layers composing a PLSMC module.

Both active and passive nanostructured electrodes have been obtained by screen-printing (and subsequent thermal treatment) of viscous pastes containing engineered metal-oxide (plasmonic) nanocrystals. A configuration employing tungsten oxide and cerium oxide layers, interspersed by a lithium-ion electrolyte, has been implemented. Upon application of an external potential, lithium ions migrate towards the WO<sub>x</sub> layer, inducing an alteration in its crystalline structure. This structural modification directly affects the material's optical properties, particularly its absorption spectra. Concurrently, the cerium oxide layer not only acts as a counter electrode, aiding in the ion migration process, but also contributes to the stability of the system. Importantly, the cerium oxide layer provides memory effects, ensuring the retention of distinct optical stationary states the device can adopt. Reversing the potential causes the lithium ions to depart from the WO<sub>x</sub> matrix, returning the device to its original optical characteristics.

Modules of both 55x45 cm<sup>2</sup> and 70x130 cm<sup>2</sup> have been fabricated by using a semi-automated screen-printing machine (FIG. 3a) equipped with a stainless-steel screen mesh stretched under 20 N m<sup>-1</sup> tension in an aluminium frame. Screen-printed coatings, both the PLSMC active electrode and the counter electrode, have been dried for 15 minutes at 180°C in an IR oven and then subjected to thermal sintering in a ceramic furnace at 450°C with an optimised heating ramp-up. A set of sintered 45x55 cm<sup>2</sup> PLSMC films is shown in Fig. 3b.

The two coated glass panes were then assembled to form the PLSMC sandwich by laminating a UV-curable gel electrolyte cast onto one of two electrodes (Fig. 3b). The sandwich was exposed to UV radiation for 30 minutes (Fig. 3c) and then sealed at the edges with silicone resin that prevents moisture penetration. To reduce the ohmic resistance and improve the current distribution homogeneity, a copper current collector tape was attached to the edges of the TCO-glass panes.

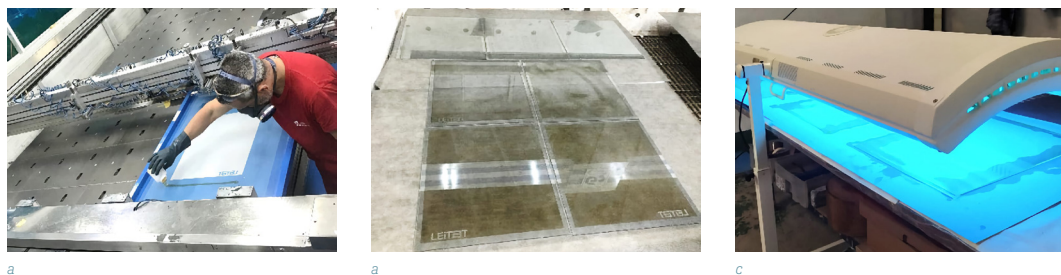


FIG. 3 (a) Semi-automated screen-printing machine. (b) Image of the PLSMC device assembled. (c) UV treatment of the prototype under a 365 nm wavelength light.

A 70x130 cm<sup>2</sup> PLSMC module is shown in Fig. 4, both in the bleached (WARM) and the coloured (DARK) state. Challenges have been identified in fabricating PLSMC modules exceeding dimensions of 70x130 cm<sup>2</sup>. The primary concerns revolve around issues such as paste non-uniformity and inconsistencies in electrolyte deposition. Given that the technology is still in its developmental stages, with a current Technology Readiness Level (TRL) of 5, certain hurdles remain unaddressed.



FIG. 4 70x130 cm<sup>2</sup> PLSMC module respectively in the a) WARM and b) DARK state.

## 2.2 MODELLING OF A PLSMC IGU

The comprehensive performance evaluation of a glazing system heavily relies on the measurement of key parameters as well as the solar heat gain coefficient ( $g$ -value), the total visible transmittance ( $T_{LUM}$ ), the total solar transmittance ( $T_{SOL}$ ), and the thermal transmittance ( $U$ -value). These numbers have been obtained from the experimental transmittance and reflectance spectra of PLSMC devices, which have been properly processed with Optics (Optics, n.d.).

The insulating glass configuration selected for this study consists of a double-glazing unit (DGU) where the PLSMC module is laminated on the inner side of the exterior glass plate. Clear float glass has been chosen for both the exterior and interior glass to fully exploit the prerogatives of the PLSMC technology in the WARM state.

The thickness and type of the IGU typically depend on the application and associated insulating glass materials, which comprise metallic spacer, desiccant, sealants, laminating interlayer materials, and wiring. We have opted for a 31mm-thick IGU that embeds a low-emissive coating applied to the inner side of the interior glass and a 16 mm cavity filled with a mixture of argon (90%) and air (10%). See Fig. 5.

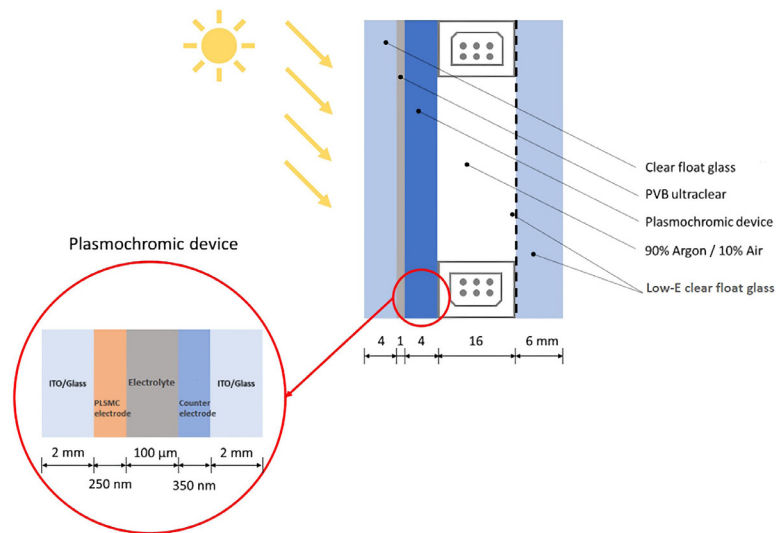


FIG. 5 Longitudinal section of a PLSMC DGU with a close-up section of the PLSMC device integrated in the DGU.

These properties have been calculated by means of the software tools Optics (Optics, n.d.) and WINDOW (WINDOW, n.d.) according to the formulas defined by ISO EN 410 (Standardization, ISO EN 410:1998. Glass in building. Determination of luminous and solar characteristics of glazing., 1998) and ISO EN 673 (Standardization, ISO EN 673:1997. Glass in building. Determination of thermal transmittance (U-value) - Calculation method., 2011):

$$T_{LUM} = \frac{\int_{380nm}^{780nm} D_{\lambda} V(\lambda) T(\lambda) d\lambda}{\int_{380nm}^{780nm} D_{\lambda} V(\lambda) d\lambda} \quad [-]$$

$$T_{SOL} = \frac{\int_{300nm}^{2500nm} I_{AM\ 1.5,\lambda} T(\lambda) d\lambda}{\int_{300nm}^{2500nm} I_{AM\ 1.5,\lambda} d\lambda} \quad [-]$$

$$g - value = T_{SOL} + q_i \quad [-]$$

$$U - value = \left( \frac{1}{h_e} + \sum R_i + \sum \frac{s}{\lambda} + \frac{1}{h_i} \right)^{-1} \quad [W \cdot m^{-2} \cdot K^{-1}]$$

In formula (1),  $D$  denotes the relative spectral distribution of illuminant D65,  $V(\lambda)$  is the spectral luminous efficiency for photopic vision, which defines the standard observer for photometry, and  $T(\lambda)$  is the transmission value at a certain wavelength.  $\lambda$  represents the radiation wavelength in nm. In formula (2),  $I_{AM\ 1.5}$  stands for the relative spectral distribution of solar radiation at 1.5 Air Mass. In formula (3),  $q_i$  represents secondary internal heat transfer towards the inside, accounting for the temperature difference between glass panes and the indoor environment. Formula (4) defines the U-value. Here,  $h_i$  and  $h_e$  are the internal and external surface heat transfer coefficients, respectively,  $R_i$  represents the thermal resistance of the  $i$ -layer,  $s$  refers to the thickness, and  $\lambda$  denotes thermal conductivity.

To provide a realistic estimation of the most relevant thermal and optical properties of the PLSMC IGU, a set of commercially available glazing and shading solutions have been taken as benchmarks, namely:

- SageGlass SR2.0, an EC glass incorporated in a DGU with an internal low-E coating for dynamic control of light and heat transmission.
- Hella AR92S, a DGU with an internal low-E coating and an external blind, enabling flexible control over solar heat gain and light transmission.
- Pellini V95, triple glazing unit (TGU) featuring internal blinds and an internal low-E coating, offering superior thermal insulation and seamless control of light and privacy.

### 3 RULE-BASED CONTROL STRATEGIES FOR SMART GLAZING SYSTEMS

The potentialities of dynamic glazing with extended solar control properties are evident even to the most sceptical observers. However, the effectiveness of smart EC glazing systems strongly depends on their automatic regulation functionalities, underscoring the importance of adopting advanced control strategies to fully harness their potential.

Rule-Based Control (RBC) strategies are the most frequently utilised control algorithms for managing active glazing systems. These strategies are designed to trigger specific control actions when certain conditions are met. The most common driving variables used nowadays in RBC-based strategies include indoor temperature, outdoor temperature, solar radiation, illuminance, heating or cooling requirements, and occupancy levels.

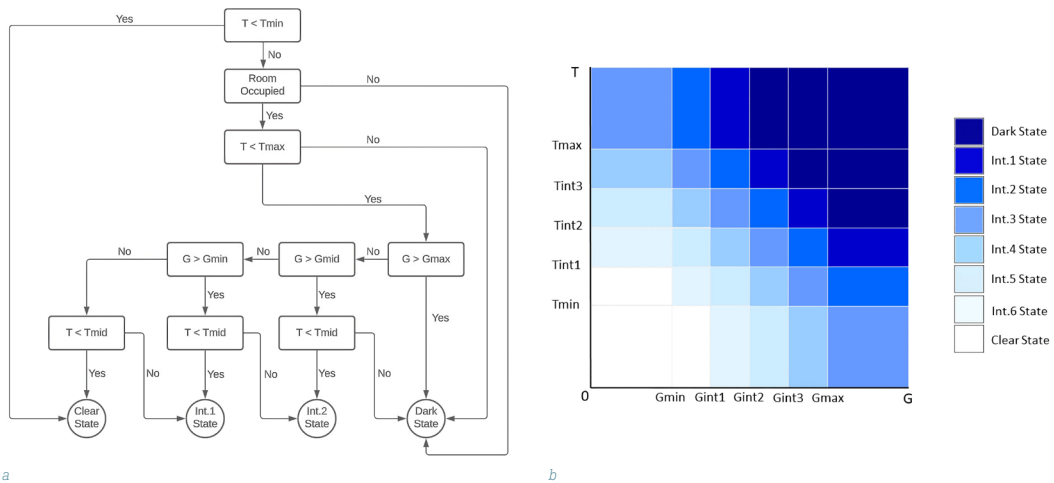


FIG. 6 (a) Flowchart of an RBC strategy based on internal air temperature (T) and incident solar irradiance on the window (G) made up of  $T_{min}$ ,  $T_{mid}$  and  $T_{max}$  as indoor temperature thresholds, and  $G_{min}$ ,  $G_{mid}$ ,  $G_{max}$  as incident solar irradiance thresholds. (b) Cartesian representation of the same type of algorithm, using indoor temperature ( $T_{min}$ ,  $T_{int1}$ ,  $T_{int2}$ ,  $T_{int3}$ ,  $T_{max}$ ) and incident solar irradiance ( $G_{min}$ ,  $G_{int1}$ ,  $G_{int2}$ ,  $G_{int3}$ ,  $G_{max}$ ) thresholds.

An example of an RBC approach that may fit properly with the functional features of the PLSMC windows is depicted in the flowchart in Fig. 6a, which is based on the sequential consideration of three main variables: occupancy state, indoor temperature (T), and incident solar irradiance (G) (Roberts, De Michele, Pernigotto, Gasparella, & Avesani, 2022).

Based on the definition of n threshold values for indoor temperature T and incident solar irradiance G (in addition to the occupancy state), this algorithm can select and implement a number of discrete

states of the EC glazing to maximize both visual and thermal comfort. In Fig. 6b, the possible window's states are represented in the T vs G plane, where various regions are demarcated by the respective colour indicative of the EC state.

This control strategy may fit very well with the extended solar control prerogatives of PLSMC glazing, as its spectral selectivity would enable a finer balance between the (often competitive) needs for natural light and optimal indoor temperature. This key advantage of PLSMC systems with respect to "traditional" EC ones can be exploited with an advanced RBC algorithm capable of independently regulating  $T_{LUM}$  and the g-value. In Fig. 7, it is schematically represented as the combination of two 1-dimensional grids responding respectively to changes of G (horizontal tuning of  $T_{LUM}$ ) and T (vertical tuning of g-value). As red gets more intense, the g-value of the PLSMC glazing gets lower (Fig. 7a). As blue gets more intense,  $T_{LUM}$  of the PLSMC glazing gets lower (Fig. 7b). The combination of two algorithms results in a comprehensive RBC strategy encompassing 36 distinct optical states (in comparison to the 8 states available with a "traditional" EC system) identified by a unique combination of  $T_{LUM}$  and g-value (see Fig. 7c).

This approach may, in principle, be able to account for seasonal variations in sunlight intensity and angle, as well as daily weather changes. For example, on a hot summer day with high solar irradiance, the system might trigger a state that reduces solar heat gain while maintaining adequate daylight. Conversely, on a cold but sunny winter day, it might allow for more solar heat gain while controlling the brightness levels.

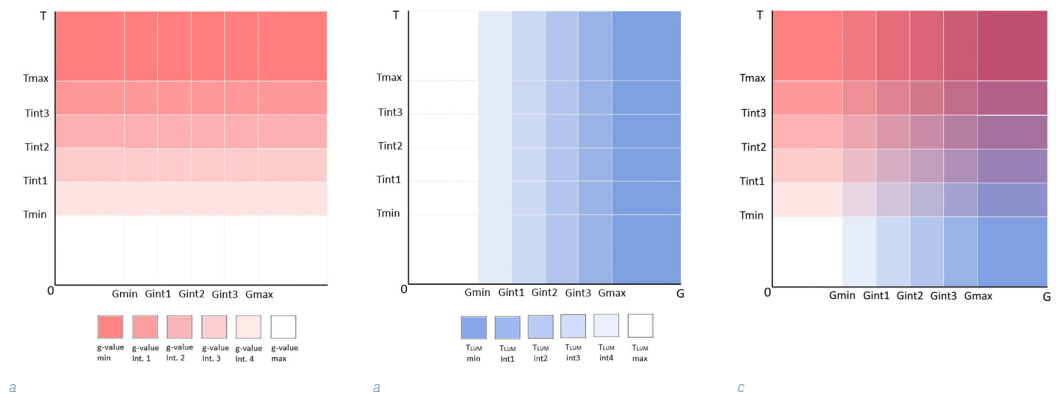


FIG. 7 (a) and (b) illustrate two complementary RBC algorithms optimized for PLSMC technology. The figures, using colour intensity scales, demonstrate how the algorithms modulate near Infrared and visible light transmittance based on varying indoor temperature and irradiance conditions. These algorithms use both the same indoor temperature (T<sub>min</sub>, T<sub>int1</sub>, T<sub>int2</sub>, T<sub>int3</sub>, T<sub>max</sub>) and incident solar irradiance (G<sub>min</sub>, G<sub>int1</sub>, G<sub>int2</sub>, G<sub>int3</sub>, G<sub>max</sub>) thresholds. In figure (c), the combination of the previous two algorithms led to a 36 states, with high thermal and visible modulation capability.

Nevertheless, the effects of incoming solar radiation on the indoor environment can be both immediate and long-lasting, as it heats the thermal mass and air within the space. Sophisticated control strategies can leverage these interconnected impacts, for instance, by adjusting solar gains in the short term to address immediate effects on occupant thermal and visual comfort while managing the building's thermal mass to optimise energy demand under comfort constraints. This aim can be realised by employing a control strategy that considers the building's thermal response to changes in input variables while effectively managing competing objectives. Among these strategies, Model Predictive Control (MPC) stands out for its capability to predict dynamic system response and calculate the optimal sequence of future inputs to minimize a specific cost function.

Isaia et al. have recently developed an innovative and efficient MPC (Isaia, Fiorentini, Serra, & Capozzoli, 2021), demonstrating its effectiveness in managing EC windows. This method successfully considers both continuous and discrete variables, resolving conflicting requirements and outperforming traditional rule-based controllers in key areas such as energy consumption, peak power, and discomfort hours.

An advanced MPC strategy may, in principle, further optimise the performances of PLSMC glazing. Depending on the priority, the controller can focus more on energy conservation or on maintaining indoor temperature for visual comfort, achieving a balance between these two objectives.

The performance of this MPC is largely determined by its specific configuration. For instance, prioritizing the heating/cooling system in the setup leads the controller to focus more on energy conservation. In contrast, when maintaining indoor temperature is given higher importance, the controller puts more effort into keeping optimal comfort levels instead of simply maximizing energy savings.

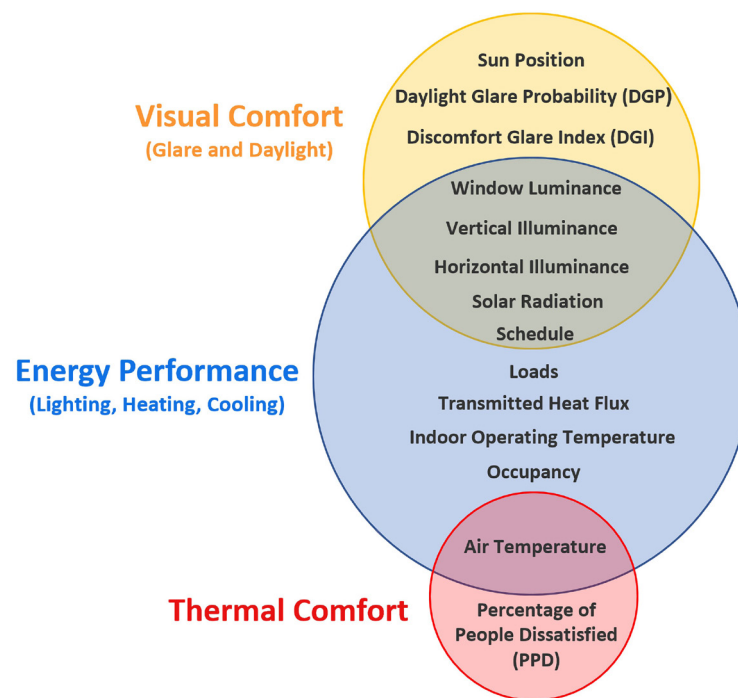


FIG. 8 Schematic representation of the main performance parameters, sensors and variables involved in optimizing energy and comfort conditions within a built environment.

Fig. 8 comprehensively illustrates the variables involved in optimising energy and comfort performances within a built environment. For instance, in terms of visual comfort, the MPC considers several factors such as the sun's position, Daylight Glare Probability (DGP), Discomfort Glare Index (DGI), window luminance, and solar radiation. It also takes into account changes over time, such as the shifting position of the sun and seasonal variations in daylight availability.

Thermal comfort is another crucial aspect, with key indicators like the temperature of the inner glass surface and the Percentage of People Dissatisfied (PPD). These factors demand a sophisticated understanding of the building's thermal characteristics and the ability to anticipate and respond to changes in the external environment and occupant behaviour.

For energy performance, a wide range of variables are considered, such as window luminance, solar radiation, transmitted heat flux, loads, indoor operating temperature, occupancy, and air temperature. The MPC must be designed to adapt dynamically to changing conditions and demands to optimise the energy efficiency of the building.

The possibility to adjust light and heat transmittance independently allows for a greater degree of control in balancing the multiple dimensions of building performance. This feature aligns seamlessly with an MPC's ability to dynamically adapt and manage a wide range of variables. The synergy between PLSMC technology and an advanced MPC system can definitively provide a uniquely adaptable solution to the multidimensional challenge of optimizing building performances.

While advanced control strategies like Rule-Based Control harness the potential of dynamic glazing systems, the research presented in Section 4 delves deeper into the optical and thermal features of the PLSMC and the implications for building performance.

## 4 PERFORMANCE OUTCOMES AND DATA ANALYSIS

Emerging from the foundational research on plasmochromic materials, we now turn our attention to their practical application within Insulated Glazing Units. Their energy efficiency and potential to enhance occupant comfort are scrutinised, drawing direct comparisons with conventional glazing systems prevalent in sustainable building design.

### 4.1 OPTICAL AND THERMAL CHARACTERISATION OF PLSMC MODULES

The transmittance spectra of PLSMC modules at different optical states (corresponding to specific values of a bias voltage applied between the PLSMC electrode and counter electrode) are reported in Fig. 9c. The high transparency these modules showcase over the entire solar spectral range when in the initial bleached (OFF) state must be remarked. In this state, the solar transmittance ( $T_{\text{sol}}$ ) and luminous transmittance ( $T_{\text{LUM}}$ ) values register at an impressive 79% and 75%, respectively, revealing the module's substantial transmissive capabilities.

Upon applying moderate bias potentials, a progressive attenuation of the optical transmittance within the NIR region begins to emerge. This perceptible change evolves until it eventually culminates in a complete extinction of incident solar radiation within the range of 780 to 1600 nm (this corresponds to  $T_{\text{NIR}}$  values of less than 1%). This intriguing occurrence of NIR light shielding is contrastingly paired with a modest decline in visible transmittance, maintaining  $T_{\text{LUM}}$  values greater than 46% even for applied biases of less than -1.5 V.

However, as the voltages decrease further, there is a noticeable impact on  $T_{\text{LUM}}$ , which also begins to decline. This leads to the glass acquiring a characteristic deep blue hue. The emergence of this scattering phenomenon is intrinsically linked with the appearance of a powerful optical extinction band, which subsequently causes an increase in the reflectance within the NIR range. Pushing the bias to its maximum sustainable potential, approximately -2.7 V, results in a steep drop in  $T_{\text{LUM}}$  values to below 5%, which transpires around 15 minutes from the initial bleaching state.

This decrease in optical contrast is primarily driven by a blue shift of the absorption band, thereby causing a dominant blue tone. This is a characteristic property of significantly reduced tungsten oxide. However, its spectral response is not entirely aligned with the human eye's response (approximately 400 to 700 nm). This mismatch presents a considerable limitation for the luminous transmittance (TLUM) and, hence, inevitably affects the value of the ratio of luminous to solar transmittance (TLUM/TSOL).

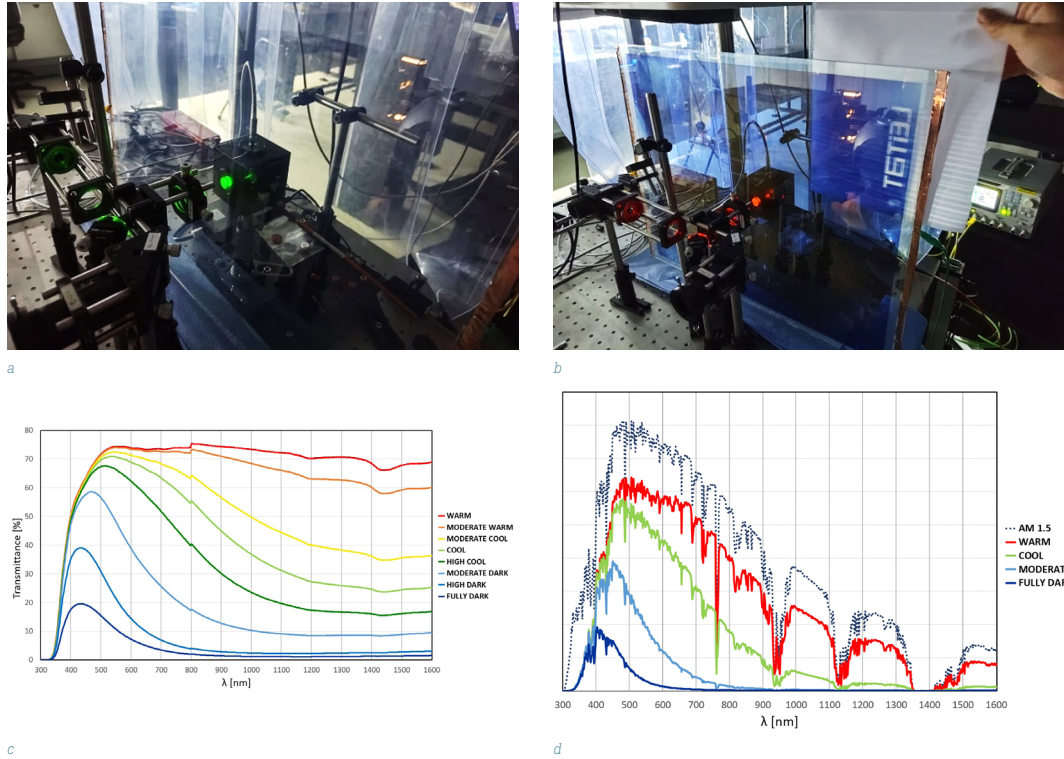


FIG. 9 a,b) The set-up adopted to measure the transmittance spectra of PLSMC modules. c) Transmittance spectra and d) solar irradiance spectra at different applied voltages to the PLSMC device.

The most meaningful features of the above presented PLSMC modules – namely the dynamic range of optical modulation both in the VIS ( $T_{LUM}$ ) and NIR ( $T_{NIR}$ ) – and the corresponding colouring and bleaching time (namely  $t_c$  and  $t_b$ ) are summarised in TABLE 1.

TABLE 1 Main parameters and properties of a PLSMC module

INFINITE PLSMC modules	
PLSMC IGU size	Not integrated into IGU
	$3\% < T_{LUM} < 75\%$ (EN 410)
	$5\% < T_{NIR} < 79\%$ (EN 410)
Maximum Optical Modulation	$2\% < T_{SOL} < 79\%$ (EN 410)
Spectral Selectivity	$T_{LUM}/T_{SOL}$ (in cool mode) $> 1.5$
Switching Speed	$t_{col}@600nm < 10$ min / $t_{bleach}@600nm < 15$ min
	$t_{col}@1500nm < 3$ min / $t_{bleach}@1500nm < 25$ min
SHGC (dynamic range)	To be measured upon integration in IGU
Abs. Power Density	$< 300$ mW/m <sup>2</sup>
Electrochemical Stability	$> 1000$ colouring/bleaching cycles @ RT
Thermal Stability	$> 500$ cycles @ 85°C & 40% RH

To illustrate this effect, we conducted a comprehensive examination, presenting a semi-quantitative analysis of the reversible temperature modulation observed on the PLSMC glass surface, as well as on a black surface situated directly behind it, as depicted in Fig. 10. In this experimental series, a VarioCAM® HR InfraTec camera was employed to capture a series of infra-red images of the device under varying bias and exposure conditions. A representative depiction of the experimental setup is provided in Fig. 10. The IRBIS 2.2 software, supplied by InfraTec, was utilised for editing the acquired IR images.

The experiment involved a 12x12 cm<sup>2</sup> device, which was subjected to sunlight radiation via a solar simulator, with a light source casting a nominal intensity of one sun on an AM1.5 filter. The device then underwent exposure to the previously mentioned bias voltages. The observable outcomes reveal that, after an exposure period of 40 minutes at the OCP with  $T_{LUM} = 75\%$  and  $T_{SOL} = 79\%$ , there is a notable increase in temperature on the top surface by approximately 7°C, changing from 26°C to 33°C. Simultaneously, the surface of the background black paper registered a temperature surpassing 40°C.

Following this, the experimental setup underwent a cooling process back to Room Temperature (RT), and the device was then shifted into a NIR-blocking state, with  $T_{LUM} = 54\%$  and  $T_{SOL} = 34\%$  at -1.5V. The temperature measurement procedure was then repeated, as seen in Fig. 10e-h. Under these conditions, the temperature recorded behind the glass did not rise above 38°C, while the top of the glass registered a temperature of 35°C.

At a lower bias potential, specifically at -2.7V, the black surface appeared almost completely protected by the PLSMC device in its fully absorbing state, with  $T_{SOL}$  dropping below 2%. The surface temperature of this black surface was only marginally higher than the surrounding unexposed environment, as illustrated in Fig. 10i-l. After a 40-minute exposure period at 1sun, the PLSMC device itself reached a temperature of 42°C.

In comparison with commercially available EC glazing, the devices presented in this study demonstrate considerable advantages, showcasing an expansive modulation of the overall solar radiation ( $\Delta T_{SOL} = 77\%$ ). They exhibit high visible light transmission in the bleached state ( $T_{LUM} = 75\%$  at OCP), coupled with strong optical contrast ( $\Delta T_{LUM} = 72\%$  between OCP and -2.7 V). These parameters indicate a robust performance across various spectrums and voltage conditions. However, a unique distinction is worth noting. Typically, for EC devices, a reduction in  $T_{LUM}$  corresponds to a proportionate decrease in  $T_{NIR}$ , and consequently in  $T_{SOL}$ , across the entire control range. In contrast, PLSMC systems at low to moderate bias potentials provide the ability to substantially lower  $T_{SOL}$  by about 40% while still retaining a  $T_{LUM}$  value above 50%.

It is crucial to emphasise that these data should only be applied to carry out a meaningful quantitative analysis when considering the precise set of experimental conditions under which they were acquired. These conditions include specific characteristics of the light source (a 150 W xenon short arc lamp was used for this experiment), the distance between the lamp and the glass (approximately 15 cm in this case), the ventilation conditions, the emissivity of the thermocamera, and several other factors.

This unique attribute can be strategically exploited to optimise energy consumption in buildings and enhance both thermal and daylight comfort levels. For instance, in climates dominated by cooling requirements, the considerable reduction in solar thermal radiation entering the glazing can help decrease energy usage without significant compromise to the transparency of the glass.

This feature thus has the potential to mitigate overheating problems while minimally impacting daylight infiltration. Conversely, during the heating season or in climates primarily requiring heating, PLSMC devices can be adjusted to allow higher levels of solar energy transmission. This is achievable because a high  $T_{LUM}$  can be maintained, which can effectively offset a substantial portion of the building's heating energy requirements. As such, PLSMC devices serve as a versatile solution, catering to varying energy needs across diverse climatic conditions.

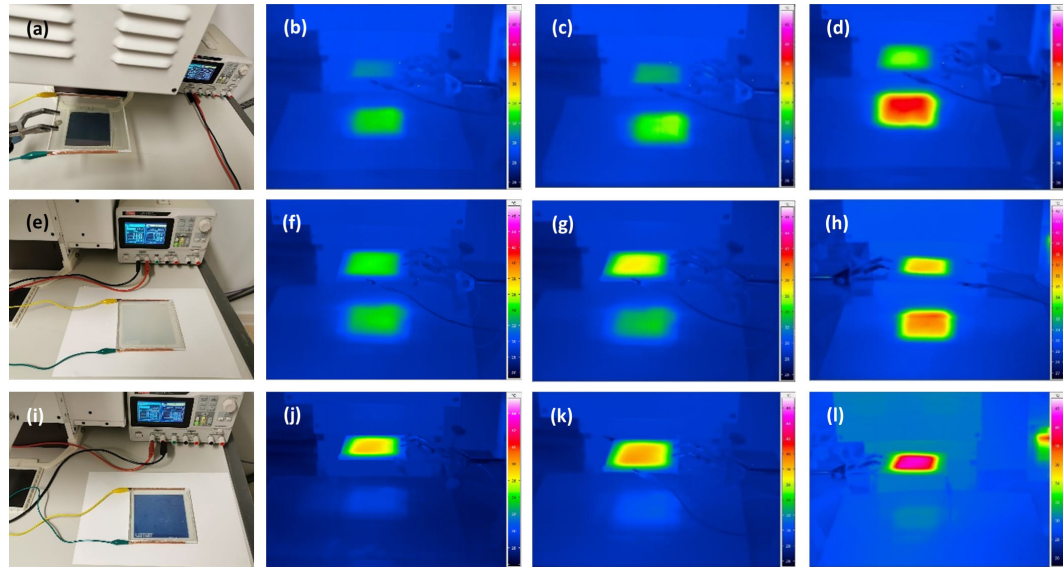


FIG. 10 Thermo-camera pictures of a PLSMC device exposed to sunlight radiation. (a) Initial picture of the setup before turning on the solar simulator; (c-d) changes observed until reaching 40 min of solar irradiation. (e) Picture of the device after 40 min at an applied potential of  $-1.5V$  and the corresponding IR-images (f-h) during 40 min of continuous illumination. Finally, (i) picture taken at  $-2.7V$  after 40 min under solar light exposure and (j-l) its IR-images (Cots, et al., 2021).

Nevertheless, to comply with the requirements of some extreme building façade operative conditions (Poláková, Schäfer, & Elstner, 2018), a marketable EC technology should guarantee adequate thermal and electrochemical stability. PLSMC modules have been tested in a CTS climatic chamber (Mod. CL-30/1000-BF+) by running a series of colouring/bleaching cycles at  $85^{\circ}C$ . The I-t curve (collected by an SP-150 Potentiostat/Galvanostat) is shown in Fig. 11b. The data reveal that no significant reduction in the galvanostatic current occurred over the first 500 cycles, as attested by the WARM and DARK transmittance spectra measured (again) upon the thermal ageing test.

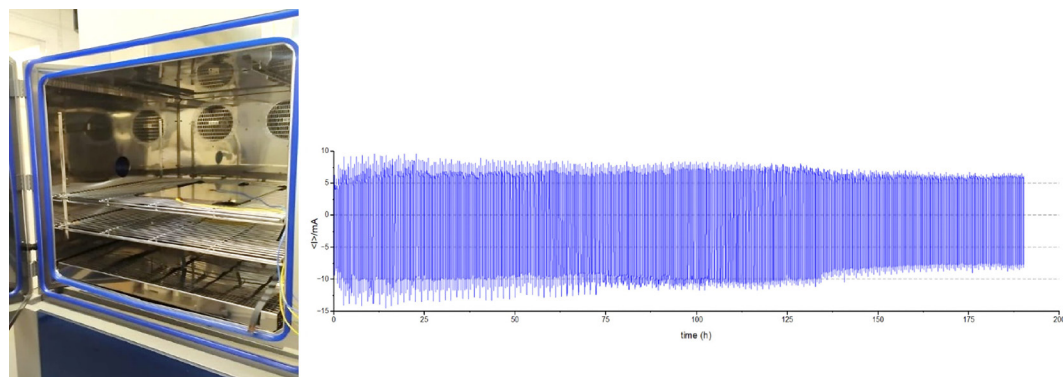


FIG. 11 (a) Climatic chamber used for the thermal ageing test of the PLSMC devices. (b) Variation of the electric current measured over 200 hours (about 500 cycles) under cycling a  $45 \times 55 \text{cm}^2$  PLSMC device at  $85^{\circ}C$  and 40% RH.

A good compromise between EC performance and environmental stability can be claimed. However, it is pertinent to note that achieving this balance will necessitate additional industry-driven design optimisation efforts. These efforts will be crucial in ensuring that the PLSMC modules adhere to both technical standards and international norms.



FIG. 12 (a), (b) and (c) are photos of the 45x50 cm<sup>2</sup> PLSMC prototype module realized in the frame of the INFINITE project. (d) Represent a schematic drawing of the demonstrator embedding an ad-hoc implemented control circuit.

While the experimental observations demonstrate the capabilities of the PLSMC devices, Section 4.2 delves deeper into the design and benchmarking of an efficient PLSMC IGU, highlighting its potential advantages in building envelopes compared to commercial alternatives.

## 4.2 DESIGN OF AN EFFICIENT PLSMC IGU AND COMPARISON WITH BENCHMARK TECHNOLOGIES

The energy-saving potential of PLSMC modules can be fully exploited in a building envelope only if they are integrated into a well-designed IGU, which must also account for a low thermal transmittance (U-value), typically within the range of 1.0 to 1.4 W/m<sup>2</sup>K for a well-designed DGU. To this purpose, the appropriate choice of glass panes, interlayer coatings, and cavity gas is of crucial importance. In particular, the proper choice of a low-E coating permits increasing the modulation range of the g-value and maximises the peculiar benefits of the PLSMC system in terms of energy saving and visual/thermal comfort.

As mentioned before in paragraph 2.2 and represented in Fig. 5, the PLSMC DGU considered and modelled in this article presents a layer structure made of clear float glass, a PVB interlayer, the PLSMC device, a 16 mm air gap with a gas mixture made of 90% Argon and 10% air, and a Low-E clear float glass ( $\epsilon = 0.04$ ).

The KPIs of this DGU have been compared with those of three benchmark DGUs chosen based on their common usage in contemporary architecture and their distinctive features.

The first benchmark is an EC DGU made with commercial EC glass, specifically SageGlass Classic SR2.0, and it has an internal low-E coating ( $\epsilon = 0.04$ ) that reduces the amount of UV and IR light that can pass through the glass without compromising the amount of visible light transmission. This combination of EC technology and low-E coating allows for dynamic control of light and heat transmission.

The second benchmark is a DGU with an internal low-E coating and an external blind, specifically the Hella AR92S blind. This system represents a more traditional approach to managing solar heat gain and light transmission, combining the energy-efficient properties of low-E glass with the flexibility of external blinds.

Finally, the third benchmark is a triple glazing unit (TGU) with an internal low-E coating and internal blinds, specifically the Pellini V95. Triple glazing offers superior thermal insulation compared to double glazing, making it a popular choice for high-performance buildings in colder climates. Pellini V95 blinds are integrated into the window system, allowing for seamless control of light and privacy without affecting the window's thermal performance.

By comparing the performance of the PLSMC-based DGU with these benchmarks, the study aimed to understand how this novel technology stacks up against existing solutions in terms of thermal comfort, visual comfort, and energy efficiency. TABLE 2 summarises the most meaningful characteristics of the selected benchmarks together with one of the PLSMC DGU.

TABLE 2 Thermal and optical features of the PLSMC DGU and of three commercial glazing systems

IGU	STATE	U-value	g-value	T <sub>LUM</sub>	T <sub>SOL</sub>
		[W/m <sup>2</sup> K]			
<b>PLSMC (DGU)</b> Clear float Glass 6mm / PVB/ PLSMC device/16mm 90% Argon, 10% Air/ Low-E clear float glass 6mm	WARM	1.2	0.64	0.73	0.52
	MODERATE WARM		0.54	0.71	0.45
	MODERATE COOL		0.40	0.64	0.31
	COOL		0.32	0.56	0.23
	HIGH COOL		0.24	0.43	0.16
	MODERATE DARK		0.17	0.28	0.11
	HIGH DARK		0.12	0.17	0.09
	FULLY DARK		0.07	0.03	0.02
<b>SAGEGLASS EC (DGU)</b> SageGlass SR2.0 9mm/ 16mm 90% Argon, 10% Air/ Low-E clear float glass 6mm	BLEACHED	1.2	0.40	0.57	0.33
	TINTED 1		0.22	0.34	0.16
	TINTED 2		0.14	0.20	0.08
	TINTED 3		0.09	0.05	0.02
	FULLY TINTED		0.08	0.01	0.05
<b>HELLA AR92S (DGU)</b> Hella AR92S/ Clear float glass/ 16mm 90% Argon, 10% Air/ Low-E clear float glass 6mm	TILT 0 °	1.2	0.63	0.73	0.52
	TILT 55 °		0.08	0.06	0.04
	TILT 90 °		0.02	0.00	0.00
<b>PELLINI V95 (TGU)</b> Clear float glass 6mm/ Pellini V95/ Clear float glass 6mm/ 14mm 90% Argon, 10% Air/ Low-E clear float glass 6mm	TILT 0 °	0.7	0.53	0.68	0.45
	TILT 55 °		0.17	0.18	0.04
	TILT 90 °		0.02	0.00	0.00

The data detailed in the table has been subjected to a thorough analysis; Fig. 13 presents the results in a plot of  $g$ -value versus  $T_{LUM}$ . This approach to data representation facilitates a more intuitive comparison of the various technologies under consideration. The  $g$ -value vs  $T_{LUM}$  plot serves as a tool to provide a visual representation of how each technology allows for the transmission of light ( $T_{LUM}$ ) and heat ( $g$ -value), which are both critical factors in determining the overall performance of a window system. The horizontal axis of the plot represents the  $g$ -value, an important measure of a window's ability to transmit solar energy and, hence, contribute to the heating of a space. The vertical axis, on the other hand, represents  $T_{LUM}$ , the percentage of visible light that passes through a window system.

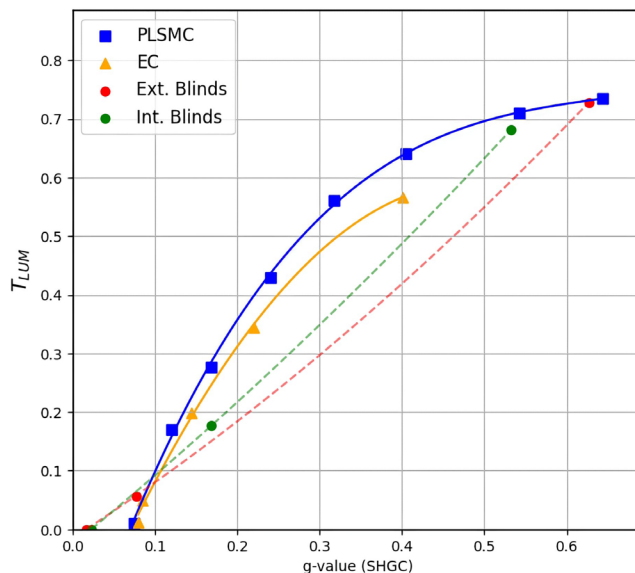


FIG. 13  $T_{LUM}$  vs  $g$ -factor (SHGC) curves for the glazing and shading technologies considered.

These data reveal that the integration of PLSMC technology into a correctly designed IGU may turn in the considerable improvements over some of the existing advanced shading systems taken as benchmarks shown in TABLE 3:

TABLE 3 Characteristics and benefits of PLSMC DGUs in comparison to the selected benchmarks

Features/Advantages	Description
<b>Wide Modulation Capability</b>	PLSMC DGUs have a $\Delta g$ of 0.57, with over 0.30 in visible transmission above $T_{LUM} > 60\%$ , reducing solar loads and balancing cooling with daylight. In cold climates, the wide $\Delta g$ enhances solar heat on sunny days.
<b>Optical Contrast in VIS Range</b>	PLSMC DGU's $T_{LUM}$ ranges from 0.73 to 0.03, ensuring ample daylight in buildings with a low $g$ -value and options down to 3% $T_{LUM}$ for visual comfort.
<b>Flexibility Over Benchmarks</b>	Compared to Pellini internal blinds and Hella external blinds, PLSMC boasts greater flexibility, offering precise control over light modulation and dynamic adjustment of light transmittance and $g$ -value.
<b>Overall Benefits of PLSMC DGU</b>	The technology enhances $g$ -value modulation and solar gain across climates, impacting energy and thermal comfort. Its luminous transmittance is on par with blind benchmarks, ensuring better visual comfort.

To summarise, the advantages of the PLSMC DGU with respect to the chosen benchmarks are a wider modulation capability of the  $g$ -value, which improves the possibility of using this glazing as a solar gain modulator, useful both in heating and cooling-dominated climates and with a direct effect on energy needs and thermal comfort; a large luminous transmittance range, even comparable to the benchmarks with blinds, which ultimately allows the PLSMC DGU to guarantee better levels of visual comfort. Moreover, the peculiar shape in the  $T_{LUM}$ - $g$  plot suggests an interesting potential in managing high  $g$ -values while not compromising  $T_{LUM}$  (useful in heating periods, where solar gains are a plus and the possibility of maintaining high transmittances is appreciated for visual purposes).

## 5 CONCLUSIONS & PERSPECTIVES

We have been working on the development of EC glazing with extended control functionalities in the NIR region. In this paper, we presented the most recent achievements and prospected their competitive advantages with respect to analogous commercial solutions. IGUs integrating PLSMC technology have indeed great potential in terms of the capability to modulate solar loads and visible light beyond what is currently achievable with full solid-state EC devices. They ultimately impact the total building energy use (lighting, cooling, and heating) and the occupant comfort (visual comfort, in terms of daylight availability and perceived glare discomfort, and thermal comfort).

Future efforts will focus on enhancing PLSMC materials and module design. Spectral selectivity can be improved using alternative electro-active materials that align with the photopic human eye normalisation spectrum. The visible blue appearance in the "DARK state" can be adjusted for better colour neutrality. The next steps will assess this potential and aim to optimise control, reducing building energy use, and occupant discomfort. Separating the NIR and VIS ranges facilitates superior control strategies, a concept unexplored thus far. Past adaptive glazing system designs balanced thermal and visual domains. This separation invites new control strategies that consider these aspects independently, simplifying the controller and improving indoor environment influence. The insights derived from this process were not only informative but also invaluable for shaping the future trajectory of PLSMC technology in the field of modern building design.

### Acknowledgements

---

This publication was funded by the European Union from the European Union's Horizon Europe Research and Innovation Programme under Grant Agreement No 958397, INFINITE. Views and opinions expressed are however those of the author(s) only and do not necessarily reflect those of the European Union. Neither the European Union nor the granting authority can be held responsible for them.

This work was partially supported by the Spanish Ministry for Science and Innovation (MICINN) through the "Ramon y Cajal" grant awarded to Dr. Michele Manca (ref. RYC2018-024399-I).

## References

---

- Barawi, M., Veramonti, G., Epifani, M., Giannuzzi, R., Sibillano, T., Giannini, C., . . . Manca, M. (2018). A dual band electrochromic device switchable across four distinct optical modes. *Journal of Materials Chemistry A*, *6*, 10201–10205. Retrieved from <https://doi.org/10.1039/C8TA02636J>
- Cao, S., Zhang, S., Zhang, T., & Lee, J. Y. (2018). Fluoride-Assisted Synthesis of Plasmonic Colloidal Ta-Doped TiO<sub>2</sub> Nanocrystals for Near-Infrared and Visible-Light Selective Electrochromic Modulation. *Chemistry of Materials*, *30*, 4838–4846. Retrieved from <https://doi.org/10.1021/acs.chemmater.8b02196>
- Cao, X., Dai, X., & Liu, J. (2016). Building energy-consumption status worldwide and the state-of-the art technologies for zero-energy buildings during the past decade. *Energy and Buildings*, *128*, 198–213. Retrieved from <https://doi.org/10.1016/j.enbuild.2016.06.089>
- Cots, A., Dicorato, S., Giovannini, L., Favoino, F., & Manca, M. (2021). Energy Efficient Smart Plasmochromic Windows: Properties, Manufacturing and Integration in Insulating Glazing. *Nano Energy*, *84*, 105894. Retrieved from <https://doi.org/10.1016/j.nanoen.2021.105894>
- Danza, L., Barozzi, B., Bellazzi, A., Belussi, L., Devitofrancesco, A., Ghellere, M., . . . Scrosati, C. (2020). A weighting procedure to analyse the Indoor Environmental Quality of a Zero-Energy Building. *Building and Environment*, 107155. Retrieved from <https://doi.org/10.1016/j.buildenv.2020.107155>
- Favoino, F., & Overend, M. (2015). A Simulation Framework for the Evaluation of Next Generation Responsive Building Envelope Technologies. *Energy Procedia*, *78*, 2602–2607. Retrieved from <https://doi.org/10.1016/j.egypro.2015.11.302>
- Garcia, G., Buonsanti, R., Runnerstrom, E. L., Mendelsberg, R. J., Llordes, A., Anders, A., . . . Milliron, D. J. (2011). Dynamically Modulating the Surface Plasmon Resonance of Doped Semiconductor Nanocrystals. *Nano Letters*, *11*, 4415–4420. Retrieved from <https://doi.org/10.1021/nl202597n>
- Giannuzzi, R., Scarfiello, R., Sibillano, T., Nobile, C., Grillo, V., Giannini, C., . . . Manca, M. (2017). From capacitance-controlled to diffusion-controlled electrochromism in one-dimensional shape-tailored tungsten oxide nanocrystals. *Nano Energy*, *41*, 634–645. Retrieved from <https://doi.org/10.1016/j.nanoen.2017.09.058>
- Giovannini, L., Favoino, F., Pellegrino, A., Lo Verso, V. R., Serra, V., & Zinzi, M. (2019). Thermo-chromic glazing performance: From component experimental characterisation to whole building performance evaluation. *Applied Energy*, *251*, 113335. Retrieved from <https://doi.org/10.1016/j.apenergy.2019.113335>
- Isaia, F., Fiorentini, M., Serra, V., & Capozzoli, A. (2021). Enhancing energy efficiency and comfort in buildings through model predictive control for dynamic façades with electrochromic glazing. *Journal of Building Engineering*, *43*, 102535. Retrieved from <https://doi.org/10.1016/j.jobe.2021.102535>
- Li, S. Y., Niklasson, G. A., & Granqvist, C. G. (2012). Plasmon-induced near-infrared electrochromism based on transparent conducting nanoparticles: Approximate performance limits. *Applied Physics Letters*, *101*, 07190. Retrieved from <https://doi.org/10.1063/1.4739792>
- Manthiram, K., & Alivisatos, A. P. (2012). Tunable Localized Surface Plasmon Resonances in Tungsten Oxide Nanocrystals. *Journal of the American Chemical Society*, *134*, 3995–3998. Retrieved from <https://doi.org/10.1021/ja211363w>
- Optics. (n.d.). Retrieved from Windows and Daylighting: <https://windows.lbl.gov/software/optics>
- Pallonetto, F., De Rosa, M., D'Etto, F., & P. Finn, D. (2020). On the assessment and control optimisation of demand response programs in residential buildings. *Renewable and Sustainable Energy Reviews*, 109861. Retrieved from <https://doi.org/10.1016/j.rser.2020.109861>
- Poláková, M., Schäfer, S., & Elstner, M. (2018). Thermal Glass Stress Analysis – Design Considerations. *Challenging Glass Conference Proceedings*, *6*, 725–740. Retrieved from <https://doi.org/10.7480/cgc.6.2193>
- Roberts, J. A., De Michele, G., Pernigotto, G., Gasparella, A., & Avesani, S. (2022). Impact of active façade control parameters and sensor network complexity on comfort and efficiency: A residential Italian case-study. *Energy and Buildings*, *255*, 111650. Retrieved from <https://doi.org/10.1016/j.enbuild.2021.111650>
- Standardization, E. C. (1998). *ISO EN 410:1998. Glass in building. Determination of luminous and solar characteristics of glazing*. Brussels.

- Standardization, E. C. (2011). *ISO EN 673:1997. Glass in building. Determination of thermal transmittance (U value)- Calculation method*. Brussels.
- Tsuboi, A., Nakamura, K., & Kobayashi, N. (2016). Chromatic control of multicolor electrochromic device with localized surface plasmon resonance of silver nanoparticles by voltage-step method. *Solar Energy Materials and Solar Cells*, 145, 16-25. Retrieved from <https://doi.org/10.1016/j.solmat.2015.07.034>
- WINDOW. (n.d.). Retrieved from Windows and Daylighting: <https://windows.lbl.gov/software/window>
- Xu, J., Zhang, Y., Zhai, T.-T., Kuang, Z., Li, J., Wang, Y., . . . Xia, X.-H. (2018). Electrochromic-Tuned Plasmonics for Photothermal Sterile Window. *ACS Nano*, 12, 6895–6903. Retrieved from <https://doi.org/10.1021/acsnano.8b02292>

# Implementation of a multifunctional Plug-and-Play façade using a set-based design approach

David Masip Vilà<sup>1\*</sup>, Grazia Marrone<sup>2</sup>, Irene Rafols Ribas<sup>3</sup>

\* Corresponding author, david.masip.vila@upc.edu

1 Universitat Politècnica de Catalunya – BarcelonaTech (UPC), Barcelona School of Architecture (ETSAB), Department of Architectural Technology (TA), Barcelona, Spain

2 Politecnico di Milano, Architecture, Built Environment and Construction Engineering Department, Milan, Italy

3 Eurecat, Centre Tecnològic de Catalunya, Product Innovation & Multiphysics Simulation Unit, Cerdanyola del Vallès, Spain.

## Abstract

*An immediate paradigm shift is needed to transform the deep renovation market for improved building performance and expanded energy efficiency horizons. The financial, social, and sustainability challenges of the EU targets suggest research towards reliable, inter-compatible, and interoperable solutions aiming at combining different energy conservation measures. This work proposes the implementation of a lightweight Plug-and-Play (PnP) building system for façade renovation using a set-based design approach. The PnP module, based on a main structure in the form of a Light Steel Frame (LSF) and a metal-faced sandwich panel, is combined with various market-ready components. The efficient integration of these third-party products is highlighted by defining and demonstrating the design process, implementing a solution driven by the reach of a highly industrialised solution, easy to assemble and install, customizable, scalable, and adaptable to the existing buildings. With the set-based design matrix, different integration scenarios are investigated through virtual prototypes. Moreover, to facilitate the shift from design to construction of the integrated PnP module, the study proposes three prototyping levels to demonstrate the efficiency of the design integration methodology and the technical feasibility of both the various module's configurations and the overall module, exploring them through the realisation of preliminary, full-scale façade and actual environment-applied prototypes.*

## Keywords

*plug-and-play façade, off-site construction, set-based design, integrated design, building renovation*

## DOI

<http://doi.org/10.47982/jfde.2023.2.T4>

# 1 INTRODUCTION

In the framework of the European Green Deal (European Commission, 2020), the construction sector is acknowledged as the second-largest responsible for greenhouse gas emissions (Haigh et al., 2021). With the launch of the Renovation Wave, the European Union (EU) identifies the upcoming years as crucial for the transition to a carbon-neutral future. The EU gave a strong signal towards changing the building industry with modifications to the Energy Performance of Buildings Directive (European Commission, 2018), highlighting the importance of buildings' performance. Within this context, the need for forward-thinking strategies toward the improvement of the overall construction process in building renovation interventions has seen off-site construction techniques gaining interest from researchers in light of the industrialisation of the construction process toward the improvement of the construction rate (Correia Lopes, Vicente, Azenha, & Ferreira, 2018). Certainly, given the diverse range of commercial solutions in the market and the utilization of disparate criteria and inconsistent semantics among the prevailing categorization and classification systems for construction products, there persists a crucial requirement for standardization concerning the principal Prefabricated Enclosure Wall Panel Systems (PEWPS).

The construction sector is now shifting in a direction that has already been taken in other industries like automotive, design, and shipbuilding, where products' subparts are preassembled off the main assembly line, producing high-quality, optimised, and specialised products (Kieran & Timberlake, 2004). Although the renovation practice is increasing, according to the 2022 Global Status Report for Buildings and Construction (United Nations, 2022), the progress of the building sector is far from the targets set. As a result, the trends of recent research projects supported by the EU also confirm the rising interest in off-site and multifunctional construction technologies for the building envelope (D'Oca et al., 2018) and particularly Zero Energy Renovation Kits, which are considered pivotal to accelerating the Renovation Wave (Van Oorschot, Di Maggio, Op 't Veld, & Tisov, 2022) and potentially overcoming the existing technical, financial and social obstacles (D'Oca et al., 2018). In this context, there is significant opportunity and room for improvement of Plug-and-Play (PnP) solutions (Piaia, Turillazzi, Longo, Boeri, & Giulio, 2019). The term "plug and play" is widely known in the computer industry, referring to the ability to easily implement an existing system without manual intervention. In the last years, the term has also been used in the construction sector (Sebastian et al., 2018). PnP solutions are primarily off-site components, which, due to standardisation and ease of on-site assembly, contribute to (i) speeding up the renovation time by up to 50%, (ii) avoiding the disturbance of people, (iii) reducing the overall cost, allowing at least 15% savings, (iv) increasing performance and resource efficiency in both energy and material terms, and (v) the possibility for urban mining and re-use of building materials (D'Oca et al., 2018; Op't Veld, 2015; Piaia et al., 2019).

Although the goal of this work is not to provide a state-of-the-art of off-site and industrialised technologies developed within the EU-funded programs, many research projects deepened the topic (Li & Chen, 2022). The projects focus on improving building energy, thermal, and environmental performance, emphasising façade retrofitting, which accounts for 20-30% of energy consumption (Dall'O', Galante, & Pasetti, 2012). One of the possible measures to address façade retrofitting is to adopt Energy Conservation Measures (ECMs) (Sarihi, Mehdizadeh Saradj, & Faizi, 2021). Various ECMs to renovate buildings that adhere to the standards established by the most recent European and international directives can be developed: (i) passive ECMs aim to reduce building energy consumption by increasing thermal resistance, replacing windows, and using bioclimatic strategies, (ii) active ECMs replace Heating, Ventilation and Air Conditioning (HVAC) components with energy-efficient sources, (iii) renewable energy source ECMs, like solar panels, photovoltaic panels, and wind turbines, and (iv) control ECMs optimise energy supply technologies, rationalising

fossil fuel use (Sarihi et al., 2021). However, the application of each ECM will allow only certain improvements in the building performance; thus, recent studies focus on the combination of ECMs in the same system (D'Oca et al., 2018), investigating multifunctionality.

In considering the combination strategies, the MEEFS project, launched in 2012, focused on multifunctional façade modules with composite materials and renewable energy sources. Although the integration of renewable energies in the façade's modules is of common interest (Du, Huang, & Jones, 2019), many other projects deepen mainly the integration of active and passive technologies, such as high-performance lighting systems and energy-efficient HVAC. The E2VENT project proposed a comprehensive strategy for the retrofit of residential buildings employing a cutting-edge ventilated façade with heat recovery units, solar cells, and envelope insulation technologies and a latent system integrating Phase Changing Materials (Basso, Mililli, Herrero, Sanz, & Casaldiga, 2017). Furthermore, several projects investigated the manufacture of industrialised solutions in terms of process and product optimisation. The MORE-CONNECT project suggested process and product innovation for prefabricated modular façade elements, combining multifunctional components for temperature control, energy savings, building physics, aesthetics, and developing PnP connections (Veld, 2015). Consistently, the BERTIM project improved a prefabricated wood-based module integrating windows, balconies, insulation, collective HVAC systems, and renewable energy systems, addressing the complexity and multidisciplinary of the multifunctional building envelope.

Although the projects focused on the application of both products and renovation methodologies, new concepts, such as building envelope adaptability, have expanded in recent years. There has been a renewed emphasis on improving energy efficiency, overall sustainability, and cost-effectiveness of off-site technologies in the last five years, proposing fast PnP façade solutions, including implementation within the BIM environment (D'Oca et al., 2018). The P2ENDURE project focused on prefabricated PnP solutions that are ready to use, scalable, adaptable, and effective, implementing prefabricated and multifunctional façade integrating windows, water ducts, and pipes, air supply and/or even ventilation ducts, heating, and cooling functions. On the same page, project 4RinEU also developed a prefabricated multifunctional façade integrating active components, proposing a risk evaluation method to address the effectiveness of the proposed technologies and implementations (D'Oca et al., 2018).

Even though research has shown that off-site façades for building renovation are cutting-edge in terms of sustainability, energy, and environmental efficiency (Capeluto, 2019), the literature identifies obstacles to their advancement. One of the main barriers is the lack of knowledge and experience among architects, engineers, and contractors in designing and constructing off-site façades. Moreover, the high initial costs associated with implementing these technologies compared to traditional construction techniques (D'Oca et al., 2018) form a bottleneck. Although many concepts have been created, only a few have reached market maturity and are now being used in building renovations (Capeluto, 2019). As a result, another method consisted of making these systems more competitive by merging several market-ready components. For example, the project BRESAER developed an innovative and adaptable industrialised system combined with a lightweight and versatile structure, using market-ready products, thus allowing the study of the mutual interaction between the components (Capeluto, 2019).

In light of the above, industrialisation is recognised as fundamental towards upscaling these solutions (Capeluto, 2019), highlighting the need for mass production strategies to boost them. In addressing the complexity of the new technological solutions, industrial manufacturers will be key players in upscaling the solutions through industrialisation (Torres et al., 2021). On the one hand,

there is a need to implement innovative paradigms to design flexible and effective multifunctional complex construction systems (Simões et al., 2019), also considering that different stakeholders might be involved and, on the other hand, that there is the need for new holistic methods to evaluate and design renovation interventions (Colajanni, Rotilio, Di Santo, & Marrone, 2022). Although it might seem that prefabricated elements allow for limited adaptability, if the system is conceived as a combination of different components and implemented according to the demand, the possibilities are significant (Negrão, Godinho Filho, & Marodin, 2017).

This work uses a set-based design methodology to implement a PnP façade module for deep renovation. The PnP façade module's core is made by lightweight industrialised technologies, particularly Light Steel Frame (LSF) and sandwich panels. The role in the optimisation of resource use and reduction of building's embodied energy allowed by industrialised lightweight construction technologies which effectively use less material is generally recognised (Gervásio, Santos, Da Silva, & Lopes, 2010; Marrone, Sesana, & Imperadori, 2023).

Considering the need to shift towards more resilient and sustainable design, the main aim of this study is to offer a paradigm shift to transform the market of deep building renovation technologies by defining and demonstrating a design and production process of a PnP façade module which relies on the integration of industrialised products, avoiding commitment to a particular design and instead generating and assessing sets of design alternatives. In following such aim, the current research has two main objectives. The first objective is to explore the use of set-based design principles (Singer, Doerry, & Buckley, 2009) to investigate different levels of prefabrication, thus improving a multifunctional lightweight PnP façade system for deep renovation interventions. The second objective is to show the viability and benefits of the set-based design methodology in facilitating the exploration of various scenarios, in a virtual environment, which facilitates collaboration between companies for product development. This methodology allows for identifying potential design conflicts and optimising the system's performance before physical prototypes are created. The demonstration phase of the design methodology is discussed, providing three levels of full-scale prototyping. According to the objectives, the manuscript proceeds as follows: Section 2 describes the methodology used to implement innovative façade solutions. The results of the applied methodology are presented in Sections 3 and 4; the first dealing with the outcomes of the set-based design method to the design phase of the implemented PnP module; the latter presenting the outcomes of the PnP module's demonstration phase through full-scale prototypes. Section 5 reports the conclusion and further research developments.

## 2 METHODOLOGY

The PnP module has been implemented and integrated using interoperable and interconnected third-party products (TPP) available in the market to provide a highly industrialised off-site solution through a set-based design methodology. This section describes the methodology adopted. The first part gives an overview of the PnP module and provides the classification of the TPPs to be integrated into the module. In the second part, the set-based design methodology is presented, highlighting how it has been applied in this study.

## 2.1 THE PLUG-AND-PLAY FAÇADE MODULE

### 2.1.1 Module design

The façade module object of the study is a PnP complex system composed of different layers which can be integrated and varied depending on the project needs. The PnP concept applied to the façade is connected to a high level of prefabrication; thus, the façade design incorporates a certain degree of standardisation for fast on-site assembly and user-friendliness to reduce human intervention. Therefore, the implementation of the PnP module includes market-ready components which are already tested and validated in different scenarios, complying with regulations. The final design of the PnP façade module has been developed by an Italian company with expertise in industrialised steel-based products such as LSF structures and metal-faced sandwich panels. The main core of the module is composed of metal-faced sandwich panels assembled on an LSF structure. The modules are produced off-site and installed as a single element on the existing building through a flexible anchoring system fixed to the LSF, allowing movements in three directions. Flexibility is assured, on the one hand, by the anchoring system, which allows interventions to a wide range of existing buildings and, on the other hand, by the adaptability of the PnP module. The modularity of the design allows the PnP to be customised in terms of dimensions, with heights ranging from 2.5 to 4 meters and widths ranging from 1.30 to 3 meters. Depending on the project requirements, the module's thickness can range from 20 to 35 centimetres, while from an energy performance perspective, the system enables achieving U-values below  $0.2 \text{ W/m}^2\text{K}$ . To streamline the layers that constitute the PnP module, its composition can be simplified into five main layers as represented in FIG 1.

Starting from the outside, the PnP module is composed of a ventilated façade (Layers 1 and 2). The first layer will be addressed throughout the work as the "External layer" and refers to the exterior finish of the façade, while the second layer is defined as "Air gap & substructure" and consists of the air cavity inherent to ventilated façades, including aluminium profiles for the exterior finish. The third layer is the main core of the module and will be addressed as "Structure and sandwich panels". It is constituted by the metal-faced sandwich panels attached to the LSF structure made of vertical and horizontal cold-formed steel profiles 3 millimetres thick. Metal-faced sandwich panels consist of a core layer of polyurethane or mineral wool skinned with two steel sheets. The sandwich panels provide thermal insulation, air and water tightness, acoustic insulation, and a good reaction to the fire. The sandwich panels allow the installation of the ventilated façade through anchoring elements installed on the ribs of the sandwich. The fourth layer is addressed as the "Air gap and anchoring system". It consists of the anchoring systems for the installation of the module on the existing envelope, thus creating a non-ventilated air gap in between.

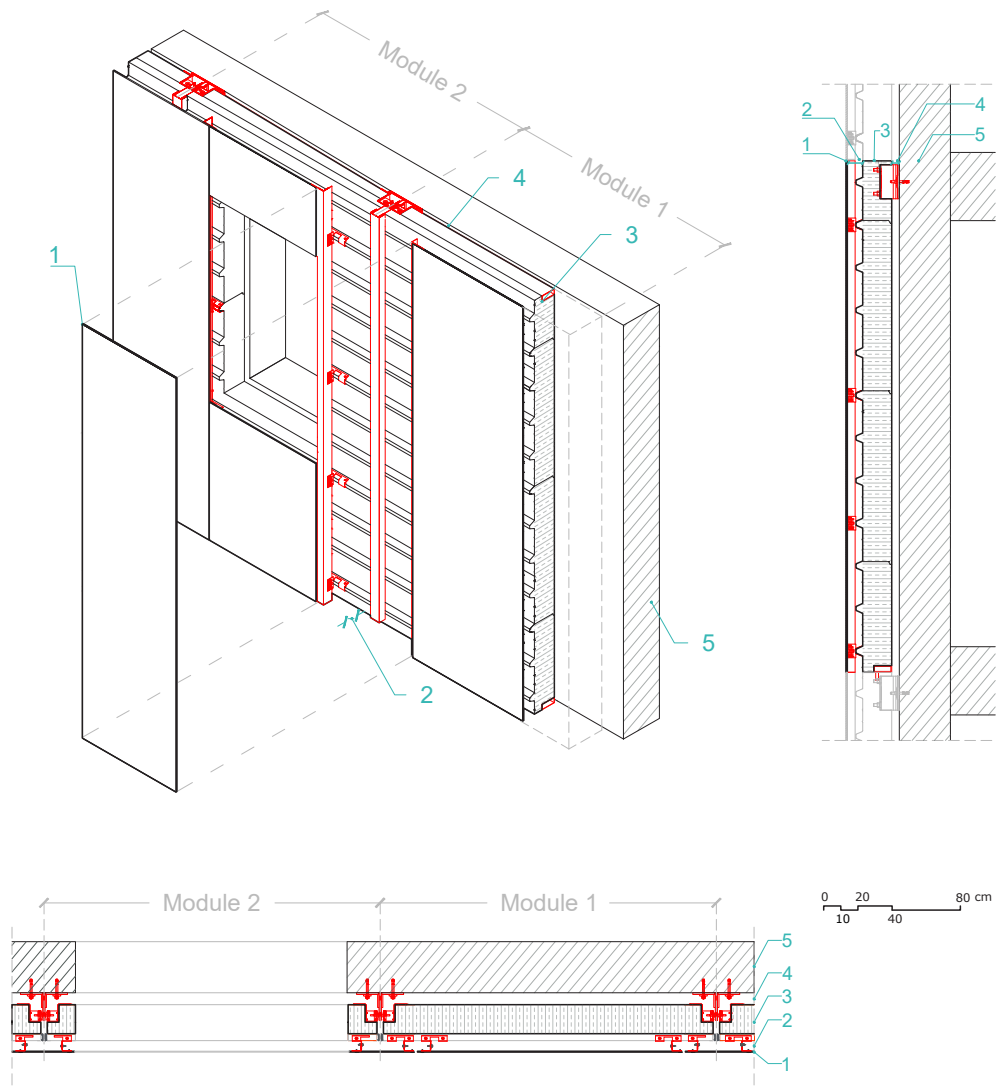


FIG. 1 Representation of the PnP module's details: a) 3D representation; b) Vertical section; c) Horizontal section.  
 1. External Layer | 2. Air gap & Structure | 3. Structure & Sandwich panel | 4. Air gap & Anchoring System | 5. Existing Envelope

The fifth layer is intended to be the structural element of the building and is not part of the PnP module but constitutes the complete envelope. The PnP module can accommodate pipes and other services in the Air gap and substructure (layer 2). The object of the study is the implementation of this basic PnP module with selected TPPs already available in the market through the set-based design approach described in section 2.2.

### 2.1.2 Integration of third-party products

According to the state of the art of PnP systems, it is necessary to propose fast and adaptable solutions to boost this market. As the demand for building renovation continues to grow, it is essential to keep exploring new solutions and technologies. In this context, the interoperability of TPPs needs to be studied in detail, focusing on already market-ready products. The products integrable in the PnP module have been selected using a structured protocol (Batallé, Masip, Ràfols, Lupi, & Donnerup, 2022) to ensure interoperability and inter-compatibility between components.

The protocol outlines six principles that the TPP must follow: industrialisation, customisation, compatibility and interoperability, circularity, open information exchange, and adherence to certification and regulation requirements. By adhering to industrialisation and customisation principles, the selected product allows off-site assembly, ease of installation, and adaptability to various architectural geometries and aesthetics, thus enhancing the overall easy and time-saving installation of the PnP module. Besides the variety of innovative and established solutions in the building renovation market, efforts have mostly focused on two main concepts: the reduction of energy demand and the optimisation of energy production through the combination of different ECMs, which include passive, active, and energy production systems. Passive systems are those methods that help the building perform the function of heat transfer and storage with no assistance from energy sources. These systems include external cladding, high-performance windows, and solar protection. On the other hand, active systems maintain demanded environmental conditions within a space. The energy production systems consider all technologies integrated into the building that can produce energy, such as photovoltaic panels. The technologies considered in this paragraph are those that can be integrated into the façade according to the protocol: comfort and salubrity (Demand-Controlled Ventilation, DCV) and energy production (Photovoltaic panels, PV). The integration of a heating and cooling system has been discarded since any TPP meets the PnP protocol. The TPPs identified to be integrated into the module are listed in Table 1.

TABLE 1 TPPs potentially integrable into the PnP façade module.

Third-Party Products (TPP) potentially integrable into PnP module	
Passive systems	1. External Cladding
	2. High-performance windows
	3. Solar Protection or Sun Shading
Active systems and energy production	4. Demand Controlled Ventilation (DCV)
	5. Photovoltaic (PV) panels

## 2.2 A SET-BASED DESIGN MATRIX FOR PNP FAÇADE DEVELOPMENT

This section describes the methodology used to implement the PnP module with TPPs. The design of such complex systems and their product development means that different parties must collaborate to deliver the expected outcome, highlighting the need for a structured methodology. Considering the integration of TPPs in the PnP façade module, this work investigated the application of the set-based design methodology to address the complexity of the problem.

Among other design methodologies, set-based design (Sobek & Ward, 1996) allows resilient design solutions; thus, it is one of the main methods adopted in product development. Known as a pillar of lean thinking, set-based design is a structured approach which allows the exploration of a wide range of possible alternatives to gradually converge to the best possible solution while handling the uncertainties typical of the early design stages (Sobek & Ward, 1996). The main characteristic of the approach is keeping design freedom in the earliest phases of design, conversely to a point-based approach (Singer et al., 2009). The traditionally used design practice tends to consider engineered design as an iterative process which, step by step, reaches the final solution without any guarantee that the solution will be the best one (Inoue, Takahashi, & Ishikawa, 2013).

Although the approach with its hybrid applications has been used in designing different products, structural building solutions, construction management, and BIM environments (Serugga, Kagioglou, & Tzortzopolous, 2020), to the authors' best knowledge, it hasn't been explored widely in the technical implementation of off-site building façades.

In this paper, the authors propose a design method for implementing an industrialised façade for building renovation using the set-based design method as the main theoretical framework to develop a set-based design matrix to investigate inter-compatible and interoperable sets of design alternatives. Although the set-based design has been consistently used in product development, according to the literature, there is a need to develop its knowledge-based environment through techniques able to increase the comprehension and application of the methodology, such as prototyping and testing. The development of an innovative industrialised PnP building system, potentially upgradeable, is a complex task that has been further investigated by enriching the set-based design methodology with a prototyping phase developed with three different levels of detail. The proposed methodology assesses the decision-making in developing the PnP modular façade, allowing both the main developer and the third-party companies to collaborate in a virtual environment and integrate their products, exploring an open set of design solutions. In this study, the authors focused on the feasibility of the façade module integration with existing TPPs to attempt to boost the industrialised production process.

Considering that the set-based design methodology highly depends on the object of the study, the boundary conditions and the design phase, the literature cannot outline a specific set of actions to apply it (Parrish, 2009). Although there is a different complexification according to each project, the key concepts to implement a set-based design methodology have been synthesised: (i) understand the design space considering a wide range of design alternatives, (ii) specialists have to be allowed to think about the problem from their perspective, and (iii) the intersection of many sets may be used to enhance a design and determine its feasibility before committing to it.

Starting from breaking down the design problem into smaller and manageable components, this study suggests the application of set-based design methodology according to the following phases: (i) identification of the main layers of the façade module, (ii) identification of potential integrable TPPs, (iii) identification of the possible scenarios of TPPs integration, (iv) demonstrate the scenario in a virtual environment, (v) develop technical design alternatives for each scenario, (vi) prediction of future performance requirements according to the technical constraints, (vii) demonstration of the selected options through prototyping at different levels of detail, and (viii) validation phase through different performance tests to qualify the final product. Although the validation phase is considered necessary to allow the market readiness of the solutions, this phase has not been included in this study.

To commit to the definition of all the possible TPP integration scenarios into a PnP façade module and the technical requirements, a set-based design matrix has been outlined. The matrix provides the designer with the visualisation of several scenarios assisting the exploration of the possible effect on the façade module in terms of technical requirements and feasibility. Particularly, the set-based design matrix presents three different inputs: the TPPs selected, the PnP modular façade's layers, and hypothesized performance requirements. The reading process of the matrix is reported in Table 2.

TABLE 2 Example of the set-based design matrix's reading process and identification of a possible scenario.

		PNP MODULE'S LAYERS					Technical requirements of each scenario	
		1	2	3	4	5		
		External Layer	Air gap & Substructure	Structure & Sandwich Panel	Air gap & Anchoring System	Existing Envelope		
[1] →	N	Name	-	-	Scenario N1 <input checked="" type="checkbox"/>	-	-	← [3]
			R <sub>n</sub>	R <sub>n</sub>	R <sub>1</sub> , R <sub>2</sub> , ...	R <sub>n</sub>	R <sub>n</sub>	
	X	Name	-	-	-	Scenario X2 <input checked="" type="checkbox"/>	-	
			R <sub>n</sub>	R <sub>n</sub>	R <sub>n</sub>	R <sub>1</sub> , R <sub>2</sub> , ...	R <sub>n</sub>	

The integration of the TPP into the PnP module involves identifying scenarios where it can be effectively incorporated. The two factors that define a scenario are, from one side, the TPP potentially integrable into the module (arrow [1]) and the layer of the PnP module in which the TPP is installed (arrow [2]). Once a potential scenario is identified, a list of requirements (arrow [3]) that must be fulfilled is proposed to ensure smooth integration and functionality across the various layers in which the TPP is installed. The requirements, identified and numbered subsequently as "Rn", can involve not only the specific layer in which the TPP is integrated but also the adjacent layers, which can be potentially influenced by the TPP integration. Thus, the matrix may present requirements in multiple layers at once, influencing different layers. Each scenario is studied and technically implemented within a virtual environment by the PnP module designers and the third-party companies which provide the product to be integrated. To fast-track the deep renovation, the possible solutions of integration are successively prototyped and demonstrated at three different levels: a preliminary prototype, a full-scale prototype, and a real environment prototype on a case study building. This method allowed the collaboration between the different companies towards the industrial production of a complex PnP façade system incorporating different ECMs.

### 3 DESIGN SOLUTION SET FOR PLUG-AND-PLAY MODULE: APPLICATION OF THE SET-BASED DESIGN MATRIX

The main objective of the set-based design methodology is to guide the technical development of the PnP module by integrating existing technologies available in the market through the exploration of different scenarios. Moreover, it is considering the technical requirements and the feasibility of its integration. However, this means that to fulfil a correct integration of a TPP into the PnP, the requirements presented in this paper should be met. Table 3 offers a summary of the possible scenarios identified for the TPPs integration into the PnP module. To clarify the scenarios along with their list of requirements (addressed as Rn and numbered progressively), the following paragraphs will describe each case.

TABLE 3 Overall matrix of the scenarios identified to integrate potential TPPs into the PnP module.

		PNP MODULE'S LAYERS							
		1	2	3	4	5			
		External Layer	Air gap & Substructure	Structure & Sandwich Panel	Air gap & Anchoring System	Existing Envelope			
TPP potentially integrable into the PnP module	A	External Cladding (3.1)	<b>Scenario A1</b> ✔ $R_1, R_2, \dots$	- $R_n$	- $R_n$	- $R_n$	- $R_n$	$R_n$	
			- $R_n$	<b>Scenario A2</b> ✔ $R_1, R_2, \dots$	- $R_n$	- $R_n$	- $R_n$	$R_n$	
		B	High performance windows (3.2)	- $R_n$	- $R_n$	<b>Scenario B1</b> ✔ $R_1, R_2, \dots$	- $R_n$	- $R_n$	$R_n$
				- $R_n$	- $R_n$	- $R_n$	- $R_n$	<b>Scenario B2</b> ✔ $R_1, R_2, \dots$	$R_n$
	C		Solar Protection or Sun Shading (3.3)	- $R_n$	<b>Scenario C1</b> ✔ $R_1, R_2, \dots$	- $R_n$	- $R_n$	- $R_n$	$R_n$
				- $R_n$	<b>Scenario C2</b> ✔ $R_1, R_2, \dots$			<b>Window</b> - $R_n$	$R_n$
		D	Demand Controlled Ventilation (3.4)	- $R_n$	- $R_n$	<b>Scenario D1</b> ✔ $R_1, R_2, \dots$	- $R_n$	- $R_n$	$R_n$
				- $R_n$	- $R_n$	- $R_n$	- $R_n$	<b>Scenario D2</b> ✔ $R_1, R_2, \dots$	$R_n$
	E		PV or ST Panels (3.5)	<b>Scenario E1</b> ✔ $R_1, R_2, \dots$	- $R_n$	- $R_n$	- $R_n$	- $R_n$	$R_n$
				- $R_n$	<b>Scenario E2</b> ✔ $R_1, R_2, \dots$	- $R_n$	- $R_n$	- $R_n$	$R_n$

Technical requirements of each scenario

### 3.1 EXTERNAL CLADDING

The integration of TPPs in the external layer of the PnP module affects the part of the envelope in contact with the exterior, i.e., the ventilated façade, which directly involves the external layer (1) and its substructure (2). The cavity between the external layer and the sandwich panel is a ventilated gap. The integration of the external cladding deals with the capability to offer different types of geometries and aesthetic finishes, in other words, providing a high degree of customisation. Two possible scenarios have been identified for this integration. The first scenario, named A1, sees the TPP adapting their system to the basic substructure of the PnP module. In this case, the main challenge is to ensure a secure union between the substructure and the external cladding.

The second scenario, named A2, explores the case in which the TPP provides its own substructure for the ventilated façade. In this case, a reliable anchoring system is necessary to ensure the structural stability and safety of the façade. The installation of the substructure to the ribs of the sandwich panels is guaranteed by a flexible anchoring system with the capability to integrate different substructures, thus allowing these two scenarios.

As can be seen in Table 4, a list of requirements to be fulfilled by the TPP to be integrated into the modules is provided. Regarding scenario A1, the first requirement ( $R_1$ ) highlights the need for the external cladding's dimensions to be between 2.5 and 3 metres to be adaptable to the PnP envelope size, ensuring the correct transportation and the assembling process. The second requirement ( $R_2$ ) is the compliance of a maximum weight, which is related to the mechanical and load-bearing capacity of the façade, while the third ( $R_3$ ) requires the adaptability of the system to the existing substructure.

TABLE 4 Set-based design matrix for the integration of external cladding as TPP in the PnP module

		PNP MODULE'S LAYERS					
		1	2	3	4	5	
		External Layer	Air gap & Substructure	Structure & Sandwich Panel	Air gap & Anchoring System	Existing Envelope	
A	External Cladding	<b>Scenario A1</b> ✔	-	-	-	-	
		$R_1$ : The external cladding should be adaptable to PnP envelope size between 2.5 - 3 mt and different configurations.	$R_3$ : Anchoring system adaptable to the existing substructure.				$R_n$
		$R_2$ : The external cladding elements should not be heavier than 60 kg/m <sup>2</sup>					
		-	<b>Scenario A2</b> ✔	-	-	-	
$R_3$ : Adapt to PnP envelope size specifications.	$R_1$ : The provided substructure should be attached either to the sandwich panel or the brackets.				$R_n$		
	$R_2$ : The anchoring system must fit in the ventilated facade air gap.						

The main objective of the PnP module is to be able to offer third parties the option to integrate their products without limitations. It should be mentioned that the sandwich panel can also be placed vertically, opening a wide range of possibilities.

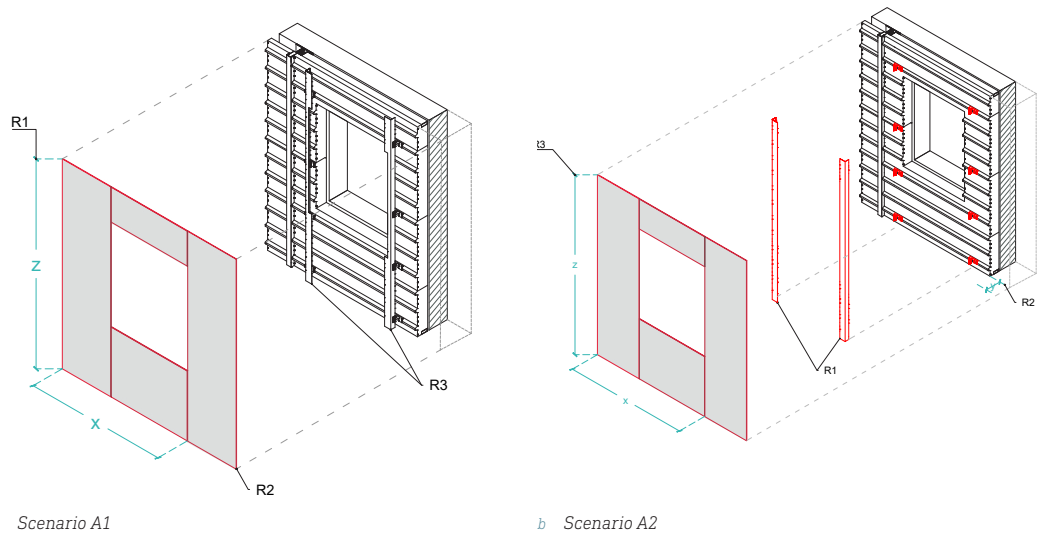


FIG. 2 Representation of integration scenarios and relative requirements (Rn) - Scenario A1: Integration of TPP external cladding in the external layer of the PnP module; Scenario A2: Integration of TPP external cladding in the air gap and structure layer of the PnP module through a provided substructure.

### 3.2 HIGH-PERFORMANCE WINDOWS

TABLE 5 Set-based design matrix for the integration of high-performance window as TPP in the PnP module.

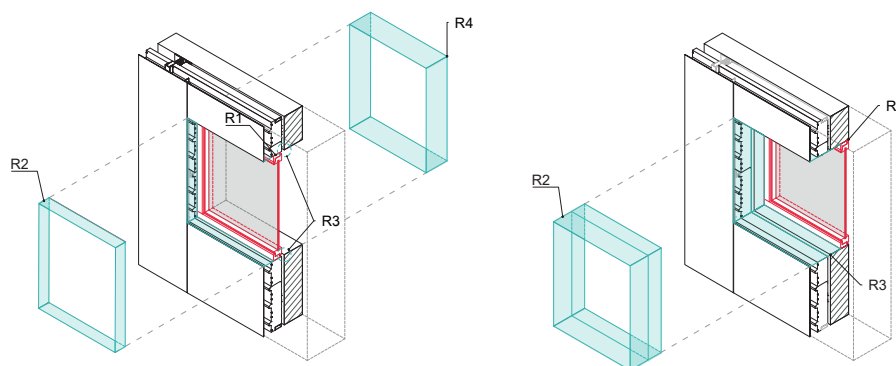
		PNP MODULE'S LAYERS					
		1	2	3	4	5	
		External Layer	Air gap & Substructure	Structure & Sandwich Panel	Air gap & Anchoring System	Existing Envelope	
B	High performance windows	-	-	<b>Scenario B1</b> ✓	-	-	R <sub>n</sub>
		R <sub>2</sub> : The installation of a perimetral frame is needed to seal the window hole.		R <sub>1</sub> : The substructure of the window must be compatible with the sandwich panel.	R <sub>3</sub> : The air chamber should be sealed.		
					R <sub>4</sub> : The installation of a perimetral frame from the interior is needed to provide an optimal interior finish.		
		-	-	-	-	<b>Scenario B2</b> ✓	R <sub>n</sub>
R <sub>2</sub> : The installation of a perimetral frame is needed to seal the window hole. A double frame should be provided.					R <sub>1</sub> : The existing building must allow the window frame installation.		
				R <sub>3</sub> : The continuity of the isolation layer should be solved, otherwise the implementation would present thermal bridges.			

High-performance windows are decisive elements that complement the building's envelope, providing natural light and ventilation while also contributing to aesthetic and thermal properties. The integration of high-performance windows depends on the bioclimatic strategy and the solar orientation of the building. Table 5 offers an overview of the identified scenarios and relative requirements to be fulfilled to ensure correct integration of the TPP in the PnP module.

Scenario B1 considers the window's installation within the sandwich panel, thus substituting the windows installed in the existing building, while scenario B2 explores the hypothesis in which the window is kept or substituted in the existing envelope. The location of the windows also affects the placement of other components, such as sun shading systems.

Diving deeper into the main features of scenario B1, it can be said that it assures the continuity of the thermal envelope throughout the façade plane. However, the integration of a window frame in an industrialised component, such as the sandwich panel, is an issue that highlights the need for compatibility between the two products. Moreover, the placement of the window in the third layer of the PnP module is possible if considering the installation of a perimetral frame and sealing the air gap between the existing building and the PnP module. Another detail related to scenario B1 is the need to complete the module installation with an interior frame to ensure an aesthetic internal finishing. This action must be carried out on-site, accommodating the tolerances of the building.

Scenario B2 describes the situation in which the installed windows to be renovated are left in their location. In this case, the technical solution proposed is the integration of a perimetral frame to seal the opening made in the PnP module corresponding to the window. In this case, a double frame or a frame that allows both thermal and mechanical movements should be integrated into the PnP module. The technical detail adopted in the installation of this frame could help ensure the continuity of the insulation layer to avoid thermal bridges. This second scenario allows the potential integration of solar protection systems in the PnP module, which will be discussed in the next paragraph.



a Scenario B1

b Scenario B2

FIG. 3 Representation of integration scenarios and related requirements (Rn) - Scenario B1: Integration of TPP high-performance window in the structure and sandwich panel layer of the PnP module; Scenario B2: Integration of TPP high-performance window in the existing envelope.

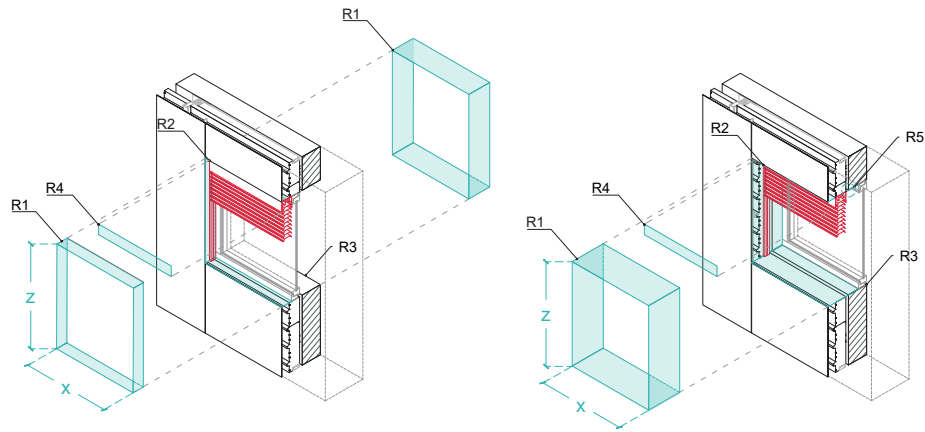
### 3.3 SOLAR PROTECTION | SUN SHADING

Solar protection and sun shading are crucial elements in the building envelope since they must be implemented depending on the climate analysis and the building's location and orientation. These features must be designed aiming at the user's comfort; thus, every situation is different. For example, buildings in hot and sunny climates benefit from external shading devices such as solar blinds or shades, while buildings with less sun exposure may benefit from internal shading devices such as blinds or curtains. The integration of solar protection or sun shading systems into the PnP façade module, if correctly designed, can significantly contribute to reducing the cooling demand of a building by limiting the solar gains. Additionally, by lowering glare and heat accumulation, sun protection systems can increase building occupants' comfort. Although there are various types of solar protection systems and sun shadings, their implementation within the PnP module is related to the window location. When it comes to integration, solar protection or sun shading installation can be made directly onto the metal frame installed in the window opening, already described in the previous paragraph, thus making the integration process relatively straightforward. Table 6 provides the set-based design matrix of solar protection and sun shading integration within the PnP module, highlighting two possible scenarios and the relative technical requirements, addressed in the figures and tables as "Rn".

While scenario C1 considers the integration of the solar protection and sun shading systems when the window is installed within layer 3 of the PnP module, scenario C2 explores the integration of the TPPs when the window is in the existing envelope.

TABLE 6 Set-based design matrix for the integration of solar protection or sun shading as TPP in the PnP module.

		PNP MODULE'S LAYERS					
		1	2	3	4	5	
		External Layer	Air gap & Substructure	Structure & Sandwich Panel	Air gap & Anchoring System	Existing Envelope	
C	Solar Protection or Sun Shading	-	<b>Scenario C1</b> ✔	<b>Window</b>	-	-	R <sub>n</sub>
		R <sub>4</sub> : The structure of the Sun shading needs to be covered by an external layer.	R <sub>1</sub> : The TPP should provide a system adaptable to a frame sheet. R <sub>2</sub> : Dimensions of the Sun shading should be compatible with building dimensions.		R <sub>3</sub> : Installation for the sun shading control should be solved.		
		-	<b>Scenario C2</b> ✔			<b>Window</b>	R <sub>n</sub>
		R <sub>4</sub> : The structure of the Sun shading needs to be covered by an external layer.	R <sub>1</sub> : The TPP should provide a system adaptable to a frame sheet. R <sub>2</sub> : Dimensions of the Sun shading should be compatible with building dimensions.	R <sub>5</sub> : The continuity of the thermal envelope should be solved in this layer. Otherwise, the implementation of the window would have thermal bridges.	R <sub>3</sub> : installation for the sun shading control.		



a Scenario C1

b Scenario C2

FIG. 4 Representation of integration scenarios and relative requirements (Rn) - Scenario C1: Integration of TPP solar protection when the window is installed in the structure and sandwich panel layer of the module; Scenario C2: Integration of TPP solar protection when the window is in the existing envelope.

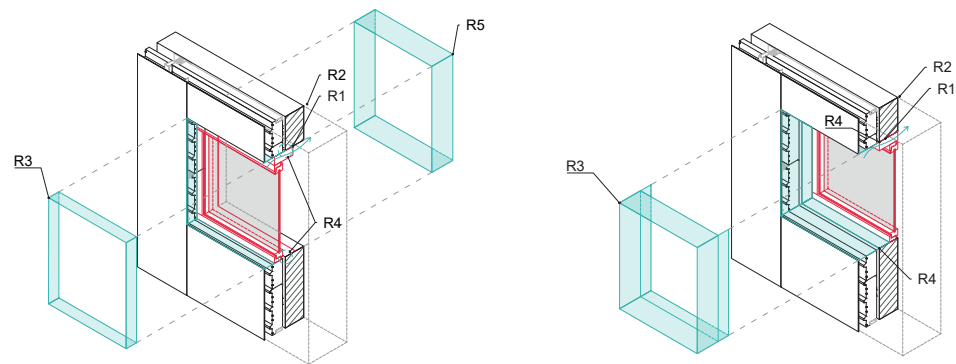
### 3.4 DEMAND CONTROLLED VENTILATION

TABLE 7 Set-based design matrix for the integration of the DCV as TPP in the PnP module.

		PNP MODULE'S LAYERS						
		1	2	3	4	5		
		External Layer	Air gap & Substructure	Structure & Sandwich Panel	Air gap & Anchoring System	Existing Envelope		
D	Demand Controlled Ventilation	-	-	<b>Scenario D1</b> ✓	<b>Window</b>	-	-	R <sub>n</sub>
		R <sub>3</sub> : The installation of a perimetral frame is needed to seal the window hole. A double frame should be provided.		R <sub>1</sub> : The DCM system should allow the physical installation on the PnP module through the window system.		R <sub>4</sub> : The air chamber should be sealed.		
				R <sub>2</sub> : The connection with the electrical facilities should be solved.		R5: The installation of a perimetral frame from the interior is needed to provide an optimal interior finish.		
		-	-	-	-	-	<b>Scenario D2</b> ✓	<b>Window</b>
R <sub>3</sub> : The installation of a perimetral frame is needed to seal the window hole. A double frame should be provided.				R <sub>1</sub> : The existing envelope must allow physically the installation of DCM.		R <sub>2</sub> : The existing envelope must allow/provide the electrical facilities.		
		R <sub>4</sub> : The continuity of the thermal envelope should be solved, otherwise the implementation could present thermal bridges						

A smart ventilation system adjusts ventilation rates in a building to one or more of the following parameters: occupancy, temperature, and air quality conditions. The main purpose is to ensure efficient air filtration in the interior spaces. Table 7 provides the set-based design matrix of a DCV integration within the PnP module, highlighting two possible scenarios.

The integration of DCV in the module is related to the window location; thus, the two scenarios have been identified according to the scenarios identified for the window integration (paragraph 3.2, scenarios B1 and B2). The identified technical requirements, addressed in the figures and tables as “Rn”, are related to scenarios B1 and B2 but include the electrical connection of the DCV system.



a Scenario D1

b Scenario D2

FIG. 5 Representation of integration scenarios and relative requirements (Rn) - Scenario D1: Integration of DCV system when the window is in the structure and sandwich panel layer; Scenario D2: Integration of DCV system when the window is in the existing envelope.

### 3.5 PHOTOVOLTAIC PANELS

The integration of photovoltaic panels (PV) into the PnP module contributes to reducing the energy consumption of the building. Although the amount of electricity generated by a PV panel depends on several factors, installing PV panels in the façade is a topic of growing interest, considering that the panels are becoming more efficient and affordable due to technological advancements. Table 8 shows the set-based design matrix, which identifies two main scenarios

Scenario D1 represents the case in which the TPP can adapt its system to the existing substructure. Scenario D2 investigates the case that the TPP system provides its own substructure or anchoring system. The integration of PV panels into the PnP module has been validated by various companies; thus, it is considered reliable especially due to the presence of a ventilated gap. On the one hand, the presence of the ventilated gap helps dissipate heat generated by the PV panels, preventing any potential damage or decrease in efficiency due to overheating. On the other hand, the available space allows the allocation of the technical connection and facilities of the panel, ensuring easy installation, maintenance, and accessibility.

TABLE 8 Set-based design matrix for the integration of PV panel as TPP in the PnP module.

		PNP MODULE'S LAYERS					
		1	2	3	4	5	
		External Layer	Air gap & Substructure	Structure & Sandwich Panel	Air gap & Anchoring System	Existing Envelope	
E	PV or ST Panels	<b>Scenario E1</b> ✓ R <sub>1</sub> : Adapt to PnP envelope size specifications.	-	-	-	-	R <sub>n</sub>
		R <sub>2</sub> : Ground wires R <sub>3</sub> : The anchoring system of panels must be compatible with PnP module's substructure.					
		-	<b>Scenario E2</b> ✓ R <sub>1</sub> : Adapt to PnP envelope size specifications.	-	-	-	R <sub>n</sub>
		R <sub>2</sub> : Ground wires R <sub>3</sub> : The substructure must be compatible with the brackets or attachable to sandwich panel. R <sub>4</sub> : The anchoring system must fit into the air gap of the ventilated façade.					

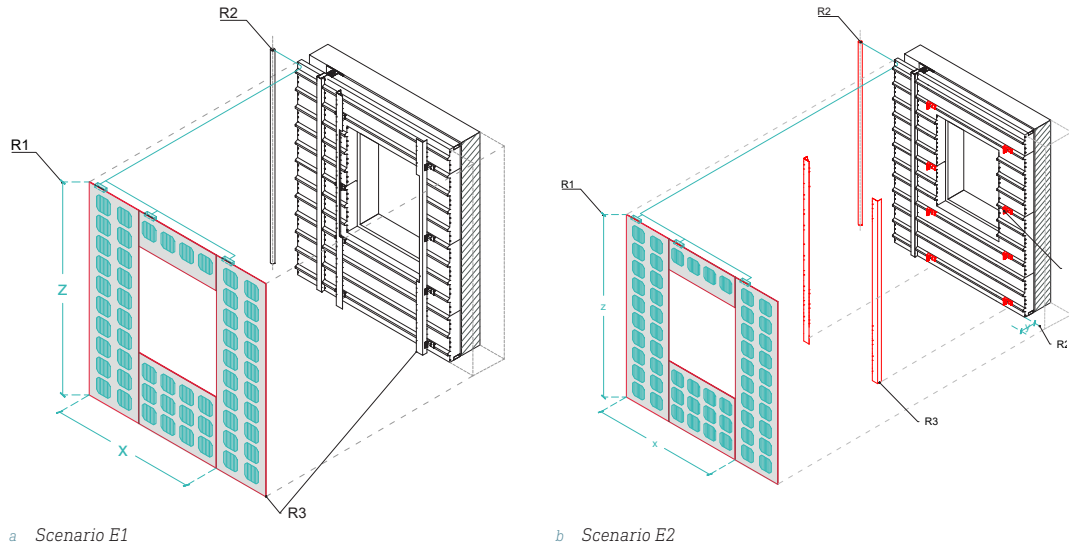


FIG. 6 Representation of integration scenarios and relative requirements (Rn) - Scenario E1: Integration of PV Panels when the TPP can adapt their system to the existing structure; Scenario E2: Integration of PV Panels when TPP provides a new substructure or anchoring system.

## 4 FULL-SCALE DEMONSTRATION

One of the main objectives of this work is to practically demonstrate the feasibility of the scenarios previously explored in a virtual environment through the set-based design methodology. To eliminate the weakest solutions in the set and thus concentrate on the design options which can ensure flexibility, discovery, and innovation, the set-based design approach uses prototypes to facilitate successful product development. According to the literature, one of the aspects that require more evaluation in future research is both virtual and physical prototyping, which is considered necessary to allow an informed convergence process (Toche, Pellerin, & Fortin, 2020).

Considering the above, this section presents the demonstration phase of the solution set explored with the set-based design methodology. If the virtual modelling represented a preliminary level of investigation serving as feasibility prototypes, the physical demonstration was implemented to streamline the transition from research to real-scale applications. The methodology used in the prototyping phase allows the demonstration of the integrated PnP systems in real scenarios considering three levels of investigation: preliminary level, demonstration level, and final level. The three levels of prototyping aim at exploring various aspects respectively.

The first level of prototyping consisted of investigating the PnP module at a preliminary level, diving deeper into a portion of the module to study the interfaces between various TPPs. The second prototype intends to demonstrate a full-scale façade made of six complete PnP modules. The third prototype demonstrates the shift from design to construction of a real façade solution applied on a real case study building.

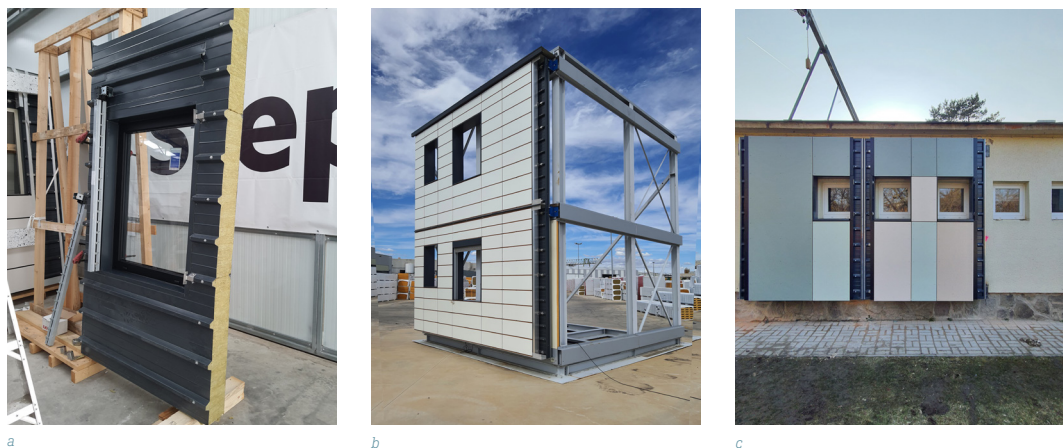


FIG. 7 Full-scale demonstration of the PnP module at three levels. a) preliminary module prototype; b) full-scale façade prototype; c) façade prototype in a real environment.

The prototyping phase is a physical demonstration of the scenarios virtually explored with the set-based design matrix. Hence, for reasons of space, the TPP integration validation addressed in this study are the external cladding, high-performance windows, and solar protection. During the prototyping phase, an active collaboration between technology providers was established to reach the best technical solution. Particularly, the three demonstrators investigated the inter-compatibility of (i) a ventilated façade system developed by a sandwich panel producer: the system enables the integration of different finishes such as perforated sheets, HPL, WPC, wood, and composites through visible or concealed fastening, (ii) a high-performance window composed of aluminium

profiles developed by a company specialised in façades and curtain wall manufacturing, and (iii) an aluminium folding shutter developed by a company specialised in the production of solar protection solutions. The shutter can be oriented from 0° to a maximum of 115° and can be moved up and down until achieving total closure. The results of the prototyped TPP integration in the PnP module are reported in the following paragraphs.

#### 4.1 FIRST LEVEL OF DEMONSTRATION: THE PRELIMINARY PROTOTYPE

The first level of prototyping aimed at addressing the feasibility of the set of solutions investigated in a virtual environment following the set-based methodology. This phase has been a crucial step to deepen the inter-compatibility between the TPPs and components, solving many technical issues. Only a portion of the PnP module has been used to focus mainly on the interface between the substructure and sandwich panel, with first the high-performance window and then the sun shading system. The physical dimensions of the PnP module were 1.3 meters in width and 2.2 meters in height. The LSF structure and the sandwich panel have been assembled on a horizontal working station, as shown in FIG 8.



FIG. 8 Preliminary prototype: a) LSF structure on horizontal working station; b) Assembling the PnP module on the horizontal working station; c) Lifting of the module vertically once preassembled.

The first TPP integration consisted of prototyping the window allocation in the structure and sandwich panel layer (Scenario B1). A designed aluminium frame attached to the steel sheets of the sandwich panel made it easy to install the high-performance window since the sandwich panel's technical characteristics allow the window's load. The second TPP integration prototype consisted of the integration of the sun shading system. Here, some shortcomings were identified. One major issue was the lack of information about the main production and workability features of each TPP. Without this information, the design team was unable to detect potential technical incompatibilities between the different components, given that the goal was to produce the PnP module in an industrialised manner. The first attempt supposed the integration of the sun shading system in the structure and sandwich panel layer (Scenario C2). Although the connection was possible, the aesthetic and functional result was deemed insufficient. Particularly, it was impossible to easily hide the blinds inside the sandwich panel when they were not all the way down, thus impacting the quantity of light entering the existing building's window. This issue highlighted the need for a more thorough analysis of the TPP integration process to ensure seamless compatibility between the technologies. Additionally, it emphasised the importance of considering both functionality, aesthetics, and feasibility in the integration of TPP in the PnP module to smooth the industrialisation process and meet the desired standards.

Considering the above, the integration of the sun shading system inside the air and substructure layer has been addressed with a second prototype (Scenario C1). This prototype successfully achieved the desired aesthetic and functional results by allowing for easy concealment of the blinds when they are not in use. However, there was the need to study an anchoring system for the sun shading system to ensure compatibility with the sandwich panels' ribs; such a system was not available in the market. The need to study an anchoring system for the sun shading system suggests that the TPPs selected should allow modifications or at least be flexible in case some adjustments are needed. The exploration of these three scenarios revealed the significance of close collaboration between the design team, manufacturers, and suppliers of TPPs. The more accurate the technical information on the TPPs, the more precise the integration into the PnP modular system. When the 3D drawings were not detailed enough, some critical intersections had to be solved during the prototyping phase. By involving all stakeholders early in this process, technical constraints have been addressed, leading to more effective solutions and smoother integration of the different products.



FIG. 9 Preliminary prototype: a) Integration of aluminium folding shutter in PnP module; b) Integration of high-performance window in PnP module.

## 4.2 SECOND LEVEL OF DEMONSTRATION: FULL-SCALE FAÇADE PROTOTYPE

While the first level of demonstration has been used for the decision-making process in the early TPP integration attempts in the PnP module, the second level of prototyping aims at deepening both the production phase and the installation phase of a PnP module with a higher integration level, including three TPPs. Six complete PnP modules, integrated with high-performance windows, an aluminium folding shutter sun shading system, and an external cladding in HPL, have been produced to be installed on a sample structural frame which simulates an optimal condition for an existing building. This prototype aims to identify the potential issues and challenges that may arise during the production, transportation, and installation phases of a complete PnP module. This is crucial to enable necessary adjustments for a smoother industrial implementation and allow upscaling of the solution.



FIG. 10 Demonstration prototype: a) Assembly of TPP in the PnP using a vertical working station; b) Movement of the PnP module using a crane; c) Final asset of the prototype; d) Detail of window and sun shading integration.

Regarding the production phase of the modules, some shortcomings have been identified. During this activity, the workers found it uncomfortable to assemble the module on a horizontal working station since it was impossible to easily view the whole module assembly at once, resulting in poor aesthetic quality. Moreover, the horizontal assembly of the integrated PnP module and the following repositioning to place it on the transportation frames, again followed by installing it on the building in two modules, caused misalignments of the external cladding. Despite the difficulties listed above, the installation of the PnP modules with the anchoring systems on the existing structure was smooth, and the six modules were installed in three hours without any major issues.

The main outcome of this phase was the validation of strategies to enhance efficiency in module assembly by developing a new vertical working station on which the entire module can be assembled to streamline the process and favour the industrialisation of the PnP module (see FIG. 10 a). Moreover, to speed up the installation phase, the definition of design limitation dimensions of the modules as 2.5 metres in width and 3.7 metres in height was validated. However, an optimisation strategy must be developed to limit unnecessary movements and prevent potential damages during the installation phase. Overall, this initial prototype has provided valuable insights into simulating at an early stage the real production and installation conditions. Further refinement and demonstrations of the installation process are required to minimise any potential difficulties that may arise through a complete full-scale building application of this new technology on a large scale.

#### 4.3 THIRD LEVEL OF DEMONSTRATION: PROTOTYPE IN A REAL ENVIRONMENT

The last demonstration level is the final prototype, which implies the installation of the PnP system on a real case study application, a kindergarten in Budapest in need of deep renovation. In this study, the objective is to highlight the transition from the design of the system to its construction, addressing mainly the benefits and shortcomings identified in the production and installation phases. The case study building was chosen to showcase the adaptability of the PnP module in interacting with the existing large windows left in the existing building envelope. By selecting a building with a high ratio of transparent and opaque parts, the study aimed to evaluate how well the module could seamlessly integrate with existing geometry.



FIG. 11 Final prototype: a) Placement of the anchoring system on the existing building structure; b) Transportation and installation of the PnP module; c) Final façade configuration after the renovation with the PnP module.

Additionally, this comprehensive analysis allowed for an assessment of the time required to produce a high number of modules, thus providing valuable insights in terms of time and technical feasibility of the technology's scalability and its industrialisation process. For the renovation intervention, 38 PnP modules have been produced to cover a façade area of 200 m<sup>2</sup>. According to the façade's characteristics, the PnP module has been designed with different dimensions, varying from 1.3 m and 2.5 m in width and from 2.6 m and 3 m in height due to dimension limitations in the transportation phases. The production phase of the modules lasted three weeks, considering the off-site production of the sandwich panels and light steel frame structures and the assembly of the complete integrated module by a working team of six people. One of the outcomes of this stage is that the developed vertical working station for module production requires specialised workers able to handle lifting platforms and install ventilated façade technologies.

In this context, the transportation phase strategy has been tested as well. The modules have been placed on a wooden structure designed to carry two modules at a time, already placed vertically and ready to be lifted for the installation. The placement of the module allowed a smooth transportation phase in terms of space used for the shipment in the truck, ensuring a safe and time-efficient delivery of the modules. During the prototyping phase in a real environment, a deep study of the A1 and B2 scenarios mentioned above has been done. Besides the integration of an HPL cladding in the PnP module (scenario A1), there was a need to investigate the scenario involving the direct interaction between a new prefabricated façade system and a window left in the existing building (scenario B2). This scenario is one of the most challenging to address in terms of its implementation since the objective is to prevent thermal bridges and air infiltrations, which can compromise the thermal efficiency of the PnP module. In this specific case, the window intradoses were not industrialised and had to be resolved on-site. The fitting between the dimensions of the current window openings and those of the PnP module was difficult in this case. Considering this, it is essential for the success of the renovation intervention that the technology provider and the architects work together to develop a shared solution to avoid additional costs and on-site time.

Regarding the installation phase, the importance of a preliminary geometry definition of the existing building must be highlighted. An architectural survey plays a crucial role in ensuring the measurements of the existing building. It helps identify potential obstacles or irregularities in the existing geometry that may impact the installation process. By combining the data from the laser scanning and architectural survey, a comprehensive understanding of the site's conditions can be achieved, enabling a seamless and efficient installation of the modules.

## 5 DISCUSSION AND CONCLUSIONS

An instant paradigm change is required to commit to the urgent energy efficiency frontiers with affordable solutions that can revolutionise the deep renovation market. In this context, the role of industrialised systems is recognised as a key towards the upscaling of the solutions. The deep renovation solution presented in this study is a Plug-and-Play (PnP) façade module which integrates existing third-party products (TPPs) already available in the market. This strategy aims at providing a solution which relies on high-level industrialisation, resulting in an off-site façade system whose configuration can be customized according to the project's requirements. However, while significant progress has been made in the development of PnP façades, their complexification due to the integration of many energy conservation measures has hindered products being available on the market.

Considering the above, the study proposes the application of a set-based design methodology to facilitate and coordinate the design phase of a PnP module integrated with TPPs already available in the market. The integration of TPPs in the PnP module is investigated with a scenario approach through a set-based design matrix. The set-based design approach aims to investigate and understand the inter-compatibility between different TPPs, thus minimising feasibility issues by predicting technical requirements and 3D models. Once a set of design solutions has been explored during the theoretical phase, the study proposes a further step to demonstrate the effective feasibility of the designed solutions by realising the three levels of prototypes.

Starting from a core technology of the PnP module, composed of a light steel frame structure, a sandwich panel, and an anchoring system, the proposed methodology sets solid bases for smooth TPP integration. The set-based design methodology allows the exploration of TPPs integration scenarios, including external claddings, high-performance windows, sun shading systems, PV panels and demand-controlled ventilation systems. The evidence from this proposed application of the set-based design approach suggests effective possible customisation through a wide set of different configurations that are easy to assemble. With this objective in mind, the set-based design methodology was used as a tool to improve the coordination and sharing of knowledge between different companies and developers of building components, facilitating the detection of potential technical limitations already in the design phase.

The demonstration phase of the proposed set-based design approach suggests that successful integration of TPPs in the PnP module requires an effort in the early stage of technology selection. To allow easy and industrial-oriented production of the integrated PnP module, the selected TPPs should allow modifications or at least be flexible in case some adjustments are needed. The exploration of different scenarios of TPP integration through iterations on preliminary prototyping revealed the significance of precise technical details as well as the importance of close collaboration between the design team, manufacturers, and suppliers of TPPs towards a smoother integration of the different products. While the first level of demonstration was used for the decision-making process in the early TPP integration attempts in the PnP module, the second level of prototyping deepened the production and installation phase of the designed integrated module. Further refinement and demonstrations of the installation and production process have been reached through the development of the prototype in a real environment, highlighting the transition from the design to construction. The case study building was chosen to showcase the adaptability of the PnP module, simulating some scenarios identified in the set-based design matrix, allowing a better understanding of how the PnP module can be integrated into different architectural designs, validating its potential for widespread use in construction projects.

Although the study aims to boost the renovation wave in the European context by demonstrating a PnP façade system as a result of a broad research-based design study, further considerations for future research are needed. To allow the market breakthrough and the boost of these technologies, the authors want to focus the reader's attention on two main topics: performance assessment and economic evaluations. The final validation of such complex systems must include testing their mechanical, fire, air and water tightness, acoustic, and thermal performances to permit qualification and commercialisation. As the combination of different components cannot be studied by harmonised testing procedures, this verification must be part of the process to ensure the safety and reliability of the systems. Considering their market position, other parameters must be quantified as well in comparison with existing building technologies for renovation. Further studies are recommended to evaluate the costs related to the design, production, and installation phases of the PnP modules in comparison with traditional construction systems are suggested.

Starting from this methodology as a theoretical background, more TPPs could be integrated into the PnP module and tested in building demonstrators to further develop the set-based design methodology. Based on this work, the constitution of a "technology-provided consortium" will be proposed in collaboration with producers of third-party technologies that complement the PnP module. The consortium aims to enhance the interaction between third-party providers to develop modular solutions. Additionally, it might offer a mutually advantageous arrangement for prominent technology producers, enabling them to provide their customers with direct access to a comprehensive array of solutions while simultaneously promoting an open innovation environment for the technological advancement of off-site building envelopes. Considering the evidence of this study, further research should deepen the application of set-based design methodology in an informed environment. Through more detailed digital models of the integrable TPPs, the design integration process could be seamlessly implemented and validated in a BIM environment, allowing the exchange not only of geometrical information but also performance ones, opening the perspectives for the application of PnP integrated modules in new buildings.

### Acknowledgements

---

The content presented in this contribution is the result of close collaboration between various research partners. Acknowledgements belong to MANNI GROUP for the technical design of the Plug-and-Play (PnP) module and the building of all the full-scale prototypes and ISOPAN for providing the sandwich panels; GRADERMETIC and COPERMO for providing the solar protection system and the high-performance windows integrated into the full-scale prototypes, respectively.

The authors would like to thank the StepUP consortium for their contributions to the project development. Specifically, acknowledgements belong to Giulia Barbano, Anna Batallé, UniSMART and Eurecat for setting up the third-party products' selection protocol on which this work relies.

### Fundings

---

This work has been developed in the context of the StepUP project, which received funding from the European Union's Horizon 2020 research and innovation programme under grant agreement no. 847053.

## References

---

- Breakthrough Solutions for Adaptable Envelopes for Building Refurbishment Project Information Summary of the Context and Overall Objectives of the Project. | BRESAER Project | Fact Sheet | H2020 | CORDIS | European Commission. Retrieved February 26, 2023 (<https://cordis.europa.eu/project/id/637186>).
- Building Energy Renovation through Timber Prefabricated Modules | BERTIM Project | Fact Sheet | H2020 | CORDIS | European Commission. Retrieved February 26, 2023 (<https://cordis.europa.eu/project/id/636984>).
- Plug-and-Play Product and Process Innovation for Energy-Efficient Building Deep Renovation | P2Endure Project | Fact Sheet | H2020 | CORDIS | European Commission. Retrieved February 27, 2023 (<https://cordis.europa.eu/project/id/723391/it>).
- Robust and Reliable Technology Concepts and Business Models for Triggering Deep Renovation of Residential Buildings in EU | 4RinEU Project | Fact Sheet | H2020 | CORDIS | European Commission. Retrieved February 27, 2023 (<https://cordis.europa.eu/project/id/723829/it>).
- Basso, P., Mililli, M., Herrero, F. J. M., Sanz, R., & Casaldiga, P. (2017). E2VENT - Design and integration of an adaptable module for residential building renovation. *Journal of Facade Design and Engineering*, 5(2), 7–23. <https://doi.org/10.7480/jfde.2017.2.1678>
- Batallé, A., Masip, D., Ràfols, I., Lupi, M., & Donnerup, M. V. (2022). Deliverable D2.5: StepUP Plug&Play Protocol. Retrieved from <https://www.stepup-project.eu/download/d2-5-stepup-plugplay-protocol/?wpdmdl=3108&refresh=647b272b-9b04e1685792555>
- Capeluto, G. (2019). Adaptability in envelope energy retrofits through addition of intelligence features. *Architectural Science Review*, 62(3), 216–229. <https://doi.org/10.1080/00038628.2019.1574707>
- Colajanni, S., Rotilio, M., Di Santo, N., & Marrone, G. (2022). ACTIVE HOUSE PROTOCOL APPLICATION IN MEDITERRANEAN CLIMATE An energy-efficient kindergarden in Coppito | APPLICAZIONE DEL PROTOCOLLO ACTIVE HOUSE IN CLIMA MEDITERRANEO Un asilo ad alta efficienza energetica a Coppito. *Sustainable Mediterranean Construction*, 2022(15), 75–80.
- Correia Lopes, G., Vicente, R., Azenha, M., & Ferreira, T. M. (2018). A systematic review of Prefabricated Enclosure Wall Panel Systems: Focus on technology driven for performance requirements. *Sustainable Cities and Society*, Vol. 40. <https://doi.org/10.1016/j.scs.2017.12.027>
- D'Oca, Ferrante, Ferrer, Pernetti, Gralka, Sebastian, & Op't Veld. (2018). Technical, financial, and social barriers and challenges in deep building renovation: Integration of lessons learned from the H2020 cluster projects. *Buildings*, 8(12). <https://doi.org/10.3390/buildings8120174>
- Dall'O, G., Galante, A., & Pasetti, G. (2012). A methodology for evaluating the potential energy savings of retrofitting residential building stocks. *Sustainable Cities and Society*, 4(1). <https://doi.org/10.1016/j.scs.2012.01.004>
- Du, H., Huang, P., & Jones, P. (2019). Modular facade retrofit with renewable energy technologies: The definition and current status in Europe. *Energy and Buildings*, Vol. 205. <https://doi.org/10.1016/j.enbuild.2019.109543>
- European Commission. (2018). Directive (EU) 2018/844. Official Journal of the European Union.
- European Commission. (2020). European green deal: Circular economy action plan for a cleaner and more competitive Europe. European Union.
- European Parliament. (2018). DIRECTIVE (EU) 2018/2002 on Energy Efficiency. Official Journal of the European Union, 328(October 2012).
- Gervásio, H., Santos, P., Da Silva, L. S., & Lopes, A. M. G. (2010). Influence of thermal insulation on the energy balance for cold-formed buildings. *Advanced Steel Construction*, 6(2), 742–766.
- Haigh, L., Wit, M. de, Daniels, C. von, Collorichio, A., Hoogzaad, J., Fraser, M., ... Heidtmann, A. (2021). The Circularity Gap Report 2021. In *Circle Economy*.
- Inoue, M., Takahashi, M., & Ishikawa, H. (2013). A design method for unexpected circumstances: Application to an active isolation system. 20<sup>th</sup> ISPE International Conference on Concurrent Engineering, CE 2013 - Proceedings. <https://doi.org/10.3233/978-1-61499-302-5-155>
- Kieran, S., & Timberlake, J. (2004). *Refabricating ARCHITECTURE: How Manufacturing Methodologies are Poised to Transform Building Construction*. McGraw-Hill Education. Retrieved from <https://books.google.it/books?id=PkxQKyGxe2cC>

- Li, Y., & Chen, L. (2022). Investigation of European modular façade system utilizing renewable energy. *International Journal of Low-Carbon Technologies*, 17, 279–299. <https://doi.org/10.1093/ijlct/ctab101>
- Marrone, G., Sesana, M. M., & Imperadori, M. (2023). Life-cycle assessment of light steel frame buildings: A systematic literature review. In F. Biondini & D. M. Frangopol (Eds.), *Life-Cycle of Structures and Infrastructure Systems: PROCEEDINGS OF THE EIGHTH INTERNATIONAL SYMPOSIUM ON LIFE-CYCLE CIVIL ENGINEERING (IALCCE 2023), 2-6 JULY, 2023, POLITECNICO DI MILANO, MILAN, ITALY (1<sup>st</sup> ed.)* (pp. 2405–2412). CRC Press. <https://doi.org/10.1201/9781003323020-293>
- Negrão, L. L. L., Godinho Filho, M., & Marodin, G. (2017). Lean practices and their effect on performance: a literature review. *Production Planning and Control*, 28(1). <https://doi.org/10.1080/09537287.2016.1231853>
- Op't Veld, P. (2015). MORE-CONNECT: Development and advanced prefabrication of innovative, multifunctional building envelope elements for modular retrofitting and smart connections. *Energy Procedia*, 78. <https://doi.org/10.1016/j.egypro.2015.11.026>
- Parrish, K. D. (2009). Applying a Set-Based Design Approach To Reinforcing Steel Design.
- Piaia, E., Turillazzi, B., Longo, D., Boeri, A., & Giulio, R. Di. (2019). Plug-and-Play and innovative process technologies (Mapping/Modelling/Making/ Monitoring) in deep renovation interventions. *Techné*, (18), 215–225. <https://doi.org/10.13128/techné-7533>
- Sarihi, S., Mehdizadeh Saradj, F., & Faizi, M. (2021). A Critical Review of Façade Retrofit Measures for Minimizing Heating and Cooling Demand in Existing Buildings. *Sustainable Cities and Society*, 64. <https://doi.org/10.1016/j.scs.2020.102525>
- Sebastian, R., Gralka, A., Olivadese, R., Arnesano, M., Revel, G. M., Hartmann, T., & Gutsche, C. (2018). Plug-and-Play Solutions for Energy-Efficiency Deep Renovation of European Building Stock. 1157. <https://doi.org/10.3390/proceedings2151157>
- Serugga, J., Kagioglou, M., & Tzortzopolous, P. (2020). A utilitarian decision-making approach for front end design-a systematic literature review. *Buildings*, Vol. 10. <https://doi.org/10.3390/buildings10020034>
- Simões, I., Simões, N., Santos, I., Brett, M., Tadeu, S., & Silva, H. (2019). Energy and sustainable performance of a multifunctional façade. *WIT Transactions on Ecology and the Environment*, 237, 51–61. <https://doi.org/10.2495/ESUS190051>
- Singer, D. J., Doerry, N., & Buckley, M. E. (2009). What is set-based design? *Naval Engineers Journal*, 121(4). <https://doi.org/10.1111/j.1559-3584.2009.00226.x>
- Sobek, D. K., & Ward, A. C. (1996). Principles from toyota's set-based concurrent engineering process. *Proceedings of the ASME Design Engineering Technical Conference*, 4. <https://doi.org/10.1115/96-DETC/DTM-1510>
- Toche, B., Pellerin, R., & Fortin, C. (2020). Set-based design: A review and new directions. *Design Science*. <https://doi.org/10.1017/dsj.2020.16>
- Torres, J., Garay-Martinez, R., Oregi, X., Torrens-Galdiz, J. I., Uriarte-Arrien, A., Pracucci, A., Cea, A. M. (2021). Plug and play modular façade construction system for renovation for residential buildings. *Buildings*, 11(9). <https://doi.org/10.3390/buildings11090419>
- United Nations. (2022). 2022 Global Status Report for Buildings and Construction. Retrieved from [www.globalabc.org](http://www.globalabc.org).
- Van Oorschot, J., Di Maggio, M. S., Op 't Veld, P., & Tisov, A. (2022). Boosting the Renovation Wave with Modular Industrialized Renovation Kits: mapping challenges, barriers. Retrieved from <https://circulareconomy.europa.eu/platform/en/knowledge/boosting-renovation-wave-modular-industrialized-renovation-kits-mapping-challenges-barriers-and-solution-strategies>
- Veld, P. O. t. (2015). MORE-CONNECT: Development and Advanced Prefabrication of Innovative, Multifunctional Building Envelope Elements for Modular Retrofitting and Smart Connections. *Energy Procedia*, 78, 1057–1062. <https://doi.org/10.1016/J.EGYPRO.2015.11.026>

# Off-site prefabricated hybrid façade systems

A holistic assessment

**Ioannis A. Atsonios<sup>1\*</sup>, Emmanouil Katsigiannis<sup>1</sup>, Andrianos Koklas<sup>1</sup>, Dionysis Kolaitis<sup>1</sup>, Maria Founti<sup>1</sup>, Charalampos Mouzakis<sup>2</sup>, Constantinos Tsoutis<sup>3</sup>, Daniel Adamovský<sup>4</sup>, Jaime Colom<sup>5</sup>, Daniel Philippen<sup>6</sup>, Alberto Diego<sup>7</sup>**

\* Corresponding author: atsoniosgiannis@central.ntua.gr

1 Laboratory of Heterogeneous Mixtures and Combustion Systems, School of Mechanical Engineering, National Technical University of Athens, Zografou, Greece.

2 Laboratory for Earthquake Engineering, School of Civil Engineering, National Technical University of Athens, Zografou, Greece

3 Proigmenes Erevnitikes & Diahiristikes Efarmoges (AMSolutions), Acharnes, Greece

4 University Centre for Energy Efficient Buildings, Czech Technical University in Prague, Bustehrad, Czechia

5 Denvelops, Arquitectura y planificación, Igualada, Cataluña / Catalunya, Spain

6 University of Applied Sciences HSR, SPF Institute for Solar Technology, Rapperswil-Jona, Switzerland

7 Product Quality Department, Catalonia Institute of Construction Technology (ITeC), Barcelona, Spain

## Abstract

*The residential sector is responsible for the largest share of global energy consumption, while the existing building stock in Europe is relatively old. This issue, in combination with the low rate of new constructions, highlights the necessity for deep renovation of existing buildings to reach NZEB standards. At the same time, in the last decades, off-site prefabricated solutions have gained popularity in the building market, allowing the reliable and effective integration of diverse components and reducing the total renovation cost and occupants' disturbance. The current study describes three all-in-one "Plug & Play" prefab renovation solutions and their assessment in terms of thermal, static, acoustic, and fire performance. The assessing performance is selected depending on their incorporated element as well as the national regulations of the country where the renovation solution is going to be installed. The assessment aims to ensure their characteristics' satisfaction with the European and national requirements. In parallel, the assessment identifies the accurate behaviour of prefab façade systems both in passive and active mode and improves/optimises any possible design drawbacks.*

## Keywords

*deep renovation, prefabricated façade, structural performance, thermal performance, fire performance*

## DOI

<http://doi.org/10.47982/jfde.2023.2.A1>

# 1 INTRODUCTION

The European Commission established the European Green Deal as a policy initiative for Europe to become a climate-neutral continent by 2050. The Energy Performance of Buildings Directive (EPBD), as part of the EU Green Deal, is key to achieving the EU's goals of reducing energy consumption in buildings, which accounts for 40% of energy consumption and 36% of total greenhouse gas emissions in the EU (European Commission, *In focus: Energy efficiency in buildings*, 2020). Since 85-95% of the existing buildings will be standing in 2050 (Maduta, Melica, D'Agostino, & Bertoldi, 2022) and roughly 75% of the European building stock is estimated to be energy-inefficient (European Commission, *In focus: Energy efficiency in buildings*, 2020), the renovation of buildings with energy efficient solutions is a viable and feasible measure for achieving the European energy goals.

The required annual renovation rate has to be 3%, with deep renovations accounting for 70% of the total, to achieve climate neutrality by 2050 (BPIE, *On the way to a Climate-Neutral Europe: Contributions from the building sector to a strengthened 2030 climate target*, 2022). However, the annual renovation rate in Europe is below 1%, of which only 0.2% concerns deep renovation (Filippidou, Nieboer, & Visscher, 2017). These low rates are due to the high cost of renovation solutions, the long duration of work, and the occupant disturbance. In this context, the application of prefabricated modular building elements constitutes an innovative way for a deep renovation of existing buildings, reducing the renovation cost and time while at the same time minimising occupant disturbance (Pihelo, Kalamees, & Kuusk, 2017) (Masera, Iannaccone, & Salvalai, 2014). In prefabrication technologies, the design, manufacturing, and assembling of the building components take place in a specialised industrial environment before their installation at the final construction site (Kamali & Hewage, 2016). The concept of prefabricated building elements is fast construction with fewer resources (Naji, Çelik, Alengaram, Jumaat, & Shamshirband, 2017).

Recently, off-site hybrid prefabricated façade systems, which combine highly efficient insulation façade panels integrated with HVAC and renewable harvesting systems, are an upcoming topic for research, innovation development and policymakers (Du, Huang, & Jones, 2019). Combining innovative HVAC components with renewable energy systems constitutes a cost-efficient all-in-one solution for the renovation of a building towards nearly zero energy building (NZEB) status with significant cost, time, material, and waste savings (Torres, et al., 2021). Several such all-in-one deep renovation façade solutions have been explored and developed within EU-funded research projects demonstrating the extended work done to reach NZEB state after the renovation (D'oca, et al., 2018), such as MORE-CONNECT, BERTIM, E2VENT, iNSPiRe, and 4RinEU. In some cases, prefabricated modules combine HVAC units and integrated RES that are designed as a prefabricated box, while in other cases, the HVAC and energy harvesting systems are incorporated into the wall assembly (Katsigiannis, et al., 2022).

It is vital for these underdeveloped off-site hybrid prefabricated façade systems to be in line with the European and national/regional regulatory requirements in order to penetrate the market. The European Union has put in place a comprehensive legislative and regulatory framework for the construction sector. Health and safety in construction and the free movement of engineering/construction services and products are important policy priorities. However, there is a lack of regulatory framework regarding the installation of prefabricated elements/façades and, in general, kits that combine structural parts with electromechanical equipment because this renovation concept is relatively new. The most relevant regulation regarding hybrid prefabricated façade systems is the Construction Products Regulation (CPR). The objective of the CPR is to achieve the proper functioning of the internal market for construction products by establishing harmonised

rules on how to express their performance. The key points of the CPR are: a) to set out the conditions for the marketing of construction products, and b) to set out methods and criteria for assessing and expressing the performance of construction products and the conditions for the use of CE marking. CPR establishes seven basic requirements for construction works: a) mechanical resistance and stability, b) safety in case of fire, c) hygiene, health and the environment, d) safety and accessibility in use, e) protection against noise, f) energy economy and heat retention, and g) sustainable use of natural resources.

Despite the large number of EU projects that develop modular and industrialised prefabricated renovation solutions, there are still many barriers that hamper speeding up market uptake, such as performance verification and the mistrust for the performance of innovative components (Oorschot, Maggio, Veld, & Tisov, 2022). The current study presents the methods that are followed to verify the structural, thermal, and fire performance of three off-site hybrid prefabricated deep renovation façade systems that are developed in the frame of the PLURAL EU funding project (PLURAL EU project, 2020-2024). Each façade system is planned to be installed in a different EU country (Greece, Spain, and the Czech Republic). Selected performance assessment methods of façade systems are implemented to identify their accurate behaviour and to ensure and verify the satisfaction of their characteristics with the European and national requirements. The structural performance of façade panels is investigated in terms of the analysis of their anchoring system or the seismic resistance, where necessary, while the fire performance analysis is carried out in terms of reaction to fire tests. The thermal performance is assessed by calculating all incorporated thermal bridges and the equivalent thermal transmittance of façade panels and investigating the impact of the embodied HVAC systems on thermal transmittance when they are in operation (active mode) and stopped (passive mode).

## 2 DESCRIPTION OF PREFABRICATED FAÇADES

The present study assesses three different off-site prefabricated hybrid façade systems developed in the frame of the PLURAL project: the SmartWall, the Denvelops Comfort Wall, and the ConExWall (Adamovský, et al., 2022).

### 2.1 SMARTWALL

SmartWall is a multifunctional façade system that combines active with passive technologies developed by AMS (AMS coatings and advanced materials, 2023). The concept of SmartWall is to integrate various prefabricated elements (such as windows, doors, and balcony doors) and a wide range of HVAC technologies (e.g. fan coils, split units, air ducting systems, radiators, and convectors) in order to reduce installation time and construction faults during installation. It is a compact, versatile prefabricated façade panel which can be installed externally or internally (in case there are space or aesthetic restrictions) in existing building envelopes, introducing an innovative, dynamic, and flexible retrofitting solution (Katsigiannis, et al., 2022). The SmartWall is easily adjustable to any dimension up to 4 m of height per panel and can be decorated with any kind of finishing material.

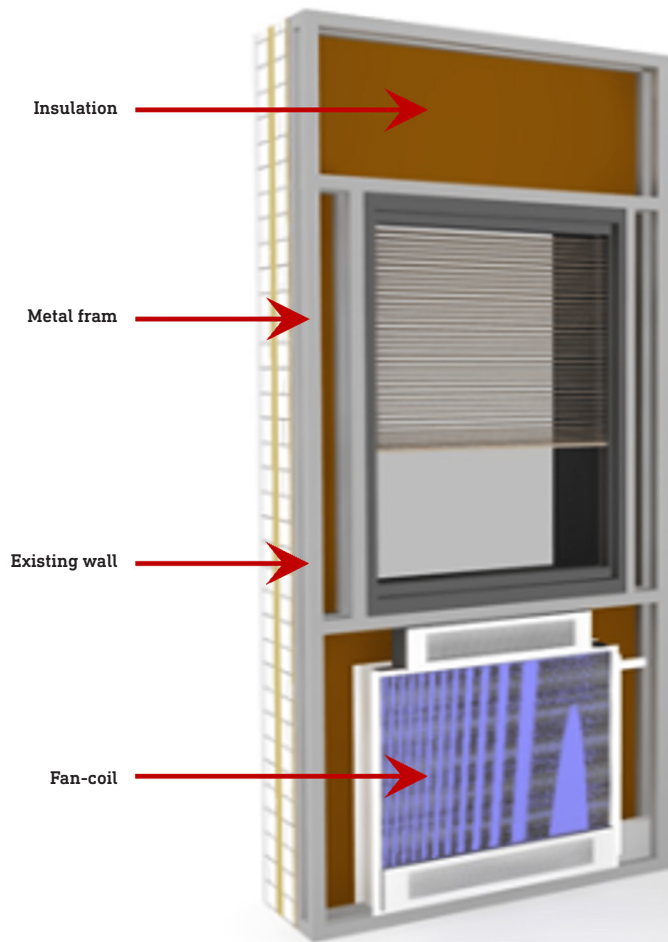


FIG. 1 The concept of SmartWall

The general concept of the SmartWall is presented in FIG. 1 (Katsigiannis, et al., 2022). The basic material for the frame is steel S245, using lightweight 50 x 50 mm members welded in a frame. The concept allows for the design and manufacture of a large variety of panel sizes with various frame strength to accommodate the multitude of materials and technologies that can be integrated into the SmartWall. The basic insulation material is mineral wool, but several alternatives can be used (rockwool, glass wool, EPS, cellulose). Finishing surfaces differ according to the use of the façade system in interior or exterior position, while a large variety of boards containing cement, gypsum, fibre, timber, etalbond®, etc. can also be utilised. The SmartWall is constructed containing flexible piping and electrical wiring connections that can accommodate either the existing or a new heating/cooling system and electrical services (switches, plugs, etc.), which significantly reduces on-site installation time. Photovoltaics can be part of the external SmartWall or can be installed on the roof of the building if the geometry includes balconies or volumes that shade the vertical external surfaces. FIG. 2 illustrates the four different configurations of SmartWall:

- Type A – The module contains no fan coil or window (Blank Type).
- Type B - The module contains a slim type fan coil, but it does not contain any windows.
- Type C - The module contains a window, but it does not contain any fan coils.
- Type D - The module contains both a fan coil and a window.

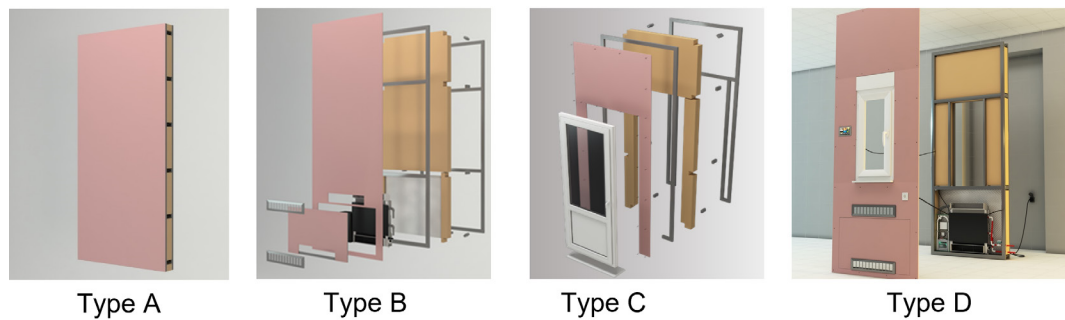


FIG. 2 Four different SmartWall configurations

In the present study, the materials of the SmartWall are anchored on two frames made by Hollow Rectangular Section (HRS) structural steel members with sections of 50x30 mm and 1.8 mm thick. Spacers made by the heat breaker structure are placed in the fixing points to ensure movement treatment, except on the bottom side, where the spacers are made from the HRS frame for structural reasons. The space between the frames (160 mm width) is filled with mineral wool. A gypsum board layer (12.5 mm thick) covers the internal side of SmartWall, while a mineral wool layer with aluminium foil (30 mm thick) is placed on the opposite side that rests against the existing envelope. Moreover, in the cases where the fan coil exists, a Vacuum Insulation Panel (VIP) layer, 20 mm thick, is installed at the back side of the fan coil.

## 2.2 DENVELOPS® COMFORT WALL

The Denvelops Comfort Wall is an off-site prefabricated ventilated façade system composed of vertical stainless-steel guidelines and connectors that allow to attach and bear loads of the cladding (Denvelops, 2022). The cladding system (FIG. 2a) is made of 1 mm thick painted aluminium cladding tiles with resistant powder coating. PV panels are integrated into the façade, locally replacing the final cladding. The thermal insulation is made of mineral wool and is protected by a weathering layer. Both are attached to the system's vertical guidelines in order to achieve the required thermal and water-tightness performance. The mineral wool is covered by a glass-fibre layer that can protect against mechanical damage. Thermal resistance equal to  $2.90(\text{m}^2\cdot\text{K})/\text{W}$  is achieved with a 100 mm thick Denvelops Comfort Wall façade, considered the optimum passive measure.

The Denvelops Comfort Wall contains an innovative HVAC system called Air Handling Unit (AHU) developed by Czech Technical University (Zavřel, Zelenský, Macia, Mylonas, & Pascual, 2022), located in a vertical position. As presented in FIG. 2b, the AHU incorporates two stages of heat recovery: the first is a passive heat exchanger (plate), and the second is an active heat exchanger with thermoelectric modules that provides supply air temperature control. The unit is connected to the interior space via supply and extract channels. The electric power for the thermoelectric modules is derived from the PVs or the grid.

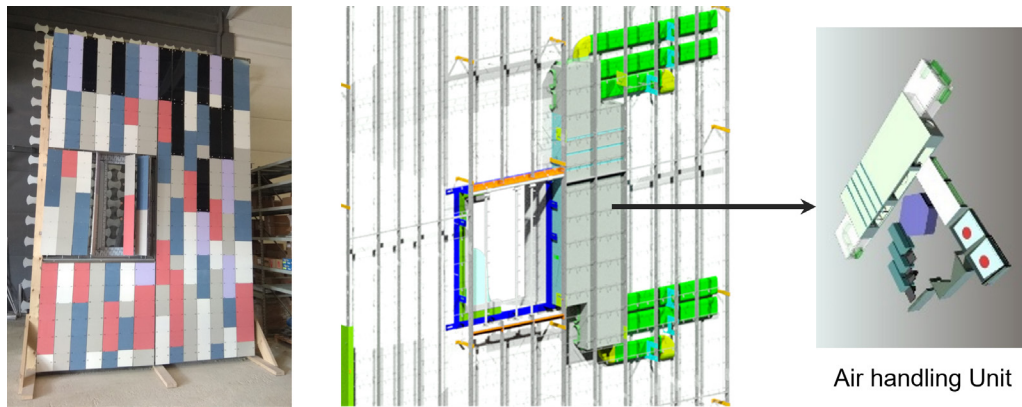


FIG. 3 The Denvelops Comfort Wall façade system

## 2.3 CONEXWALL

The ConExWall is a façade system that integrates a heating/cooling piping system, and it is specifically designed to be used in colder climatic zones, such as alpine and continental locations. The basic configuration of the ConExWall is illustrated in FIG. 4. The fundamental material for the frame is timber because of its low carbon footprint, thermal conductivity avoiding thermal bridges, high flexibility in shape dimensions, and the variety of connection techniques available. The outer layers serve as load-bearing timber and include the main thermal insulation. Its purpose is to ensure the best and maximum contact of the heating/cooling pipes with the existing façade wall accounting for wall irregularities. This enables the element to adapt to uneven sections of the wall (Material: wood fibre, sheep wool, hemp wool, glass and rock wool). The internal side of the ConExWall is a 20 mm layer of wood board with embodied heating pipes and a 60 mm thick flexible layer (Isover Orsik insulation). Next, a layer of 50 mm thick gypsum board is anchored on a timber frame with vertical studs with sections of 180 x 80 mm and stud spacing equal to 750-650 mm. The gap inside the frame is filled with insulation (180 mm thick), while a layer of hard wood insulation (STEICOprotect H) 50 mm thick is anchored on the external side of the frame. A 40 mm thick ventilated timber frame is placed at the external side of the STEICOprotect layer, while a layer of 20 mm thick timber cladding is placed on the finishing layer of the façade panel. The anchoring system of the ConExWall consists of L-shaped (200 x 190 mm and 15 mm thick) metal profiles with a spacing of 1.19 m that penetrates the façade panel and anchors on the existing wall.

The advantage of this heating concept is the thermal activation of the whole existing façade, which allows for using the existing wall as thermal storage. In the case of a heating system with a heat pump and PV, this enables running of the heat pump longer and to higher temperatures during times of excess electricity gains from the PV system, and on the other hand, to run it for shorter times during periods when electricity must be purchased from the electricity grid. Additionally, such an operational mode overcomes the energy shortage delivered to a room, which strongly depends on the opaque external wall area. An integrated control system, utilising an advanced monitoring system, measures weather data, the supply temperature of the heating system, room temperature, and CO<sub>2</sub> concentration and will control the thermal comfort as well as the indoor air quality.

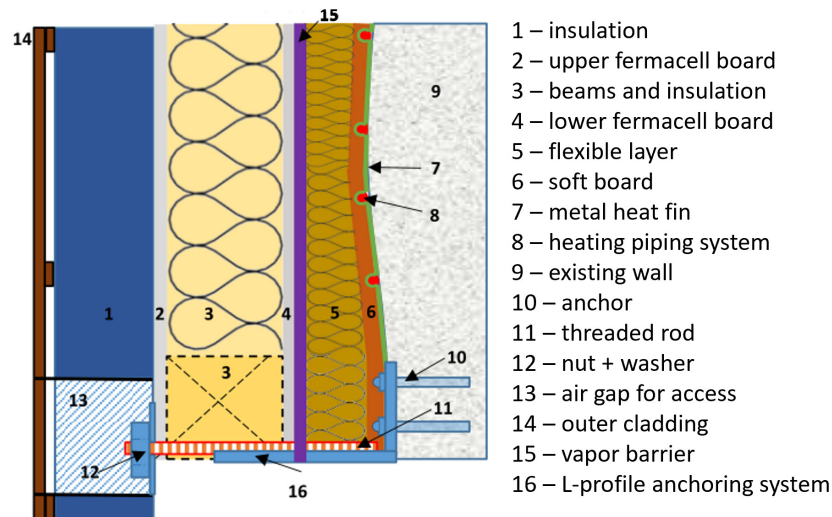


FIG. 4 The ConExWall façade system and its incorporated building elements.

### 3 METHODOLOGY

Each of the previously described prefabricated hybrid façade systems is applied for the renovation of an existing residential building located in a different country with different climate conditions and national building requirements. The SmartWall is implemented in a Greek (Athens), the Denvelops ComfortWall in a Spanish (Terrassa), and the ConExWall in a Czech (Kasava) residential building. The performance in terms of structural, fire and thermal behaviour of each façade system is verified using standardised methods. Each method was selected taking into account the national requirements and the incorporated components. Table 1 summarises the country and the performance assessment method that was carried out for each façade system.

TABLE 1 Application of hybrid system in different countries and the assessment performant tests

Hybrid façade system	Country	Performance Assessment		
		Structural	Fire	Thermal
SmartWall	Greece	Seismic resistance	Reaction to fire test	Equivalent U-value ( $U_{eq}$ ) – Thermal bridges – Impact of HVAC systems
Denvelops Comfort Wall	Spain	Anchoring	No need	
ConExWall	Czechia	Anchoring	No need	

#### 3.1 STRUCTURAL PERFORMANCE ASSESSMENT

FIG. 5 illustrates the European seismic hazard map displaying the ground motion expected to be reached or exceeded with a 10% probability in 50 years, according to Eurocode 8 (Eurocode 8). As indicated on the map, the Spanish and the Czech buildings are located in low-hazard areas, while the Greek building is located in a high-hazard area. For this reason, the verification of

the structural performance of the SmartWall façade system in terms of seismic resistance is mandatory. So, the SmartWall that is planned to be installed in Greece is assessed using the Floor Response Spectrum (FRS) method by conducting seismic shaking table testing (Panoutsopoulou, Meimaroglou, & Mouzakis, 2023).

On the other hand, according to national legislation, ČSN EN 1998-1 for the Czech case and NSCE-02 (NSCE-02) and CTE DB-SE (CTE DB-SE) for the Spanish case, it is not necessary to conduct structural assessment of façade systems in terms of seismic resistance. The structural performance of these façade systems is investigated in terms of the mechanical properties of connections and anchoring systems, self-weight, wind and snow loads, using the Eurocode methods (Eurocode 1, Action on structures – Part 1-1: General actions – Densities, self-weight, imposed loads for buildings).

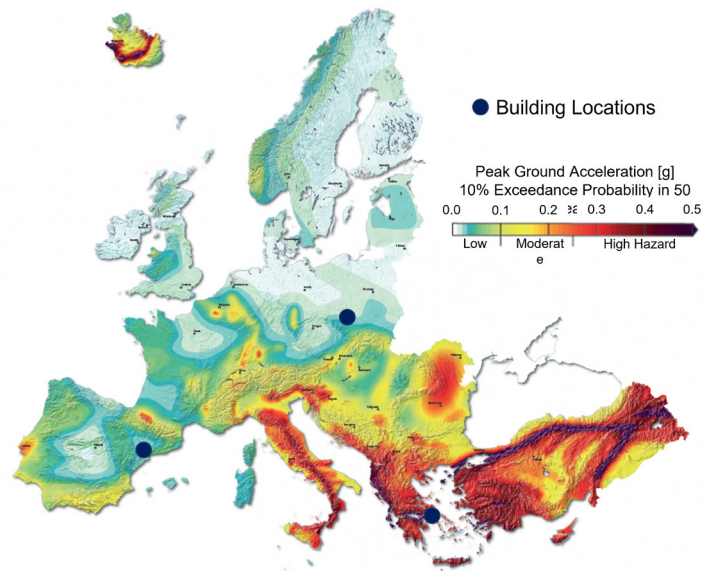


FIG. 5 The European Seismic Hazard Map (European Commission, Mapping Europe's earthquake risk, 2014).

## 3.2 FIRE PERFORMANCE ASSESSMENT

The fire requirements are also dealt with in different approaches for each case, depending on the national requirements, the incorporated materials, and their certifications. The SmartWall façade system, applied in a Greek building, is investigated by performing standard “reaction to fire” tests, following the EN 13823 standard (EN 13823:2020+A1:2022). The results of these tests are used for the classification of the innovative façade system based on EN 13501-1.

This test requires either a corner specimen or two specimens of the examined walls to be joined as a corner. The height of the tested specimen was 1.5 m, while the width was 0.5 m for the short wing and 1 m for the long wing. During the first part of the test procedure, an auxiliary burner is ignited in order to precisely calculate the fire-power level and smoke production of the burner itself. After that, the auxiliary burner is turned off, and the main burner is ignited. The main burner is located at the internal corner of the specimen, providing a steady fire-power level of 30 kW. The duration of the test is 20 minutes, and during this period, the combustion gas products (used to calculate

the heat release rate), the smoke production, and the potential creation of burning droplets are measured. Based on the heat release rate, two main parameters are calculated: the fire growth rate (FIGRA), which is an indication of how fast the maximum heat release rate is achieved and the total heat release 600 s after the fire test initiation ( $THR_{600s}$ ). Equations 4 and 5 are used to estimate the aforementioned parameters.

$$FIGRA = 1000 \times \max\left(\frac{HRR_{av}(t)}{t}\right) \quad 1$$

$$THR_{600s} = \frac{\sum_0^{600}(\max[HRR(t),0])}{1000} \quad 2$$

In addition, two smoke production parameters are calculated with the smoke growth rate (SMOGRA) and the total smoke production 600 s after the fire test initiation ( $TSP_{600s}$ ), according to the following equations:

$$SMOGRA = 10000 \times \max\left(\frac{SPR_{av}(t)}{t}\right) \quad 3$$

$$TSP_{600s} = \sum_0^{600}(\max[SPR(t),0]) \quad 4$$

The criteria for the “reaction to fire” classification are according to the EN 13501-1: 2019 standard (EN 13501-1 : 2019). For the classification of a specimen in a certain category (heat release rate, smoke production, and droplets), both the involved parameters must be within the range; otherwise, it is classified as the worst category.

TABLE 2 EN 13501-1 Classification criteria

		A2/B	C	D	E	s1	s2	s3	d0	d1	d2
Heat release rate	FIGRA	<120	<250	<750	>750	-	-	-	-	-	-
	$THR_{600s}$	<7.5	<15	>15	>15	-	-	-	-	-	-
Smoke production	SMOGRA	-	-	-	-	<30	<180	>180	-	-	-
	TSP	-	-	-	-	<50	<200	>200	-	-	-
Droplets	d < 10s	-	-	-	-	-	-	-	0	>0	>0
	d > 10s	-	-	-	-	-	-	-	0	0	>0

The applicable Spanish regulation CTE DB-SI (CTE DB-SI) establishes requirements on reaction to fire and resistance to fire for external walls. As for reaction to fire, the applicable requirement (class D-s3, d0 for façades up to 10 m height) is met by the individual Denvelops Comfort Wall integrated components and their relevant certification (metallic cladding elements and substructure, mineral wool insulation, etc.). Therefore, it is unnecessary to carry out any additional investigation according to EN 13501-1. As for resistance to fire, the applicable requirement (Integrity & Insulation (EI) - 60 for the external wall as a whole) is already met by the existing wall. The addition of the Denvelops Comfort Wall system does not adversely affect the performance, except for the penetration of the ventilation pipework. In such points, the resistance to fire of the existing external wall is reinstated by the installation of an intumescent fire sealing collar. The resistance to fire performance of the intumescent collar is addressed by its product certification or, at least, by the relevant test according to EN 1366-3 and classification according to EN 13501-2. Therefore, it is unnecessary to carry out any additional test of the Denvelops Comfort Wall system or its components. Finally, the CTE DB-SI does not establish any requirement for large-scale testing for façade elements.

The ConExWall, composed of a commercial basic structure, does not include materials without fire certification (e.g. gypsum boards, insulation) or materials not classified in fire codes (e.g. wood). The ConExWall façade can be installed at an existing wall in two different ways: the basic type and the load-bearing external walls. The basic type is the installation of a façade system as an external insulation complex on an existing external wall. In this case, external walls are constructed from non-flammable materials – typical concrete, bricks, and stones. Fire regulations require load-bearing structures from materials with certain fire resistance, but the ConExWall façade is not a load-bearing structure. The ConExWall only influences fire risk areas, which limit neighbouring buildings. The dimensions of the fire risk area, calculated according to fire protection codes for each specific case, depend on specific layer composition, surface layer (e.g. plaster, wood cladding) and window dimensions. The installation of ConExWall as load-bearing external walls, placed on the uppermost floor, requires specific fire resistance. Fire resistance is achieved by using gypsum board/fiberboard plates from the interior with existing fire. The impact of the façade system on the fire risk area is individually calculated, as in the previous case.

### 3.3 THERMAL PERFORMANCE ASSESSMENT

The thermal performance analysis of the façade systems is carried out following the ISO 10211 (ISO 10211, 2017) methodology, which is a steady-state approach aiming to calculate the equivalent thermal transmittance (U-value) or equivalent thermal resistance (R-value) taking into account all incorporated thermal bridges. The presence of the frame (metal or wooden), the anchoring system, the window or the incorporated heating system into the façade systems creates non-negligible thermal bridges.

The equivalent U-value,  $U_{eq}$ , taking into account the impact of thermal bridges, is calculated by the equation:

$$U_{eq} = U_{clear} + \frac{\sum_k(\Psi_k \cdot l_k)}{A} + \frac{\sum_n \chi_n}{A} \quad 5$$

Where  $U_{clear}$  is the thermal transmittance without the effect of thermal bridges, calculated according to ISO 6946 standard,  $\Psi_k$  expressed in [W/(m·K)] is the linear thermal transmittance of the linear thermal bridges,  $l_k$  [m] is the length over the which the  $\Psi_k$  value applies,  $\chi_n$  expressed in [W/K] is the point thermal transmittance of the point thermal bridges and  $A$  [m<sup>2</sup>] is the total surface of the façade system.

The window frame, if present in a façade panel, is assumed to be made of aluminium, with  $U_f=1.4$ W/(m<sup>2</sup>K), while the glazing system is assumed to be double pane Argon filled with  $U_g=1.2$ W/(m<sup>2</sup>K).

TABLE 3 Boundary conditions for the thermal performance analysis

Boundary Condition	SmartWall	Denvelops Comfort Wall	ConExWall
Outdoor temperature	0° C	-2° C	-15° C
Indoor temperature	20° C	22° C	20° C
External heat transfer coefficient, $h_{out}$		25 W/(m <sup>2</sup> K)	
Internal heat transfer coefficient, $h_{in}$		7.69 W/(m <sup>2</sup> K)	
Temperature of medium	28° C	22° C	25° C

For the calculation of the equivalent thermal transmittance/resistance, each façade system is simulated by means of the commercial CFD package (COMSOL and ANSYS) in steady-state conditions. The boundary conditions are summarised in Table 3.

The total heat flow,  $Q$ , which passes through each façade configuration, is obtained by the simulation results. Hence, the equivalent U-value,  $U_{eq}$ , is calculated by the following equation:

$$U_{eq} = \frac{Q}{A(T_{in}-T_{out})} \quad 6$$

When the HVAC system is active in heating mode, an equivalent thermal transmittance is also calculated following the methodology described in (Kisilewicz, Fedorczak-Cisak, & Barkanyi, 2019). This method takes into account the temperature of the medium fluid, but in the current study, a constant temperature for each system is assumed, as presented in Table 3.

For the geometries, which include window or glass door, the equivalent U-value is calculated by the equation:

$$U_{eq} \cdot A = U_{eq,opWall} \cdot A_{opWall} + U_{Win} \cdot A_{Win} \quad 7$$

Where  $U_{opWall}$  is the equivalent thermal transmittance of the opaque area of the façade, including the effect of all thermal bridges,  $A_{opWall}$  is the opaque area of the façade panel (area without the window opening),  $U_{Win}$  and  $A_{Win}$  are the U-value and the window area (including the glass and the frame), respectively.

## 4 RESULTS / DISCUSSION

### 4.1 SMARTWALL

#### 4.1.1 Structural performance

The structural performance of the SmartWall façade system is investigated with the shaking table test, allowing for proper validation of the structural response under different earthquake tests. A real-scale steel frame structure with a brick masonry infill wall (supporting structure) fitted with SmartWall was tested at the Laboratory for Earthquake Engineering (LEE) of the National University of Athens (NTUA), using the shaking table facility. The SmartWall (FIG. 6a) was fixed to the brick wall using Z-shape steel plates (hanging brackets) at three positions through its height. Additionally, it was anchored to the brick wall with two chemical anchors at the top to ensure no vertical and in-plane movements of the module independent of the infill wall during an earthquake. Thus, the SmartWall is considered an acceleration-sensitive non-structural component, and damage could occur from inertial forces.

The Floor Response Spectrum (FRS) method is used for the analysis of the SmartWall façade. The FRS was calculated for Peak Ground Acceleration (PGA) equal to 0.36 g (highest seismic zone for Greece) and EC8 soil category B for the two horizontal directions, resulting in a 0.86 g peak floor acceleration. The vertical component spectrum was set equal to 0.80 of the horizontal ones. Compatible floor acceleration time histories were generated and used as the input motion.

The characteristic periods of the FRS were chosen to cover floor spectra for buildings with 1 to 10 storeys, and the non-structural component was assumed to be located on the upper floor (roof). This spectrum is considered the Required Floor Response Spectrum (RFRS) for the present study. The acceleration time histories used as base motion were modified from the Landers earthquake that occurred on June 28, 1992, near the town of Landers, California, in order to be compatible with the RFRS.

The specimen was subjected to triaxial ground motion time history with base acceleration increased stepwise corresponding to the different limit states to investigate the response of SmartWall. Prior to and after the execution of the shaking table tests, the dynamic properties of the specimen were measured through logarithmic sine sweep excitation along the X, Y, and Z main axes.



FIG. 6 Structural performance test of SmartWall: a) the experimental set-up and b) the anchoring system

The main conclusions that can be derived from the structural performance test:

- No visible damage is observed in steel members, brick walls, and the SmartWall panel during triaxial shaking table tests.
- For the SmartWall façade system, frequencies and corresponding damping ratios are close to the dynamic characteristics before testing in both horizontal and vertical directions.
- For the brick wall, a reduction of frequency and an increase in damping ratio is found in the X direction. This may be attributed to very light, invisible damages, such as sliding along the bed and head mortar joints, as well as sliding between the brick wall and surrounding steel frame.
- The two chemical anchors (FIG. 6b) used at the top of the SmartWall could withstand the imposed inertial forces for the tested level of base acceleration.
- The selected method of fixing the SmartWall onto the brick wall with Z-shape plates is found to be adequate for the tested level of base motion.

#### 4.1.2 Fire performance

The fire performance of SmartWall is carried out by standard “reaction to fire” tests, following the EN 13823 standard (EN 13823:2020+A1:2022), also known as Single Burning Item (SBI) test. Two different SmartWall types are examined: a) Type A, serving as a “blank type”, was a simple configuration constructed by the metal frame, gypsum plasterboards, and mineral wool (FIG. 7a) and b) Type B corresponded to a SmartWall panel with the fan coil unit (FIG. 7b).

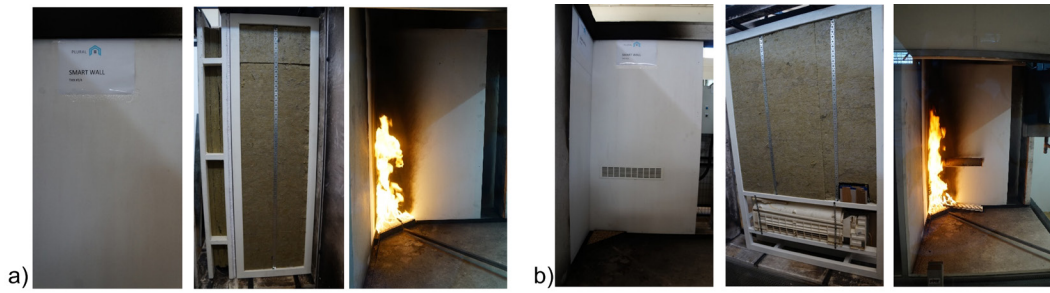


FIG. 7 The examined SmartWall samples (front side, back side and during the test): a) Type A and b) Type B.

Table 4. summarises the results of the standard EN 13823 test. Based on these results and the classification according to EN 13501 (EN 13501-1 : 2019) both the SmartWall Types are classified as B-s1, d0 and have similar behaviour as far as the test is concerned. The presence of a fan coil results in a heat release reduction of 45% in comparison with the blank type of SmartWall, while the smoke production is almost the same.

TABLE 4 EN 13823 results for the examined SmartWall types

Parameter	SmartWall - Type A	SmartWall - Type B	Classification
FIGRA	0.00	0.00	B
THR <sub>600s</sub>	0.79	0.44	B
SMOGRA	0.00	0.00	s1
TSP	43.34	44.85	s1
d < 10s	No	No	d0
d > 10s	No	No	d0

In the frame of the fire performance tests, a number of additional thermocouples (Type K, 1.5 mm diameter) were added to the specimens in order to achieve a better understanding of their fire behaviour. The thermocouples were added at the gypsum plasterboard at the unexposed side, at heights of 100 mm, 400 mm (fan coil height for the SmartWall Type B) and 800 mm and at the metal frame at the height of 400 mm. In the SmartWall with the fan coil (Type B), an extra thermocouple was added at the centre of the fan coil unit.

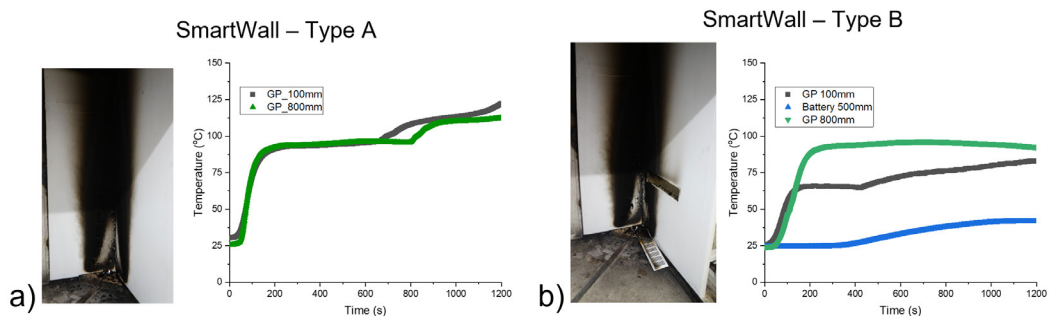


FIG. 8 The SmartWall after the test procedure and the measured temperatures for Type A (a) and Type B (b)

FIG. 8 depicts the temporal variation of the temperature at the aforementioned measuring locations. In both test cases, the temperature in the back of the specimen did not exceed 100°C. There was no

major difference in the fire performance of the two specimens, judging by both the EN 13823 results and the additional thermocouples. As a result, the existence of the fan coil unit and the incorporated battery does not seem to have a significant effect on the fire performance of the specimen (the rise of the temperature at the height of 400 mm was due to a crack in the gypsum board).

### 4.1.3 Thermal performance

The thermal performance investigation of the SmartWall façade panel is carried out for the four different types of the façade system, depending on the presence of a fan coil and/or window on the façade panel (Types A - D). The thermal transmittance of the blank type SmartWall (Type A), without considering any thermal bridge,  $U_{clear}$  is calculated according to ISO 6946 equal to  $U_{clear} = 0.176 \text{ W}/(\text{m}^2\text{K})$ . Table 5 summarises the equivalent U-values of the whole SmartWall, including ( $U_{eq}$ ) and excluding ( $U_{eq,op}$ ) the window. It is observed that the presence of the metal frame increased the U-value of the opaque wall by  $0.05 \text{ W}/(\text{m}^2\text{K})$ , the presence of the window by a further  $0.05 \text{ W}/(\text{m}^2\text{K})$  and the fan coil by a further  $0.03 \text{ W}/(\text{m}^2\text{K})$ .

For the types with a fan coil, two alternatives are assumed depending on the operation of the fan coil: passive and active. In passive mode, the temperature of the fan coil depends on the temperature of the adjacent materials, but in active mode, a constant temperature of ca.  $25^\circ \text{C}$  (low-temperature system) is assumed. When the fan coil is stopped, it acts as a thermal bridge, increasing the U-value by 43% compared with  $U_{clear}$ . However, when the fan coil is in operation (active), it acts as a heat source, reducing the equivalent U-value of the whole façade area by 13%. The change of the U-value depending on the operation of the incorporated fan coil seems to be significant for the overall thermal performance assessment of the system.

TABLE 5 Thermal transmittance (U-values) of all types of SmartWall, including the effect of thermal bridges

SmartWall type	$U_{eq}$	$U_{eq,op}$	U-value difference	
	$\text{W}/(\text{m}^2\text{K})$	$\text{W}/(\text{m}^2\text{K})$	$[\text{W}/(\text{m}^2\text{K})]$	$[\%]$
Type A	0.23	0.23	0.05	+29%
Type B – fan coil passive	0.25	0.25	0.08	+43%
Type B – fan coil active	0.12	0.12	-0.06	-32%
Type C	0.46	0.28	0.10	+58%
Type D– fan coil passive	0.48	0.31	0.13	+74%
Type D – fan coil active	0.35	0.15	-0.02	-13%

FIG. 9 illustrates the U-values for the four investigated SmartWall types, as provided by the COMSOL environment. It is obvious that the most severe thermal bridges occurred at the window and the bottom side of the metal frame. The last is due to the presence of HRS spacers at the bottom side for structural reasons instead of heat breakers. The fan coil does not create significant thermal bridges due to the use of VIP behind it, creating a relatively homogenous thermal resistance at the central part of SmartWall. All thermal bridges (window, metal frame, and fan coil) increase the opaque wall U-value by 74% (from  $U_{clear} = 0.18 \text{ W}/(\text{m}^2\text{K})$  to  $U_{eq} = 0.31 \text{ W}/(\text{m}^2\text{K})$ ).

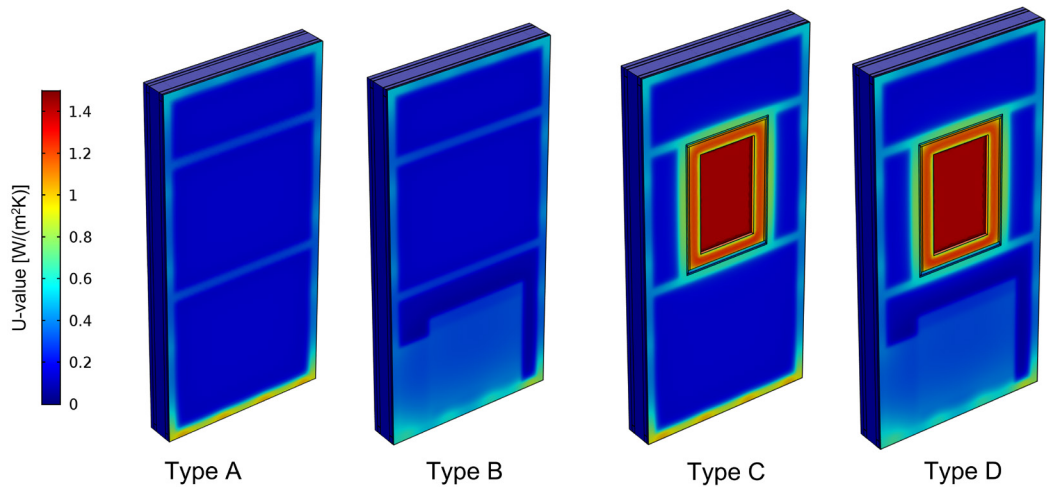


FIG. 9 U-value contour for the four types of SmartWall system in COMSOL software

## 4.2 DENVELOPS COMFORT WALL

### 4.2.1 Structural performance

The Denvelops Comfort Wall is considered, according to the Spanish Resistance Construction Standard, as an add-on constructive element and, therefore, not part of the building structure (NSCE-02). For such cladding systems, only the mechanical resistance of the connections between the add-on element and the building structure must be verified. For this reason, the present study only investigates the structural performance of the anchoring system of the Denvelops Comfort Wall for the Spanish building.

The structural performance and anchoring system analysis is carried out in accordance with Eurocodes and Spanish adjustment "Documento Básico de Seguridad Estructural" (CTE DB-SE). The structure is considered a main façade, and the loads are divided into permanent, variable, and accidental loads. Specific weights for permanent and variable loads are assumed according to Eurocode 0, while the accidental loads have not been taken into account. For the design of steel structures, the parameters and criteria described in the Eurocode 3 and the DB-SE-EA are used, assuming stainless steel  $79 \text{ kN/m}^3$ , for self-weights and wind load,  $q_e$ , for wind pressure, expressed by the equation:

$$q_e = q_b \cdot c_e \cdot c_p \quad \delta$$

where  $q_b$  is the wind dynamic pressure,  $c_e$  is the exposure's factor, and  $c_p$  is the pressure's factor. Two possible wind pressures are investigated: at the centre of the mesh, applying the values of  $c_e=1.9$  and  $c_p=0.8$  ( $q_{e,m}=1.20\text{kPa}$ ) and on the side of the mesh, applying the values of  $c_e=1.9$  and  $c_p=1.2$ , ( $q_{e,s}=0.80\text{kPa}$ ).

The obtained criteria for the structural performance of Denvelops Comfort Wall are summarised in Table 6.

TABLE 6 Criteria for the structural performance of Denvelops Comfort Wall

Criterion	Explanation
<p>When the section is subjected to an axial force, <math>N_{t,Rd}</math>, must be less than design plastic resistance, <math>N_{pl,Rd}</math>:</p> $N_{t,Rd} \leq N_{pl,Rd} = A \cdot f_{yd}$	<p><math>f_{yd}</math>: Design resistance determined by:</p> $f_{yd} = f_y / \gamma_M$ <p><math>f_y</math>: Characteristic value of the particular resistance determined with characteristic or nominal values for material properties and dimensions  <math>\gamma_M</math>: the global partial factor for the particular resistance</p>
<p><b>Cross section</b></p> <p>For sections subjected to the combination of <math>N_{Ed}</math>, <math>M_{y,Ed}</math> and <math>M_{z,Ed}</math>, the following criteria should be met:</p> $\frac{N_{Ed}}{N_{Rd}} + \frac{M_{y,Ed}}{M_{y,Rd}} + \frac{M_{z,Ed}}{M_{z,Rd}} \leq 1$	<p><math>N_{Rd}</math>: Design value of the resistance depending on the cross-sectional classification.  <math>M_{y,Rd}</math>: Design value of the resistance depending on the elastic resistance.  <math>M_{z,Rd}</math>: Design values of the resistance depending on the plastic resistance.</p>
<p>The design value of the shear force, <math>V_{Ed}</math>, at each cross section shall satisfy:</p> $V_{y,Ed} \leq V_{pl,Rd} = A_v \cdot \frac{f_{yd}}{\sqrt{3}}$	<p><math>V_{Ed}</math>: Design value of the shear force  <math>V_{pl,Rd}</math>: Design plastic resistance</p>
<p><b>Buckling</b></p> <p>A laterally unrestrained member subject to major axis bending should be verified against lateral-torsional buckling as follow:</p>	<p><math>M_{Ed}</math>: Design value of moment and <math>M_{b,Rd}</math>: Design buckling resistance moment</p>

The structural performance analysis of wind and load anchors was carried out by means of finite element simulation in ANSYS software. The wind anchor, consisting of two parts (FIG. 10), is the part of the mesh in which the wind strength is applied to the façade. The maximum wind force applied to the wall is 3.046 N perpendicular to the façade, applied to both parts of the anchor. The results of the analysis are presented in FIG. 10b. The maximum force applied in the load anchor is 1.334 N perpendicular and 1.512 N parallel to the façade (FIG. 11). The results of both anchors show that the von Mises tensions satisfy the criteria.

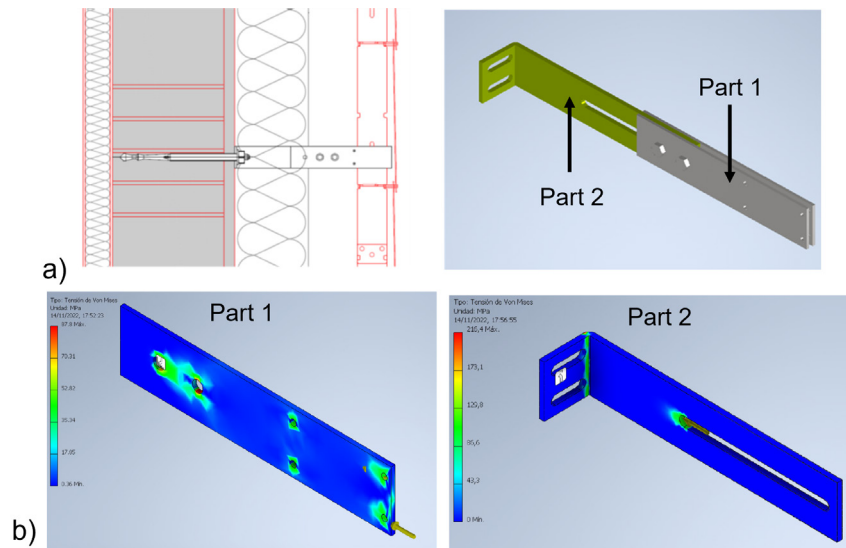


FIG. 10 The wind anchor of Denvelops Comfort Wall: a) Geometry and b) Von Mises Strength study in ANSYS software.

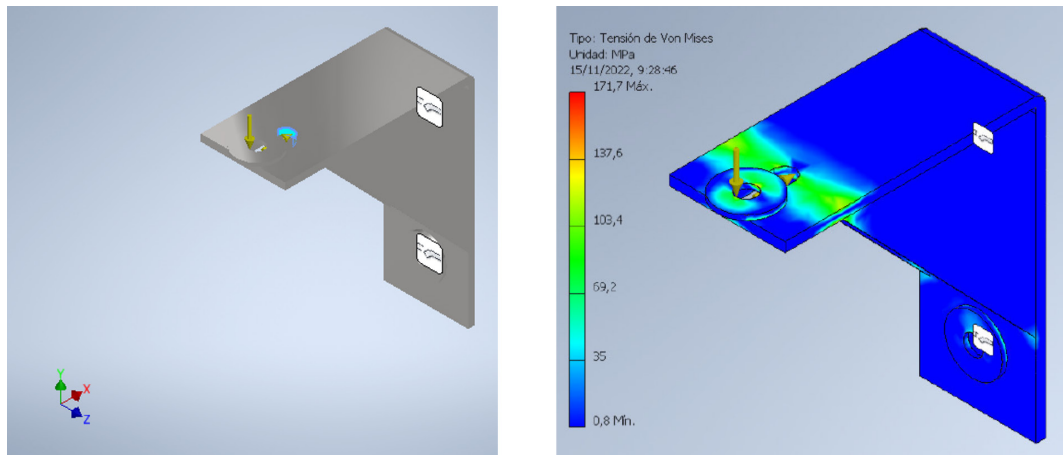


FIG. 11 The load anchor of Denvelops Comfort Wall: a) Geometry and b) Von Mises Strength study in ANSYS software.

#### 4.2.2 Thermal performance

The thermal performance of the Denvelops Comfort Wall is carried out by means of the ANSYS Fluent software, following the methodology described in section 3.3. The analysis focuses on the calculation of all incorporated thermal bridges on the façade system, especially the thermal bridges created by the presence of the air handling unit (AHU). A 3D façade panel is modelled, including the different layers of the structure (wall, thermal insulation layers, closed air cavity, and the AHU). Since the Denvelops Comfort Wall is a ventilated insulation system with an air gap in front of the thermal insulation, the external cladding was not considered in the model. The AHU model is also simplified, excluding fans, control system, and heat exchangers. The geometry of the model is illustrated in FIG. 12, indicating the air handling unit and the vertical plane for the calculation of thermal bridges.

The analysis is performed for three different cases:

- For the façade panel without the AHU (reference case)
- For the façade panel with the AHU unit off
- For the façade panel with AHU in operation

The dimensions of the wall model are 2 m (width) and 2.7 m (height), while the dimensions of the AHU are 0.6 m (width) and 1.5 m (height). The simulations were performed for an interior temperature of 22°C and an exterior temperature of 2°C (Table 3). The anchoring system of the building envelope is not modelled but is taken into account in the calculation by a surcharge U-value of 0.02 W/m<sup>2</sup>K. Thermal resistance in AHU channels  $R_{AHU}$  is assumed to equal 0.01 (m<sup>2</sup>K)/W.

Table 7 summarises the simulated results of the Denvelops Comfort Wall for the three examined cases. The results show that the façade panel with switched off AHU has a higher U-value (0.231 W/m<sup>2</sup>K) by 18.5% than the façade without the AHU (0.195 W/m<sup>2</sup>K), indicating the high thermal bridge created by AHU. However, when the AHU is in operation, the thermal transmittance decreases by 3.6% (0.188 W/m<sup>2</sup>K) in relation to the panel without AHU due to the circulation of warmer air and creating an active insulation area.

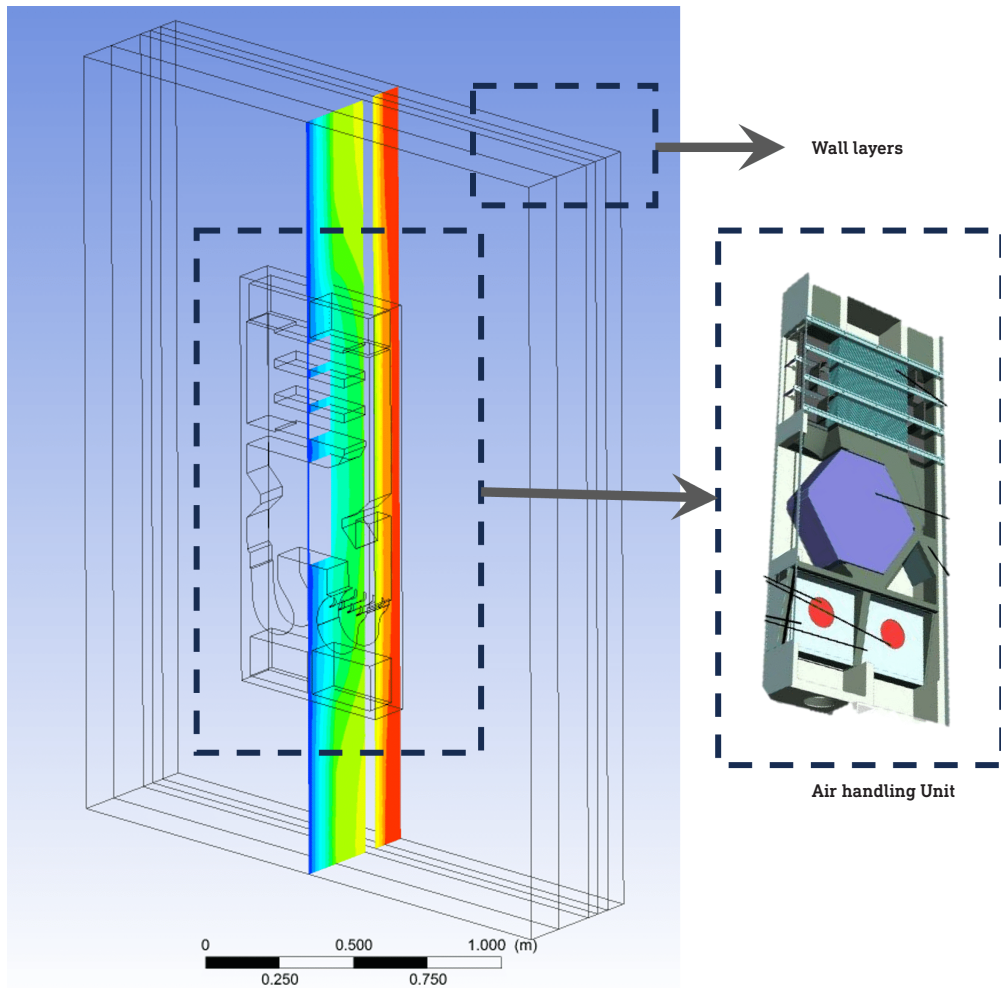


FIG. 12 Geometry of Denvelop Comfort Wall in ANSYS Fluent

TABLE 7 Equivalent thermal transmittance ( $U_{eq}$ ) for the three cases of Denvelops Comfort Wall

	$U_{eq}$	Increase of U-value
	W/(m <sup>2</sup> K)	%
<b>Façade panel without the AHU</b>	0.195	
<b>Façade panel with AHU stopped</b>	0.231	18.5%
<b>Façade panel with AHU in operation</b>	0.188	-3.6%

FIG. 13 presents the temperature contour for a section of the simulated façade in the three examined cases. In the case without AHU, the total heat flux value equals 18.9 W, while the calculated U-value equals 0.175 W/m<sup>2</sup>K (without anchoring system). The temperatures in the wall layers are homogenous, indicating that there is not any severe thermal bridge. The presence of AHU (when it is stopped) creates a severe thermal bridge at the middle height of the façade panel, changing the temperature homogeneity of the insulation layers. However, when the AHU is in operation, the insulation layer behind the AHU is warmer due to the air circulation and the operation of the heat exchanger.

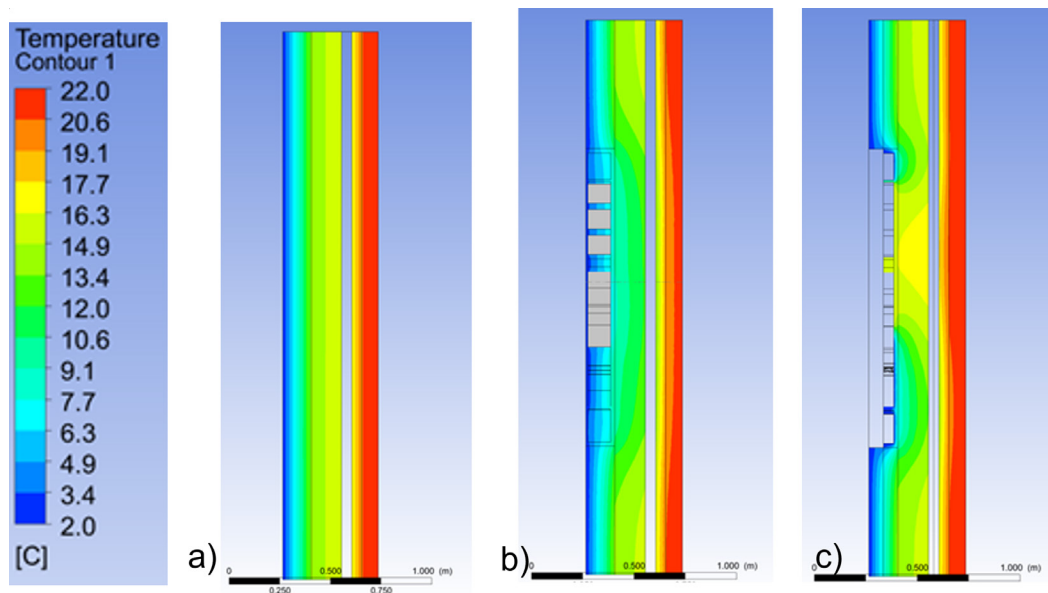


FIG. 13 Temperature contour of the Denvlops Comfort Wall for the three examined cases: a) without AHU, b) AHU stopped and c) AHU in operation

## 4.3 CONEXWALL

### 4.3.1 Structural performance

The structural performance of the ConExWall façade system is carried out by investigating the mechanical performance of the anchoring system. The ConExWall panels are anchored on the existing load-bearing walls using point steel anchors. Each anchor consists of a steel element and chemical anchors for masonry or concrete. The following basic parameters need to be taken into account for the design of panel anchors:

- The material of the main construction of panels and joints
- The material of the existing structure of the building into which it will be anchored

The ConExWall, planned to be installed in a Czech residential building, is designed as large-format wood-based panels. So, pressed structural joints of timber panel elements are structurally more advantageous than tensile joints. The existing load-bearing walls of the building are made of solid ceramic bricks, while there are sandwich walls underground (inside solid bricks and outside stones). The inner part is made of ceramic solid bricks on lime cement mortar, with a total thickness of 150-300 mm. The outer part is faced with hack-lite stone masonry (sandstone).

The general rules and the methodology for the structural performance analysis follow the standard of the Eurocodes (Eurocode 1, Action on structures – Part 1-1: General actions – Densities, self-weight, imposed loads for buildings) and Czech adjustment ČSN EN 1991-1-1, 03/2004 (incl. National Annexes – ČSN EN 1990 NA, ed.A, 02/2021). The requirements for mechanical resistance and stability take into consideration: a) the existing structures of the building, b) the anchoring of panels, and c) the panel construction. The loads are divided into permanent, variable, and accidental loads. The expected load derived from:

- self-weight of the panel:  $g_k=1.0 \text{ kN/m}^2$ ,  $g_d=1.350 \text{ kN/m}^2$
- wind load: for  $v_{b,0}=25.0 \text{ m/s}$ ,  $w_{e,k}=-0.490 \text{ kN/m}^2$ ;  $w_{e,d}=0.735 \text{ kN/m}^2$  (Eurocode 1, Actions on structures - Part 1-4: General actions - Wind loads)
- snow load (irrelevant for this case)
- pre-stress axial load: set by experiment:  $P_{Sk}=0.9 \text{ kN/m}^2$ ,  $P_{Sd}=1.215 \text{ kN/m}^2$

The steel part of the anchor depends on the geometry of the panel. The size is chosen so that the panel can be supported, and the steel part of the anchor is designed with a large margin from a structural point of view. The anchor must be able to withstand vertical  $V_{sd}=3.645 \text{ kN}$  and horizontal loads (tension),  $N_{sd}=3.316 \text{ kN}$ . The estimated scheme of anchors is illustrated in FIG. 14, while the design values of the most loaded row of anchors are summarised in Table 8.

TABLE 8 Design values of the most loaded row of anchors in ConExWall

Design value	Value
Vertical loading	$V_{sd} = 3.645 \text{ kN/m}$
Horizontal load	$N_{sd} = 3.316 \text{ kN/m}$
Number of chemical anchors per meter (Fischer anchors M10)	$N_1 = V_{sd}/V_{Rd} + N_{sd}/N_{Rd} = 7,5$ $V_{Rd} = 1.00, N_{Rd} = 0.86$
Number of chemical anchors per meter (Hilti HIT-HY 270 anchors M10)	$N_2 = V_{sd}/V_{Rd} + N_{sd}/N_{Rd} = 7.062$ $V_{Rd} = 0.50, N_{Rd} = 2.80$

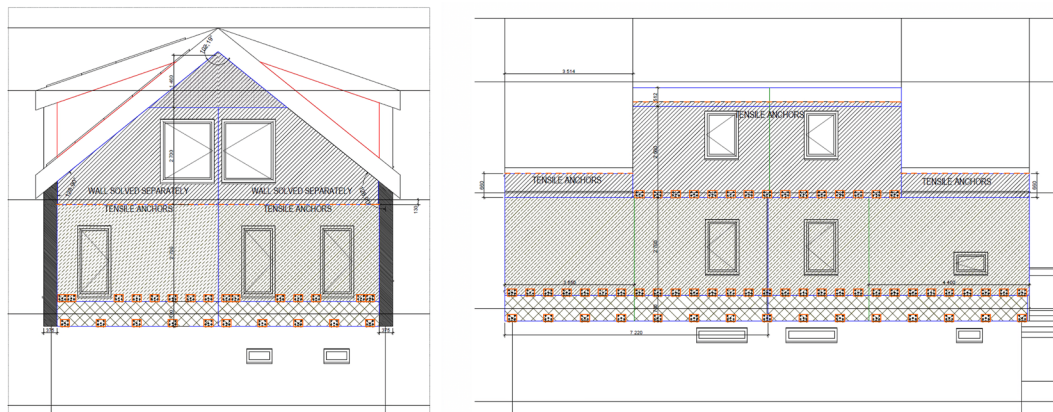


FIG. 14 The scheme of anchors for the Czech building

### 4.3.2 Thermal performance

The thermal performance of the ConExWall façade panel is investigated using COMSOL software and the methodology described in section 3.3 for a representative geometry in accordance with the panel that is planned to be installed in the Czech building. The simulated geometry (FIG. 15) has dimensions of 7.035 m length and 3.400 m height, and it is considered to be installed on the external side of an existing wall. The under-investigation façade panel contains two windows (3.95 m<sup>2</sup> area for each window) and two ventilation systems. The window frame is assumed to be wood-aluminum, with  $U_f=1.4 \text{ W/(m}^2\text{K)}$ , while the glazing system is assumed to be triple pane Argon filled with  $U_g=0.58 \text{ W/(m}^2\text{K)}$ . The thermal transmittance of the overall window is equal to  $U_w=0.74 \text{ W/(m}^2\text{K)}$ .

The ventilated system is assumed to be a box with a metal case and still air, without being operated. For the thermal performance analysis of ConExWall, the vapour barriers are excluded. Based on the above, the thermal transmittance of the ConExWall (for 180 mm insulation thick), without considering any thermal bridge,  $U_{clear}$  is calculated according to ISO 6946 equal to  $U_{clear,ConExWall}=0.125 \text{ W}/(\text{m}^2\text{K})$ .

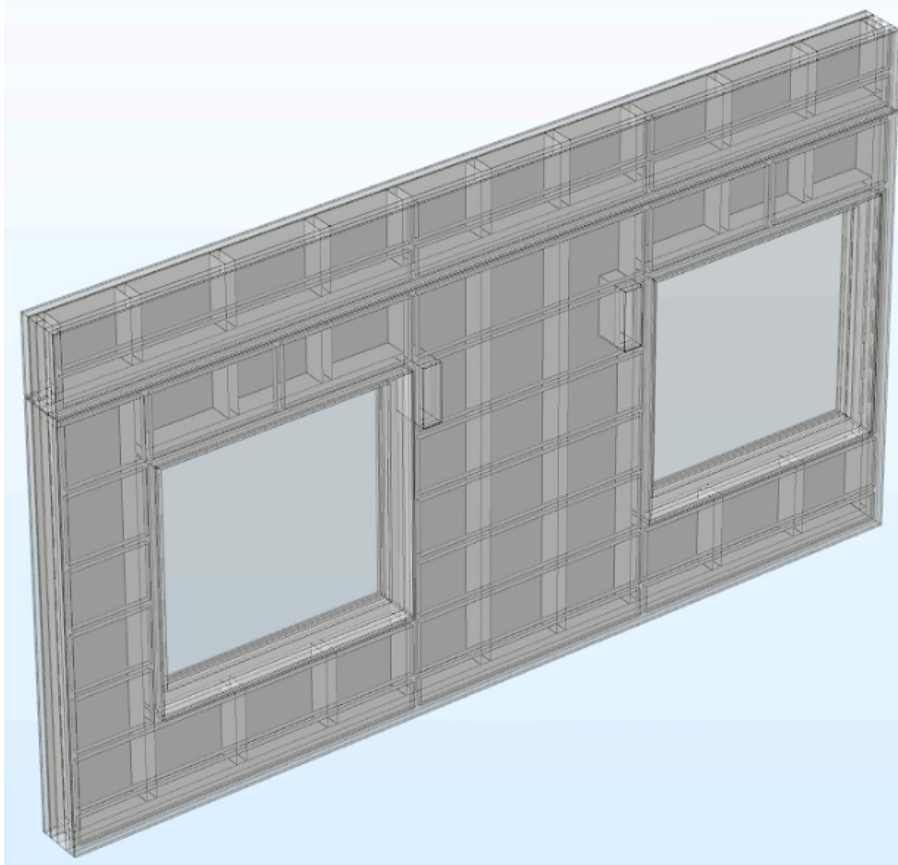


FIG. 15 The simulated geometry of ConExWall in Comsol software.

For the thermal performance analysis of ConExWall, the piping system is considered to be either in passive mode, meaning that the water temperature is changed depending on the boundary conditions, or in active mode, meaning that the water temperature is stable and around 30°C. Due to the complexity of the geometry, the heating pipes are impossible to simulate along with the whole ConExWall geometry. For this reason, the contribution of heating pipes is calculated in the layer of wood fibre board. The layer is simulated with the heating pipes, and an equivalent thermal conductivity is calculated, taking into account the effect of the water and piping system, according to the following equation:

$$k_{eq} = \frac{d_{layer}}{A(T_{in}-T_{out}) \frac{1}{Q} \frac{1}{h_{in}} \frac{1}{h_{out}}} \quad 9$$

where  $d_{layer}$  is equal to the layer of the soft heating board (20 mm),  $Q$  is the heat that penetrates the soft heating layer in [W],  $A$  is the total area of the equivalent layer in [ $\text{m}^2$ ], and  $T_{in}$ ,  $T_{out}$ ,  $h_{in}$  and  $h_{out}$  are the internal/external temperatures and heat transfer coefficients, respectively, according to the Table 3.

The wood fibre board (the layer that incorporates the piping system) is simulated without and with the embodied heating pipes. In the case without the piping system, the average heat flow of the layer is  $58.78 \text{ W/m}^2$ , while in the second case (with the piping system), the average heat flow is increased by  $4.83 \text{ W/m}^2$  (Table 9). This increase can be achieved if, in the first case (layer without the heating pipes), the thermal conductivity is  $0.053 \text{ W/(m}\cdot\text{K)}$  instead of  $0.047 \text{ W/(m}\cdot\text{K)}$ . So, the complex geometry of the wood fibre board ( $k=0.047 \text{ W/m}\cdot\text{K}$ ) with the water heating pipes can be replaced by another layer with thermal conductivity equal to  $0.053 \text{ W/(m}\cdot\text{K)}$  without heating pipes.

TABLE 9 Results of the analysis of wood fibre board with and without the piping system

	Heat $\text{W/m}^2$	Thermal conductivity $\text{W/(m}\cdot\text{K)}$
Wood fibre board without heating pipes	58.75	0.047
Wood fibre board with heating pipes	63.61	0.053 (equivalent)

Table 10 summarises the equivalent thermal transmittance ( $U_{eq}$ ) of the whole ConExWall (including the window,  $U_{eq,ConExWall}$ ) and the opaque wall (excluding the window,  $U_{eq,opConExWall}$ ) for passive and active heating system and for two different insulation thicknesses (120 mm and 180 mm). For the passive systems, it is observed that the presence of ventilation units, anchoring systems, windows, and wooden frames almost double the U-value of the opaque wall. The wooden frame, the anchoring system, the ventilation unit, and the window further increase the U-value by  $0.11 \text{ W/(m}^2\text{K)}$ . The increase of insulation thickness by 60 mm reduces the U-value by only 7%. When the heating system is active in heating mode, the whole wall surface acts as a heat source, resulting in a very low thermal transmittance of the opaque wall equal to  $0.05 \text{ W/(m}^2\text{K)}$ . This value is similar to values found in the literature (Kisilewicz, Fedorczak-Cisak, & Barkanyi, 2019).

TABLE 10 Equivalent thermal transmittance of the ConExWall for two insulation thicknesses

Insulation thickness mm	$U_{clear}$ $\text{W/(m}^2\text{K)}$	Piping heating system	$U_{eq,opConExWall}$ Excluding windows	$U_{eq,ConExWall}$ Including windows
			$\text{W/(m}^2\text{K)}$	$\text{W/(m}^2\text{K)}$
120	0.153	Passive	0.27	0.40
		Active	0.05	0.24
180	0.125	Passive	0.25	0.38
		Active	0.05	0.23

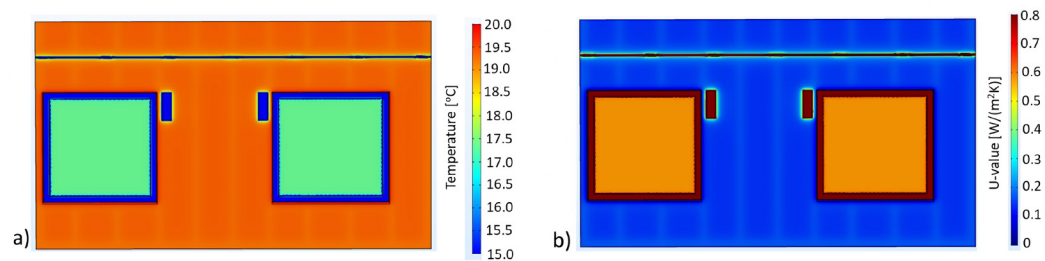


FIG. 16 Temperature and U-value contour of the simulated geometry at the internal side

FIG. 16 presents the temperature and the U-value contours of the internal side (the surface contacting the existing wall) of the ConExWall façade panel for 180 mm insulation thickness in the case that the heating system is passive mode. Except for the window area, whose U-value is much higher than the opaque wall, the ventilation units and the air gap in the height of the anchoring system (L-profiles) create significant thermal bridges providing temperatures lower than 15°C.

## 5 CONCLUSIONS

This study presents a holistic assessment of three innovative hybrid prefabricated façade systems (SmartWall, Denvelops Comfort Wall, and ConExWall) in terms of structural, fire, and thermal performance. These systems, developed in the frame of the PLURAL project, are planned to be installed in existing residential buildings in three countries (Greece, Spain, and the Czech Republic). The methodology applied for the investigation of their assessment takes into account the European and national codes that must be met for the implementation of the façade systems as a deep renovation solution in the proposed existing buildings. The structural performance of the façade system that will be installed in a building in Greece was assessed in terms of its seismic resistance due to the high-risk seismic location, while the other systems are not required to be stimulated in such seismic tests. The study presented a part of the pathway that must be followed for the certification of such façade systems for the renovation of existing buildings in order to penetrate the market, highlighting the importance of being in line with the Construction Products Regulation (CPR).

The special challenge of the three hybrid façade systems is that they incorporate HVAC systems: fan coil for the SmartWall, air handling unit for the Denvelops Comfort Wall, and heating piping system for the ConExWall. This study investigates their thermal performance, calculating the equivalent thermal transmittance using the most accurate method (ISO 10211) both in the case where their systems are stopped (passive mode) and in operation (active mode). The results showed that in passive mode, the presence of these systems creates significant thermal bridges, but in active mode, part of the wall or even the whole wall acts as a heat source, drastically reducing the equivalent wall thermal transmittance.

### Acknowledgements

---

The work has been funded by the European Union's Horizon 2020 Research and Innovation Programme in the frame of the H2020 project: "Plug-and-Use Renovation with Adaptable lightweight Systems" – PLURAL (<https://plural-renovation.eu/>), Grant Number 958218.

## References

---

- Adamovský, D., Vcelak, J., Mlejnek, P., Colon, J., Prochazkova, Z., Tsoutis, C., . . . & Founti, M. (2022). Technology concepts for rapid renovation using adaptable lightweight façade systems. *CLIMA 2022 Conference*. doi:<https://doi.org/10.34641/clima.2022.42>
- AMS coatings and advanced materials. (2023, February). Retrieved from <https://amsolutions.gr/materials/>
- BPIE, *On the way to a Climate-Neutral Europe: Contributions from the building sector to a strengthened 2030 climate target*. (2022). Retrieved from [https://www.bpie.eu/wp-content/uploads/2020/12/On-the-way-to-a-climate-neutral-Europe\\_Final.pdf](https://www.bpie.eu/wp-content/uploads/2020/12/On-the-way-to-a-climate-neutral-Europe_Final.pdf)
- CTE DB-SE. (n.d.). Código Técnico de la Edificación – Documento Básico de Seguridad Estructural (Building Technical Code – Basic Document of Structural Safety).
- CTE DB-SI. (n.d.). Código Técnico de la Edificación – Documento Básico de Seguridad en caso de incendio (Building Technical Code – Basic Document of Safety in case of fire).
- Denvelops. (2022, January 13). *Denvelops Smart system*. Retrieved from <https://www.denvelops.com/new-construction-system/>
- D’oca, S., Ferrer, C., Perneti, R., Gralka, A., Sebastian, R., & Velp, P. (2018). Technical, financial, and social barriers and challenges in deep building renovation: Integration of lessons learned from the H2020 cluster projects. *Buildings*, 8(12).
- Du, H., Huang, P., & Jones, P. (2019). Modular façade retrofit with renewable energy technologies: The definition and current status in Europe. *Energy and Buildings*, 205. doi:<https://doi.org/10.1016/j.enbuild.2019.109543>
- EN 13501-1: 2019. (n.d.). Fire classification of construction products and building elements – Part 1: Classification using data from reaction to fire tests.
- EN 13823:2020+A1:2022. (n.d.). Reaction to fire tests for building products - Building products excluding floorings exposed to the thermal attack by a single burning item.
- Eurocode 1. (n.d.). Action on structures – Part 1-1: General actions – Densities, self-weight, imposed loads for buildings.
- Eurocode 1. (n.d.). Actions on structures - Part 1-4: General actions - Wind loads.
- Eurocode 8. (n.d.). Actions of structures for earthquake resistance - Part 1: General rules, seismic actions and rules for buildings.
- European Commission. (2014). *Mapping Europe’s earthquake risk*. Retrieved from <https://ec.europa.eu/research-and-innovation/en/horizon-magazine/mapping-europes-earthquake-risk>.
- European Commission. (2020, February 17). *In focus: Energy efficiency in buildings*. Retrieved from [https://commission.europa.eu/news/focus-energy-efficiency-buildings-2020-02-17\\_en](https://commission.europa.eu/news/focus-energy-efficiency-buildings-2020-02-17_en).
- Filippidou, F., Nieboer, N., & Visscher, H. (2017). Are we moving fast enough? The energy renovation rate of the Dutch non-profit housing using the national energy labelling database. *Energy Policy*, 109, pp. 488 - 498. doi: <https://doi.org/10.1016/j.e>
- ISO 10211. (2017). Thermal bridges in building construction – Heat flows and surface temperatures – Detailed calculations.
- Kamali, M., & Hewage, K. (2016). Life cycle performance of modular buildings: A critical review. *Renewable and Sustainable Energy Reviews*, 62 (Supplement C), pp. 1171 - 1183.
- Katsigiannis, E., Gerogiannis, P. A., Atsonios, I., Bonou, A., Mandilaras, I., Georgi, A., . . . Founti, M. (2022). Energy assessment of a residential building renovated with a novel prefabricated envelope integrating HVAC components. *1078*. doi:10.1088/1755-1315/1078/1/012130
- Kisilewicz, T., Fedorczak-Cisak, M., & Barkanyi, T. (2019). Active thermal insulation as an element limiting heat loss through external walls. *Energy and Building*(205).
- Maduta, C., Melica, G., D’Agostino, D., & Bertoldi, P. (2022). Towards a decarbonised building stock by 2050: The meaning and the role of zero emission buildings (ZEBs) in Europe. *Energy Strategy Reviews*(44). doi: <https://doi.org/10.1016/j.esr.202>
- Masera, G., Iannaccone, G., & Salvalai, G. (2014). Retrofitting the Existing Envelope of Residential Buildings: Innovative Technologies, Performance Assessment and Design Methods. *Advanced Building Skins - 9<sup>th</sup> Energy Forum*.
- MORE-CONNECT, EU-funded project, <https://www.more-connect.eu/more-connect/>. (n.d.).

- Naji, S., Celik, O., Alengaram, U. J., Jumaat, M., & Shamshirband, S. (2017). Structure, energy and cost efficiency evaluation of three different lightweight construction systems used in low-rise residential buildings. *Energy and Buildings, 84 (Supplement C)*, pp. 727 - 739.
- NSCE-02. (n.d.). Norma de Construcción Sismorresistente (Seismic Resistance Construction Standard).
- Oorschot, J. v., Maggio, M. S., Veld, P. O., & Tisov, A. (2022). Boosting the Renovation Wave with Modular Industrialized Renovation Kits: mapping challenges, barriers and solution strategies. *Architects' Council of Europe*.
- Panoutsopoulou, L., Meimaroglou, N., & Mouzakis, C. (2023). Shaking table tests on single-bay timber-framed wall specimens with fired brick and adobe block infills and mortise-tenon joints. *Journal of Building Engineering*, (76).
- Pihelo, P., Kalamees, T., & Kuusk, K. (2017). nZEB Renovation of Multi-Storey Building with Prefabricated Modular Panels. *IOP Conference Series: Materials Science and Engineering, 251*(1).
- PLURAL EU project. (2020-2024). <https://www.plural-renovation.eu/>.
- Torres, J., Garay-Martinez, R., Oregi, X., Torrens-Galdiz, J., Uriarte-Arrien, A., Pracucci, A., . . . Arroyo, N. (2021). Plug and Play Modular Façade Construction System for Renovation for Residential Buildings. *Buildings, 11*(419), pp. 1-21. doi:<https://doi.org/10.3390/buildings11090419>
- Zavřel, V., Zelenský, P., Macia, J., Mylonas, A., & Pascual, J. (2022). Simulation aided development of a façade-integrated air handling unit with a thermoelectric heat exchanger. *Clima 2022, REHVA 14<sup>th</sup> HVAC World Congress*.



# Automation process in data collection for representing façades in building models as part of the renovation process

**Kepa Iturralde<sup>1\*</sup>, Asier Mediavilla<sup>2</sup>, Peru Elguezabal<sup>2,3</sup>**

\* Corresponding author: kepa.iturralde@tum.de

1 Technical University of Munich, Chair of Engineering Geodesy, TUM School of Engineering and Design, Germany

2 TECNALIA, Basque Research and Technology Alliance (BRTA), Spain

3 University of the Basque Country UPV/EHU, Department of Electrical Engineering, Spain

## Abstract

*A key barrier in building façade renovation processes versus new designs is that an initial building model on which the design process is based rarely exists and that the technologies usually employed to create it (e.g., based on point cloud scanning) are costly or require modelling skills. This situation is a clear limitation, especially in early decision stages, where the level of detail required is not very high and the analysis and studies to consider the renovation plan (e.g., simplified energy simulations and renovation potential, or estimation of the number, types, and dimensions of the prefabricated modules incorporating solar panels) highly depend on such digital models. This paper introduces a process that, based on freely available data such as open GIS sources (local cadasters, OpenStreetMap...) and façade images, can semi-automatically generate the 3D building model of the existing conditions and, in a second step, can also suggest the prefabricated façades module layout for building upgrades. Additionally, no on-site visit is needed. When the upgrade is focused on the façade, a big opportunity is identified for generating the building model and a realistic representation of its envelope, only using online data sources as input. The process developed consists of a set of easy-to-use software tools that can be used independently or combined in a workflow, depending on the available data and starting conditions. Time-saving is the main benefit, which also contributes to reducing costs.*

## Keywords

*semi-automated data acquisition, prefabricated façade panels, building envelope renovation, open data, interoperability, IFC*

## DOI

<http://doi.org/10.47982/jfde.2023.2.A2>

# 1 INTRODUCTION

Critical success factors in the construction industry are multiple and diverse due to the high number of stakeholders, disciplines, and technologies that coexist in this sector. According to Knotten et al. (2017), communication and decision-making are key in building design management, while other authors (Oluleye et al., 2023) also highlight data-driven digital tools and pre-demolition auditing as principal success factors.

The importance of a well-managed project in every construction work highly affects the quality of the result. The better managed the project is, the better the intervention will be. This is important with new buildings but especially relevant for renovation activities (Noori et al., 2016), where the built environment and surroundings strongly affect and condition the potential upgrading designs. In such a situation, the project needs to be defined using a reliable and descriptive basis of the building that is about to be renovated, also implying a good radiography of the actual status.

When alternative interventions and potential renovations are assessed, getting a fair representation of the existing building becomes a necessary input to properly make the assessments needed (Wang et al., 2022). But at the same time, the effort to capture that information needs to be proportional to these initial steps of the process when the decision to renovate has not yet been adopted and when the resources and budget are still very limited. The use of BIM technology has rapidly grown among AECO (Architecture, Engineering, Construction, and Operations) professionals but is still primarily used for new designs and with several challenges, such as the cost of equipment and software, lack of skilled workforce, and a very fragmented industry, mainly composed of SMEs (European Construction Sector Observatory, 2021). Considering the existing building stock, the available digital information is scarce and dispersed across various owners, formats, and accessibility levels. There is a growing research interest in GIS-BIM interoperability (Zhu & Wu, 2022). Still, practical implementation is typically limited to large vendors such as ESRI or Autodesk (ESRI, 2023), skilled users, and extensive construction or infrastructure projects. The equation gets more complex if we add energy estimation aspects to the data flow automation (buildingSMART, 2022).

In parallel, there is an urgent need to quickly upgrade the current building stock, which is why several initiatives are strongly promoting this change by means of renovation to significantly reduce the impact of the buildings and the AEC sector on the environment. Europe's decarbonisation strategy is fully oriented and aligned with these rehabilitation goals, and the impact of the façade and its insulation and the benefits of on-site renewable energy capture are labelled as two of the most critical. The use of industrialisation and prefabrication has also been identified as a key driver to support this transformation. The main advantages of adopting this manufacturing strategy when envelope refurbishment is considered are less obtrusive work for the inhabitants, shorter periods on-site, better and safer working conditions, and, in general, higher quality control of the overall intervention along its different phases. Moreover, adopting such a prefabrication approach also enables the possibility to incorporate additional systems and solutions, rather than conventional ones used in envelopes, representing a clear opportunity to incorporate solar collecting solutions into the building envelope (Elguezabal & Arregi, 2018).

However, compared to manual processes, renovation processes with prefabricated modules require more data and a better data flow. With manual methods, the operator manipulates the material based on the measurements made by themselves directly on the site while working with it. With prefab technologies, the products are produced off-site, requiring major coordination with the building measurement, as well as high accuracy when the on-site assembly process is materialised.

Previous studies for façade data acquisition have focused on 3D Laser Scanning (Omar & Nehdi, 2016; Alizadehsalehi & Yitmen, 2016). Preliminary approaches for data acquisition with 3D laser scanners were focused on matching geometries for as-built documentation. These cases involved graphic documentation that could be compared, meaning the CAD file. One of the preliminary studies was developed (Bosché, F. 2009). It comprised matching a two-phase construction steel profile recognition to a previously drafted 3D CAD. It was not an automatic procedure, though, but rather mainly used for as-built documentation. Later, the automatic reconstruction of as-built building information models from laser-scanned point clouds was developed (Kim, C., Son, H., Kim, C., 2013). However, these are time-consuming and relatively expensive procedures that cannot be used in the early stages of a façade renovation project because, at that point, the financing is usually unclear.

Summarising, there is a critical necessity to renovate a large number of buildings in a quick and efficient process, supported by digital tools and prefabrication techniques. But, for doing that, the early decision-making process establishes the starting point to 1) make the owners of bad-performing buildings aware of their actual situation, 2) describe the potential impact and benefits of a renovation intervention, and overall, 3) assist the owner in adopting the decision to renovate using studies and data that support that resolution.

Thus, there is a clear need to “democratise” the BIM adoption, especially in early decision stages, by offering solutions that 1) reduce the number of needed tools and license costs, 2) automate the capture of existing free data sources, and 3) have almost no learning curve. Using online data such as GIS and OpenStreetMap can improve this situation because it adds extra information to the generation of the building model.

According to this context, the main contribution of the research is an online data flow or tool that generates a building model based on open BIM formats. This is a semi-automatic process, which is fast and accurate enough for our needs. Furthermore, it can be achieved without visiting the site, only requiring pictures of the different façades. Among other aspects, building owners, promoters, or engineers should have a comprehensive understanding of the building’s geometry, orientation, location, and other data that is needed to consider alternative renovation scenarios and to make estimates in an early stage of the project about the costs of investment, the need for insulation or the capabilities for harvesting solar energy. To achieve this, it is necessary to have a geo-located 3D model of the building that can accurately depict the building’s shape and structure and the ability to fit the prefabricated modules as an over-cladding system. This is where the layout of the prefabricated walls and solar panels comes into play. A proper layout can give a clear idea of how many solar panels can fit on the building envelope, what cumulated irradiation they receive, how much insulation is needed, and how much investment is required. This paper explains the latest updates on a tool that allows for semi-automated online building modelling and the layout of prefabricated modules with solar panels. This tool generates a detailed 3D building model and layout of the prefabricated modules by using building images and OpenStreetMap floor plans. The tool provides two main outputs. One is the building model that can be used as the basis to estimate, with some other specific tools, the potential energy savings. The second output is the layout of the prefabricated modules, which includes and optimises the placement of solar panels. The major benefit of the tool is that it can be used without the need for on-site measurements by technicians. By using the outputs of this tool, building owners, promoters, and engineers can make informed decisions about the installation of prefabricated modules with solar panels and get an initial estimation of how economically viable and energy-efficient the renovation project could be.

## 2 SOA AND INNOVATION

Different stakeholders participating in building envelope renovation agree that façade upgrading with prefabricated modules needs to be more efficient, as stated by the European Commission (European Commission, 2020). There is a general need for a more automated process to achieve a safer and more effective process. The renovation of building envelopes using modules has not taken off, as anticipated, despite the effort put forth in the research programs. The European Commission's latest call for research project proposals (European Commission, 2020) was asked to, among other things:

- A "Demonstrate retrofitting plug & build solutions and tools reaching NZEB standards suitable for mass production by the industry for buildings under deep renovation."
- B "Decrease of retrofitting time and costs by at least 50% compared to current renovation process for the same building type."

These issues highlight the fact that there are still problems in the field of prefabricated module-based building refurbishment. The requirement for mass customisation is still present, as seen in point a). Contrarily, point b) reveals that the "current renovation process" or, in other words, the manual process is more practical, affordable, and effective than approaches that use prefabricated modules. Therefore, there is a real need for improvement in façade renovation with prefabricated modules.

Figure 1 explains all stages. Please note that the prefabricated modules are supported by connectors

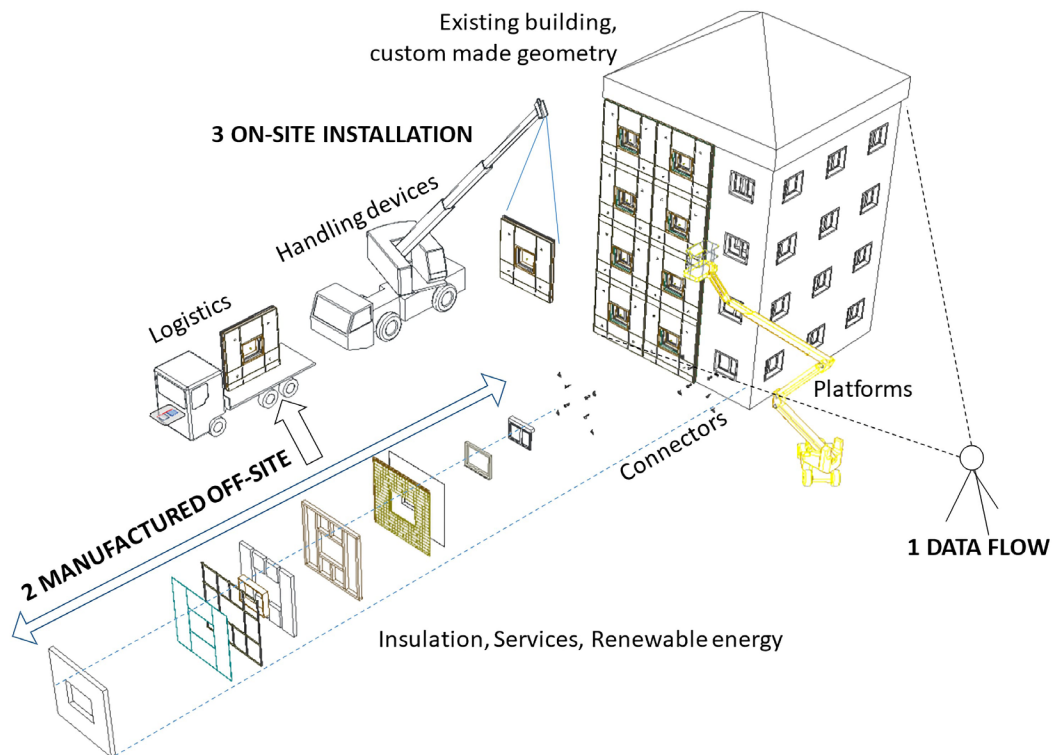


FIG. 1 Building renovation process with prefabricated panels for the envelope

Records obtained in previous research projects (Iturralde, K. et al., 2022) show that the time for on-site data acquisition of the building was 0.15 hours per façade square meter. In the analysed cases, data acquisition was made with a Total Station and targets. Besides, according to these previous studies, the prefabricated layout definition takes 0.34 hours per square meter. Defining the layout of the prefabricated modules means adjusting a standard or normalised façade type (i.e., from a certain company) to the geometry of the existing building's façade. For the initial stages of the project, when the decision-making takes place, the objective of this research is to reduce the time for façade and building modelling as well as the layout definition by at least 90 per cent; a reduction that directly impacts cost savings. This percentage was determined as a benchmark during the research project proposal and based on previous studies (Iturralde, K. et al., 2022). The objective is to minimise the time of data flow during the renovation processes of existing buildings. These previous studies, such as research projects such as BERTIM (BERTIM, 2019), have shown that, in the initial stages, it is essential to reduce iterative measurements of the building and that reducing the data flow to almost zero is crucial. Since reducing the time of the entire data flow process to zero is predicted to be difficult, 90% has been defined as a challenging objective.

### 3 METHODOLOGY

The implementation of the workflow is a two-step process. The first step involves the creation of a 3D model of the building and its various features. Once this is done, parametric algorithms can be applied to the façade, which are able to generate prefabricated module placements on the building.

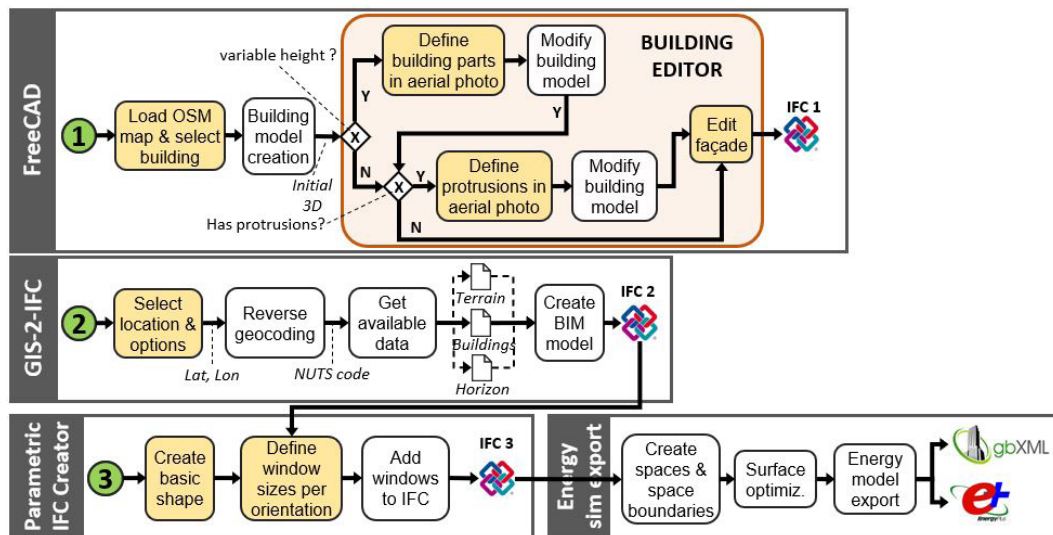


FIG. 2 Workflow for online building modelling methods

#### 3.1 ONLINE BUILDING MODELLING OF EXISTING CONDITIONS

Before proceeding to any digital workflow, the first step is to model the existing conditions since old buildings rarely have any digital representation (Volk et al., 2014). To manually create it could be time-consuming and require basic modelling skills (Kadhim et al., 2021). In addition, there is an increasing availability of open data sources and digital formats concerning the building stock,

although at different levels of detail, quality, availability, or reliability. In general, these sources provide information about the building layout or footprints and some basic attributes, although they do not usually inform about the internal distribution of the building. However, when the renovation process only involves interventions in the façade, this can be sufficient for our purpose.

**Figure 2** shows the workflow covered in this paper for the online data acquisition part and its further use for other purposes, e.g., energy simulation. Numbered circles 1, 2, and 3 represent different possible starting points, which will depend on the available information about the existing building or the user type. They can be used independently and produce an IFC of the existing building (namely IFC 1 and IFC 2), but could also be combined in more complex workflows, even involving external tools. Yellow-shaded boxes represent user-driven actions, whereas the rest represents automated processes executed in the background with no user interaction.

### Option 1: FreeCAD-based approach

This approach (starting point 1 in Figure 2) focuses on the information from OpenStreetMap and pictures given by the client/building owner. The tool creates a building model while the promoter interacts with it. OpenStreetMap (OSM, 2023) was used for preliminary semi-automated data acquisition and the subsequent initial building modelling. For that purpose, an algorithm was developed to semi-automatically generate the shape of the building (see **Figure 4**). Computational design tools and software, such as FreeCAD (FreeCAD, 2023), were used to merge information taken from online databases.

First, the user exports a map section from OSM as an XML file. The user then opens FreeCAD and uses the 'Load.osm' file command to select the exported map file. The command creates a CAD object for each building in the OSM file with the correct layout (**Figure 3**). However, at this point, the exact height of the building and the roof shape are unknown; thus, the height is indirectly estimated from the number of floors (assuming a typical floor height, e.g., 3 m).

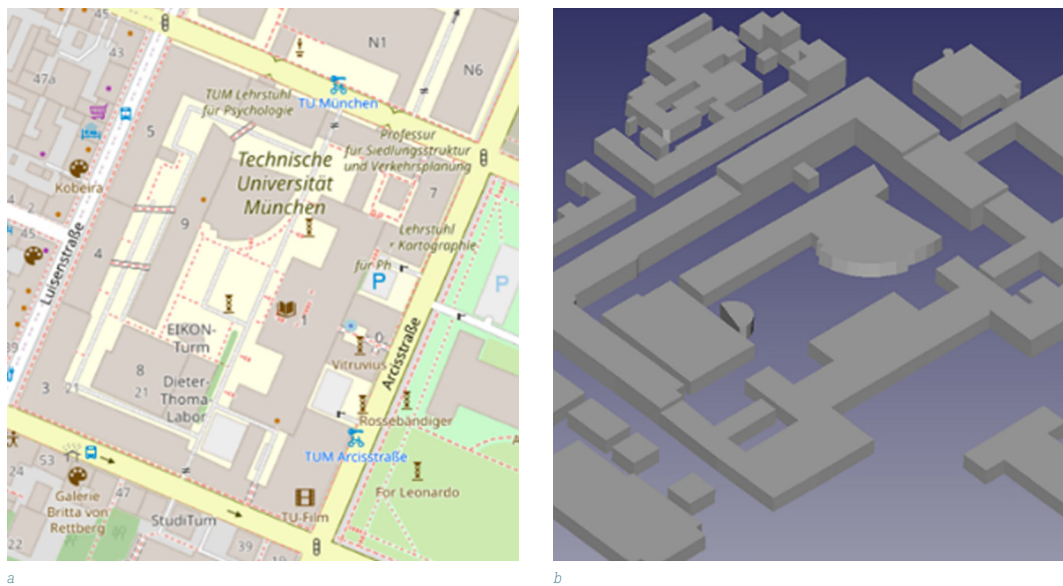


FIG. 3 A map section in OpenStreetMap (left) and the same map section after import in FreeCAD as a 3D model (right)

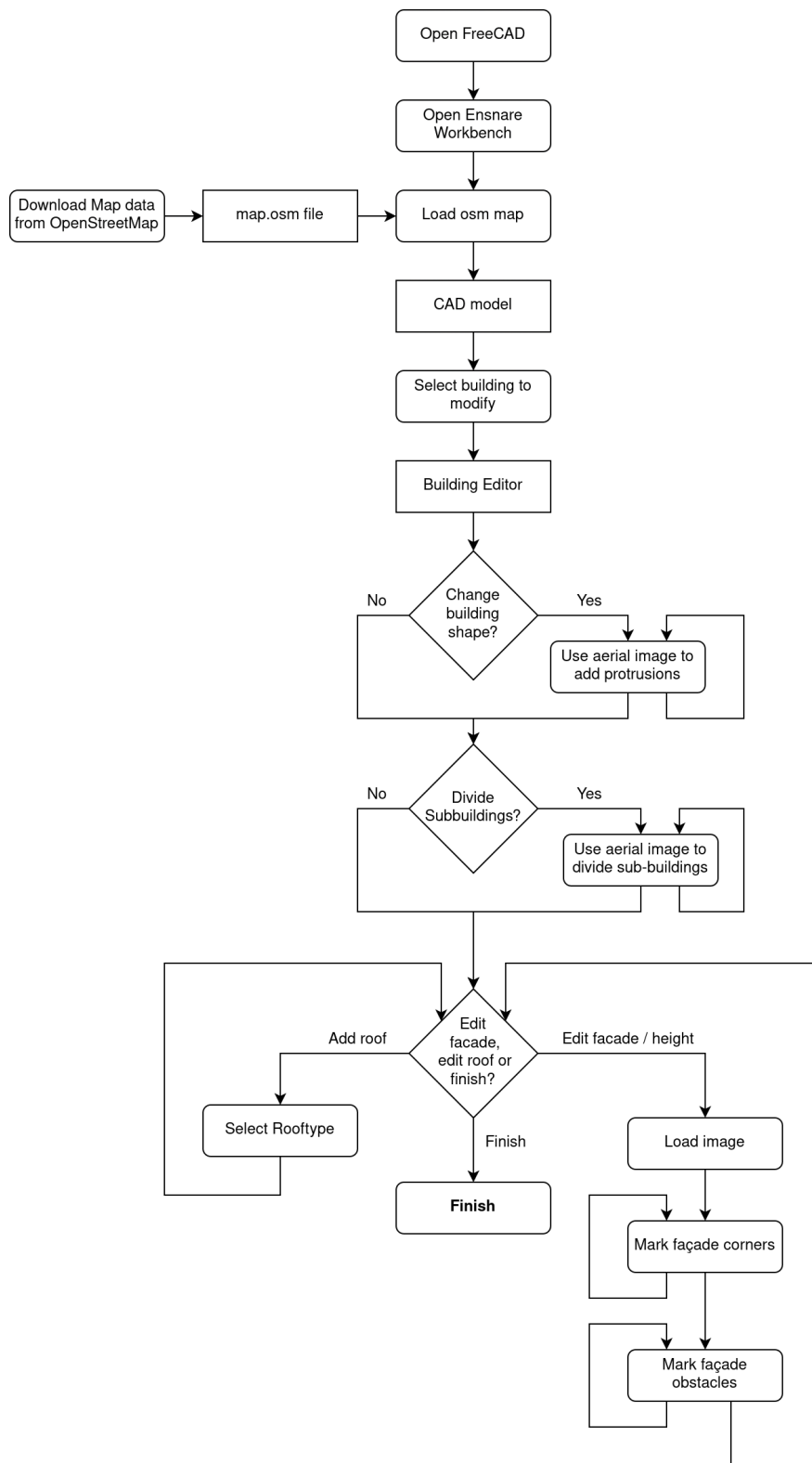


FIG. 4 Scheme of the online data processing

Next, the user selects a façade in the 3D view and uses the 'Adjust façade' command. The user then selects a previously taken photo of the façade, which is opened in a new window. In this window, the corners of the façade can be marked. With the corners given and by assuming a rectangular façade, we can locate the vanishing points. Through a series of geometrical operations based on the plane folding of the quadrangle, we were able to obtain the geometrical restitution. In this way would could revert the projection of the façade and determine the original proportion between width and height, as shown in **Figure 5**, right. This is a well-known procedure of geometry techniques (Izquierdo Asensi, F., 2000). Note that the image of the visual interface generated in Python itself is not linear; it only serves to visualise the algorithm (the code itself in Python is linear). Since the length of the façade is known from OpenStreetMap data, we can multiply it by the proportion to calculate the building height. The height is then adjusted in the 3D model (see **Figure 5**).



FIG. 5 Left, Tartu demo building façade with marked façade and gable area. Right, screenshot of the Python code, the algorithm for computing the height-width proportion from a façade image on the very same Tartu demo building

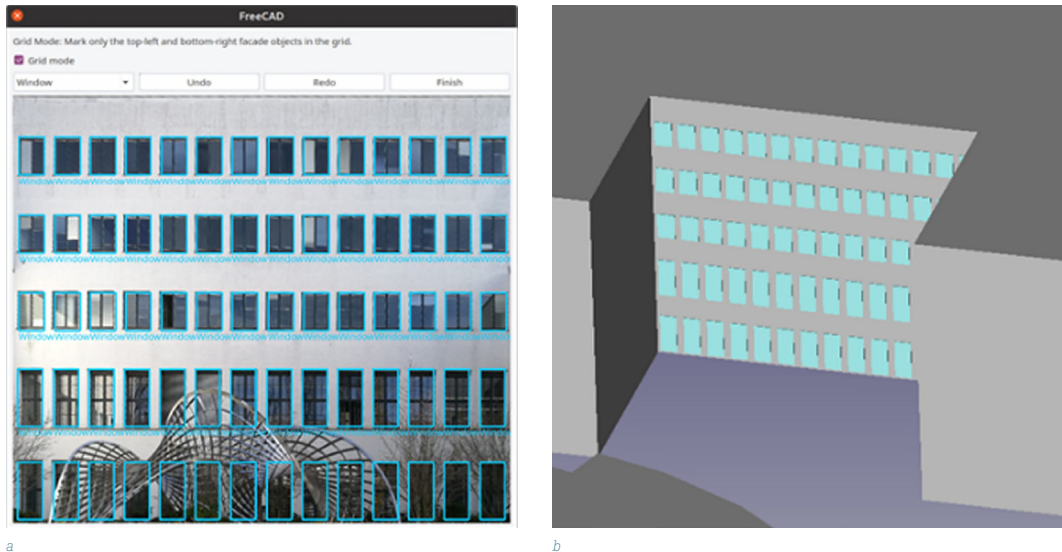


FIG. 6 Marked windows with the grid function on the transformed façade image of the main building of the Technical University of Munich.

In the following step, a perspective transformation is performed on the façade area to make it rectangular. In this transformed façade image, the user draws bounding boxes around façade objects and selects the appropriate object type, for example, a door or window. A grid selection mode is available for marking many objects in one step since objects like windows are frequently positioned in a grid. When the user has marked all objects on the façade, they can finish the step, and the objects are added to the 3D model (see **Figure 6**). To better explain this step, a façade with a grid of multiple windows is shown, in this case, one of the façades of the main building of the Technical University of Munich (see **Figure 6**).

When the user marks more than four corners for the façade, the additional points are interpreted as roof points. The roof shape is then extruded along the length of the building to create the roof in the 3D model (see **Figure 7**).



FIG. 7 Different types of marked façade elements and pitched roofs

With the process described above, the building model can be defined. Several tests have been carried out with satisfactory results, as shown in **Figure 6** and **Figure 7**. The difference between the obtained data and the measured building sizes ranges between 1 and 3 per cent of the building. The differences are tolerable because this solution is supposed to be used at the first stages of the façade renovation project; the initial phase where the model's reliability level is still expected to be lower than the one required for later detailing phases (Polly, Kruijs & Roberts, 2011). The measurements at this stage are used only for estimation. With this building model, the layout of the modules for the renovation intervention can also be determined automatically.

Several tests were carried out with different buildings, such as a demo building in Milan (depicted in the following **Figure 8**), and Level of Detail 4 (Löwner, M. O et al., 2013) was approached.



FIG. 8 The demonstration building in Milan, the original on the left, the version obtained with the aforementioned tool on the right

Sometimes, the user of the tool might not be able to manually select the elements in a façade. For this reason, automated detection of building limits and windows using CNNs (Convolutional Neural Network) was approached. This can facilitate the detection of corners, as can be seen in **Figure 9** and **Figure 10**. This capability will be re-adapted to link the process with the BIM generation.



FIG. 9 Automatic building edge detection in the demo building located in Tartu (Estonia)



FIG. 10 Automatic detection of windows

### Option 2: IFC generation from GIS and open cadastral data.

The starting point 2 in **Figure 2** covers the automated IFC generation from open GIS data sources. The process starts with a location selected by the end user (e.g., by selecting it in a web map). Next, location-based information must be retrieved. Typically, open data sources can be universal, e.g., OpenStreetMap, which is collaboratively maintained by individuals, or limited to some geographical scope (national, regional, or city level), which is the case with cadastral systems maintained by public administrations. Thus, the location-based information must be obtained from the selected coordinates (usually given in latitude and longitude), a process known as “reverse-geocoding”. Many equivalent services exist for this purpose; for this work, Nominatim has been used, a service offered by OpenStreetMap. However, the output of the web service does not offer a standardised output; neither in terms of language (although we could force it to use English or the local language), having a homogeneous naming convention (and output language), nor in terms of attribute naming. This is more difficult to address since administrative units are not the same in Europe: Spain has provinces, France has departments and regions, and so on; thus, the output tags vary greatly (**Figure 11**, left). This will happen with any reverse geocoding service. To solve this, Eurostat provides a unified framework named Nomenclature of Territorial Units for Statistics or NUTS (European Commission, 2021a). Thus, from the country code (e.g., “es” or “fr”) and the postcode, which is offered by the reverse geocoding, the NUTS code was obtained using the correspondence tables which are freely offered by the EC (European Commission, 2021b). NUTS codes follow a hierarchical coding (e.g., Spain is “ES”, the Basque Country is “ES21”, and the province of Biscay is “ES213”).

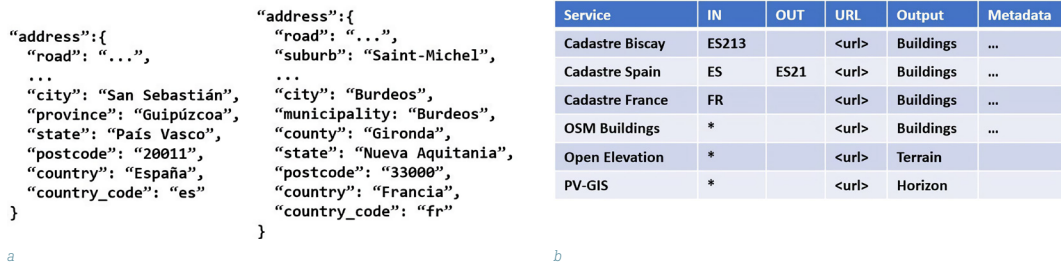


FIG. 11 Sample Nominatim outputs (left) and internal service configuration mapping (right)

Then, an internal configuration file was created (see the simplified concept in **Figure 11**, right) where, for each open data service, the applicable (or eventually excluded) NUTS code(s) are defined: e.g., the Spanish cadastre applies to all of Spain (ES), except the Basque Country (ES21), and the cadastre for Biscay is only applicable at the province level (ES213). Additionally, OSM is universally available in Europe and not filtered by location. Thus, from a given NUTS code, we can filter out which data sources (and their URL) we can access (or not). This configuration file provides metadata

(such as the type of output or detail), which has helped to better filter the information or select the most appropriate one with several available. Finally, for some use cases like solar analysis, it can be interesting to include the terrain and solar masks (visible horizon) in the output model. This is done by accessing two extra web services: 1) Open Elevation API (Lourenço, 2017) to obtain a grid of points with their elevations and 2) the horizon values are obtained through PV-GIS (European Commission, 2022), an online tool for solar panels production estimation, which offers an API-based access. A simple web application has been developed to seamlessly integrate this workflow and make it available for any non-expert, as shown in **Figure 12**. The user only needs to click the location in a web map, and the model is automatically created and displayed in 3D within a few seconds while also being configurable in dimensions and level of detail. This can be implemented in web browsers and viewed online thanks to the cesium.js JavaScript library and downloaded in IFC, optionally with horizon and terrain, as shown in the rightmost image.

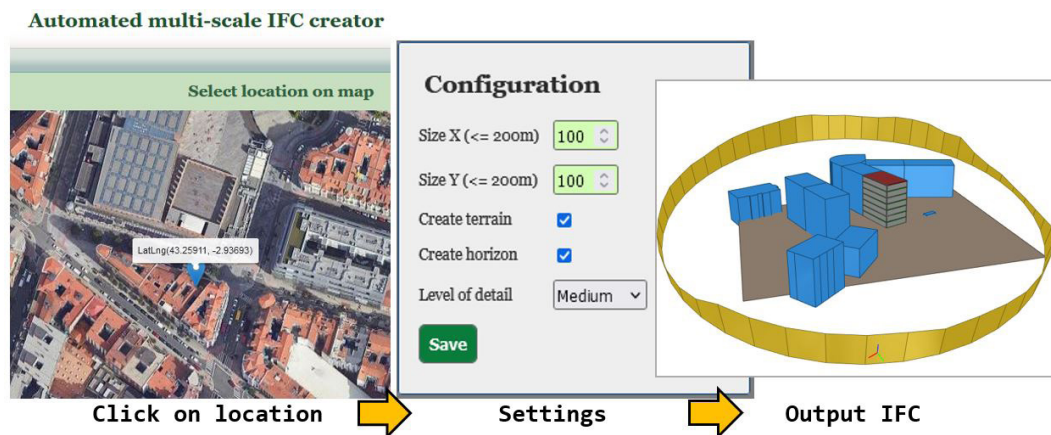


FIG. 12 Web application implementing the GIS-2-IFC workflow

The main benefit of this approach is that simplified models of any residential building from many EU countries can be obtained in BIM/IFC format in a few seconds, online, with a couple of clicks. This enormously reduces the initial data acquisition time. The obtained model can be sufficient for merely estimating some façade dimensions or orientations or other kinds of outputs. However, using it for energy simulation purposes requires additional information, such as windows or internal spaces. These use cases have been tested by integrating the generated output with external tools, as explained in the following sections, thanks to the benefits of relying on open BIM formats (IFC).

### Option 3: Integration with external tools and automated export to energy simulation

The output generated via Option 1 or 2 is an open format (IFC), which means it can be integrated with other tools in a chained workflow. To showcase this process, an integration with the Parametric IFC Creator was conducted. The tool (bottom lane marked as Option 3 in Figure 2) permits creating from scratch an IFC from basic shape parameters, orientation, window sizes per orientation, etc. In this case, the shape was already generated from the cadastral import; thus, only the windows needed to be added to the tool, saving time. This tool also implements the algorithms for BIM-2-BEM conversion proposed by Mediavilla et al. (2023), which permits obtaining a ready-to-simulate file with no BIM or energy modelling expertise required on the user's side. This presents a big potential for early decision stages in building renovation since no detailed model is needed but an estimation of the possible alternatives and their expected impact.

**Figure 13** shows a workflow conducted using the Milano demo building (Italy). The steps can be described as follows: (1) Overview of the building in a satellite image; (2) the result of generating the basic IFC model from OSM with the approach previously explained (Option 1); (3) the model obtained by creating regular windows in Parametric IFC Creator; (4) the same building but with a highly irregular window layout (without the user interface); (5) the previous model exported to gbXML, the standard for model exchange between energy simulation engines (Green Building XML, 2022) and seen in a Aragog web viewer (Ladybug Tools, 2020), and (6) a single storey (space) of the gbXML building.

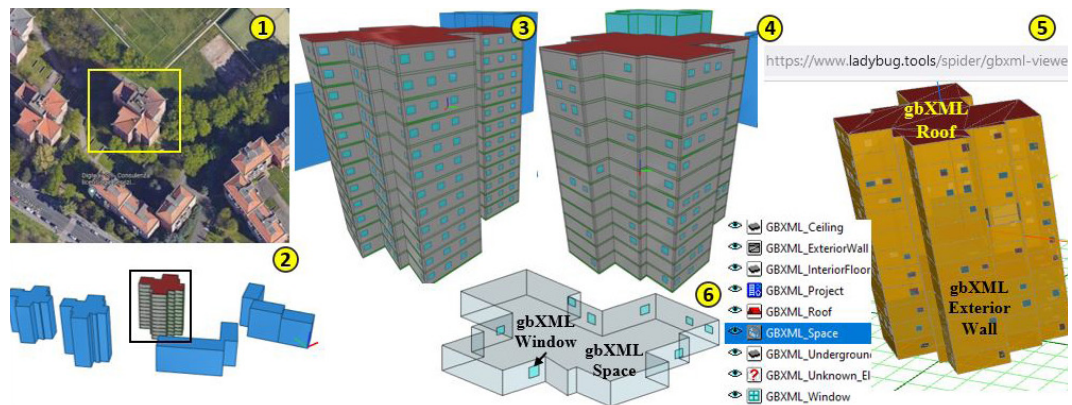


FIG. 13 Model preparation for energy simulation with the demo-building in Milano

However, even if this approach has a real potential, it still has some limitations. In a real building, not all floors are identical; some could include balconies, which can affect the energy demand calculations but also affect the estimation and layout of the prefabricated panels we need to install for renovation. Thus, an additional integration path is being explored in the ongoing research by considering both previously mentioned IFC generation methods in an integrated way, as explained next.

#### Integration of both IFC generation approaches

The different methods to generate the existing IFC presented earlier have their own benefits and limitations, so it seems reasonable to try to extract the best features of each and integrate them into a more optimised workflow, as shown in **Figure 14**, which is part of ongoing research. It starts from the GIS-2-IFC approach based on the online tool presented before. The main difference is that instead of generating an IFC, it generates a JSON file, which will be further used to create the IFC, i.e., the IFC generation logic is encapsulated into a new JSON-2-IFC component (the third one in **Figure 14**), so the workflow between different tools is limited to manipulating the base JSON file. **Figure 15** shows the basic structure of this JSON file, which primarily originates from the GIS-2-IFC module but still lacks windows and other salient elements, which are added in the building edition part approach 1 in **Figure 2**. This, in turn, produces a new JSON file of higher façade resolution, which is the input for generating the final IFC file, compatible with energy analysis tools.

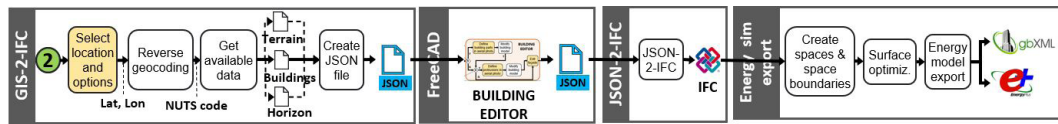


FIG. 14 Integrated workflow

```

"buildings": [
  {
    "orientation": 63.074172200141557,
    "name": "314648932",
    "position": "-9.992625921324358, 19.57854034891352, 0.0",
    "storeys": [
      {
        "elevation": 0,
        "objects": [
          {
            "geometries": [
              {
                "extrusion_direction": "0,0,1",
                "extrusion_length": 3,
                "style": {
                  "surface_colour": "144,144,144"
                },
                "type": "extrusion",
                "extrusion_profile": "-11.5273,-8.6883,0.0 11"
              }
            ],
            "name": "Wall_0_1",
            "ifc_class": "IfcWallStandardCase",
            "name": "Wall_0_1",
            "ifc_class": "IfcWallStandardCase",
            "openings": [
              {
                "start_x": 0.995649136626974,
                "start_y": 1,
                "name": "Window 0-2-1",
                "width": 1.3055435837050867,
                "ifc_class": "IfcWindow",
                "height": 1.002726513102079
              },
              {
                "start_x": 4.196729416460875,
                "start_y": 1,
                "name": "Window 0-2-2",
                "width": 1.370731398929089,
                "ifc_class": "IfcWindow",
                "height": 0.9528239516519759
              }
            ]
          }
        ]
      }
    ]
  }
]

```

FIG. 15 Structure of the exchange JSON file

The JSON file is a hierarchy representing the building, its storeys and heights, the objects in each storey, and their 3D geometries. Each object is tagged with the IFC class name (slab, wall, roof, window, etc.) and different types of geometries are supported (extrusions, boundary representations, and boolean operations). It resembles the IFC structure, but it is much simpler and easier to implement and modify by developers; thus, it is being used to store all the temporary modifications of the building model before generating the final IFC. A snippet of the JSON file is shown in **Figure 15**, where the GIS-2-IFC approach creates the main structure and then, in the image-based editor, window and balcony objects are added relative to the corresponding walls.

### 3.2 PREFAB LAYOUT DEFINITION

As said before, the design of the prefabricated modules for building renovation can lead to time-consuming procedures. In the tool developed for this research, a parametric algorithm determines the prefabricated layout automatically, including the optimisation of the solar panels' surface. This is achieved by applying a set of parameters that are adjusted to different façade topologies. For greater accuracy, extra data given by the building owner can be helpful, such as the vertical distance of the window from the floor.

The foundations of the developed FreeCAD model are a sketch and a spreadsheet. In the sketch, an abstracted two-dimensional drawing defines and visualises the placement and size of the elements of a module. The desired placement and size are controlled through adjustable parameters, which in FreeCAD are addressed as constraints. Most of these constraints are defined in the spreadsheet, while the rest are referenced in the sketch. Constraints (such as the height of the window) are first

accessed through the spreadsheet, where they are given a value, then referenced with an alias, and finally linked in the constraints of the sketch in the form of a formula. This way of linking the data offers a parametric workflow. For modifying the constraints, it is only necessary to change the value of that constraint in the spreadsheet, and the model will be adjusted accordingly.

Regarding the solar panel's dimensions, several panel sizes are selected in this research project. Their dimensions are listed in the spreadsheet. For every case, the correct size of the solar panel for the module needs to be chosen, and its dimensions then need to be selected as values for the constraints.

The three-dimensional module model comprises several building elements belonging to the back frame and the panels on top. This is optimised for the later module assembly.

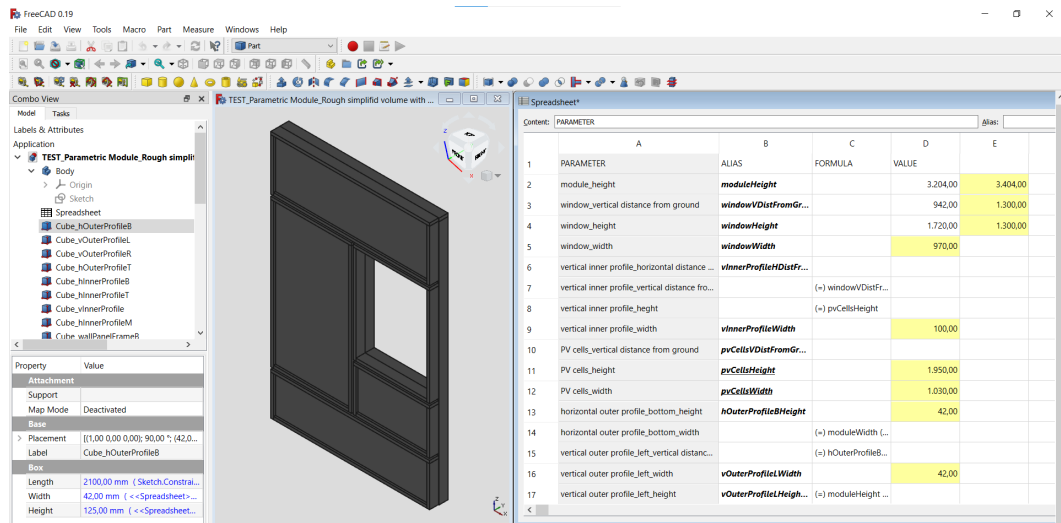


FIG. 16 Different types of marked façade elements

Currently, a scenario is developed in which the façade symmetrically admits modules that are all geometrically equivalent. In this scenario, the problem simplifies placing a solar panel and accompanying registration area within just one module since it can be used to reconstruct the rest of the façade. Tackling more complex façades is a future task.

The façade, module, solar panel, registration, and window must be abstracted as 2D regions in the plane. Under this abstraction, the placement of the solar panel and registration area is a packing problem with the additional goal of maximising the solar panel area.

A module is represented as a rectangular region in the plane whose lower left vertex is at the origin, as shown in Figure 17. The other features (the window, the solar panel, and the registration area) are rectangular regions subjected to the following constraints:

- A feature must be contained within the module.
- No two features may overlap.
- The registration area and solar panel must maintain some proximity.
- The registration area must be placed in a way that it can be reached by a neighbouring module.

The approach is a greedy method that finds the first feasible configuration for a given solar panel. To ensure maximal surface area, the approach starts with the solar panel of maximal area and then moves on to the solar panel of second maximal area, and so on, until all possible solar panels have been exhausted (see red boxes in Figure 17). The layout of the modules also includes the registration area of the pipes and cables (see yellow boxes in Figure 17), the perimeter of each module (see blue boxes in Figure 17), and the perimeter of each window (see green boxes in Figure 17). The size of the façade is shown on the x and y axes in Figure 17.

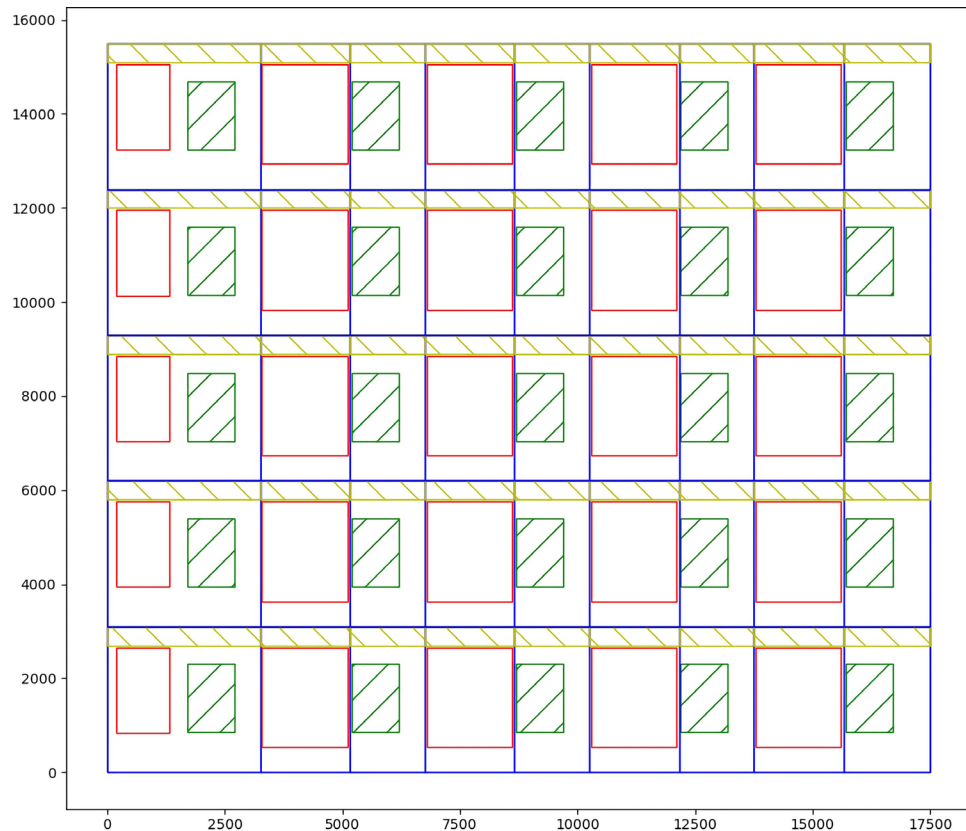


FIG. 17 Automated maximisation of the solar panels (red) and sub-division of the modules (blue), including the registrable area of two façades (yellow)

The implementation of the approach is done using Python (version 3.6.9) without any external libraries. The solution is found by the function optimal placement based on the following inputs:

- The length and height of the module
- The local coordinates of the bottom left corner of the window, its length, and its height
- A list of dimensions of potential solar panel
- A list of dimensions of possible registration areas
- A margin that specifies the distance between features, and the boundary of the module
- A step size which controls how many configurations are tested.

With the definition of the existing building model and the prefabricated module layout, the demo building in Milan can be drafted as shown in Figure 18.



FIG. 18 Visualisation of the automated generation of the layout in the Milano demo building

## 4 RESULTS AND DISCUSSION

The main contribution of the research presented describes a flexible workflow for drastically reducing the time and cost of the IFC model generation process of an existing building for façade renovation purposes. It combines automated, georeferenced multi-building IFC model generation from open data sources with easy-to-use interfaces for façade details edition (e.g., windows or balconies). The tool has been proven in more than 25 apartment buildings, with successful results, as shown in Figure 19.

Depending on the final use and taking this initial digital representation of the building as a baseline, it also covers modules for generating a simplified energy model or for generating a prefabricated panel layout of the renovation project. This layout is automatically generated based on the dimensional criteria and constraints of the modular solution. Figure 20 shows the results of the semi-automated generation of the layouts in some buildings.

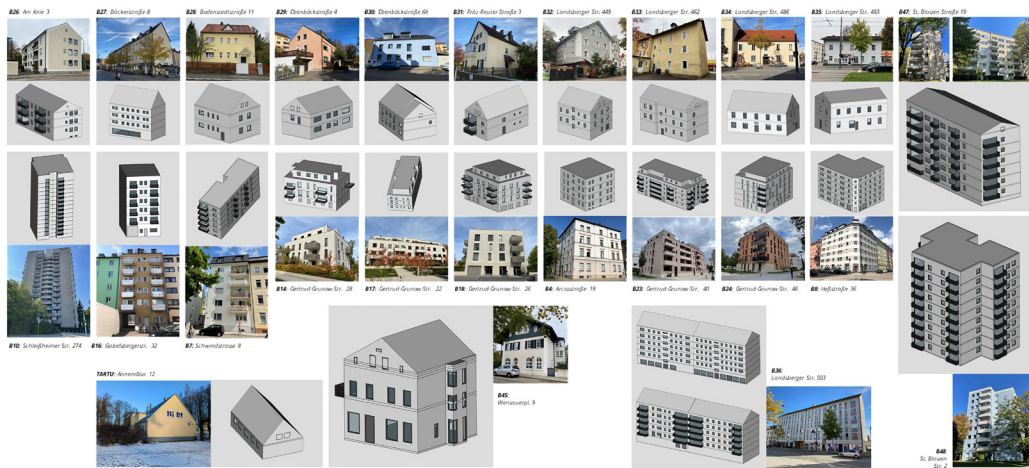


FIG. 19 Some of the building models generated with the tool



FIG. 20 Prefabricated layout definitions by using the tool

The time reduction in the initial stages is obvious. The techniques developed in this research open the possibility for a competitive building renovation with prefabricated modules compared to current manual means. The main objective of the tool was to reduce time, especially in the early stages of the project when the client does not necessarily have the economic means to finance a building model. With the tools explained in this paper, a complex building like the demonstration building in Milan can be generated in less than 20 minutes or 0.33 hours. The demo building in Milan has approximately 3000 m<sup>2</sup> of building envelope. According to the data given in section 2, by manual means, the whole data acquisition and detailed building modelling should, in theory, take about 450 hours (0.15\*3000). This data is high because it implies the necessary and accurate data for manufacturing the prefabricated modules. Therefore, it is not comparable to the time results of the tool described in this paper. On the other hand, defining the prefabricated layout manually can take up to 1020 hours (0.34\*3000). With the tools described in this paper, it can take about 25 minutes, although with less accuracy but still sufficient for the early decision-making process.

*Therefore, in order to compare the whole data flow, the next stages of the research project will monitor the whole process in a demonstration building. However, it remains difficult to compare the time spent in previous stages because there is no benchmark for such tasks.*

## 5 CONCLUSIONS

The generation of BIM-based digital models of existing buildings has a big potential, and the investment done can easily be recovered during the operation phase due to more efficient and data-driven processes (facility management, digital twins, etc.). Emerging frameworks such as Digital Building Logbooks could boost all the potential of BIM models. However, building owners are frequently reluctant to incur such costs when the decision about renovating has not yet been taken, or its future savings and payback are still unclear.

The obtained building model can be used for an early phase where the client/building owner and other stakeholders can decide whether it is feasible or not to carry out the façade upgrading process. The working time has been reduced to a minimum, and therefore, the engineering work that is needed to guide the decision-making is almost eliminated. This facilitates a more agile process. Thus, the market demands low-cost and easy-to-use tools to orient owners in the early decision-making process, where only go/no-go decisions are needed with some comparative estimation of renovation alternatives. The work presented demonstrates that these decisions can be taken using simplified BIM models that can be generated with high levels of automation and using existing open data sources, some of them freely accessible, complemented with algorithmically created renovation layout alternatives. Once the building owner or the client approves the initial budget given and, thus, unlocks a budget for expending economic resources, travelling to make an on-site measurement of the building becomes possible. This will greatly increase the level of detail and definition of the model, reaching the necessary accuracy that the manufacturing and installation processes demand.

Furthermore, since the output is the open source IFC format, it can be further used for energy simulation, web visualisation or export to dedicated BIM software for detailed design and fabrication once the decision for renovation is taken. This approach enables the possibility to consider alternative data sources to generate the building's digital representation, depending on the different data availability, and it also provides a solution that does not require any expertise level in building modelling.

One key aspect of ensuring workflow integration and its future extensions has been the definition of an exchange JSON file, together with JSON-2-IFC synchronisation mechanisms. Thus, it enables quick adoption and implementation by software developers. Another key aspect for its future success is to import/export information from open sources and based on open formats, e.g., GML or geoJSON for cadastral data or gbXML for energy modelling tools.

This paper also shows the path for a future opportunity to apply machine learning on big data sets of images to detect windows and balconies and to match with BIM models or the application of generative design techniques (i.e., for the automatic proposal and optimisation of façade panels). The recent boom in AI techniques (deep learning for image segmentation, natural language processing, generative design, etc.) showcases the interest in the research community and the potential of the technology.

A final aspect to consider is that the availability and quality of freely available data is rapidly increasing, mainly due to the rise in awareness of data providers (e.g., public administrations) to share data with the public. For instance, although the work presented can work on OpenStreetMap data, it can also process local and regional cadastres, which at the moment of writing are only available as web services for a few EU countries and regions, but its support (e.g., by means of

INSPIRE directives) is growing. It is expected that coverage for all EU countries will be possible at some point. These sources provide more reliable and curated data.

In parallel, there is also a rapid increase in the number of publicly available datasets of various types (building façade images, aerial imagery, material and building typology datasets, energy certificates, etc.), which can be used for machine learning and data fusion with BIM models to recreate not only the geometry but its material and performance properties.

## ACKNOWLEDGEMENTS

---

This project has received funding from the European Union's Horizon 2020 research and innovation programme under grant agreement No 958445. This publication reflects only the author's views and the Commission is not responsible for any use that may be made of the information it contains.

## REFERENCES

---

- Alizadehsalehi, S., & Yitmen, I. (2016). The Impact of Field Data Capturing Technologies on Automated Construction Project Progress Monitoring. *Procedia Engineering*, 161, 97–103. DOI: <https://doi.org/10.1016/j.proeng.2016.08.504>
- Bertim. (2019). Viewed on the 28 August 2023. [Online]. Available: <https://cordis.europa.eu/article/id/125299-digitising-building-energy-renovation>
- Bosché, F. (2009). Automated recognition of 3D CAD model objects in laser scans and calculation. *Advanced Engineering Informatics*, pp. 107-119.
- European Commission. (2020). Industrialisation of building envelope kits for the renovation market (IA). Viewed on the 14 March 2020. [Online]. Available: <https://ec.europa.eu/info/funding-tenders/opportunities/portal/screen/opportunities/topic-details/lc-eeb-04-2020;freeTextSearchKeyword=;typeCodes=0,1;statusCodes=31094501,31094502,31094503;programCode=null;programDivisionCode=null;focusAreaCode=null;cross>.
- European Commission. (2021a). NUTS - Nomenclature of territorial units for statistics. Retrieved from <https://ec.europa.eu/eurostat/web/nuts/background>.
- European Commission. (2021b). Correspondence tables - Postcodes and NUTS. Retrieved from <https://ec.europa.eu/eurostat/web/nuts/correspondence-tables/postcodes-and-nuts>.
- European Construction Sector Observatory. (2021). Digitalisation in the Construction Sector. Analytical Report. Retrieved from <https://ec.europa.eu/docsroom/documents/45547>.
- European Commission. (2022). PVGIS API Non-Interactive Service. Retrieved from [https://joint-research-centre.ec.europa.eu/pvgis-photovoltaic-geographical-information-system/getting-started-pvgis/api-non-interactive-service\\_en](https://joint-research-centre.ec.europa.eu/pvgis-photovoltaic-geographical-information-system/getting-started-pvgis/api-non-interactive-service_en).
- Green Building XML (2022). gbXML schema. Retrieved from <https://gbxml.org>.
- Iturralde, K., et al. (2022). Solution Kits for automated and robotic façade upgrading. In *Proceedings of the 39<sup>th</sup> International Symposium on Automation and Robotics in Construction, 2022*, pp. 414–421. DOI: <https://doi.org/10.22260/ISARC2022/0057>
- Iturralde, K., et al. (2021). Compilation and assessment of automated façade renovation, in *Proceedings of the 38<sup>th</sup> International Symposium on Automation and Robotics in Construction, 2021*, pp. 797-804. DOI: <https://doi.org/10.22260/ISARC2021/0108>
- Izquierdo Asensi, F. (2000). *Geometría Descriptiva*. Editorial Paraninfo. ISBN: 9788493366872.
- João Ricardo Lourenço (2017), Open elevation. Retrieved from <https://www.open-elevation.com/>.

- Kadhim, N., Mhmood, A. D., & Abd-Ulabbas, A. H. (2021). The creation of 3D building models using laser-scanning data for BIM modelling. *IOP Conference Series: Materials Science and Engineering*, 1105(1), 012101. DOI: <https://doi.org/10.1088/1757-899X/1105/1/012101>
- Kim, C., Son, H., Kim, C., (2013). Fully automated registration of 3D data to a 3D CAD model for project progress monitoring. *Automation in Construction*, pp. 587-594.
- Knotten, V., Lædre, O., & Hansen, G. K. (2017). Building design management – key success factors. *Architectural Engineering and Design Management*, 13(6), 479–493. DOI: <https://doi.org/10.1080/17452007.2017.1345718>
- Ladybug Tools. (2020). Aragog gbXML viewer. <https://www.ladybug.tools/spider/gbxml-viewer/r12/gv-app/gv-app.html>
- Löwner, M. O., Benner, J., Gröger, G., & Häfele, K. H. (2013). New Concepts for Structuring 3D City Models – An Extended Level of Detail Concept for CityGML Buildings. In *Computational Science and Its Applications – ICCSA 2013*, pp. 466–480. DOI: [https://doi.org/10.1007/978-3-642-39646-5\\_34](https://doi.org/10.1007/978-3-642-39646-5_34)
- Mediavilla, A., Elguezabal, P., & Lasarte, N. (2023). Graph-Based methodology for Multi-Scale generation of energy analysis models from IFC. *Energy and Buildings*, 282, 112795. DOI: <https://doi.org/10.1016/j.enbuild.2023.112795>
- Noori, A., Saruwono, M., Adnan, H., & Rahmat, I. (2016). Conflict, Complexity, and Uncertainty in Building Refurbishment Projects. In *InCIEC 2015*, pp. 251–258. DOI: [https://doi.org/10.1007/978-981-10-0155-0\\_24](https://doi.org/10.1007/978-981-10-0155-0_24)
- Oluleye, B. I., Chan, D. W. M., Antwi-Afari, P., & Olawumi, T. O. (2023). Modeling the principal success factors for attaining systemic circularity in the building construction industry: An international survey of circular economy experts. *Sustainable Production and Consumption*, 37, 268–283. DOI: <https://doi.org/10.1016/j.spc.2023.03.008>
- Omar, T., & Nehdi, M. L. (2016). Data acquisition technologies for construction progress tracking. *Automation in Construction*, 70, 143–155. DOI: <https://doi.org/10.1016/j.autcon.2016.06.016>
- Polly, B., Kruis, N., Roberts, D.R. (2011). *Assessing and improving the accuracy of energy analysis for residential buildings*. US Department of Energy, Energy Efficiency and Renewable Energy, Building Technologies Program, National Renewable Energy Laboratory. URL: <https://www.nrel.gov/docs/fy11osti/50865.pdf>
- Volk, R., Stengel, J., & Schultmann, F. (2014). Building Information Modeling (BIM) for existing buildings – Literature review and future needs. *Automation in Construction*, 38, 109–127. DOI: <https://doi.org/10.1016/j.autcon.2014.03.001>



# Comparative cost analysis of traditional and industrialised deep retrofit scenarios for a residential building

**Martino Gubert<sup>1\*</sup>, Jamal Abdul Ngoyaro<sup>1</sup>, Miren Juaristi Gutierrez<sup>1</sup>, Riccardo Pinotti<sup>1</sup>, Davide Brandolini<sup>2</sup>, Stefano Avesani<sup>1</sup>**

\* Corresponding author, [martino.gubert@eurac.edu](mailto:martino.gubert@eurac.edu)

<sup>1</sup> Eurac research, Institute for Renewable Energy, Energy Efficiency Buildings – Building envelope technologies team, Bolzano, Italy

<sup>2</sup> BIT, servizi per l'investimento sul territorio S.P.A., Parma, Italy

## Abstract

*In this paper, the economic competitiveness for deep retrofit actions between the industrialised off-site and the traditional on-site approaches are discussed by using a comparative Life Cycle Costing (LCC) analysis. This assessment was based on a deep analysis of all renovation-related cost and timing processes, from design to operation and maintenance phases. The study was based on three retrofit scenarios for an existing building in Italy undergoing a deep renovation. The Life Cycle Inventory (LCI) was developed starting from real costs and a list of bills collected by the design team and the industrialised technologies developers. Afterwards, the LCC modelling was performed for all scenarios. The results show that the two deep retrofit approaches (traditional and industrialised) are comparable in terms of investment costs, even if a gap of around -7% and +16% still exists. This highlights a potential for technological optimisation. Moreover, the operation and maintenance phase has shown to be key to transforming the expected higher quality of the industrialised components into a prolonged life expectancy, hence highly impacting the whole cumulated Net Present Value. Finally, the analysis of the End of Life (EoL) phase in case of possible reusing of some dismantled components in the industrialised scenario resulted in contributing in a relevant way to increase the final value of such an approach.*

## Keywords

*deep retrofit of existing building, industrialised approach, prefabricated envelopes, multifunctional envelopes, LCC*

## DOI

<http://doi.org/10.47982/jfde.2023.2.A3>

# 1 INTRODUCTION

Buildings in the EU are responsible for 40% of energy consumption and 36% of greenhouse gas emissions (International Energy Agency (IEA), 2019). Hence, the buildings sector is the largest energy consumer in the EU and one of the largest CO<sub>2</sub> emitters (European Commission - Energy Department., 2020).

Building stock retrofit is a crucial aspect and a primary concern in the European agenda as a reflection of the relevant role played by existing buildings in terms of energy consumption and CO<sub>2</sub> emissions, as demonstrated through the launching of the Energy Performance of Buildings Directive EPBD recast (2018/844) and the Renovation Wave strategy, presented in 2020 by the European Commission to boost building renovation in Europe (European Commission, 2020). 75% of the existing buildings in the EU are energy inefficient, with an energy label below A (European Commission - Energy Department., 2020). European regulations regarding building retrofit in Member States, therefore, aim to improve the energy performance of the existing building stock (Annunziata et al., 2013). Three main categories of energy renovations can be identified: light, medium, and deep retrofit actions, with a building performance respectively less than 30%, between 30% and 60%, and above the 60% of final primary energy as declared in (European Commission, 2019). In terms of shallow and deep renovation solutions and related impacts, a theoretical techno-economic comparative study was conducted by (Semprini et al., 2017) for the city of Bologna. Given the ambitious target of CO<sub>2</sub> neutrality in Europe by 2050, set by the European Green Deal, a deep energy renovation of the building stock is a must, and the current renovation rate needs to be quickly and dramatically increased (Hélène Sibileau, 2021), (Semprini et al., 2017).

To achieve this vision, the deep retrofit of buildings has to be empowered through innovations able to trigger quicker renovation while assuring long-lasting performances. A potentially relevant game changer to trigger this transition is building industrialisation (through digitalisation and prefabrication), given the proven advantages evident from the new building sector. The implementation of an industrialised retrofit approach was deeply studied in different research and innovation projects, as summarised in (D'Oca et al., 2018). This approach consists of the off-site production of prefabricated envelope modules (for the roof and the façades) ready to be directly installed on-site on the existing building, generally without the use of scaffolding, supported by a very detailed design grounded on the exploitation of different digital tools. The main envisaged advantages are related to construction site time reduction, cost compression, and low disturbance for the inhabitants (Andaloro et al., 2019), in parallel with improving the general building efficiency, exploiting an increased interconnection between the envelope and the energy systems (Sandberg et al., 2016). The current practices and future potential for such an industrialised approach were presented in (Konstantinou & Heesbeen, 2022). Moreover, the expected impacts of modularity and prefabrication in terms of sustainability were deeply investigated by (van Oorschot et al., 2021) for prefabricated timber façades.

In literature, a quite wide variety of solutions and a number of studies on their performances can be found. The hygro-thermal performances of multifunctional prefabricated timber frame façades integrating solar thermal panels, windows, decentralised ventilation machines, and shading systems were investigated by (Riccardo Pinotti, 2019). Another prefabricated façade system integrating a micro-heat pump and semi-centralised ventilation was studied and tested by (Ochs et al., 2015). Another study about the improvements in the indoor environmental quality and the energy consumption of an existing office building through the use of a prefabricated module was done by (Pungercar et al., 2021), showing 77% energy consumption reduction for a temperate climate.

Prefabrication and modularity could also trigger the creation of new spaces added to the existing buildings to increase energy performance, as discussed in (Fotopoulou et al., 2018). Finally, it is worth mentioning that a retrofitting intervention with an industrialised approach without relocating the inhabitants during the work was studied by (Zanni et al., 2023) and implemented in a real building, achieving structural and energy performance improvements. From a structural point of view, the retrofit solution entailed the adoption of a wooden shell made of CLT prefabricated panels.

Despite the development of several prefabricated technical solutions and the constant improvements in their technologies, the topic of the costs was hardly discussed due to many reasons: confidentiality, lack of standardised methodology, lack of reliable primary data, and sensitive calculation procedure. The costs of the actual implementations of low-tech industrialised renovation solutions (with a very low level of multifunctionality) were reported in (ECSO, 2017) based on the Energiesprong experience in the Netherlands. Energiesprong is heavily promoting such an industrialised approach through a series of real cases of implementation of low-tech retrofit solutions, aiming at activating such a market and optimising the final renovation costs through mass activation.

The off-site industrialised retrofit approach considered in this analysis aims at providing a prefabricated solution set to achieve the nearly Zero Energy Building (nZEB) energy target, minimising the on-site work by integrating the needed components directly in the new envelope. The building renovation's underlying energy concept is based on energy demand electrification, generating energy with a heat pump system to deliver hot-cold water for both Domestic Hot Water (DHW) and space heating-cooling. The DHW distribution exploits the existing building hydraulic network, while a new water distribution system runs into the new prefabricated façade to a semi-centralised mechanical ventilation system, part of the so-called Energy and Fresh air prefabricated façade kit. Such an innovative system comprises a double-flow ventilation machine with heat recovery, with an added water-air heat exchanger to control the air inlet temperature. This allows to supply each flat with both fresh air and heating/cooling power, depending on the season. Finally, a Building Integrated Photo Voltaic (BIPV) cladding with appealing innovative finishing allows to generate on-site solar energy, eventually storable in a battery, to increase self-consumption and lower the final energy building demand. FIG. 1 shows the kind of industrialised façade and roof module concepts considered in this analysis.

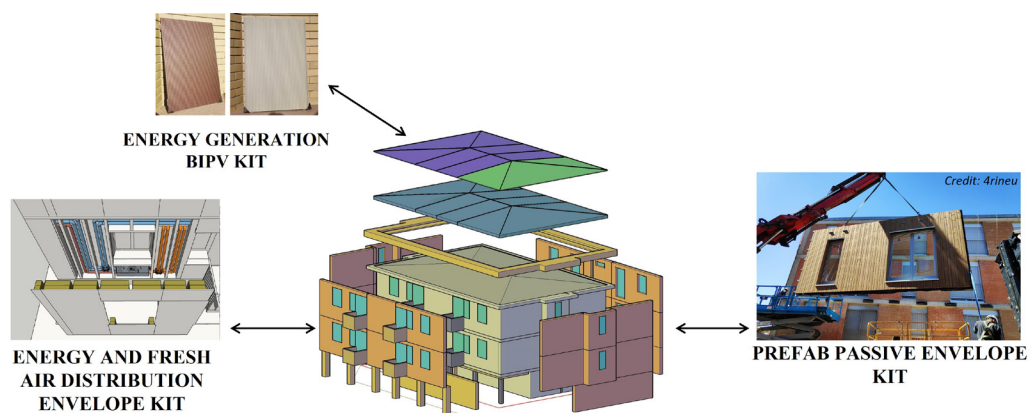


FIG. 1 Schematic representation of the prefabricated envelope (roof and façade) solutions used in the industrialised deep retrofit approach.

Given the technical complexity of the multifunctional prefabricated envelope solutions and the urgency to provide reliable and market-acceptable solutions for the deep renovation, the topic of the overall renovation cost was tackled. The aim of this study was to assess such an industrialised deep building retrofit approach from a cost perspective to better understand its competitiveness. The main research questions were the following: (i) How far is the industrialised retrofit approach competitive against the traditional one? (ii) What is the cost distribution of current and industrialised deep renovation?

## 2 METHODOLOGY

To answer these questions, a comparative economic analysis of different retrofit scenarios was developed to better understand the advantages and limits of an industrialised retrofit process over a traditional one. Specifically, a Life Cycle Costing (LCC) comparative analysis was performed for an existing building in Italy undergoing a deep industrialised retrofit process. The LCC is a lifecycle-based technique that evaluates an anthropic system from the economic point of view, from design to dismissal and disposal phases. This kind of approach allows for assessing the full cost of long-life goods, in this case, buildings which imply long-term maintenance and use phase, as well as high installation costs (Ciroth et al., 2011).

### 2.1 THE REFERENCE BUILDING

The LCC comparison was done at the building level, based on an actual building located in Greve in Chianti (Florence, Italy), under the Italian climatic zone E. It is a social housing block of four apartments constructed in 1979. The apartments are distributed across two floors above a *pilotis* ground level, for a total net heated area of around 400 m<sup>2</sup>. Each apartment has a gross area of 97 m<sup>2</sup>. The façade gross area is around 415 m<sup>2</sup>, of which 55 m<sup>2</sup> are windows (FIG. 2). The 8° pitched roof covers an extension of about 215 m<sup>2</sup>, and the eight balconies cover a total surface of 21 m<sup>2</sup>. In TABLE 2, the main building envelope and internal partition features are reported in detail. The choice of the building was made to ensure the collection of reliable primary data related to the building features and to the different retrofit strategies, given the availability of the building owners, designers, and retrofit technologies suppliers.



FIG. 2 Reference building pictures from different sides (from left to right, East, West, North).

TABLE 1 Construction details of the reference building in its state of the art.

Envelope construction typology description													
Walls	Materials	Thickness	U-value	Walls	Materials	Thickness	U-value						
		m	W/m <sup>2</sup> K			m	W/m <sup>2</sup> K						
External walls M1 - Empty box masonry (40cm)	Plaster	0,01	1,362	Ground floor P1 - Concrete masonry on Pilotis	Ceramic tiles	0,015	0,626						
	Hollow brick	0,08			Plant screed	0,055							
	Not Ventilated Interspace	0,19			Concrete load distribution screed with mesh	0,04							
	Solid brick	0,12			Brick slab thickness 18 cm	0,18							
External walls M2 - Empty box masonry - WC (40cm)	Plaster	0,01	1,362		Plaster	0,005		1,38					
	Hollow brick	0,08			EPS	0,04							
	Not Ventilated Interspace	0,09			Plaster	0,005							
	Solid brick	0,12											
Internal walls M2 - Empty box masonry - Stairwell (30cm)	Plaster	0,01	1,227		Ground floor P2 - Concrete masonry on Cellars	Ceramic tiles		0,015	1,38				
	Hollow brick	0,08				Plant screed		0,055					
	Not Ventilated Interspace	0,08		Concrete load distribution screed with mesh		0,04							
	Solid brick	0,12		Brick slab thickness 18 cm		0,18							
Roof	Concrete load distributed screed with mesh	0,04	1,953	Whole windows		Wood		1,7					
										Brick slab thickness 18 cm	0,18		
												Plaster	0,01

TABLE 2 Schemes of the retrofit scenarios' main features.

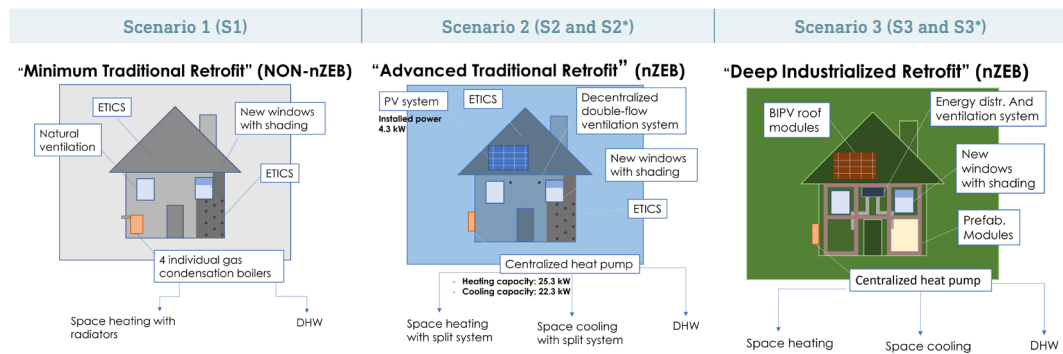


TABLE 3 Resume of the considered envelope characteristics and HVAC technologies for each of the developed retrofit scenarios

	S1: Traditional shallow retrofit	S2: Traditional deep retrofit	S2*: Traditional deep retrofit	S3 and S3*: Industrialized deep retrofit
<b>Thermal insulation wall</b>	ETICS (120 mm of EPS) for the whole envelope excluding the structural pillars and the roof.	ETICS (120 mm of EPS) for the whole envelope, excluding the roof.	Ventilated façade composed of 120 mm of EPS for the whole envelope, excluding the roof.	Ventilated façade composed of a 160 mm mineral wool layer directly installed in the wood frame of the prefabricated façade panels.
<b>Thermal insulation roof</b>	Insulation of the last floor under the roof with a 100 mm layer of mineral wool (keeping the old roof)	Insulation of the last floor under the roof with a 100 mm layer of mineral wool (keeping the old roof)	Insulation of the last floor under the roof with a 100 mm layer of mineral wool (keeping the old roof)	Ventilated roof composed of a 160 mm mineral wool layer directly installed in the wood frame of the prefabricated roof panels (new roof)
<b>Windows</b>	New double-glazing windows with $U = 1.3 \text{ W}/(\text{m}^2 \text{ K})$ .	New double-glazing windows with $U = 1.3 \text{ W}/(\text{m}^2 \text{ K})$ .	New double-glazing windows with $U = 1.3 \text{ W}/(\text{m}^2 \text{ K})$ .	New double-glazing windows with $U = 1.3 \text{ W}/(\text{m}^2 \text{ K})$ .
<b>Ventilation</b>	Natural ventilation.	Decentralised mechanical ventilation machines with double fluxes (supply and exhaust).	Centralised mechanical ventilation machines with the distribution that arrive in each room (fault ceiling in the corridor).	Fresh air and energy distribution system integrated into the façade (semi-centralised mechanical ventilation with double flux).
<b>Heating &amp; Cooling</b>	Condensing gas boiler for each apartment connected to existing hot water radiators in each room. Air conditioning units in each room.	Centralised heat pump connected to new split units in each room. SH and SC powers of 25.3 kW and 22.3 kW.	Centralised heat pump connected to new split units in each room. SH and SC powers of 25.3 kW and 22.3 kW.	Centralised heat pump hydraulically connected to the integrated fresh air and energy distribution system.
<b>Renewable Energy Sources</b>	Absent.	Traditional PV modules installed on the roof (4.3 kWp).	Traditional PV modules installed on the roof (4.3 kWp).	BIPV modules, installed on the roof as cladding elements of the prefabricated modules (4.3 kWp).

## 2.2 RETROFIT SCENARIOS

Three retrofit scenarios were defined as listed below and described in TABLE 2 and TABLE 3: (i) Scenario 1 (S1): Traditional shallow retrofit (non-nZEB), used as the benchmark. (ii) Scenario 2 (S2): Traditional deep retrofit (reaching the nZEB energy performance target after the retrofit). (iii) Scenario 3 (S3): Industrialised deep retrofit (reaching the same energy performances as Scenario 2).

S1 considers a state-of-the-art retrofit energy target of “two energy classes improvements”, as required by the 110% incentive available in Italy from 2020 to 2023 (DECRETO LEGGE, 2020), (Governo Italiano Presidenza del Consiglio dei Ministri, 2023). Such technical targets were achieved by changing windows and the boiler and by applying a 120 mm External Thermal Insulation Composite System (ETICS). S2 and S3 were dimensioned, aiming at achieving the Italian nZEB minimum requirements of at least 50% of the energy demand (heating, cooling, and DHW) covered by RES (with at least 50% for DHW energy demand). The PV sizing method followed is defined in the nZEB Italian norm (Verdi, 2015). Space Heating (SH); Space Cooling (SC) thermal powers for the heat pump were calculated based on the thermal peak loads derived from a building and energy system dynamic thermal model developed in TRNSYS, with the PV system localisation through a dedicated tool. Such a modelling procedure is described in (Gazzin et al., 2022).

To obtain a clear comparison between the traditional deep retrofit and the industrialised deep retrofit approaches, two additional cases were studied, resulting in the five scenarios summarised in TABLE 3. Scenario 2\* (S2\*) was defined to be directly comparable with S3. A centralised double-flux ventilation system with an indoor ducting network (instead of a fully decentralised machine, as in S2) was considered. This assumption is highly impacting in a traditional retrofit intervention because of the kind of indoor construction work to be done to host ducting and ventilation systems. Moreover, instead of an ETICS, an on-site mounted ventilated façade was included. Hence, the expected façade finishing and façade cladding lifetime are directly comparable with S3. Still, S2 allows us to benchmark the ETICS as the most widely used insulation system with painted finishing. Scenario 3\* (S3\*) was introduced to take into consideration that the features and costs of the S3 were reflecting a set of products still under development (Technology Readiness Level<sup>1</sup> TRL= 7). Hence, a 20% reduction of the final price of each prefabricated module installed on the existing building was applied to take into account ongoing processes and technology optimisations as well as the potential of market critical mass activation on the demand side. This reduction rate was discussed with the industrialised solutions technologies providers. Finally, a reduced yearly maintenance rate for the building envelope elements from 1.5% to 1% of the construction costs was considered in the S3\* scenario to give value to the higher quality of the prefabrication process against the on-site one. This reduction was chosen based on the study of the industrialised mock-up maintenance procedures defined with the product developers.

## 2.3 LCC METHODOLOGY

### 2.3.1 Introduction

The LCC methodology followed in this study is based on the LCA and LCC reference norms (ISO 14040:2006; ISO 15686-5:2017). Given the study goal reported in the previous chapter, the functional unit (FU) of the study – crucial to compare different systems in a fair way – was defined as a building providing a living environment to the inhabitants over a reference study period of 50 years with the characteristics reported in the following TABLE 4.

TABLE 4 Characteristics of the living environment considered in the three systems under study.

Parameter	Value
Indoor air temperature (winter)	19°C -21°C
Indoor air temperature (summer)	25°C-27°C
Indoor humidity (winter)	30%
Indoor humidity (summer)	50%
Max CO <sub>2</sub> concentration	1000 ppm
Final energy consumption	12'000 kWh/y

Fifty years was considered as a reference study period because the life span of a building envelope is linked to the service life of the building (Hildebrand, 2014). This means that the industrialised renovation components related to the renovation will end their service life. The rest of the building is kept without generating either costs or revenue. Even though the reference service life of a component can be longer than the remaining reference study period (after maintenance), if the component is not reused, it will end its service, keeping a residual value which was accounted for.

### 2.3.2 System boundaries

As the study is a comparative one, manufacturing and installation of all building components in the current status were excluded from the study boundaries, as they would be the same for all systems. The following life cycle steps were included in the study: (A0) Building renovation design, (A1-A3) Product manufacturing and packaging, (A4-A5) Transport and on-site installation, (B1-B7) Operation and maintenance of the building renovated with industrialised technologies, and (C1-C4 and D) EoL phase. And eventual circular practices such as materials and components EoL were considered in a simplified and preliminary way, given the uncertainties in the market readiness for the definition of alternative circular scenarios.

### 2.3.3 LCC analysis workflow

The whole LCC analysis workflow is depicted in FIG. 3. After the definition of the goal and scope, the subsequent step was the data gathering phase (Life Cycle Inventory – LCI), based on 2021-2022 costs data available from other renovation projects occurring in the same region (Tuscany, Italy) and from the same design team. A list of bills was created for the application of all retrofit scenarios for the reference building: all processes were listed, detailing, where meaningful, both labour and materials costs. For the industrialised retrofit technologies, primary data gathered from the envelope, PV, and ventilation system manufacturers were used. For the traditional scenarios, the primary data of the design team were used, given the availability of a set of offers for traditional retrofit actions. Such dataset was finally cross-checked against the regional prices tables generally used for public procurements (Il Prezzario 2023 dei lavori della Toscana, 2023). A freely downloadable Excel-based tool developed by the H2020 CRAVE zero (Pernetti et al., 2019) was used to perform the LCC analysis. The core of the LCC calculation is the Net Present Value, calculated each year as the sum  $C_n$  of the discounted costs, revenue streams, and value during the phases of the selected period of the life cycle (ISO 15686-5, 2017). The NPV used formula at year  $p$  is

$$NPV_p = \sum_{n=1}^p C_n / [(1 + d)^n]$$

Besides the NPV, the Total Cost of Ownership (TCO) was calculated as cumulated life cycle expenses and revenues after EoL. Primary data were used as pure costs, on which a fixed 25% increase was applied to take into account profit and general expenses. VAT was not considered.

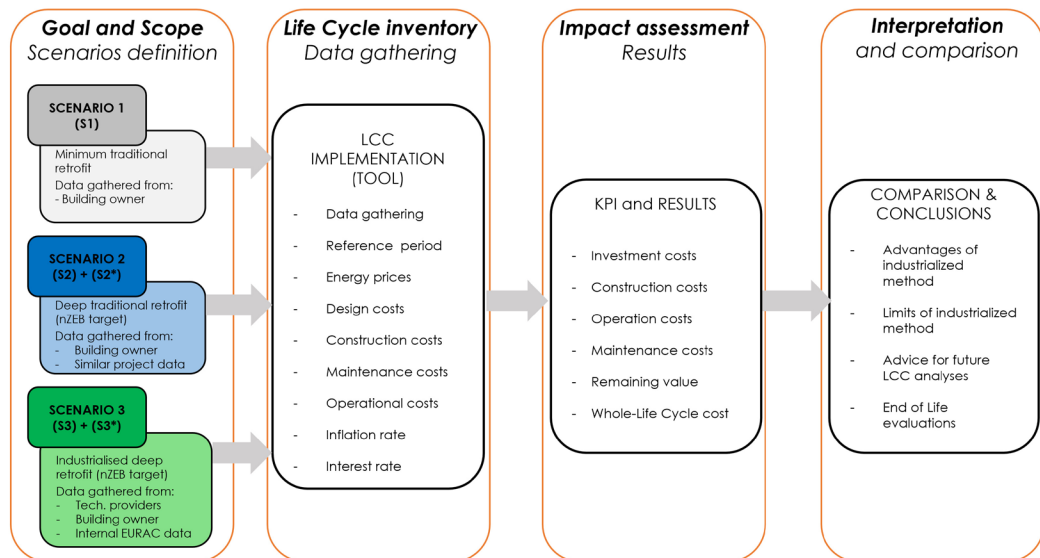


FIG. 3 Scheme of the LCC workflow used for the analysis.

## 2.4 LCC HYPOTHESES

### 2.4.1 Design costs

The design phase-related costs were taken into account as percentual values of the total construction costs, as defined by the Italian regulation (DECRETO 20 luglio 2012, 2012) and (LEGGE 2 marzo 1949, 1949) for the minimum design fees for architects-engineers association. Such values were then validated by the designers involved in the renovation. All these costs were defined for each phase of the project (preliminary, definitive, executive), including also energy certification fees and all the building site management and safety. This turned out to be, in total, 17 % for the traditional retrofit. Further assumed were a design cost increase of +1% for the deep traditional and +3% for the industrialised scenarios (resulting in total design costs of 18 % and 20 %), based on the current renovation experiences of the design team.

### 2.4.2 Construction costs

The construction costs were analysed in detail, as they represent a key factor both for the investors and for the purchasers. These specific costs were subdivided into the two following macro-categories. The first one is the "Building envelope costs", where the total costs for the manufacturing and installation of the building envelope components were included. These costs comprehend all that is related to insulation materials, prefabricated substructures, anchoring and fixing systems, windows, shading systems, passive cladding (or finishing), BIPV modules, and so on. A second cost category was labelled "Additional items cost". This category considers all the costs for all the other interventions and phases, as listed in the following: supply and installation of the building services, working site operations, preparation and rent of the working vehicles and systems, and on-site transportation costs.

### 2.4.3 Maintenance costs

The maintenance costs include both a yearly rate (as a percentual of the total construction cost) for ordinary maintenance and the dismantling plus reinstallation costs occurring once the items reach their service lifetime. With this approach, the yearly rate is the same among all the scenarios in relative terms. Conversely, the replacement costs are different because the technologies to be replaced are different. Hence, it is to be expected that S2 and S3 have higher maintenance costs due to the higher amount of technologies and related costs.

Building envelope systems and building services were grouped separately. The first group is the "Maintenance of the building envelope", including ETICS for S2 and the prefabricated envelope kits for S3, as well as the new windows and shadings. For all the envelope elements part of the industrialised retrofit approach, the yearly maintenance costs forecast was set as 1.5% of their construction costs, according to the Standard (ISO 15686-5, 2017). For S1 and S2, the ETICS lifespan was set equal to 25 years (Marques et al., 2018) (Tavares et al., 2020), while the industrialised envelope kits (ventilated façade) were set to 50 years.

The second category is the "Maintenance of the building services and RES", with the building HVAC system (including thermal storage, boiler or heat pump and accessories). The yearly maintenance costs, as a percentage of their construction costs, were taken from (EN 15459, 2018), as well as the lifespan of each component. In addition, the main electrical system components were considered together with the PV panels' maintenance and substitution. More precisely, the PV panels were assumed to have a typical 25-year expected life (Paiano, 2015) with a yearly 0.5% decrease in their power output (Jordan et al., 2016) and, therefore, to be entirely substituted in the 26<sup>th</sup> year of the life cycle.

### 2.4.4 Operation costs

#### Energy consumption

The yearly energy consumption of the implemented scenarios was calculated through dynamic energy simulations using the software TRNSYS (for the deep energy retrofit scenario) and national standards (for the traditional shallow retrofit), considering the different technologies involved in each case. Because of their high technological similarity and to have the same functional unit, S2, S2\*, S3 and S3\* were assumed to have the same energy consumption, as summarised in TABLE 5. This assumption might be challenged, considering that the insulation level is different between S2-S2\* and S3-S3\* because of the integration of the ducts into the façade. However, as a first assumption, given that a detailed thermal performance calculation of the S3 façade integrating ducts and piping is still missing, the final energy consumption was set identically as a "safe side" hypothesis. Finally, the use of electrical storage was taken into account in terms of investment costs for S2, S2\*, S3 and S3\*, with 100% self-consumption.

TABLE 5 Calculated energy consumption for each developed scenario.

Specific yearly energy demands	RES					Final energy consumption		
	Heating	DHW	Cooling	Ventilation	Appliances	PV prod.	Natural gas	Electricity
	kWh/(m <sup>2</sup> year)					kWh/year	kWh/year	kWh/year
S1	24.1	19.6	22.4	Not Implemented	18	0	16'180	14'260
S2, S2* S3, S3*	6.7	5.8	9.3	7	18	4'650	0	16'650

### Energy costs

The applied energy prices for the LCC analysis and their relative yearly increases were calculated from official data furnished by ARERA<sup>2</sup> (2<sup>nd</sup> trimester 2023) and are reported in TABLE 6. These data refer to the typical trend in the price of electricity and natural gas for the domestic consumer.

TABLE 6 Price of the investigated energy vector and respective yearly increase, equal for all the scenarios.

Energy carrier	Average price	Yearly energy price increase
	€/kWh	%
Natural Gas	0.085	0.62
Electricity from the grid	0.23	1.47

By defining the costs of the different energy vectors involved and their respective yearly percentage increase, the energy consumption costs for the building residents over the 50-year cycle were calculated. A yearly percentage increase in natural gas and electricity costs was considered as an average of the last ten yearly increases, excluding from the calculation 2020 and 2021, which were supposed to be influenced by the global world crises.

### 2.4.5 End of Life costs

An EoL preliminary analysis was performed as a simplified evaluation of the industrialised retrofit competitiveness potential related to its potential capability of easy dismantling and disassembling. The underlying idea is that, once the renovation lifetime is over (50 years), some of the renovation envelope systems components could be sold for reuse. This is, of course, a hypothetical scenario given the market-related administrative and technical difficulties in adopting such circular practices in the construction sector.

Such a theoretical EoL scenario of reuse was approached as follows. All envelope and technical systems costs related to dismantling, disassembling, transportation, and landfill were calculated for all scenarios. For S3, a "reuse" forecast option was assessed only for the industrialised envelope components. Dismantling, disassembling, and transportation costs were summed to a negative value

of revenues derived from the selling of a number of reusable components. Given the difficulties in finding reliable primary data on the topic, such revenues have been parametrically calculated as a portion of the components' initial construction costs, using reduction rates of 50% and 25%. Additionally, three hypotheses of component quantities to be really reusable were defined as 100%, 50% or 25% of the S3 list of bills, resulting in six theoretical options to be compared with "traditional EoL costs with no reuse". The cost source was the (Il Prezzario 2023 dei lavori della Toscana, 2023).

## 2.4.6 Inflation and discount rates

The LCC analysis proposed handles costs along a relevant time span (50 years). All costs were hence actualised via the inflation and discount rates using the coefficients included and described in (Life Cycle Cost Tool, 2023).

# 3 RESULTS

This chapter reports the results obtained from the comparative LCC analysis. Besides a first summary in terms of €, all detailed costs are reported as percentages (benchmarked against the S1 scenario investment costs) due to the confidentiality of the primary data sources.

## 3.1 OVERALL LC COSTS

The cost comparisons among the different scenarios, detailed for each LC phase, are reported in TABLE 7. It emerges that the most relevant phase is Manufacturing & Installation (M&I), followed by Maintenance, Operation, Design, and EoL. However, the use phase (as the sum of O&M) is the most expensive for all scenarios over 50 years of service life. The cheapest scenario is S1, followed by S2. Conversely, S2\* is quite well in line with S3 (slightly more expensive), while S3\* results cheaper than S2\*. These comparisons among the scenarios are clearly shown in FIG. 4, where the relative percentages are reported against the S1 investment cost (equal to 235,423.00 €). The graph shows that: materials shares have the most impact in all scenarios, with a percentage increase from 57% (S1), 101% (S2), 121% (S2\*), 131% (S3), and 118% (S3\*). The design costs, of course, increase from S1 to S3\* as a percentage of the total. Focusing on maintenance costs shows a comparable cost share. However, S2\* has less maintenance costs because of the presence of the ventilated façade with a 50-year life span against the 25 years of the painted ETICS (S2). S3 follows the S2\* trend because of the ventilated façade, while S3\* maintenance results in a reduced share under the hypothesis of highly integrated components with optimised maintenance procedures.

TABLE 7 Costs distribution per LC phase and comparative scenario. Manufacturing & Installation is M&I, Operation & Maintenance is O&M.

Scenario's	Investment		50 years O&M		
	Design	M&I	Operation	Maintenance	EoL costs (w/o remaining value)
S1	€ 33'430	€ 201'993	€268'39	€ 185'373	€ 38'371
S2	€ 59'269	€ 328'362	Same energy level, € 161'000	€ 293'425	€ 59'855
S2*	€ 68'986	€ 382'192		€ 258'269	€ 61'176
S3	€ 97'518	€ 389'294		€ 265'833	€ 59'722
S3*	€ 90'031	€ 359'405		€ 216'697	€ 59'722

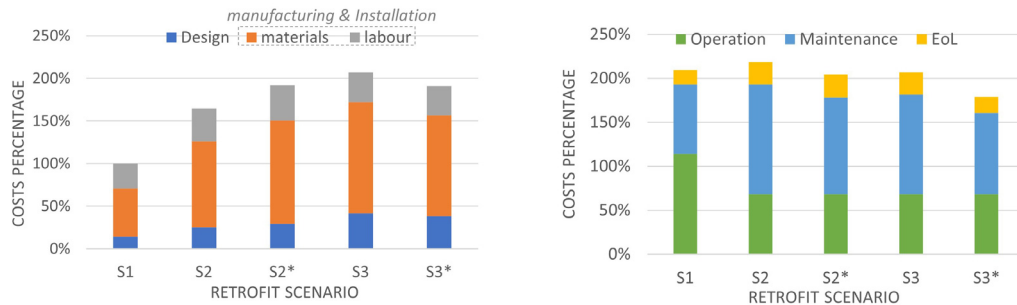


FIG. 4 Summary graphs of investment, operational and maintenance, and End of Life costs as percentages of the S1 investment costs (design, manufacturing, and installation), equal to € 235,423.00.

## 3.2 INDUSTRIALISED KIT COSTS ANALYSIS

As an exemplary result at the kit level, the BIPV and prefabricated Energy & Fresh Air façade modules are reported in FIG 5. and FIG 6. The costs expressed in percentage refer to the whole kit, including materials, manufacturing and assembling processes, packaging and all the installation activities, while the transportation costs are excluded.

It can be observed that the timber-based façade costs are the most relevant ones in the Fair kit while, in the BIPV kit, the majority of the costs refer to the coloured glass-glass PV panels. Ventilation components, which include the ventilation units and all the distribution systems, impact 23% of the total. It can also be observed that the installation costs differ substantially between the two kits (18% for the Energy & Fresh Air kit and 5% for the BIPV kit) because of two main reasons: (i) the overall costs of the BIPV kit is higher (around + 40%), so consequently the percentage impact of the installation is lower; (ii) the installation processes and effort is higher in the Energy & Fresh Air kit due to the presence of the distribution system to be "connected" to the existing building (inlet-outlet preparation, ducts and pipes connections, etc.). Regarding the prefabricated timber-based façade, the differences between kits mostly refer to assembly processes due to the integration of the Energy & Fresh Air kit distribution into the façade, while the materials still have a major impact due to the large number of components needed.

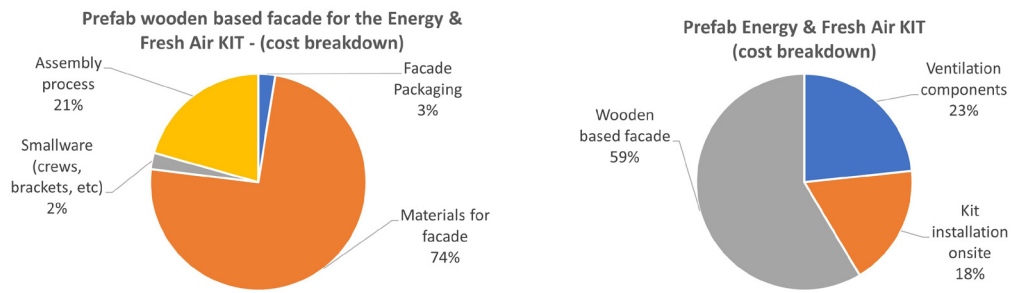


FIG. 5 Energy and Fresh air kit costs breakdown based on €/sqm and reported in %.



FIG. 6 Building Integrated PhotoVoltaic kit costs breakdown based on €/sqm and reported in %.

### 3.3 LC COSTS TRENDLINES

The work done resulted in 50-year cost analyses, allowing to generate trendlines for all assessed scenarios as depicted in FIG 7.

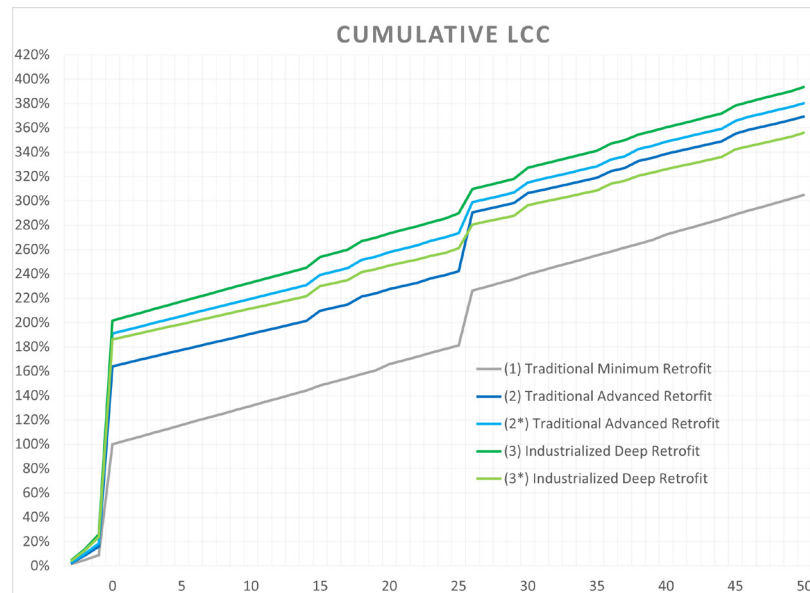


FIG. 7 Cumulative LCC Net Present Value trend along the lifetime (up to 50 years). Percentage values are defined against the S1 investment costs, corresponding to 100%.

Cumulative cost lines for scenarios 2, 2\*, and 3 present the same inclination through the considered life cycle. This is due to the assumption that these scenarios have the same yearly energy consumption and maintenance costs. By looking at the line for scenario 3\*, a decreased line gradient can be observed, which is related to the assumption of considering yearly maintenance costs for the building elements decreasing from 1.5% to 1%. The line gradient for S1, instead, is higher than the others because of the lower energy performance, mainly due to the absence of PV panels and mechanical ventilation.

All scenario trendlines show some "steeper steps" related to the substitution of the components for each retrofit action. For example, the steep increase after 25 years for S1 and S2 (traditional ones) is related to the dismissal and reconstruction of the ETICS (façade and roof) and windows after 25 years.

S2\* is characterised at year 25 by the replacement of several items (roof insulation, balconies finishings, ducts of centralised ventilation system). This does not occur for the industrialised S3 and S3\*, for which all façade-embedded components remain unvaried for 50 years, apart from the windows. For S2\*, the investment costs at year 0 become 20% higher than for S2 and, hence, closer to the costs of the industrialised deep retrofit (S3). Moreover, the optimised industrial deep retrofit approach (S3\*) with a 20% price reduction results in being competitive with S2\* already in terms of investment cost.

FIG 8. shows a set of parametric variations, starting from S3, based on reducing the scenario investment and maintenance costs. It emerges that S3 and S2\* are very similar, with a 10% of S3 investment. When acting on operation and maintenance costs, the industrialised scenario can even be economically more viable compared to a traditional advanced retrofit with a ventilated façade (S2\*).

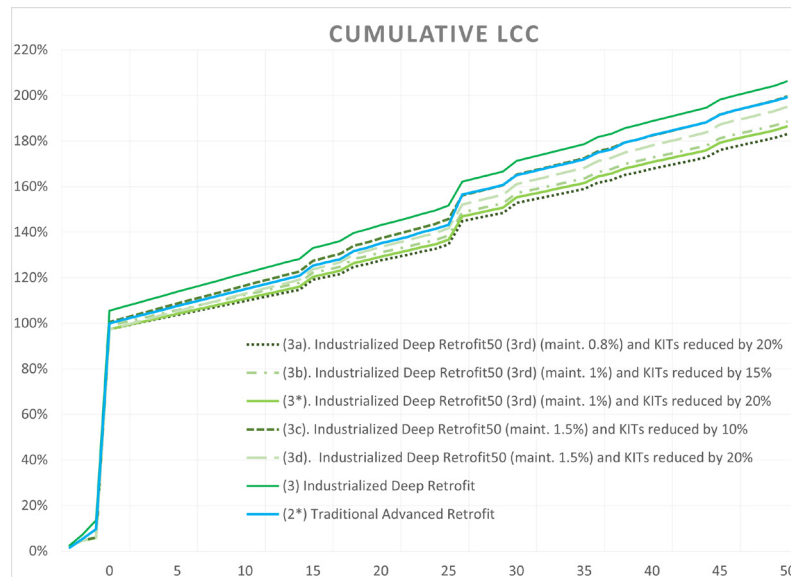


FIG. 8 Focus graph on parametric variations of investment and maintenance costs applied to S3. Reference quantity (100%) is S2\*.

### 3.4 CONSTRUCTION COSTS

The bar chart shown in FIG 9. focuses on the investment costs only related to the building envelope systems for each scenario. As expected, the industrialised approach is more expensive in terms of investment costs, mainly because of the use of additional materials and upstream processes. The most interesting comparison is between S2\* and S3, as they both have the same finishing (ventilated cladding), with a 31% discrepancy. A direct comparison between S3/S3\* against S2 is misleading because of the difference in the finishing solution (painted plaster against ventilated façade). S3\*, optimised with a 20% reduction of the investment cost related to the prefabrication processes and related materials only, is about 16% more than S2\*.

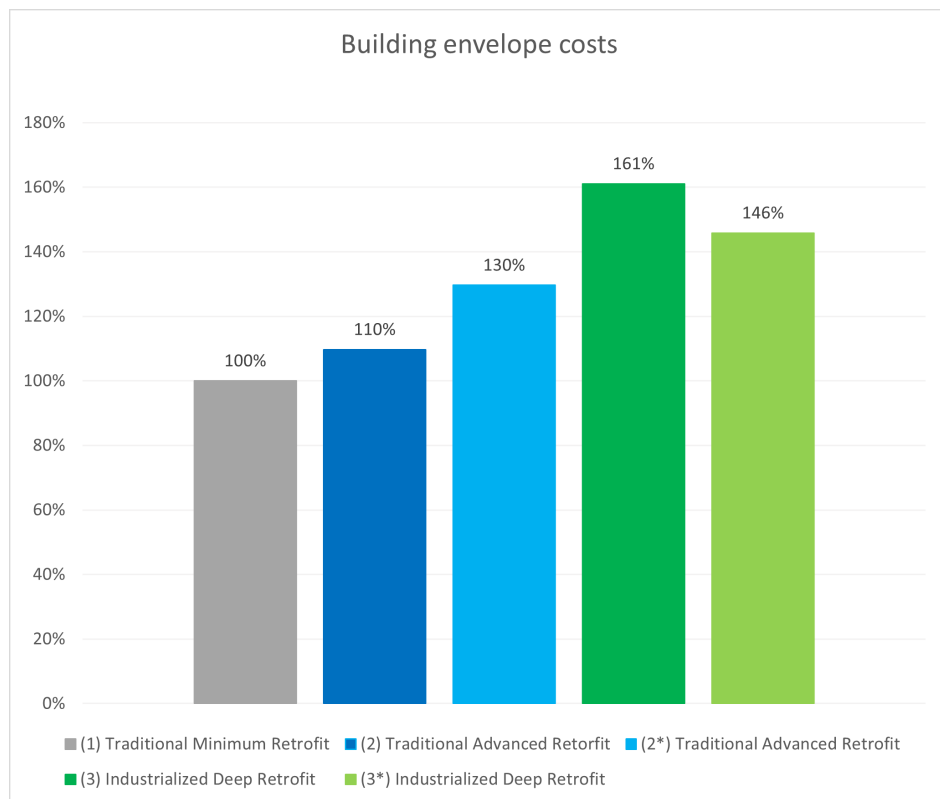


FIG. 9 Investment costs for the renovation of the building envelope for each of the analysed scenarios and their respective variations. Percentage values are defined against the 1<sup>st</sup> scenario costs (100 %).

However, FIG 10. highlights that for all the other item costs (i.e., building services installation, working site operations, preparation, and rent of the working vehicles and systems), the S3 approach provides reduced costs, thanks to time and effort savings during manufacturing and installation. For the industrialised scenario, the development of a semi-centralised double-flux ventilation system installed inside the prefabricated modules, and capable of working also as an energy distribution system, allowed to reduce the interventions inside the apartments and therefore decrease the costs related to the building services. This result is even more evident when compared to S2\* (with a traditional centralised ventilation system), where the installation costs have a 27% difference on the overall "additional items" cost. 7% reduction between S3 and S3\* is part of the cost optimisation process defined for the S3\* integrated ducts and ventilation units. As expected, the installation costs comparison S2 and S3 shows a 74% difference thanks to the fully off-site approach.

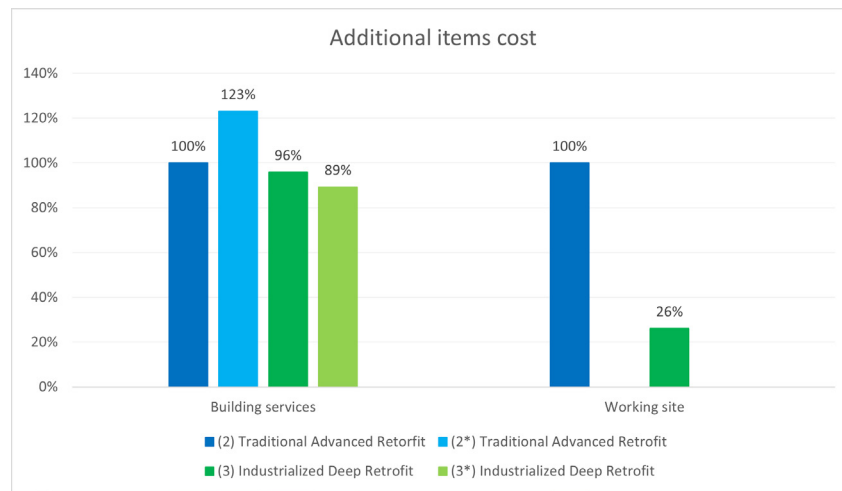


FIG. 10 Additional item costs comparison among developed scenarios and their proposed variations. Percentage values are defined about the 2<sup>nd</sup> Scenario additional item costs: correspondent to 100%.

The reduced time required for the installation of prefabricated modules was fundamental to decreasing the working site costs. Thanks to the use of the prefabricated modules, the use of a traditional scaffolding system was substituted with the utilisation of two aerial working platforms, achieving a relevant reduction in rental cost as well as time required during the on-site operation works. Transportation costs also impact the final investment cost for S3 and S3\*. The need for five lowered trucks (each one capable of transporting 120 m<sup>2</sup> of prefabricated modules) was estimated, and this cost item represents 3% of the total investment cost for S3.

### 3.5 OPERATION COSTS

A comparison between the total costs related to the energy consumed over the 50 years is shown in FIG 11. S2 and S2\* were not considered in this analysis because their energy performance is the same as S3 and S3\*.

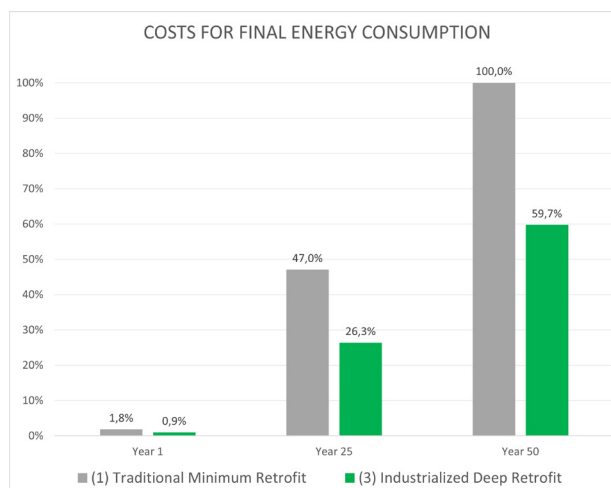


FIG. 11 Cumulative costs for final energy consumption comparison between S1 and S3. Percentage values are defined against S1 cumulated costs at year 50 (corresponding to 100%).

### 3.6 MAINTENANCE COSTS

The cumulative maintenance cost distribution for each developed scenario is depicted in FIG 12. These maintenance costs were subdivided into "building elements" and "building services."

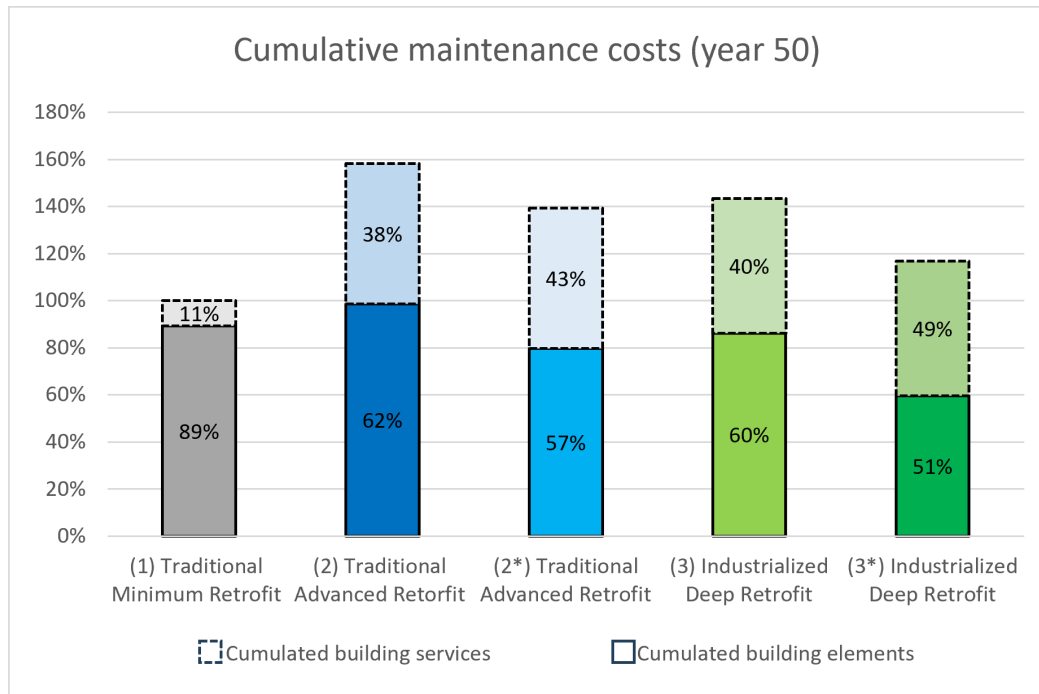


FIG. 12 Cumulative maintenance costs distribution (building elements vs building services) at the end of the life cycle. Percentage values are defined against S1 cumulative maintenance costs at year 50.

By looking at the cumulative costs for the building elements, S2 resulted in 60% more expensive than S1 because of the presence of more technologies to be maintained (and substituted). The difference between S2 and S2\* is mainly due to the substitution of ETICS in S2, while the ventilated façade is considered to last 50 years (as per S3 and S3\*). The additional S3\* has the lowest maintenance costs compared to S3 because of the lowest investment cost. Analysing the cumulative maintenance costs for the building services, instead, the S1, as expected, presents extremely limited maintenance costs for its services due to the absence of HVAC and RES systems. Conversely, in S2-S2\* and S3-S3\*, because of the similar technologies involved, the cumulative maintenance and building services costs were comparable.

### 3.7 END OF LIFE

The parametric cost-revenue EoL results are reported in FIG 13. The simplified analysis was done only on the envelope elements, aiming at assessing the theoretical potential of reusing (at least part of) the industrialised systems at year 50. It emerges how, in the case of reusing components and materials, even just for 50% of the quantities and at 50% of the price of the construction, an economic benefit for the EoL phase can be expected. To be cost-effective, the reuse quantity of the envelope components should be at least 50%, with a revenue of 25% of construction cost, and higher than 25% if the revenue is 50%.

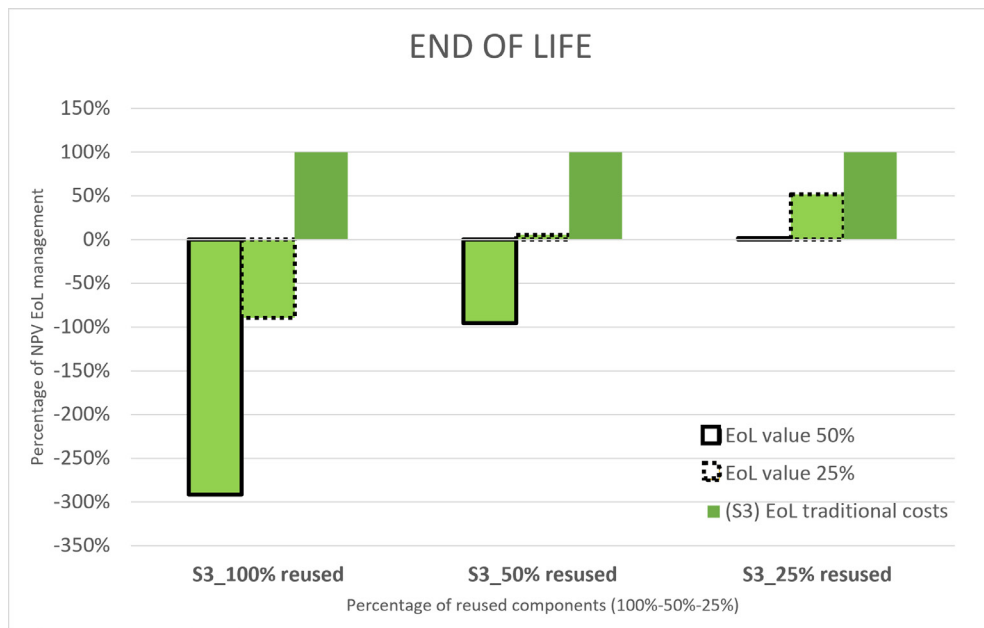


FIG. 13 End of Life scenarios for S3 considering 50% and 25% of construction costs as revenue for 100%-50%-25% of the envelope components reuse compared with the S3 costs for dismantling with no revenues.

The economic potential of a different EoL management, through the dismantling, disassembling, and reuse of sold components, is even clearer from FIG 14. In fact, the best EoL with reuse hypothesis applied to S3 shows a TCO lower than S2\* and S3, highlighting the theoretical potential of circular reuse of envelope components in terms of economic benefit on the whole life cycle. EoL revenues might play a role in reducing the TCO by around 27%.

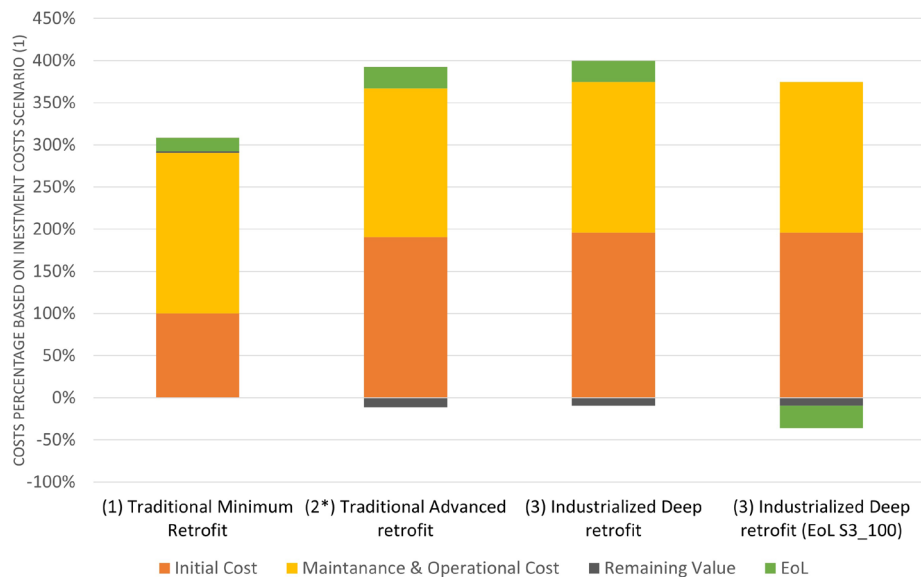


FIG. 14 Total Cost of Ownership value breakdown for the different phases. 100% reference is the investment cost of S1.

## 4 DISCUSSION

The benchmarking of traditional and industrialised scenarios, especially looking at S2\* versus S3 and S3\*, shows a substantial equivalence in terms of investment, operation, and maintenance trends. However, the industrialised approach carries some advantages that might be potentially turned into a value proposition able to impact the S3-S3\* LCC performances, lowering the investment and/or the operation & maintenance costs. Such advantages are: (i) High manufacturing and installation quality, with potentially longer components service life and lower overall retrofit intervention performance loss. (ii) The roof insulation included in the S3 family based on industrialised kits offers the value of having a brand-new roof, compared to the S2 family, with only a layer of insulation applied under the roof. (iii) The S3 and S3\* insulation thickness are actually higher than S2 and S2\* because of the ducts passing into the façade, even if an energy consumption reduction was not taken into account. S3 and S3\* are expected to perform better than S2 and S2\*. (iv) There could be a relevant economic benefit in terms of more profitable interest rates based on the use of a more robust renovation approach grounded on more durable and performing prefabricated technologies. (v) In S3 solutions family, there is the possibility to differently handle the EoL phase thanks to the increasing easiness of reuse and recycle of components and materials (Juaristi et al., 2022). Such topics will need dedicated techno-economic studies to provide robust quantitative evaluations to be used in an LCC analysis.

The comparative LCC analysis performed was a relevant step for the deepening of the market uptake potential of the industrialised deep retrofit approach compared to the traditional ones. However, the adopted LCC methodology has shown to be a tricky method because of the high cost variabilities and need for strong hypotheses. The main affecting parameters are the service lifetime of the components, the evolution of energy and material prices in time, the geographic variability of prices which hinder the generalisation of the findings, the difficulties in monetising the co-benefits and in the assessment of performance changes during time. The very low number of actual industrialised deep retrofit buildings still does not allow the creation of a robust benchmark for the industrialised solutions features characterisation over time.

Finally, the overall analysis has shown different terms of comparison. Of these, S1 and S2 should not be considered directly comparable, given the strong differences in the typologies of intervention and of the functional unit. In other words, the industrialised retrofit approach allows to obtain renovated building performance that is hardly achievable with a traditional deep retrofit. In this sense, the technical benefits of the industrialised retrofit in terms of energy efficiency should also be proven and could lead to a relevant saving in the operational phase compared to the traditional deep retrofit solutions.

## 5 CONCLUSIONS

The presented work aimed at evaluating the potential competitiveness of the industrialised against the traditional deep retrofit approaches by applying a bottom-up comparative LCC methodology. The use of innovative timber-based façade and roof kits integrating windows, highly appealing BIPV modules, and a semi-centralised mechanical ventilation machine (with the related needed aeraulic network) were considered and assessed in terms of costs and revenue trends along the life cycle.

It can be firstly concluded that the LCC methodology at the building level shows high potential to benchmark coherently the industrialised against the traditional retrofit approaches. Nevertheless,

many technical hypotheses and assumptions were made, heavily impacting the results, for which the model could be defined "sensitive". In this perspective, a sensitivity analysis will be crucial to deepen and strengthen those very influencing modelling choices. For example, materials pricing variability, industrialised retrofit co-benefits, maintenance costs, and product development optimisation can be considered crucial aspects to be further investigated.

However, a reliable cost comparison between the two renovation processes was set up, allowing a fair definition of the competitiveness of the industrialised against the traditional deep retrofit approaches. At the building's 50<sup>th</sup>-year life, a fork of plus 7% and minus 16% was calculated as the difference between the industrialised and the traditional scenarios.

The prefabricated kits LCC results highlight the need to work on reducing the materials used, which represent the highest cost share of the industrialised solutions.

In terms of cost distribution at the building level, the best industrialised and traditional scenarios (S3\*-S2\*) showed an investment cost difference of +11%. The construction cost (materials more than labour) appeared to be the main issue regarding the competitiveness of the final industrialised solution. However, given the prefabricated multifunctional envelope technologies optimisation potentials in terms of system design and materials selection, a supplementary reduction of the initial investment should be further evaluated. The investment cost for building services and the integration of renewables, besides the working site management and processes, were lower for the prefabricated scenario, more precisely 7% and 74%, respectively. Moreover, thanks to the direct installation of the major parts of the HVAC system inside the prefabricated modules, the interventions inside the building become simpler and faster, permitting the building occupants to remain in their apartments. Such co-benefits were not evaluated in this study, but their quantification should be further investigated. The operation and maintenance phase has shown to be crucial to increase the competitiveness of the industrialised retrofit. The topic of "better final quality" of this approach, however, needs to be better investigated and quantified for future integration in such LCC analyses. Moreover, the studied End of Life scenario with the possibility of reusing part of the industrialised retrofit components has shown to be a theoretically interesting option to lower the TCO by about 27%.

As a general next step, further LCC analyses should be carried out on real industrialised renovations, collecting primary data able to catch the variabilities of costs in time for different technologies and countries.

This leads to the conclusion that the industrialised approach's "co-benefits" could be the actual trigger to increase the adoption of such prefabricated solutions, contributing to a practical increase of the European building stock renovation rate. Among the most promising "co-benefits", the following need to be mentioned: improved performances in operation (final energy and maintenance), the possibility to attract better investment leveraging the reduction of the risk, reusing of disassembly-capable components as a more valuable EoL strategy, building users do not need to leave their apartments during renovation, less construction time which means less disturbance.

## Acknowledgements

---

This paper is part of the research activities of the INFINITE project, funded by the European Union's Horizon2020 research and innovation programme under grant agreement No 958397

## References

---

- Andaloro, A., Gasparri, E., Avesani, S., & Aitchison, M. (2019). *Market survey of timber prefabricated envelopes for new and existing buildings*. <http://www.holz.ar.tum.de/forschung/tesenergyfacade/>
- Annunziata, E., Frey, M., & Rizzi, F. (2013). Towards nearly zero-energy buildings: The state-of-art of national regulations in Europe. *Energy*, 57, 125–133. <https://doi.org/10.1016/j.energy.2012.11.049>
- Ciroth, A., Finkbeiner, M., Traverso, M., Hildenbrand, J., Kloepffer, W., Mazijn, B., Prakash, S., Sonnemann, G., Valdivia, S., Ugaya, C. M. L., & Vickery-Niederman, G. (2011). *Towards a life cycle sustainability assessment: making informed choices on products*.
- DECRETO 20 luglio 2012, n. 140. (2012, July 20). *DECRETO 20 luglio 2012, n. 140 - Normattiva*. <https://www.normattiva.it/uri-res/N2Ls?urn:nir:ministero.giustizia:decreto:2012-07-20;140!vig=>
- DECRETO LEGGE, Art. 119 del D. legge nr. 34. (2020). *Incentivi per efficientamento energetico, sisma bonus, fotovoltaico e colonnine di ricarica di veicoli elettrici*. [https://www.gazzettaufficiale.it/atto/serie\\_generale/caricaArticolo?art.versione=1&art.idGruppo=8&art.flagTipoArticolo=0&art.codiceRedazionale=20G00052&art.idArticolo=119&art.idSottoArticolo=1&art.idSottoArticolo1=10&art.dataPubblicazioneGazzetta=2020-05-19&art.progressivo=0](https://www.gazzettaufficiale.it/atto/serie_generale/caricaArticolo?art.versione=1&art.idGruppo=8&art.flagTipoArticolo=0&art.codiceRedazionale=20G00052&art.idArticolo=119&art.idSottoArticolo=1&art.idSottoArticolo1=10&art.dataPubblicazioneGazzetta=2020-05-19&art.progressivo=0)
- D'Oca, S., Ferrante, A., Ferrer, C., Perneti, R., Gralka, A., Sebastian, R., & Veld, P. op t. (2018). Technical, financial, and social barriers and challenges in deep building renovation: Integration of lessons learned from the H2020 cluster projects. *Buildings*, 8(12). <https://doi.org/10.3390/buildings8120174>
- ECSO. (2017). *Construction Sector Observatory Policy measure fact sheet Netherlands Energiesprong (Energy Leap)*.
- EN 15459. (2018). "EN 15459:2018" - *European Standards*. <https://www.en-standard.eu/search/?q=EN+15459%3A2018>
- European Commission. (2019). Commission Recommendation on Building Renovation (EU) 2019/786. *Commission Recommendation on Building Renovation (EU) 2019/786*.
- European Commission. (2020). *Stakeholder consultation on the renovation wave initiative*. [https://energy.ec.europa.eu/topics/energy-efficiency/energy-efficient-buildings/renovation-wave\\_en](https://energy.ec.europa.eu/topics/energy-efficiency/energy-efficient-buildings/renovation-wave_en)
- European Commission - Energy Department. (2020). *In focus: Energy efficiency in buildings*. [https://commission.europa.eu/news/focus-energy-efficiency-buildings-2020-02-17\\_en](https://commission.europa.eu/news/focus-energy-efficiency-buildings-2020-02-17_en)
- Fotopoulou, A., Semprini, G., Cattani, E., Schihin, Y., Weyer, J., Gulli, R., & Ferrante, A. (2018). Deep renovation in existing residential buildings through façade additions: A case study in a typical residential building of the 70s. *Energy and Buildings*, 166, 258–270. <https://doi.org/10.1016/j.enbuild.2018.01.056>
- Gazzin, R., Adami, J., Dallapiccola, M., Brandolini, D., Gutierrez, M. J., Bonato, P., Gubert, M., & Avesani, S. (2022). Energy performance evaluation and economical analysis by means of simulation activities for a renovated building reaching different nZEB definitions targets. *Proceedings / Building Simulation Applications BSA 2022, 5<sup>th</sup> IBPSA-Italy Conference Bozen-Bolzano, 29<sup>th</sup> June – 1<sup>st</sup> July 2022 - ISBN: 978-88-6046-191-9*. <https://bia.unibz.it/esploro/outputs/991006545098101241>
- Governo Italiano Presidenza del Consiglio dei Ministri. (2023). *Superbonus 110% | www.governo.it*. <https://www.governo.it/it/superbonus>
- Hélène Sibilleau. (2021). *Deep Renovation: Shifting from Exception to Standard Practice in EU Policy* (Hélène Sibilleau, Ed.).
- Hildebrand, L. (2014). *Strategic investment of embodied energy during the architectural planning process*.
- Il Prezzario 2023 dei lavori della Toscana. (2023). *Il Prezzario 2023 dei lavori della Toscana*.
- International Energy Agency (IEA). (2019). *Buildings – Topics - IEA*. <https://www.iea.org/topics/buildings>

- ISO 14040:2006 - *Environmental management — Life cycle assessment — Principles and framework*. (n.d.). Retrieved June 17, 2023, from <https://www.iso.org/standard/37456.html>
- ISO 15686-5. (2017). *ISO 15686-5:2017 - Buildings and constructed assets — Service life planning — Part 5: Life-cycle costing*. <https://www.iso.org/standard/61148.html>
- ISO 15686-5:2017 - *Buildings and constructed assets — Service life planning — Part 5: Life-cycle costing*. (n.d.). Retrieved June 17, 2023, from <https://www.iso.org/standard/61148.html>
- Juaristi, M., Sebastiani, I., & Avesani, S. (2022). Timber-based Façades with Different Connections and Claddings: Assessing Materials' Reusability, Water Use and Global Warming Potential. *Journal of Facade Design and Engineering*, 10(2). <https://doi.org/10.47982/jfde.2022.powerskin.5>
- Konstantinou, T., & Heesbeen, C. (2022). Industrialized renovation of the building envelope: realizing the potential to decarbonize the European building stock. *Rethinking Building Skins: Transformative Technologies and Research Trajectories*, 257–283. <https://doi.org/10.1016/B978-0-12-822477-9.00008-5>
- LEGGE 2 marzo 1949, n. 143-N. (1949). *LEGGE 2 marzo 1949, n. 143 - Normattiva*. <https://www.normattiva.it/uri-res/N2Ls?urn:nir:stato:legge:1949-03-02;143!vig=>
- Life Cycle Cost Tool. (2023). *Life Cycle Cost Tool*. <https://www.cravezero.eu/pinboard/Downloads/LCCTool.htm>
- Marques, C., de Brito, J., & Silva, A. (2018). Application of the factor method to the service life prediction of etics. *International Journal of Strategic Property Management*, 22(3), 204–222. <https://doi.org/10.3846/ijspm.2018.1546>
- Ministero Della Giustizia. (2015). *Gazzetta Ufficiale Della Repubblica Italiana Direzione E Redazione Presso Il Ministero Della Giustizia-Ufficio Pubblicazione Leggi E Decreti-Via Arenula, 70-00186 Roma Amministrazione Presso L'istituto Poligrafico E Zecca Dello Stato-Via Salaria, 1027-00138 Roma-Centralino 06-85081-Libreria Dello Stato Ministero Dello Sviluppo Economico* (Vol. 15).
- Ochs, F., Siegele, D., Dermentzis, G., & Feist, W. (2015). Prefabricated timber frame façade with integrated active components for minimal invasive renovations. *Energy Procedia*, 78, 61–66. <https://doi.org/10.1016/j.egypro.2015.11.115>
- Paiano, A. (2015). Photovoltaic waste assessment in Italy. In *Renewable and Sustainable Energy Reviews* (Vol. 41, pp. 99–112). Elsevier Ltd. <https://doi.org/10.1016/j.rser.2014.07.208>
- Pernetti, R., Garzia, F., Paoletti, G., & Weiss, T. (2019). Towards the definition of a nZEB cost spreadsheet as a support tool for the design. *IOP Conference Series: Earth and Environmental Science*, 323(1). <https://doi.org/10.1088/1755-1315/323/1/012004>
- Pungercar, V., Zhan, Q., Xiao, Y., Musso, F., Dinkel, A., & Pflug, T. (2021). A new retrofitting strategy for the improvement of indoor environment quality and energy efficiency in residential buildings in temperate climate using prefabricated elements. *Energy and Buildings*, 241. <https://doi.org/10.1016/j.enbuild.2021.110951>
- Riccardo Pinotti. (2019). *Timber Prefabricated Multifunctional Façade: Approaches And Methods For A Feasibility Analysis, System Design And Testing*.
- Sandberg, K., Orskaug, T., & Andersson, A. (2016). Prefabricated Wood Elements for Sustainable Renovation of Residential Building Façades. *Energy Procedia*, 96, 756–767. <https://doi.org/10.1016/j.egypro.2016.09.138>
- Semprini, G., Gulli, R., & Ferrante, A. (2017). Deep regeneration vs shallow renovation to achieve nearly Zero Energy in existing buildings: Energy saving and economic impact of design solutions in the housing stock of Bologna. *Energy and Buildings*, 156, 327–342. <https://doi.org/10.1016/j.enbuild.2017.09.044>
- Tavares, J., Silva, A., & de Brito, J. (2020). Computational models applied to the service life prediction of External Thermal Insulation Composite Systems (ETICS). *Journal of Building Engineering*, 27. <https://doi.org/10.1016/j.jobe.2019.100944>
- van Oorschot, J. A. W. H., Halman, J. I. M., & Hofman, E. (2021). The adoption of green modular innovations in the Dutch housebuilding sector. *Journal of Cleaner Production*, 319. <https://doi.org/10.1016/j.jclepro.2021.128524>
- Zanni, J., Castelli, S., Bosio, M., Passoni, C., Labò, S., Marini, A., Belleri, A., Giuriani, E., Brumana, G., Abrami, C., Santini, S., Venturelli, G., & Marchetti, A. L. (2023). Application of CLT prefabricated exoskeleton for an integrated renovation of existing buildings and continuous structural monitoring. *Procedia Structural Integrity*, 44, 1164–1171. <https://doi.org/10.1016/j.prostr.2023.01.150>



# Assessing the circular re-design of prefabricated building envelope elements for carbon neutral renovation

Ivar J.B. Bergmans<sup>1</sup>, Silu Bhochhibhoya<sup>1</sup>, Johannes A.W.H. Van Oorschot<sup>1\*</sup>

\* Corresponding author, john.vanoorschot@zuyd.nl

<sup>1</sup> Zuyd University of Applied Sciences, Heerlen, The Netherlands

## Abstract

*Buildings and the construction industry at large are significant contributors to the catastrophic climate breakdown. The built environment is responsible for 37% of the total global carbon emission, of which about a third arises from the energy used to produce building and construction materials, usually referred to as embodied carbon. One of the key strategies to reduce the environmental impact of buildings is to significantly improve their energy efficiency, which is referred to as deep renovation. Prefabricated building envelope elements intended to prevent heat loss through the building envelope are considered a key deep-renovation technology. Connecting prefabricated elements to a building reflects a potential stream of waste if applied linearly with severe negative environmental impact in terms of natural resource depletion and exposure to pollutants. This article reports on a quantitative Design for Disassembly (Dfd) indicator to assess future recovery potential and, subsequently, its impact on embodied carbon emission of the circular redesign of three different prefabricated building envelope elements. Although none of the redesigned elements are yet considered 100% circular, the development of these three prefabricated building envelope elements showcases that the environmental impact can be substantially reduced following a well-structured and dedicated innovation process. The reduction of the environmental impact is indicated by lower quantities of embodied carbon up to 50% and an improved design for disassembly, reflecting a higher reuse potential of building materials and components. Several limitations and directions for further research were identified to advance the development of circular, prefabricated deep-renovation building envelope elements.*

## Keywords

*deep renovation, circular design, carbon-based design, design for disassembly, embodied carbon*

## DOI

<http://doi.org/10.47982/jfde.2023.2.A4>

# 1 INTRODUCTION

The depletion of raw materials, the high embodied energy and embodied carbon levels, and the high amount of wasted materials in the construction sector in Europe require a transition from linear to circular material use. Buildings are responsible for up to 40% of global greenhouse gas (GHG) emissions, and 15% of global climate emissions come from new construction (Bajzelij et al., 2013; Joensuu et al., 2022). Moreover, 50% of all extracted materials are attributed to buildings (IPCC, 2014; United Nations, 2015; Abouhamed & Abu-Hamd, 2021; Tokede et al., 2022), and according to the European Commission (EC), construction waste accounts for 25% to 30% of all waste generated in the EU (IPCC 2014, EMF, 2015).

One of the problems with buildings' environmental impact is the limited service life, i.e. the period of time a building is in use compared to its actual technical lifespan, meaning the physical existence of a building (Grant & Ries, 2013; Rauf & Crawford, 2015). Many buildings are demolished or substantially altered even though they are still functioning well from a technical point of view (Joensuu et al., 2021). Previous studies showed that the decision to demolish and replace a building can be related to urban growth, causing pressure to increase the floor area ratio, inflexible technical and spatial design to adapt to changing functional needs or too high renovation costs. To summarize, the decision to demolish is, in many cases, the result of failure to adequately meet the demand of the intended end users and thus independent of the technical condition of a building (Huuhka & Lahdensivu, 2016; Joensuu et al., 2021). A study by Marsh (2016) showed that extending a building's lifespan reduces the environmental impact significantly by 29%, 38% and 44% for a lifespan of 80, 100 and 120 years, respectively, compared to an average lifespan of 50 years.

The concept of circular economy (CE) is considered an alternative to current environmentally destructive linear economic models and key to slowing down climate change. The transition towards full circular building practices ultimately helps decrease buildings' environmental footprint and consumption of raw materials. CE can be considered a step to implement restorative and regenerative approaches in which emissions, resource use, and waste generation are reduced through the CE principles of narrowing (efficient resource use), slowing (temporally extended use), and closing (cycling) current and future resource loops (Bocken et al., 2016; Geissdoerfer et al., 2017). In essence, a circular solution is based on 100% renewable energy, and all materials are part of infinite closed loops with the lowest value loss.

Prefabricated building envelope elements, considered a core technology of the EU renovation wave, play an essential role in improving a building's energy efficiency and prolonging its service life (Saheb, 2016). Prefabrication is a manufacturing process that takes place in a specialized facility where various materials are joined together to form a component of the final installation procedure within a controlled environment (Zairul, 2021). Prefabrication is an essential aspect of circular design strategies as it increases the reuse possibilities of building materials and products in modularity (Kuusk et al., 2022). This helps to apply CE in conventional buildings with standard measures and to close the supply chain loop and achieve waste reduction (Minunno et al. 2018). Because of this potential, prefab construction products such as prefabricated building envelope elements have gained growing interest in both science and industry. Bitar, Bergmans & Ritzen (2022) emphasized in their study that assessing Life Cycle Energy Performance (LCEP) is becoming increasingly relevant, accounting for all the operational and embodied carbon exposure during the entire lifespan of a building. Their key finding was that a substantial LCEP is possible close to 100% for a zero-energy building retrofit with circular prefabricated building elements. In a comparative study, Juaristi et al., (2022) showcased that timber-based façades have the potential to substantially

reduce the carbon footprint relative to façades constructed with inorganic construction materials (Hildebrand, 2014). Moreover, these authors calculated that the carbon footprint can be further reduced if components are reused in a second life cycle depending on the careful selection and design of construction materials and connections.

However, the application of CE indicators in isolation will not lead by default towards 'systemic circularity' and a reduced environmental footprint. Systemic circularity refers to the idea that a circular design depends on multiple interconnected indicators which influence each other in a continuous and circular manner. Improvement of a single component may adversely affect other parts within this complex system of technical, environmental, social, business, legislative, economic, and innovation impacts (Kubbinga et al., 2018; Antwi-Afari, Ng & Chen, 2022). For example, it has been found that applying DfD strategies to facilitate material reuse can lead to increased initial impact due to greater energy and resource consumption (Roberts et al., 2023). Bitar et al., (2022) emphasized that future research should address the trade-off between embodied carbon and DfD. This particularly calls for empirical studies validating 'systemic' frameworks assessing circularity in the construction industry (Attia and Al-Obaidy, 2021; Lam et al., 2022). Juaristi et al., (2022) further suggest that future works should be on the effect of ageing on reclaiming and reusing construction materials and its impact on efficient material usage, waste, and environmental footprint.

This article, therefore, attempts to contribute by answering the following research question:

Assuming the current system conditions, i.e. value proposition and business model associated with prefab façade elements, remain unchanged, what is the environmental impact in terms of the embodied carbon of circular redesigned prefab building envelope elements?

As an essential key deep-renovation technology, prefabricated building envelope elements improve the energy efficiency of buildings by preventing heat loss through the building envelope. Connecting prefabricated building envelope elements to a building reflects a potential waste stream if applied linearly with severe negative environmental impact in terms of natural resource depletion and exposure to pollutants. This article shows the impact of the circular redesign of three different prefabricated building envelope elements. It reflects on the environmental impact of building envelope elements from three cases associated with the life cycle performance of products and buildings. To gain insight into the life cycle performance, three baseline scenarios from selected partners in three Northern countries are compared with developed designs of more circular variants. Embodied carbon and disassembly potential indices are assessed to evaluate the environmental impact and level of circularity of building envelope elements. Assessing the circular performance and breaking it down into key indicators, such as embodied carbon (cradle-to-gate) and disassemble potential, provided insight into how design choices and material choices influence the life cycle performance of building elements. In this way, suppliers and designers gain insight into how they can influence the environmental footprint of their prefabricated building envelope elements. In sum, this article contributes in the following ways: first, it showcases how the environmental impact of material-intensive construction elements can be substantially reduced by following an eco-design approach and applying circular design strategies. Second, it ties together theories about circular design, life cycle assessment, and technological innovation to adhere to the EU Green Deal.

This article is structured as follows. The following section, section 2, discusses the background of the design strategies being applied in this study to reduce the environmental impacts of prefabricated building envelope elements. Section 3 addresses the methodological approach of our study, followed

by the case studies presented in section 4. Section 5 elaborates on the research findings. Finally, the last section discusses the scientific and managerial contributions and possible directions for future research.

## 2 THEORETICAL FRAMEWORK

This section presents the theoretical framework for the prefabricated building element for carbon-neutral renovation. To measure the level of circularity and the carbon emission of the prefab building envelope element, two important indicators are considered: the Design for Disassembly (DfD) index and embodied carbon.

### 2.1 PREFABRICATED CIRCULAR BUILDING ENVELOPE ELEMENTS FOR CARBON-NEUTRAL RENOVATION

Prefabricated building envelope elements have been introduced to step up the pace of building renovation to achieve European Union (EU) climate change policies for 2050, i.e. industrial building and modularity and related technological innovations are at the core of boosting the renovation wave (Renz & Zafra Solas, 2016; Saheb, 2016). The application of prefab elements aligns with industrial building principles to raise efficiency by rationalizing the construction process by adopting production technologies and methods found in highly industrialized mass-production industries like automotive. Supported by various national and international innovation programs, such as the EU Horizon and Interreg programs, the development of prefabricated façade technologies industrial has gained growing attention (Barbosa et al., 2017; Bertram et al., 2019; Hofman et al., 2009). Across Europe, multiple prefab façade systems have been developed, validated, and demonstrated, and accordingly, complementary investments have been made to tune the design process, element production, and plug-and-play installation on-site.

However, beyond efficiency gains, the full potential of prefab façade elements has not yet been met, and substantial improvements can be achieved to improve the level of sustainability, circularity, and customization in a way that does not increase project risks, complexity, and building costs of renovation projects (Juaristi et al., 2022; Lam et al., 2022). The level of circularity of prefab façade elements can be substantially improved by facilitating access to individual components of the product system, thereby facilitating refurbishing, reuse, and recycling (Chung et al., 2014; Kimura et al., 2001; Ma & Kremer, 2016; Okudan Kremer et al., 2013). This is especially relevant for components that age more rapidly than parts they interface with or that improve faster, for example, due to higher innovation clock speeds, leading to an opportunity for modular upgrades of the system. As indicated by previous studies, the two most prominent indicators to take into consideration are the design for disassembly index and embodied carbon to subsequently assess the potential to replace, reclaim, and reuse valuable construction materials and reduce the overall environmental footprint (Juaristi et al., 2022; Bitar et al., 2022).

### 2.2 DESIGN FOR DISASSEMBLY INDEX

In line with the essence of a circular economy, it is key to close material loops by being able to retrieve materials with a minimal loss of quality for the purpose of reuse (EMF, 2015). Thus, to ensure

the multi-cycle use of prefabricated building envelope elements and applied components, these elements should be able to be subtracted from the building and dismantled without loss of quality (Potting et al., 2017). To effectively close material loops specific to the building industry, various R-strategies can be applied (see Figure 1). The three most essential R-strategies include one-on-one reuse of building elements, remanufacturing reclaimed materials into new applications, and recycling materials to produce new products. Prioritized by impact, a reuse strategy is preferred over re- or downcycling as fewer natural resources are required with a minimum loss of value.

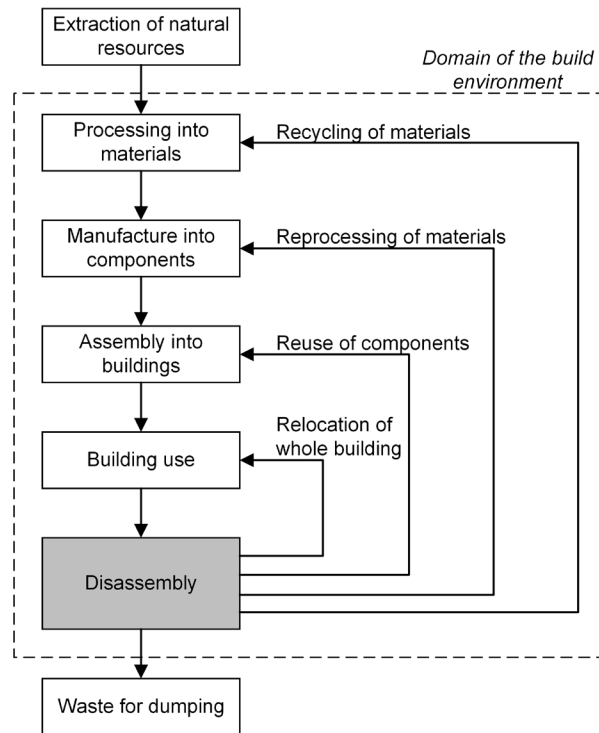


FIG. 1 R-Strategies for closing the material loop (Chini & Florida, 2001)

When closing material loops based on R-strategies, it is essential that materials and products can be easily mined from existing buildings in which they are temporarily stored. It is, therefore, of utmost importance that buildings are Designed for Disassembly (DfD). By default, in closing loops, one should not only consider end-of-life scenarios but also take into account the origin of materials and consider which materials can be reused in a new product design.

The higher the disassembly potential of a building, the easier it is to retrieve products for reuse rather than downcycling and recycling. Reusing mined materials not only contributes to efficient material consumption in the construction sector but intrinsically reduces the carbon emission associated with (re-)processing and transportation (Cottafava & Ritzen, 2021; Lam et al., 2022). In sum, DfD in the construction sector ties together value retention, efficient material use, and carbon emission reduction.

The DfD index is defined as the degree to which 'objects' can be dismantled at different levels so that the object can retain its function and high-quality reuse can be realized (Durmisevic, 2006). To determine what the above-mentioned 'objects' are and to what level of detail the calculations should be done, the authors refer to the diagram depicted in Figure 2, adopted from Durmisevic (2006), showing the subdivision of different building levels. For this study, prefabricated building

envelope elements are considered a part of the façade and, subsequently, a key subsystem of a building. Design for disassembly focuses on the potential to take apart the building envelope elements in their essential construction products and materials. Further reuse of these products and materials is beyond the scope of this study.

A methodology indicating the disassembly potential should assess the extent to which a building system and the products and materials applied in this system can be disassembled. The technical design of a building system, especially oriented on the connections between products and materials, has the most influence on disassembly. Besides the technical design of a building element, it has been suggested that process, financial and human capital aspects could also affect the disassembly potential (Akinade et al., 2017; Van Vliet et al., 2021). The assessment of the DfD index is based on the technical disassembly potential of the connection (DPc), which reflects the ability to disassemble the building envelope element as a whole, and the compositional disassembly potential (DPcp), which reflects how easily a prefabricated building envelope element can be disassembled.

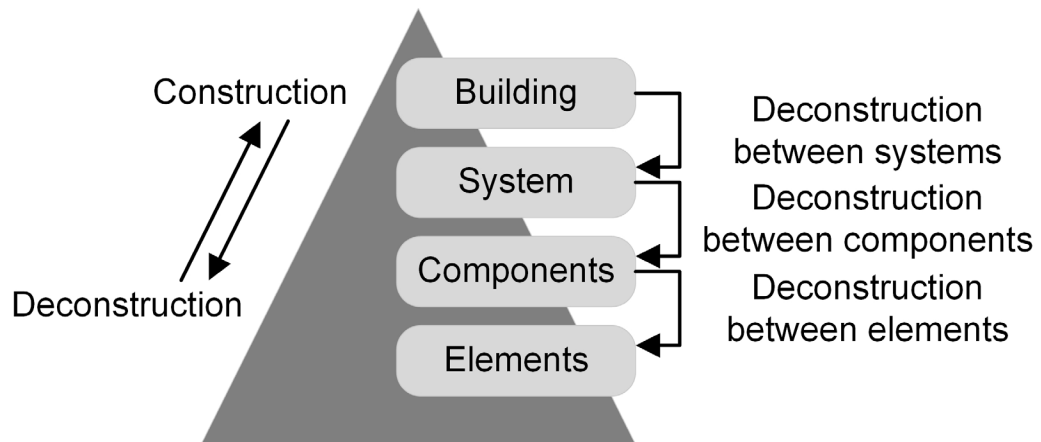


FIG. 2 Hierarchy of building materials being applied in buildings (adopted from Durmisevic, 2006)

## 2.3 EMBODIED CARBON

Embodied carbon emission is associated with the energy consumption during extraction of raw materials, transportation, manufacturing, assembly, and installation all the way to disassembly, deconstruction, and decomposition (Ritzen et al., 2016; Bhochhibhoya et al., 2016). Hammond & Jones (2011) define embodied carbon as *“the total carbon released from direct and indirect processes associated with a product or service and within the boundaries of cradle-to-gate. This includes all activities from material extraction (quarrying/mining), manufacturing, transportation and right through to fabrication processes until the product is ready to leave the final factory gate.”*

Embodied carbon has gained increased attention recently (Pomponi & Moncaster, 2016; Dutil et al., 2011). The relative importance of embodied carbon associated with building materials and elements is increasing as the GHG emission in the operational phase is substantially reduced due to significant progress in creating energy-efficient buildings (Monaha & Powell, 2011; Sartori & Hestnes, 2007; Passer, Kreiner & Maydl, 2012). However, additional energy is often required for manufacturing and transportation of the increased levels of materials and additional technologies for energy-efficient buildings (Monahan & Powell, 2011).

Much research has been conducted to investigate various strategies to reduce the embodied carbon of buildings (Akbarnezhad & Jianzhuang 2017). These strategies are divided into five categories: (1) low-carbon materials (Hammond & Jones, 2008); (2) material minimization and material reduction strategies ( Akbarnezhad & Moussavi Nadoushani, 2014); (3) material reuse and recycling strategies (Xiao et al., 2007); (4) local sourcing and transport minimization (Gonzalez & Navarro, 2006); and (5) construction optimization strategies (Guggemos & Horvath, 2005). Related to the three cases in this article, this research focused on categories 1, 2, and 3 because all collected materials for redesigning the prefabricated modular building element were calculated based on these three categories.

In line with the definition of Hammond & Jones (2011) and following the same methodological approach as Bitar et al., (2022), the embodied carbon will be calculated through a cradle-to-gate assessment.

### 3 METHODOLOGY

#### 3.1 THE ROLE OF CIRCULAR ASSESSMENT IN THE DESIGN PROCESS

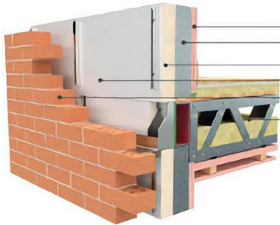
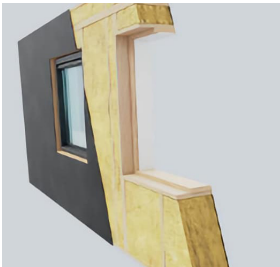
To improve the level of circularity of existing prefabricated building envelope elements, a design science approach was followed that encompasses a reflective design and analysis process consisting of succeeding stages and feedback loops (Roggema, 2016; Sipahi & Kulozu-Uzunboy, 2021; Bitar et al., 2022). The basic stages of the process are followed under the guidance of eco-design strategies, methods, and tools. Eco-design refers to the systematic integration of environmental considerations into the (re-)design process without compromising performance, quality, and cost (Knight & Jenkins, 2009; Keiller, Clements & Charter, 2013; Marques, et al., 2017). Eco-design principles concur with the circular design techniques including design for disassembly (Durmisevic, 2018; Cambier et al., 2020; Eberhardt et al., 2022) and carbon-based design (Häkkinen et al., 2015; Cottafava & Ritzen, 2021; Sobota et al., 2022).

The design process followed in this study consisted of five key stages:

- 1 Pre-design stage specifying the design challenge and outcome
- 2 Baseline assessment of environmental impacts associated with the product of its entire life cycle
- 3 Selecting circular design strategies
- 4 Circular redesign process: redesigning under the guidance of circular design strategies to reduce the carbon footprint
- 5 Post-design evaluation of environmental impact; comparing initial and revised design

During the pre-design stage, three prefabricated building elements for the deep-renovation market were selected for circular redesign. As a first selection criterium, only prefabricated building envelope elements for the deep-renovation market were taken into consideration, which have been applied beyond their demonstration status and for which the producers have the ambition to improve the level of circularity and lower the environmental impact. Secondly, we only focused on EU countries with an established market for panelized construction. See also Table 1.

TABLE 1 Case description

Case	Country	Market served	Key driver
<p>Timber frame non-structural building envelope element</p> 	Estonia	Multi-family housing	Governmental support to renovate apartment buildings (social housing) at a large scale with prefab timber frame elements.
<p>Prefab light gauge steel element</p> 	Ireland	Single family housing	Off-site construction – with prefab light gauge steel panels - is considered a fast moving field in the UK and Ireland and recently also considered in the deep-renovation market.
<p>Timber frame non-structural building envelope element</p> 	Netherlands	Single and multi-family housing	Seen as a key technology to renovate terraced housing stimulated by the Dutch Stroomversneling program.

During the second stage, a baseline environmental impact assessment was conducted based on the circular redesign ambitions identified during the pre-design stage. This included the assessment of the embodied carbon emission associated with the cradle-to-gate production of the prefab façade elements (Cao, 2017). The design for disassembly index was calculated to assess the potential reuse of materials and components. During the third stage, the circular design strategies were selected. Following the circular redesign ambitions and the baseline assessment, two circular design strategies were applied: design for disassembly (Durmisevic, 2006; Cambier et al., 2020; Eberhardt et al., 2022) and carbon reduction strategies (Akbarnezhad & Jianzhuang Xiao, 2017). Subsequently, during the fourth stage, the actual redesign of the prefab building envelope elements took place. The output of the design stage was evaluated following the same methodologies as applied in Stage 2 to compare the baseline façade elements with the revised design. If the intermediate evaluation of the conceptual design was not in line with the circular ambitions set in Stage 1, the cycle of design and evaluation was repeated. In the next section, we provide a detailed description of the assessment methodology being applied during post-design evaluation.

## 3.2 ASSESSMENT METHODOLOGY

The study reflects on the technical and environmental issues when analysing the level of circularity of prefabricated building envelope elements. Within the technical analyses, material separability rate, usage level of recycled products and technical feasibility are related to the disassembly potential. The environmental impact is indicated by embodied carbon. The calculation of the environmental impact is not connected to the disassembly potential, but the balance between both indicators is considered and reflected during the process. This study considered the cradle-to-gate boundary based on the Inventory of Carbon and Energy ICE (Hammond, 2011).

This means that design scenarios are assessed on the basis of calculating the disassembly potential index and embodied carbon, and improved scenarios can be developed based on these calculations. The following subsections describe how the DfD index and embodied carbon were subsequently calculated.

### 3.2.1 Design for Disassembly Index

The essence of the design for disassembly strategy is to close material loops by increasing the reuse potential of elements and materials. In the prefabrication of building envelope elements, the impact of DfD is crucial to the renovation wave that Europe provides. The disassembly potential, therefore, must be assessed on the element and material level.

The methodology adopted to assess the DfD index was based on Alba Concepts (van Vliet, van Grinsven, Theunizen, 2022) and ISSO assessment (ISSO, 2021). This method assesses the DfD index of the building envelope elements by assessing the connections within the prefabricated building envelope element (Bitar, Bergmans, Ritzen, 2021).

The disassembly potential of the connection (DPC) assesses the ability to disassemble the element or material at the end of its building life. The following factors are part of the disassembly potential of the connection: type and accessibility of the connection. The disassembly potential of the composition (DP<sub>cp</sub>) assessed how easily an element can be disassembled from the building envelope. The following factors are part of the disassembly potential of the composition.

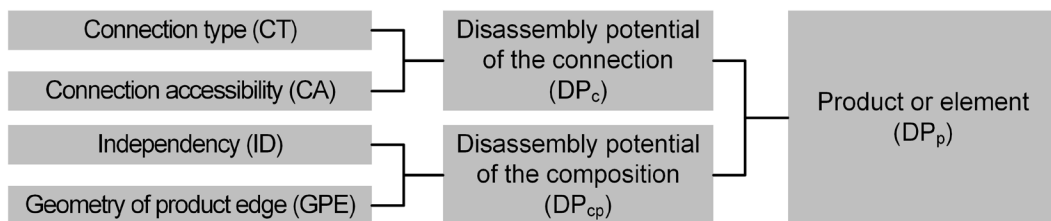


FIG. 3 Step-by-step plan for assessing the disassembly potential of the element.

Figure 3 shows the step-by-step plan for assessing the disassembly potential of the element.

The formula for assessing the disassembly potential of the connection of material n or element n (end-of-life scenarios):

$$DpC_n = \frac{2}{\frac{1}{CT_n} + \frac{1}{CA_n}} \quad [1]$$

The formula for assessing the disassembly potential of the connection and the composition of material n (maintenance scenarios):

$$DPT_n = \frac{4}{\frac{1}{CT_n} + \frac{1}{CA_n} + \frac{1}{CR_n} + \frac{1}{FC_n}} \quad [2]$$

Where:

- DPC<sub>n</sub> = disassembly potential of the connection (material or element n).
- DPT<sub>n</sub> = total disassembly potential of the connection and the composition (material n)
- CT<sub>n</sub> = type of connection of material or element n.
- CA<sub>n</sub> = accessibility of the connection of material or element n.
- CR<sub>n</sub> = independency of material n. (crossings)
- FC<sub>n</sub> = edge geometry of material n. (form containment)

TABLE 2 Scoring matrix disassemble potential (ISSO, 2021)

Type of connection		Score	Accessibility of connection		Score
Dry connection	Loose (no fastening material)	1.00	Freely accessible		1.00
	Click connection		Accessible with actions that don't cause damage		0.80
	Velcro connection		Accessible with actions causing repairable damage		0.40
	Magnetic connection		Not accessible – irreparable damage to object		0.10
Connection w. added elements	Bolt and nut connection	0.80	<b>Form containment</b>		<b>Score</b>
	Spring connection		Open. no inclusion		1.00
	Comer connection		Overlap		0.80
	Screw connection		Closed. (one side)		0.20
Direct integral connection	Pin connection	0.60	<b>Crossings</b>		<b>Score</b>
	Nail connection		No piercing		1.00
Soft chemical bond	Lute connection	0.20	Piercing by one or more objects		0.40
	Foam connection		Full integration of objects		0.10
Hard chemical bond	Glue connection	0.10			
	Pouring joint				
	Welded connection				
	Cement bound connection				
	Chemical anchors				
	Hard chemical bond				

As shown in Table 2, a dry connection scores 100% (1.0), and a hard chemical bond scores 10% (0.1). The accessibility of the connection scores 100% (1.0) if it is freely accessible and 10% (0.1) if it is not accessible and causes irreparable damage to objects. The form containment scores 100% (1.0) if there are no obstructions in removing the materials and scores 20% (0.2) if the material is closed on one side. The crossings score 100% if there are no crossings of different materials within the element with different lifespans and score 10% with full integration of materials or elements from different layers.

This study assumes that the building envelope elements are disassembled at the end of the building's life cycle. For this, it is required that parts with a shorter technical life cycle can easily be replaced (cladding), and therefore, the DfD index for these materials was calculated.

### 3.2.2 Embodied carbon

Embodied carbon is considered among the most accepted scientific indicators to assess the environmental dimension of circularity (Antwi-Afari et al., 2022). In line with the embodied carbon definition of Akbarnezhad & Jianzhuang (2017), the first three strategies were applied in this study (see section 2.3). For calculating the embodied carbon, the ICE database 2011 was used per building material (cradle-to-gate). The ICE database was developed by Hammond and Jones from the Sustainable Energy Research Team (SERT) affiliated with the University of Bath. The database includes LCA information and provides the  $ECO_2$  ( $kgCO_2$ ) on the most common building materials or components. To calculate the embodied carbon of prefabricated building envelope elements, a bill of materials has to be constructed, which provides insight into the amount and density of materials being applied. As an important intermediate step, the amount of reused material needs to be deducted from the share of virgin used materials. The embodied carbon was calculated for a functional unit of  $1 m^2$  to compare the three redesigned building envelope elements.

The formula to determine the embodied carbon of the element is:

$$ECO_{2n} = CO2Vn * Dn * V1n [3]$$

Where:

- $ECO_{2n}$  = Embodied carbon per material. (kg)
- $CO2Vn$  = Embodied carbon of the virgin material (ICE database cradle to gate).
- $Dn$  = Density per material ( $kg/m^3$ )
- $V1n$  = Volume per material ( $m^3$ ) per  $m^2$  façade area.

Note that the embodied carbon of the building envelope element per  $m^2$  façade area is the summation of the embodied carbon per material.

## 4 DESCRIPTION OF THE BUILDING ENVELOPE ELEMENTS

For this study, three demonstrator cases were selected to analyse different types of prefabricated building envelope elements in Northern Europe within the same climatic zone, i.e. a temperate zone, with various materials and designs of the façade system. The three selected building envelope elements are considered mature technologies with relevant product certification. The cases were selected on the potential of closing material loops and reducing the environmental footprint. See Table 3 for an overview of the cases with respect to the design strategy followed and an indication of the key components of the baseline and circular improved building envelope elements. For each demonstrator case, the baseline is indicated, and subsequently, a description of the circular improved design is provided. All three circular redesigned building envelope elements have been tested in mock-ups and/or applied in demonstration projects in the national context.

### 4.1 DUTCH CASE

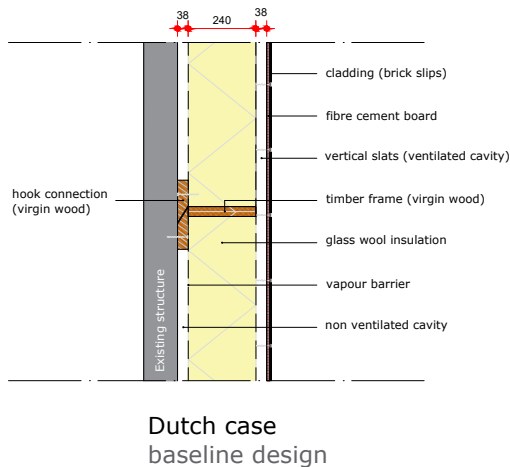


FIG. 4 Baseline set-up of the Dutch element

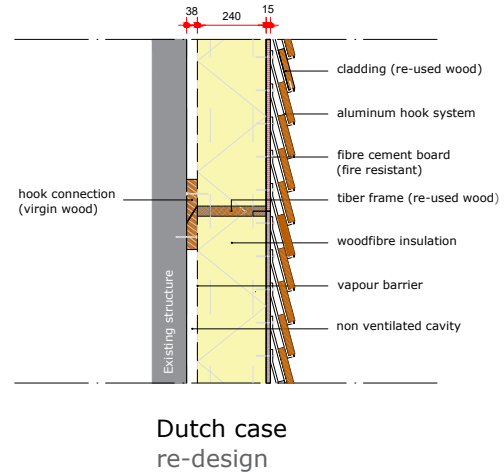


FIG. 5 Redesign set-up of the Dutch element

For the Dutch case, a Structural Insulated Panel System (SIPS) was selected, which can be applied both in newly built and deep-renovation projects, see Figure 4. The redesign (Figure 5) of the building envelope element can be best described as a demountable prefabricated plug-and-play insulation application mounted in front of an existing cavity wall, a substantial part of which consists of materials mined from donor buildings. The building element consists of an insulated timber element and structure, an air cavity, and an additional external wooden cladding. For the timber components, pine wood purlins were mined from a donor building, transported to the factory, and then purified and processed to be reused in the building envelope element. However, not all parts of the building envelope element, especially the parts that contribute to structural and fire safety, were constructed with reused materials, as this would require additional product certification. To avoid the use of chemicals and/or paint to improve durability, the cladding material underwent modification by heat treatment for ageing control (Esteves et al., 2008). The building element showcases a high reuse potential after its initial life cycle. The prefabricated external building element is fastened with screws applying a geometric plug-and-play connection. Also, the components applied in the layered design of the building envelope element are fastened with screws. The cladding is mounted with a hook system, avoiding the use of glue or other chemical connections and allowing the replacement of single components during maintenance over the life cycle of the element.

## 4.2 ESTONIAN CASE

The Estonian case also involves timber-based SIPS panels. The baseline elements consist of a timber frame-based insulation system with mineral wool insulation and cladding. For a schematic representation of the baseline, see Figure 6.

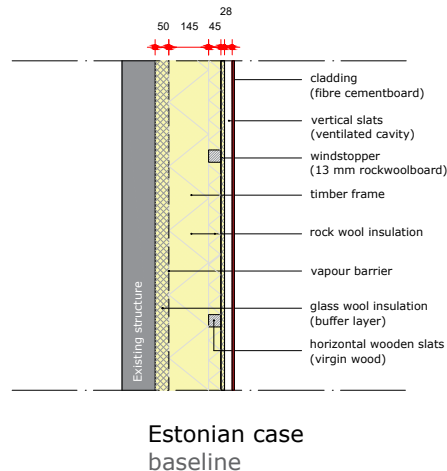


FIG. 6 Baseline set-up of the Estonian element

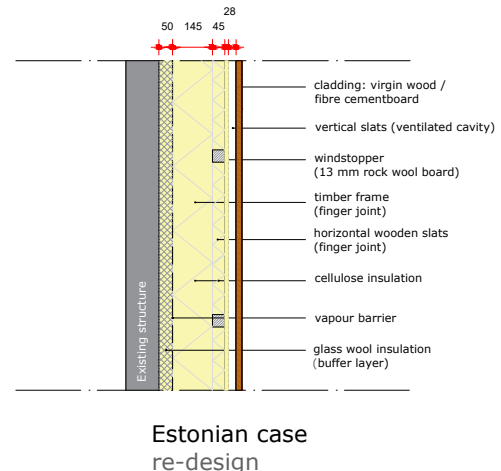
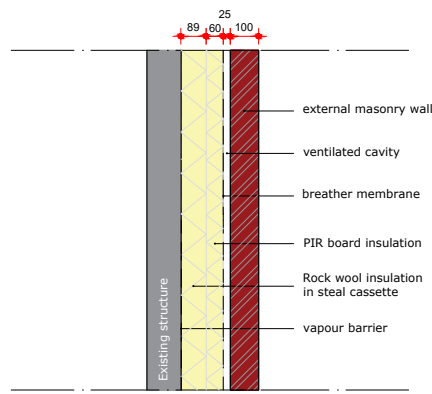


FIG. 7 Redesign set-up of the Estonian element

The focus of redesigning the building envelope element (Figure 7) was increasing the use of biobased or remanufactured materials. Also, the disassembly potential was taken into account for the whole building envelope element and its individual components. The bare structure of the insulation element consists of a 45x145 mm, high-quality (C24) timber frame (virgin material). Horizontal wooden slats (45x45 mm and 45x95 mm) were replaced by finger-jointed lumber to increase the use of remanufactured materials. Nail connections were used to form the bare structure because of higher shear strength compared to a screw connection. In contrast, screw connections can be used for horizontal wooden slats and ventilation gap wooden slats, which allow easier disassembly. Because of fire regulations, rockwool insulation was used instead of the preferred cellulose insulation with a lower carbon footprint. Rockwool board is used as a wind stopper because of its hygrothermal properties (high thermal resistance and vapour permeability). Alternatives like gypsum boards or timber-based boards (e.g., OSB, plywood) were not considered as these materials perform less in terms of thermal resistance and are more sensitive to mould growth. Fibre cement boards are used for façade cladding because of the long service life and limited maintenance. See Figure 7 for the detailed design of the building envelope element.

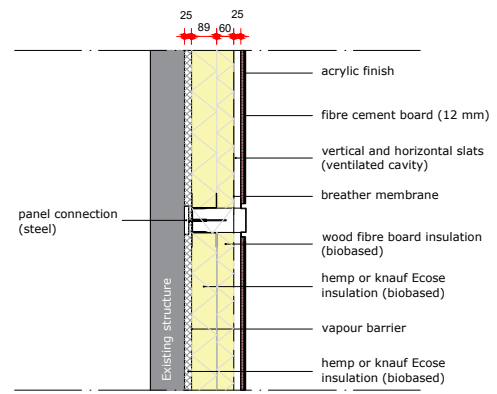
## 4.3 IRISH CASE

The Irish baseline consists of a panel system intended for the newly built inner leaf only and repurposing it as a closed panel finished system applicable to the circular renovation market. The baseline building envelope element is being developed from an existing light-gauge steel framing construction system, which is typically insulated with conventional quilt and plastic insulation board and finished with traditional brick or block outer leaves or rendered cement boards. See Figure 8.



Irish case  
baseline design

FIG. 8 Baseline set-up of the Irish element



Irish case  
re-design

FIG. 9 Redesign set-up of the Irish element

Three main alterations were introduced to improve the level of circularity of the baseline. First, reducing the structural and non-structural steel contents within the panel connection and framing to improve material efficiency and reduce the use of virgin non-renewable materials and resources; second, maximizing the extent of biobased materials and insulation application to reduce the carbon footprint; and third, off-site assembly of all components with reversibility aiming at multi-cycle circular solutions of building materials and components.

In the absence of a developed urban mining context or capacity, it was decided to focus on biobased materials, thus supporting the non-technical circularity cycle as well as associated material benefits — such as low embodied carbon. Following a detailed review of available biobased materials in the Irish market — which highlighted the limited range and notably a lack of Irish or even UK manufacturing of biobased products —, the following solutions were proposed. To replace glass or mineral wool, the insulation between the 89 mm studs will be replaced with a biobased quilt such as hemp or a recycled or enhanced conventional product such as Knauf Ecosse. The rainscreen, consisting of a PIR board, is replaced by a biobased wood fibre board such as Pavatex, Gutex, or Steico. These products were envisioned to also contribute to reducing the carbon footprint of the building envelope element and enabling the R-strategies, notably re-cycling. Hierarchical DfD has been a key principle and design strategy in the circular building envelope design, seeking to ensure that the element can be installed and removed in its entirety for potential re-stage application in its entirety and on a wall element level as well as disassembly at lower component and product/material level. For an overview of the detailed design of the building envelope element, see Figure 9.

## 5 RESULTS

In this chapter, the improved circular performance of the three different prefabricated building envelope elements is demonstrated based on embodied carbon reduction and the improvement in the design for disassembly potential. The level of circularity is assessed based on both indicators separately. The progression shown per indicator is the difference between the original baseline design and the redesign for each of the three cases separately.

## 5.1 DISASSEMBLY POTENTIAL

The disassembly potential of the prefabricated building envelope elements indicates the reuse potential of components and materials. Based on that, the baseline building envelope element is compared per case with the redesigned prefabricated building envelope element. The total score depends on the type of connection and the accessibility of the connection in the end-of-life scenario.

The DfD index was calculated for the baseline and the redesigned building envelope element for a) disassembly of the building envelope element and b) disassembly of the materials within the building envelope element.

### 5.1.1 Dutch case

Table 3 shows the scoring matrix of the disassembly potential of the baseline design of the Dutch case. The results show that the disassembly potential on the element level and material level of the baseline design are 0.83 and 0.74, respectively, whereas the disassembly potential on the element level of the redesigned building envelope element is 0.95 and 0.85 on the material level (shown in Table 4).

TABLE 3 Scoring matrix disassemble potential baseline design

		Score	
<b>Element level</b>		<b>0.83</b>	<b>Disassembly potential</b>
<b>1. Prefab 1e skin (structure)</b>		1.00	
Connection (existing construction)	Type of connection	1.00	Dry connection
	Accessibility of connection	1.00	Freely accessible
<b>2. Cladding material</b>		0.70	
Connection (wooden slats)	Type of connection	0.60	Nail connection
	Accessibility of connection	0.80	Accessible with actions not causing damage
<b>3. Wooden slats</b>		0.80	
Connection (wooden structure)	Type of connection	0.80	Screw connection
	Accessibility of connection	0.80	Accessible with actions not causing damage
<b>Material level</b>		<b>0.74</b>	<b>Disassembly potential</b>
<b>1. Cladding material</b>		0.70	
Connection (existing construction)	Type of connection	0.60	Nail connection
	Accessibility of connection	0.80	Accessible with actions not causing damage
<b>2. Wooden slats</b>		0.80	
Connection (wooden structure)	Type of connection	0.80	Screw connection
	Accessibility of connection	0.80	Accessible with actions not causing damage
<b>3. Wooden structure (HSB)</b>		0.73	
Connection (finishing material)	Type of connection	0.60	Nail connection
	Accessibility of connection	0.40	Accessible with actions causing repairable damage
Connection (insolation material)	Type of connection	1.00	Dry connection
	Accessibility of connection	0.80	Accessible with actions not causing damage
Interconnection	Type of connection	0.80	Screw connection
	Accessibility of connection	0.80	Accessible with actions not causing damage

TABLE 4 Scoring matrix disassemble potential redesign

		Score	
<b>Element level</b>		<b>0.95</b>	<b>Disassembly potential</b>
<b>1. Prefab 1e skin (structure)</b>		1.00	
Connection (existing construction)	Type of connection	1.00	Dry connection
	Accessibility of connection	1.00	Freely accessible
<b>2. Prefab 2e skin (Cladding)</b>		0.90	
Connection (wooden slats)	Type of connection	0.80	Connection with added elements
	Accessibility of connection	1.00	Freely accessible
<b>Material level</b>		<b>0.85</b>	<b>Disassembly potential</b>
<b>1. Cladding material</b>		0.95	
Connection (hook)	Type of connection	1.00	Dry connection
	Accessibility of connection	1.00	Freely accessible
Connection (wooden slats)	Type of connection	0.80	Connection with added elements
	Accessibility of connection	1.00	Freely accessible
<b>2. H20 platen</b>		0.80	
Connection (wooden slats)	Type of connection	0.80	Screw connection
	Accessibility of connection	0.80	Accessible with actions not causing damage
<b>3. Wooden slats</b>		0.90	
Connection to (wooden structure)	Type of connection	0.80	Bolt and nut connection
	Accessibility of connection	1.00	Freely accessible
<b>4. Wooden structure (HSB)</b>		0.73	
Connection (finishing material)	Type of connection	0.60	Nail connection
	Accessibility of connection	0.40	Accessible with actions causing repairable damage
Connection (insulation material)	Type of connection	1.00	Dry connection
	Accessibility of connection	0.80	Accessible with actions not causing damage
Interconnection	Type of connection	0.80	Bolt and nut connection
	Accessibility of connection	0.80	Accessible with actions not causing damage

The DfD index shows that there is a 14% and 15% improvement of disassembly potential on the redesigned prefabricated building element compared to the baseline design on the element and material level, respectively, in the Dutch case. The use of the cladding materials of the redesign connected with the hook system to the frame aiming at multiple reuses of the wood improved the disassembly potential. In contrast, nailed connections are used in the baseline design, which provides less reusability potential.

### 5.1.2 Estonian case

Table 5 shows the scoring matrix of the disassembly potential of the baseline design of the Estonian case. The results show that the disassembly potential on the element level and material level of the baseline design are 0.85 and 0.77, respectively, whereas the disassembly potential on the element level of the redesigned building envelope element is 0.85 and 0.82 on the material level (shown in Table 6).

TABLE 5 Scoring matrix disassembly potential baseline design

		Score	
<b>Element level</b>		<b>0.85</b>	<b>Disassembly potential</b>
<b>1. Prefab 1e skin (structure)</b>		0.80	
Connection (existing construction)	Type of connection	0.80	Screw connection
	Accessibility of connection	0.80	Accessible with actions not causing damage
<b>2. Cladding material</b>		0.90	
Connection (wooden slats)	Type of connection	0.80	Screw connection
	Accessibility of connection	1.00	Freely accessible
<b>3. Wooden slats</b>		0.70	
Connection (wooden structure)	Type of connection	0.60	Nail connection
	Accessibility of connection	0.80	Accessible with actions not causing damage
<b>Material level</b>		<b>0.77</b>	<b>Disassembly potential</b>
<b>1. Cladding material</b>		0.90	
Connection (wooden slats)	Type of connection	0.80	Screw connection
	Accessibility of connection	1.00	Freely accessible
<b>2. Wooden slats</b>		0.70	
Connection (wooden structure)	Type of connection	0.60	Nail connection
	Accessibility of connection	0.80	Accessible with actions not causing damage
<b>3. Wooden structure</b>		0.70	
Connection (finishing material)	Type of connection	0.60	Nail connection
	Accessibility of connection	0.80	Accessible with actions not causing damage
Interconnection (structure)	Type of connection	0.60	Nail connection
	Accessibility of connection	0.80	Accessible with actions not causing damage

TABLE 6 Scoring matrix disassembly potential redesign

		Score	
<b>Element level</b>		<b>0.85</b>	<b>Disassembly potential</b>
<b>1. Prefab 1e skin (structure)</b>		0.80	
Connection (existing construction)	Type of connection	0.80	Screw connection
	Accessibility of connection	0.80	Accessible with actions not causing damage
<b>2. Cladding</b>		0.90	
Connection (wooden slats)	Type of connection	0.80	Screw connection
	Accessibility of connection	1.00	Freely accessible
<b>3. Wooden slats</b>		0.80	
Connection (wooden structure)	Type of connection	0.80	Screw connection
	Accessibility of connection	0.80	Accessible with actions not causing damage
<b>Material level</b>		<b>0.82</b>	<b>Disassembly potential</b>
<b>1. Cladding material</b>		0.90	
Connection (wooden slats)	Type of connection	0.80	Screw connection
	Accessibility of connection	1.00	Freely accessible
<b>2. Wooden slats</b>		0.80	
Connection (wooden structure)	Type of connection	0.80	Screw connection
	Accessibility of connection	0.80	Accessible with actions not causing damage
<b>3. Wooden structure</b>		0.75	
Connection (finishing material)	Type of connection	0.80	Screw connection
	Accessibility of connection	0.80	Accessible with actions not causing damage
Interconnection (structure)	Type of connection	0.60	Nail connection
	Accessibility of connection	0.80	Accessible with actions not causing damage

The DfD index of the results shows that there is no change in the disassembly potential on the element level and only a 6% improvement on the material level in the baseline and the redesigned prefabricated envelope element. There is no change in the material use and connection in both scenarios except for the replacement of nail connections with screw connections.

### 5.1.3 Irish case

Table 7 shows the scoring matrix of the disassembly potential of the baseline design of the Irish case. The results show that the disassembly potential on the element level and the material level of the baseline design are 0.45 and 0.43, respectively, whereas the disassembly potential on the element level of the redesigned building envelope element is 0.80 and 0.72 on the material level (shown in Table 8).

TABLE 7 Scoring matrix disassembly potential baseline design

		Score	
<b>Element level</b>		<b>0.45</b>	<b>Disassembly potential</b>
<b>1. EWI System</b>		0.45	
Connection (existing construction)	Type	0.80	Connection with added elements
	Accessibility of connection	0.10	Not accessible - irreparable damage to objects
<b>Component Level</b>		0.45	
EWI to Window	Connection to window	0.45	
	Type of connection	0.80	Connection with added elements
	Accessibility of connection	0.10	Not accessible - irreparable damage to objects
<b>Material level</b>		<b>0.43</b>	<b>Disassembly potential</b>
<b>1. Acrylic Render</b>		0.25	
Connection (insolation)	Type	0.10	Hard chemical bond
	Accessibility	0.40	Accessible with actions causing repairable damage
<b>2. Insulation</b>		0.60	
Connection (existing wall)	Type	0.80	Connection with added elements
	Accessibility	0.40	Accessible with actions causing repairable damage

The DfD index shows that there is a 78 % and a 67 % improvement in the disassembly potential of the redesigned prefabricated building envelope element compared to the baseline design on the element and material level in the Irish case.

The disassembly potential of the redesign is improved on the type and accessibility of the connection compared to the baseline design. Furthermore, the redesign showcases an increase of 21% in the disassembly potential (material level) compared to the baseline. The disassembly potential of the redesign is improved on the material level by replacing hard chemical connections with dry connections compared to the baseline design. Hierarchical DfD has been a key principle and design strategy that results in significant improvement on the element and material level. The score on the element level is especially notable, caused by a premanufactured and modularized wall cladding panel.

TABLE 8 Scoring matrix disassembly potential redesign

		Score	
<b>Element level</b>		<b>0.80</b>	<b>Disassembly potential</b>
<b>1. Main 2D panel</b>		0.90	
Connection (existing construction)	Type of connection	1.00	Dry connection
	Accessibility of connection	0.80	Accessible with actions that don't cause damage
<b>2. Horiz. Const. Junction</b>		0.70	
Interconnection (construction)	Type of connection	1.00	Dry connection
	Accessibility of connection	0.40	Accessible with actions causing repairable damage
<b>Material level</b>		<b>0.72</b>	<b>Disassembly potential</b>
<b>1. Acrylic Render</b>		0.55	
Connection (cement board)	Type of connection	0.10	Cement bound connection
	Accessibility of connection	1.00	Freely accessible
<b>2. Cementboard</b>		0.80	
Connection (battens)	Type of connection	0.80	Screw connection
	Accessibility of connection	0.80	Accessible with actions that don't cause damage
<b>3. Timber battens</b>		0.80	
Connection (battens)	Type of connection	0.80	Screw connection
	Accessibility of connection	0.80	Accessible with actions that don't cause damage
<b>4. Breather membrane</b>		0.50	
Connection (woodfibre board)	Type of connection	0.60	Pin connection
	Accessibility of connection	0.40	Accessible with actions causing repairable damage
<b>5. Woodfibre board</b>		0.80	
Connection (metal stud)	Type of connection	0.80	Screw connection
	Accessibility of connection	0.80	Accessible with actions that don't cause damage
<b>6. Metal Stud</b>		0.80	
Connection (back strip/Gaskets)	Type of connection	0.80	Screw connection
	Accessibility of connection	0.80	Accessible with actions that don't cause damage
<b>7. Insolation</b>		1.00	
Connection (metal stud)	Type of connection	1.00	Dry connection
	Accessibility of connection	1.00	Freely accessible
<b>8. Backing Strip and Gaskets</b>		0.50	
Connection (existing structure)	Type of connection	0.60	Pin connection
	Accessibility of connection	0.40	Accessible with actions causing repairable damage

## 5.2 EMBODIED CARBON

The environmental impact is demonstrated based on the amount of carbon (cradle-to-gate) of the building envelope elements. The functional unit of this study is 1 m<sup>2</sup> of prefabricated building envelope element.

The difference in ECO<sub>2</sub> between the baseline design and the redesign reflects on material choices, materials reduction, and the share of virgin used materials compared to the share of reused materials. Figure 10 shows the comparison of embodied carbon associated with the baseline design and the redesign for all three cases.

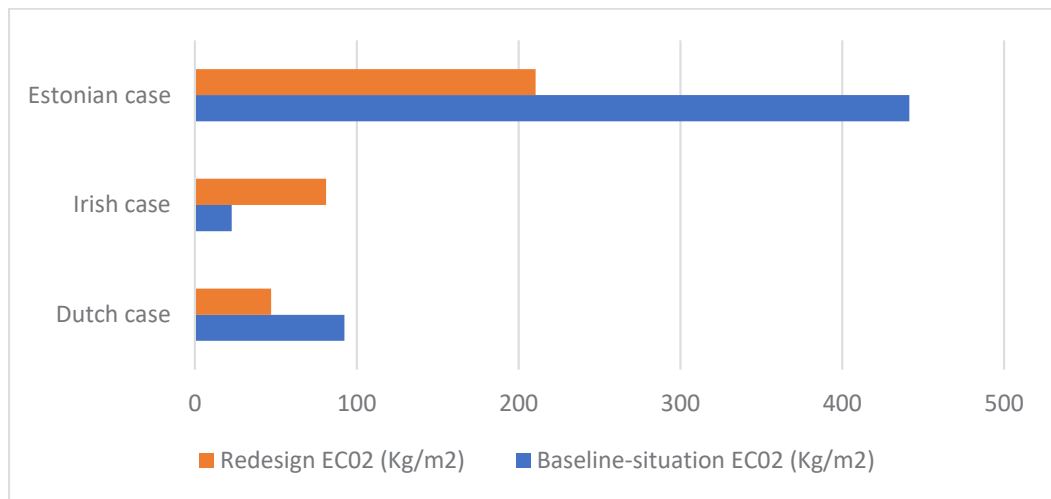


FIG. 10 Embodied carbon emission in baseline and redesign

### 5.2.1 Dutch case

Results show that the embodied carbon of the baseline design is 19.22 kg/CO<sub>2</sub> per square metre, whereas of the redesigned prefabricated building envelope element, it is 9.06 kg/CO<sub>2</sub>/m<sup>2</sup>. The embodied carbon of the redesigned prefabricated envelope element is reduced by 50% compared to the baseline design. The redesign consists of a frame (remanufactured with about 70% reused wood) and the façade cladding (100% reused wood) with a wood fibre insulation that has a high contribution of 8.04 kg/CO<sub>2</sub>. The baseline design consists of 100% virgin wood, and the use of glass wool insulation is the main culprit of higher emissions.

### 5.2.2 Estonian case

The embodied carbon of the redesigned prefabricated building envelope element is reduced by about 47% compared to the baseline design. The redesign showed a total embodied carbon of 16.79 kg/m<sup>2</sup>. The baseline design showed an embodied carbon of 31.67 kg/m<sup>2</sup>. The environmental impact is improved by a well-considered selection of biobased insulation and remanufactured materials to replace virgin materials. This selection of materials is not only considered in terms of quality and disassembly potential but also of further reuse and upscaling possibilities of the timber frame-based insulation system.

### 5.2.3 Irish case

The embodied carbon of the redesigned prefabricated building envelope element is increased by about 256% compared to the baseline design. The redesign showed a total embodied carbon of 81.05 kg/m<sup>2</sup>. The baseline design showed an embodied carbon of 22.76 kg/m<sup>2</sup>.

The cement carrier board alone contributes 68% of embodied carbon compared to other layers in the prefabricated building envelope element. The cement carrier board is used to avoid render layers and for a quality finish with impact resistance, though it contributes higher embodied carbon.

## 6 DISCUSSION

This study discussed the circular redesign of three different prefabricated building envelope elements in three demonstrator cases (Dutch, Estonian, and Irish). It was guided by the research question: what is the environmental impact in terms of embodied carbon and disassembly potential of circular redesigned prefabricated building envelope elements? By assessing the embodied carbon footprint (cradle-to-gate) and disassembly potential, direct insight is provided into how design choices and material choices influence the life cycle performance of building elements.

All three cases involve a hierarchical design for disassembly approach, resulting in a layered configuration, which facilitates future multi-cycle reuse of the building envelope element as a whole as well as its single components. In contrast to the traditional glued brick slips, the results of the Dutch demonstrator case showed that the use of the cladding materials fixed with a hook system substantially improved the disassembly potential during both maintenance and end-of-life scenarios. In the Estonian case, the improvement of the disassembly potential of redesigned envelope elements is due to separating functional layers and connecting these layers with screw connections which resulted in a higher reuse potential for horizontal and vertical wooden slats. In the Irish case, there is a significant improvement in the disassembly potential of the prefabricated building envelope by replacing traditional masonry with a rendering system that is fixed to the element with a dry connection. The redesign resulted in a demountable, premanufactured, modularized building envelope element. This study revealed that, compared to the baseline, an increase in disassembly potential of up to 100% can be achieved for an end-of-life scenario reusing the building envelope element at large and an increase of up to 49% on the level of materials and components being applied. In line with previous research (Juaristi et al., 2022), this research, therefore, advocates that, based on a careful design process and within the framework of existing product certification, it is possible to substantially increase future reuse potential contributing to improved material efficiency in the construction sector.

The environmental impact is demonstrated based on embodied carbon calculations (cradle-to-gate) of the building envelope elements. The difference in embodied carbon footprint between the baseline design and the redesign reflects the effects of avoiding the use of specific materials and careful material and connection selection to improve the overall material efficiency of building envelope elements. With respect to the material and connection selection, the application of biobased and reused materials was especially taken into account.

Results show that a reduction of 50% of embodied carbon emission can be achieved by reusing 100% of the wood for the façade cladding and 70% for the frame structure in the Dutch case and using biobased insulation and remanufactured materials in the Estonian case. In contrast to previous studies, this research showed that improving the disassembly potential of a construction element in combination with careful material selection can substantially reduce embodied carbon (Roberts et al., 2023). These findings are in line with the definition of systemic circularity, i.e. that a full circular design depends on multiple interconnected indicators with different impacts which influence each other in a continuous and circular manner (Kubbinga et al., 2018; Antwi-Afari et al., 2022).

On the other hand, the embodied carbon is significantly high due to the use of cement carrier boards and other multiple layers in the envelope elements. Designing out these materials is complex as these layers have specific functionalities (like fire safety), which are hard to meet with materials with a low(er) embodied carbon footprint. This is in line with the study by Mazzoli et al. (2022) showing that prefab multi-layered elements, required to meet the criteria of demount ability, reusability, and durability, have a greater embodied carbon due to the presence of larger quantities of materials and higher density.

Although none of the innovative prefabricated building envelope elements are yet considered 100% circular, the development of the three building envelope elements showcases that the environmental impact can be substantially reduced following a well-structured and dedicated design process. The reduction of the environmental impact is indicated by lower quantities of embodied carbon and an improved design for disassembly, reflecting a higher reuse potential of building materials and components.

## 7 LIMITATIONS AND FUTURE RESEARCH

Several limitations and directions for further research were identified. The three building envelopes redesigned for this study are not yet fully circular. Future research and development should focus on alternative designs to advance the development of fully circular deep-renovation technologies. From a holistic and systemic approach, one key strategy to arrive at fully circular deep-renovation solutions is to apply a 'tectonics of avoidance' approach. This means that at the building level, reduction and production measures — insulation versus renewable energy generation — need to be balanced with the purpose of optimal material application (Ritzen et al., 2016). A second key strategy is to increase the application of biobased materials such as hemp insulation and wood not being preserved, improved, or altered by the use of a chemical agent.

A second limitation is that additional empirical data is needed to advance our understanding of real environmental impact following an eco-design approach. First, empirical data is required to assess the reduction of embodied carbon emission under consideration of multi-cycle reuse of building elements and materials over time, which is considered a missing link in both theory and practice (Lam et al., 2022). Second, as a result of the design for disassembly strategy in combination with the reuse of mined construction materials, this study indicates that multi-cycle reuse depends on the material flow of locally available construction materials and components. Future studies could, therefore, research how to determine geographical territories by comparing the embodied carbon emission of reusing mined materials relative to other materials that can be applied, differentiating for transport distance. Such studies would contribute to the definition of territorial circular economies. They should also include the implications for the business model and supply chain set-up, which are not considered in our research project. Our research project also revealed some methodological limitations. The first methodological limitation concerns the embodied carbon calculation and the application of the ICE database since this database refers to the construction material application in the United Kingdom and is not up to date. However, because of the comparative research approach involving cases from three different countries, this limitation is considered acceptable. For absolute and country-specific impact calculations, we suggest using national-oriented databases (Bitar et al., 2022).

The third issue concerns the application of design for disassembly as a method and indicator. Coherent assessments have been suggested for the hypothesized correlation between life cycle assessment and cyclical use of construction materials, although scientific and empirical evidence is still under development. In order to form a scientific sound and good practical judgments, this coherent framework should account for:

- 1 Life cycle effects (ageing and applying R-strategies). Technical detachability tells little about the proportion and quality of the material that can be reused after disassembly and, subsequently, its effect on resource efficiency and carbon emission (Juaristi, Sebastiani, & Avesani, 2022).
- 2 The complexity of element compositions. As the number of components increases with more variation in the type of connections, this has a negative impact on carbon emission. (Lam et al., 2022; Roberts et al., 2023).
- 3 Degree of prefabrication and market forces in design choices regarding building material or component selection. This study showcased that material and component selection have a strong effect on both disassembly potential and embodied carbon emission.

Addressing the indicated, future research opportunities would be of significant importance from an academic, managerial and policy point of view. This study has contributed by offering a useful foundation for bridging circular design and the assessment of circular building indicators for materializing the transition towards a fully circular and Paris-proof built environment.

## 8 CONCLUSION

First of all, this study showcases that a reduction of up to 50% of embodied carbon emissions reduction can be achieved by closing material loops based on well-considered R-strategies and local reuse of materials. This indicates that closing material loops can lead to major consequences in terms of environmental impact and advocates treating demolition waste as a potent flow of valuable construction materials. Second, this study revealed that, compared to the baseline, an increase in disassembly potential of up to 100% can be achieved for an end-of-life scenario by reusing the building envelope element at large and an increase of up to 49% on the level of materials and components being applied. The increase in disassembly potential is due to thoughtful design choices based on accessible and dry connections and the degree of prefabrication. The increase in detachability of 50% at the level of construction materials used for the building envelope elements is of limited interest for the assembly process on-site but very important for a potential disassembly process in the factory. The design, viewed at the material level, determines how easily parts or materials of a prefab element can be recovered and/or replaced, and thus the prefab element can be adapted to changing conditions. Furthermore, in terms of eco-efficiency, the degree of reversibility in the factory can provide the opportunity to mine and reuse costly construction materials and components. However, to establish a fully circular design with a disassembly potential of materials close to 100%, further research and development are required. This advancement comes with an initial increase of embodied carbon emissions, and thus, a fully circular design will only reduce the environmental impact if multi-cycle reuse of the elements and the materials applied can be assured.

## References

---

- Antwi-Afari, P., Ng, S. T., & Chen, J. (2022). Developing an integrative method and design guidelines for achieving systemic circularity in the construction industry. *Journal of Cleaner Production*, 354, 131752. <https://doi.org/10.1016/j.jclepro.2022.131752>
- Akinade, O. O., Oyedele, L. O., Ajayi, S. O., Bilal, M., Alaka, H. A., Owolabi, H. A., ... & Kadiri, K. O. (2017). Design for Deconstruction (DfD): Critical success factors for diverting end-of-life waste from landfills. *Waste management*, 60, 3-13.
- Akbarnezhad, A. & Jianzhuang X. (2017). Estimation and Minimization of Embodied Carbon of Buildings: A Review, *Buildings* 2017, 7(1), 5; <https://doi.org/10.3390/buildings7010005>, Received: 18 November 2016 / Revised: 19 December 2016 / Accepted: 22 December 2016 / Published: 4 January 2017.
- Akbarnezhad, A. & Xiao, J. (2017). Estimation and Minimization of Embodied Carbon of Buildings: A Review. *Building*, 7(5). doi:10.3390/buildings7010005, Received: 18 November 2016 / Revised: 19 December 2016 / Accepted: 22 December 2016 / Published: 4 January 2017.
- Akbarnezhad, A.; Moussavi Nadoushani, Z.S. Estimating the costs, energy use and carbon emissions of concrete recycling using building information modelling. In *Proceedings of the 31<sup>st</sup> International Symposium on Automation and Robotics in Construction and Mining (ISARC 2014)*, Sydney, Australia, 9–11 July 2014; pp. 385–392.
- Attia, S., & Al-Obaidy, M. (2021). Design criteria for circular buildings. *Conference proceeding Crossing Boundaries Conference 2021*, March 24-25, the Netherlands. [https://orbi.uliege.be/bitstream/2268/258348/1/Criteria\\_version\\_15.pdf](https://orbi.uliege.be/bitstream/2268/258348/1/Criteria_version_15.pdf)
- Barbosa, F., Woetzel, J., Mischke, J., Ribeirinho, M.J., Sridhar, M., Parsons, M., Bertram, N., & Brown, S. (2017). Reinventing construction: A route to high productivity, p. 20. Download: <https://www.mckinsey.com/capabilities/operations/our-insights/reinventing-construction-through-a-productivity-revolution>
- Bertram, N., Fuchs, S., Mischke, J., Palter, R., Strube, G., & Woetzel, J. (2019). Modular construction: From projects to products, p. 34. Download: <https://www.mckinsey.com/capabilities/operations/our-insights/modular-construction-from-projects-to-products>
- Bhocchibhoya, S., Pizzol, M., Achten, W.M.J., Maskey R.K., Zanetti M. & Cavalli R. (2017). Comparative life cycle assessment and life cycle costing of lodging in the Himalaya. *International Journal of Life Cycle Assessment*, 22, 1851–1863. <https://doi.org/10.1007/s11367-016-1212-8>
- Bitar, A. L. B., Bergmans, I., & Ritzen, M. (2022). Circular, biomimicry-based, and energy-efficient façade development for renovating terraced dwellings in the Netherlands. *Journal of Facade Design and Engineering*, 10(1), 75-105, <http://doi.org/10.47982/jfde.2022.1.04>
- Bocken, N.M.P., Pauw, I.d., Bakker, C., Van der Grinten, B. (2016). Product design and business model strategies for a circular economy. *Journal of Industrial and Production Engineering*, 308 – 320. <https://doi.org/10.1080/21681015.2016.1172124>
- BPIE (Buildings Performance Institute Europe) (2021). Whole-life carbon: challenges and solutions for highly efficient and climate-neutral buildings. Download: <https://www.bpie.eu/publication/whole-life-carbon-challenges-and-solutions-for-highly-efficient-and-climate-neutral-buildings/>
- Cao, C. (2017). Sustainability and life assessment of high strength natural fibre composites in construction. *Advanced high strength natural fibre composites in construction*, 529-544, <https://doi.org/10.1016/B978-0-08-100411-1.00021-2>
- Cambier, C., Galle, W., & De Temmerman, N. (2020). Research and development directions for design support tools for circular buildings. *Buildings*, 10(8), 14, 10.3390/BUILDINGS10080142
- Chini, A. R. (2001). Deconstruction and Materials Reuse: Technology, Economic, and Policy. CIB Publication 266. Download: <https://www.irbnet.de/daten/iconda/CIB727.pdf>
- Chung, W.-H., Kremer, G.E.O., & Wysk, R.A. (2014). Life cycle implications of product modular architectures in closed-loop supply chains. *The International Journal of Advanced Manufacturing Technology*, 70, 2013-2028. <https://doi.org/10.1007/s00170-013-5409-8>
- Cottafava, D., & Ritzen, M. (2021). Circularity indicator for residential buildings: Addressing the gap between embodied impacts and design aspects. *Resources, Conservation and Recycling*, 164, 105120, <https://doi.org/10.1016/j.resconrec.2020.10512>
- Durmisevic, E. (2006). Transformable building structures: design for disassembly as a way to introduce sustainable engineering to building design & construction. (Doctoral dissertation), ISBN 90-902-0341-9; ISBN 978-90-9020341-6.

- Dutil, Y., Rousse, D. & Quesada, G. (2011). Sustainable buildings: an ever evolving target. *Sustainability*, 3, 443-464, 10.3390/su3020443
- Eberhardt, L. C. M., Birkved, M., & Birgisdottir, H. (2022). Building design and construction strategies for a circular economy. *Architectural Engineering and Design Management*, 18(2), 93-113 <https://doi.org/10.1080/17452007.2020.1781588>
- EMF (2015). Towards a circular economy: Business rationale for an accelerated transition. Download: <https://ellenmacarthurfoundation.org/towards-a-circular-economy-business-rationale-for-an-accelerated-transition>
- Ellen MacArthur Foundation (2015). Circularity indicators: An approach to measuring circularity. [https://www.ellenmacarthurfoundation.org/assets/downloads/insight/Circularity-Indicators\\_Project-Overview\\_May2015.pdf](https://www.ellenmacarthurfoundation.org/assets/downloads/insight/Circularity-Indicators_Project-Overview_May2015.pdf).
- Esteves, B., Domingos, I., & Pereira, H. (2008). Pine wood modification by heat treatment in air. *BioResources*, 3(1), 142-154. Download: [https://jtatm.textiles.ncsu.edu/index.php/BioRes/article/view/BioRes\\_03\\_1\\_0142\\_Esteves\\_DP\\_PineWoodMod](https://jtatm.textiles.ncsu.edu/index.php/BioRes/article/view/BioRes_03_1_0142_Esteves_DP_PineWoodMod)
- Grant A. & Ries, R. (2013). Impact of building service life models on life cycle assessment. 41, 168- 186, <http://dx.doi.org/10.1080/09613218.2012.730735>
- Guggemos, A. A., & Horvath, A. (2005). Comparison of environmental effects of steel-and concrete-framed buildings. *Journal of infrastructure systems*, 11(2), 93-101
- Gonzalez, M.J., Navarro, J.G. (2006). Assessment of the decrease of CO2 emissions in the construction field through the selection of materials: Practical case study of three houses of low environmental impact. *Building and Environment*. 2006, 41, 902-909, <https://doi.org/10.1016/j.buildenv.2005.04.006>
- Hammond, G.P.; Jones, C.I. (2008). Embodied energy and carbon in construction materials. *Proceedings of the Institution of civil Engineers*, 161, 87-9, <https://doi.org/10.1680/ener.2008.161.2.87>
- Hammond, G. & Jones, C. (2011). Embodied Carbon, The Inventory of Carbon and Energy (ICE). A BSRIA guide. Download: <https://greenbuildingencyclopaedia.uk/wp-content/uploads/2014/07/Full-BSRIA-ICE-guide.pdf>
- Häkkinen, T., Kuitinen, M., Ruuska, A., & Jung, N. (2015). Reducing embodied carbon during the design process of buildings. *Journal of Building Engineering*, 4, 1-13, <https://doi.org/10.1016/j.job.2015.06.005>
- Hildebrand, L. (2014). Strategic investment of embodied energy during the architectural planning process. Doctoral dissertation. Delft University of Technology, Faculty of Architecture and the Built Environment.
- Hofman, E., Voordijk, H., & Halman, J. (2009). Matching supply networks to a modular product architecture in the house-building industry. *Building Research & Information*, 37, 31-42. <https://doi.org/10.1080/09613210802628003>
- Huuhka, S., Lahdensivu, J. (2016) Statistical and geographical study on demolished buildings. *Building Research & Information* 44(1) , 73-96, <https://doi.org/10.1080/09613218.2014.980101>
- IPCC Climate Change (2014). *Mitigation of Climate Change (Contribution of Working Group III to the Fifth Assessment Report of the Intergovernmental Panel on Climate Change)* Cambridge University Press, Cambridge, UK
- IPCC (2023). *Climate Change 2023: Synthesis Report. Contribution of Working Groups I, II and III to the Sixth Assessment Report of the Intergovernmental Panel on Climate Change [Core Writing Team, H. Lee and J. Romero (eds.)]*. IPCC, Geneva, Switzerland, 184 pp., doi: 10.59327/IPCC/AR6-9789291691647
- ISSO (2021). *Circularity into detail*. Download: <https://documenten.isso.nl/s/uC0kWdQL2kgUqIE3p2xoRrJHK1FRH9rC/Research%20report%20Circularity%20in%20Referentiedetails.pdf>
- Joensuu, T., Leino, R., Heinonen, J., Saari, A. (2022). Developing Buildings' Life Cycle Assessment in Circular Economy-Comparing methods for assessing carbon footprint of reusable components. *Sustainable Cities and Society* 77, <https://doi.org/10.1016/j.scs.2021.103499><https://doi.org/10.1016/j.scs.2021.103499>
- Juaristi, M., Sebastiani, I., & Avesani, S. (2022). Timber-based Façades with Different Connections and Claddings: Assessing Materials' Reusability, Water Use and Global Warming Potential. *Journal of Facade Design and Engineering*, 10(2), 71-86. <https://doi.org/10.47982/jfde.2022.powerskin.5>
- Keiller, S., Clements, V., & Charter, M. (2013). *A guide for SMEs on eco-design for the construction industry*. EDECON, Jackie Walker, Enterprise Europe Network. <https://research.uca.ac.uk/id/eprint/2716>

- Kimura, F., Kato, S., Hata, T., & Masuda, T. (2001). Product modularization for parts reuse in inverse manufacturing. *CIRP Annals*, 50, 89-92. [https://doi.org/10.1016/S0007-8506\(07\)62078-2](https://doi.org/10.1016/S0007-8506(07)62078-2)
- Knight, P., & Jenkins, J. O. (2009). Adopting and applying eco-design techniques: a practitioners perspective. *Journal of cleaner production*, 17(5), 549-558, <http://dx.doi.org/10.1016/j.jclepro.2008.10.002>
- Kubbinga, B., Bamberger, M., Van Noort, E., Van den Reek, D., Blok, M., Roemers, G., Hoek, J., & Faes, K., (2018). Report. Download: <https://www.circle-economy.com/resources/a-framework-for-circular-buildings>
- Kuusk, K., Ritzen, M., Daly, P., Papadaki, D., Mazzoli, C., Aslankaya, G., Vetrsek, J., Kalamees, T. (2022). The circularity of renovation solutions for residential buildings. REHVA 14<sup>th</sup> KVAC World Congress, 22- 25<sup>th</sup> May, Rotterdam, The Netherlands. <https://doi.org/10.34641/clima.2022.333>
- Lam, W. C., Claes, S., & Ritzen, M. (2022). Exploring the Missing Link between Life Cycle Assessment and Circularity Assessment in the Built Environment. *Buildings*, 12(12), 2152, <https://doi.org/10.3390/buildings12122152>
- Ma, J., & Kremer, G.E.O. (2016). A systematic literature review of modular product design (MPD) from the perspective of sustainability. *The International Journal of Advanced Manufacturing Technology*, 86, 1509-1539. <https://doi.org/10.1007/s00170-015-8290-9>
- Marsh, R. (2016). Building lifespan: effect on the environmental impact of building components in a Danish perspective. *Architectural Engineering and Design Management*, 13 (2), <https://doi.org/10.1080/17452007.2016.1205471>
- Marques, B., Tadeu, A., De Brito, J., & Almeida, J. (2017). A perspective on the development of sustainable construction products: an eco-design approach. *International Journal of Sustainable Development and Planning*, 12(2), 304-314, doi:10.2495/SDP-V12-N2-304-314
- Mazzoli, C., Corticelli, R., Dragonetti, L., Ferrante, A., van Oorschot, J. & Ritzen, M. (2022). Assessing and Developing Circular Deep Renovation Interventions towards Decarbonisation: The Italian Pilot Case of "Corte Palazzo" in Argelato. *Sustainability*, 14(20), 13150. <https://doi.org/10.3390/su142013150>
- Minunno, R., O'Grady, T., Morrison, G.M., Gruner, R.L. and Colling, M. (2018). Strategies for Applying the Circular Economy to Prefabricated Buildings. *Building*, 8(9). 125, <https://doi.org/10.3390/buildings8090125>
- Monahan, J. and Powell, J.C. (2011). An embodied carbon and energy analysis of modern methods of construction in housing: A case study using a lifecycle assessment framework. *Energy and Buildings*, 43, 179-188. <https://doi.org/10.1016/j.enbuild.2010.09.005>
- Okudan Kremer, G.E., Ma, J., Chiu, M.-C., & Lin, T.-K. (2013). Product modularity and implications for the reverse supply chain. *Supply Chain Forum: An International Journal*, 14(2), 54-69. <https://doi.org/10.1080/16258312.2013.11517315>
- Rauf, A. & Crawford, R.H. (2015). Building service life and its effect on the life cycle embodied energy of buildings. *Energy*, 140 – 148, <https://doi.org/10.1016/j.energy.2014.10.093>
- Renz, A., Zafra Solas, M., 2016. Shaping the future of construction: A breakthrough in mindset and technology, in: Forum, W.E., Group, T.B.C. (Eds.), Geneva. Download: [https://www3.weforum.org/docs/WEF\\_Shaping\\_the\\_Future\\_of\\_Construction\\_report\\_020516.pdf](https://www3.weforum.org/docs/WEF_Shaping_the_Future_of_Construction_report_020516.pdf)
- Ritzen, M. J., Haagen, T., Rovers, R., Vroon, Z. A. E. P., & Geurts, C. P. W. (2016). Environmental impact evaluation of energy saving and energy generation: Case study for two Dutch dwelling types. *Building and Environment*, 108, 73-84, <http://dx.doi.org/10.1016/j.buildenv.2016.07.020>
- Roberts, M., Allen, S., Clarke, J., Searle, J., Coley, D. (2023). Understanding the global warming potential of circular design strategies: Life Cycle Assessment of a design-for- disassembly building. *Sustainable Production and Consumption*. 37, 331 –343 <https://doi.org/10.1016/j.spc.2023.03.001>
- Roggema, R. (2016). Research by design: Proposition for a methodological approach. *Urban science*, 1(1), , doi:10.3390/urbansci1010002
- Saheb, Y., 2016. Energy Transition of the EU Building Stock: Unleashing the 4<sup>th</sup> Industrial Revolution in Europe. OpenExp, Paris. Download: <https://apo.org.au/node/209391>
- Sartori, I. and Hestnes, A.G. (2007) Energy Use in the Life Cycle of Conventional and Low-Energy Buildings: A Review Article. *Energy and Buildings*, 39, 249-257. <https://doi.org/10.1016/j.enbuild.2006.07.001>

- Sipahi, S., & Kulözü-Uzunboy, N. (2021). A study on reducing the carbon footprint of architectural buildings based on their materials under the guidance of eco-design strategies. *Clean Technologies and Environmental Policy*, 23, 991-1005, <https://doi.org/10.1007/s10098-020-02009-4>
- Sobota, M., Driessen, I. & Holländer M. (2022), Carbon-based design: ONDERZOEK NAAR DE MILIEU-IMPACT VAN DE WONING-BOUW. Download: Carbon-Based-Design.pdf (circulairebouweconomie.nl)
- Spitsbaard, M. & Leeuwen M.V. (2021). Paris Proof Embodied Carbon: Calculation Protocol. Dutch Green Building Council, NIBE B.V. <https://www.dgbc.nl/publicaties/de-berekening-achter-paris-proof-materiaalgebonden-emissies-49>
- Thomsen, A.F., Straub,A. (2018). Lifespan assessment of dwellings. European Network for Housing Research (ENHR 2018), <http://resolver.tudelft.nl/uuid:4f2765ac-9e06-43a0-813b-9763f3ab49e3>
- Tokede, O., Rodger, G., Waschl, B., Salter, J. & Ashraf, M. (2022). Harmonising life cycle sustainability thinking in material substitution for buildings. *Resources, Conservation & Recycling*, 185, 106468, <https://doi.org/10.1016/j.resconrec.2022.106468>
- Passer, A., Kreiner, H., & Maydl P. (2012).Assessment of the environmental performance of buildings: a critical evaluation of the influence of technical building equipment on residential buildings. *International Journal of Life Cycle Assessment*, 17,1116-1130
- Pomponi, F. & Moncaster, A. (2016). Circular economy for the built environment: A research framework. *Journal of Cleaner Production*, 143 (1), 710 – 718, <https://doi.org/10.1016/j.jclepro.2016.12.055>
- Potting, J., Hekkert, M., Worrell, E., and Hanemaaijer, A. (2017). Circular Economy: Measuring Innovation in the Product Chain. PBL Netherlands Environmental Assessment Agency, The Hauge.
- United Nations (2015). Report of the Conference of the Parties on its twenty-first session, held in Paris from 30 November to 13 December 2015. In United Nations Framework Convention on Climate Change; Available online: <https://unfccc.int/resource/docs/2015/cop21/eng/10.pdf>
- Van Vliet, M., Van Grinsven, J. & Teunizen, J. (2021). Circular Buildings: A measurement methodology for Disassembly Potential Version 2.0. Download: DGBC Disassembly Potential Measurement Methodology \_ 2022.pdf
- Xiao, J.; Falkner, H (2007). Bond behaviour between recycled aggregate concrete and steel rebars. *Construction and Building Materials*. 21, 395–401, <https://doi.org/10.1016/j.conbuildmat.2005.08.008>
- Zairul, M. (2021). The recent trends on prefabricated buildings with circular economy (CE) approach. *Cleaner Engineering and Technology*, 4, <https://doi.org/10.1016/j.clet.2021.100239>



# Energy-saving potential of thermochromic coatings in transparent building envelope components

Matthias Fahland<sup>\*</sup>, Jolanta Szelwicka<sup>1</sup>, Wiebke Langgemach<sup>1</sup>

<sup>\*</sup> Corresponding author, matthias.fahland@fep.fraunhofer.de  
<sup>1</sup> Fraunhofer FEP, Germany

## Abstract

*Advances in the energy management of buildings are essential for reducing the carbon footprint in the building sector. Applying special window coatings of varying optical properties offers new chances for improved energy efficiency. Thermochromic vanadium oxide (VO<sub>2</sub>) is an important material for this development and is, therefore, one of the most investigated thermochromic materials. It changes its transmittance in the infrared spectral range in response to a changing temperature. In this study, VO<sub>2</sub> coating was deposited on ultra-thin flexible glass in a continuous roll-to-roll sputtering process. The thermochromic layer had a thickness of 70 nm, and it was embedded between two zirconium oxide layers of 170 nm each. The luminous transmittance of the stack was 50%. A solar modulation of 9.6% was reached between the low and high-temperature states. The transition temperature between the cold infrared transparent and the warm infrared opaque state was determined to be 22°C. Different application scenarios for this material were evaluated. The modulation of the solar transmittance was calculated for the combination of VO<sub>2</sub> with state-of-the-art low-e coatings. Our findings show that such a combination does not offer a benefit for reducing the energy demand of a building. However, a stand-alone implementation of thermochromic coatings has a high potential if the energy consumption of the building is dominated by cooling demands.*

## Keywords

*smart coatings, energy saving, radiative cooling, smart windows, electrochromic coatings, thermochromic coatings, energy efficiency, vanadium oxide*

## DOI

<http://doi.org/10.47982/jfde.2023.2.A5>

# 1 INTRODUCTION

The building sector in Europe is presently responsible for roughly 40% of the primary energy consumption and 36% of the greenhouse gas emissions (D'Agostino & Mazzarella, 2019). In the Scandinavian countries and Central Europe, energy is mainly used for heating and illumination. In contrast, in Southern European countries, cooling and air conditioning are the main sources of energy consumption. Several global trends support the increased energy demand for cooling the interior of buildings: climate change leads to generally increased average temperatures. Additionally, the continuous growth of both the world population and the welfare in southern countries causes an effect in the same direction. Transparent components of the buildings, i.e. windows and skylights, are crucial for the energy exchange between the interior and the surroundings. This is especially significant considering the increased window-to-wall ratio (WWR) of non-residential buildings over the last decades.

Since the 1970s, considerable improvements have been made to intentionally control the energy flux through windows. During this time, low emissivity (low-e) coatings became popular. They reduce the heat loss to the outside by thermal radiation. In contrast, solar control coatings prevent the near-infrared radiation of the sun from entering the building. These types of coatings decrease the energy demand for cooling on days with intense sunshine (Yaşar & Kalfa, 2012), (Teixeira et al., 2020). Nowadays, all these approaches are considered to be state-of-the-art. The heat exchange through the window is specified by its U-value (degree to which a building component prevents heat from transmitting between the inside and the outside of a building) and the g-factor (total solar transmittance of a window, characterizing the heat gain at sunshine conditions). Details about the definition of these values can be found in (Jelle, 2013) and (ISO 9050, EN 673:2011).

Low-e and solar control coatings have static optical properties. The preferred version can be installed in a building depending on both the design specifics and the local climate. However, as mentioned above, the optical properties of these windows cannot be adapted as a response to daily or seasonal changes. Therefore, the need for further improvements in energy efficiency has drawn increasing attention to so-called smart materials. Coatings made with these materials can change their optical properties when triggered by an external stimulus.

There exist different types of smart materials. They can be distinguished by the type of stimulus which causes the change in the optical properties. The most common ones are electrochromic, gasochromic, photochromic, and thermochromic materials. Among these, the electrochromic approach is the most popular; it has already been realized in many installations. This type of smart coating has the advantage of a large switching effect in the visible spectral range. Moreover, it can be actively controlled by a user. The effect of windows with electrochromic coatings on the energy efficiency of buildings has already been extensively investigated (Baldassarri et al., 2016).

This article focuses on the energy-saving potential of thermochromic coatings. Thermochromic coatings change their properties in response to the temperature. Different materials with such properties are presented in the literature (Wang, 2021), (Crosby & Netravali, 2022). Vanadium dioxide ( $\text{VO}_2$ ) is the most promising and well-investigated thermochromic material for energy-saving applications (Hu et al., 2023), (Wang et al., 2021). It undergoes a phase transition between a low-temperature monoclinic crystalline structure and a high-temperature tetragonal structure. This phase transition is accompanied by a change of the optical properties in the infrared spectral range, i.e. the low-temperature phase is transparent while the high-temperature phase is opaque. The optical properties in the UV and visible spectral ranges are nearly unaffected by this change.

The transition temperature of pure VO<sub>2</sub> is 68°C. Previous research has established that this value can be reduced to approximately 25-30°C by introducing small quantities of tungsten into the coating (Jin et al., 1998). However, the widespread usage of thermochromic vanadium oxide is still being prevented by various challenges (Chang et al., 2018). First, the switching effect is limited to the infrared spectral range. Thus, achievable energy modulation is lower compared to the electrochromic counterparts, which also change their properties in the visible spectral range. Secondly, the luminous transmittance of vanadium oxide thin films is only around 40%. Moreover, the absorption in the visible spectral range causes a yellowish colour of the transmitted radiation. Both aspects are undesirable optical properties which speak against the use of thermochromic coatings in windows. Furthermore, the deposition process of vanadium oxide is very demanding, as the phase diagram of the vanadium-oxygen system includes numerous other phases without thermochromic properties. Therefore, process parameters need precise adjustment to ensure the formation of the desired stoichiometry (Bahlawane & Lenoble, 2014). Different techniques have been investigated for the fabrication of thermochromic VO<sub>2</sub>, among them chemical vapour deposition (Bahlawane et al., 2014), (Mohammad et al., 2023), hydrothermal methods (Magdassi et al., 2017), and physical vapour deposition (Vu et al., 2019), (Rezek et al., 2022).

This study addresses several of the challenges of VO<sub>2</sub>. First, the VO<sub>2</sub> layer was embedded between two zirconium oxide (ZrO<sub>2</sub>) layers to increase the optical performance as well as the environmental stability compared to the single-layer vanadium oxide. Second, an improved roll-to-roll deposition process was developed as a possible pathway to the low-cost manufacturing of thermochromic coatings. This system included an inline monitoring system for the transmittance of the coated material, which resulted in increased stability compared to a process version presented in a previous work (Rezek et al., 2022). Thin flexible glass was chosen as a substrate. This bendable material has an areal weight of less than 0.3 kg/m<sup>2</sup>. Its light weight increases the suitability of the coated material for building retrofits, making the installation of thermochromic-coated materials relatively easy.

Preferably, smart coatings should be used in combination with well-established state-of-the-art solutions. Great effort has been put into answering the question of how the ability of adaptation can push the energy efficiency of buildings beyond the presently existing limits. Detailed analyses of the presently known effects on building level can be found in (Tällberg et al., 2016) and (Butt et al., 2021).

The methodology section of this article introduces the calculation scheme of different quantities. It is later used for the evaluation of the results. Based on the obtained results, different application scenarios for thermochromic coatings are evaluated. The coating process itself is only presented briefly since the deposition technique is not the focus of this paper.

## 2 METHODOLOGY

The thermochromic materials are characterized by measuring the optical properties across a temperature range of -20°C up to 80°C. The expected optical effect of vanadium oxide in a window is schematically shown in Figure 1.

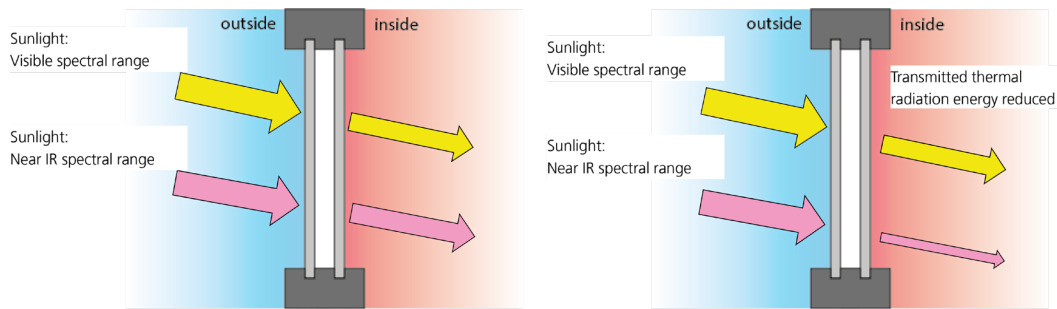


FIG. 1 Effect of a thermochromic coating on the transmission of solar radiation through an integrated glass unit in the cold state (left) and warm state (right)

The transmittance of  $\text{VO}_2$  in the visible spectral range remains nearly constant across the entire temperature range. The change in the optical properties is mainly observed in the near-infrared spectral range. Here, the transmission in the cold state is much higher than in the warm state.

The energy-saving potential can be evaluated based on both the measured luminous transmittance of the coated glass samples and the difference in the measured solar transmittance in the high- and low-temperature states. The definition of these quantities was taken from ISO 9050:2003.

The luminous transmittance  $T_{lum}$  is calculated as (1)

$$T_{lum} = \int_{380 \text{ nm}}^{780 \text{ nm}} T(\lambda) D(\lambda) V(\lambda) d\lambda / \int_{380 \text{ nm}}^{780 \text{ nm}} D(\lambda) V(\lambda) d\lambda \quad (1)$$

where  $T(\lambda)$  is the transmittance spectrum of the coated glass,  $D(\lambda)$  is the spectral distribution of illuminant D65, and  $V(\lambda)$  is the spectral luminous efficiency for photopic vision.

The change in solar transmittance  $\Delta T_{sol}$  is defined by (2) and (3) as the difference between the low-temperature and the high-temperature value measured at  $-20^\circ\text{C}$  and  $80^\circ\text{C}$ , respectively.

$$\Delta T_{sol} = T_{sol,LT} - T_{sol,HT} \quad (2)$$

$$T_{sol,(LT/HT)} = \int_{300 \text{ nm}}^{2500 \text{ nm}} T(\lambda, \Theta) S(\lambda) d\lambda / \int_{300 \text{ nm}}^{2500 \text{ nm}} S(\lambda) d\lambda \quad (3)$$

Where  $T(\lambda, \Theta)$  is the temperature-dependent transmission, and  $S(\lambda)$  the relative spectral distribution of the solar radiation. Both  $T_{lum}$  and  $\Delta T_{sol}$  are usually given in percentages.

For practical applications, it is important to know transition temperature  $\Theta_r$  between the high- and low-temperature phases. It would even be advantageous to adjust this value according to the climatic conditions of the intended installation. As already mentioned, tuning of  $\Theta_r$  is usually achieved by incorporating different amounts of tungsten into  $\text{VO}_2$ . (Jin et al. 1998). However, vanadium oxide shows a thermal hysteresis behaviour, i.e. the optical properties of the layers at a certain temperature are different depending on whether the system has been cooled down or heated up. In this work, the transition temperature  $\Theta_r$  is defined as the centre point of the hysteresis of the transmittance values measured at 2500 nm as proposed in (Houska et al., 2019).

Nevertheless, the materials reported in this paper exhibit a non-symmetrical hysteresis. Therefore, the definition of a centre point of the hysteresis must be refined to obtain reproducible values. The advanced calculation procedure of the transition temperature can be explained with the help of the quantities given in Figure 2.

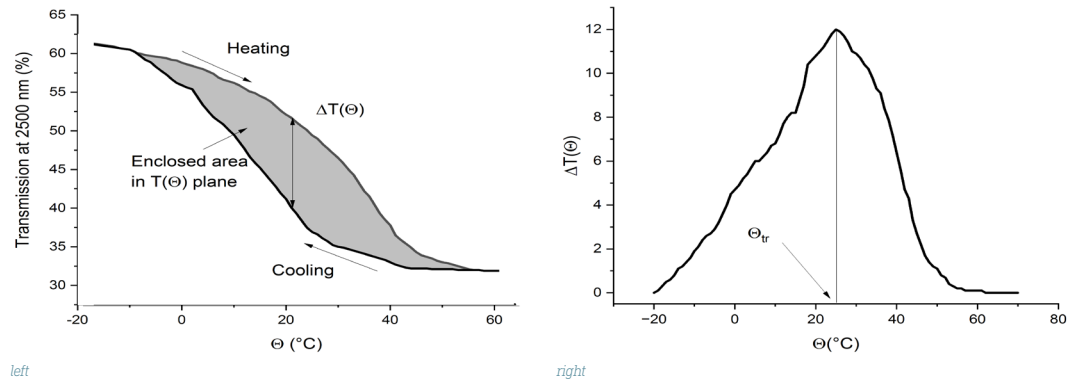


FIG. 2 Definition of the transition temperature of a thermochromic system

The left side of Figure 2 shows a typical non-symmetric hysteresis of the transmission at 2500 nm. The right side of Figure 2 shows the difference between the upper value of the transmittance (obtained for the heating curve) and the lower value (obtained for the cooling curve) as a function of the temperature ( $\Delta T(\Theta)$ ). There is a distinct maximum in this curve which can be interpreted as the transition temperature  $\Theta_{tr}$ .

An alternative approach defines the transition temperature as the abscissa value of the vertical line that divides the enclosed area in Figure 2 (left) into two equal parts. This can be expressed by the integral equation (4).

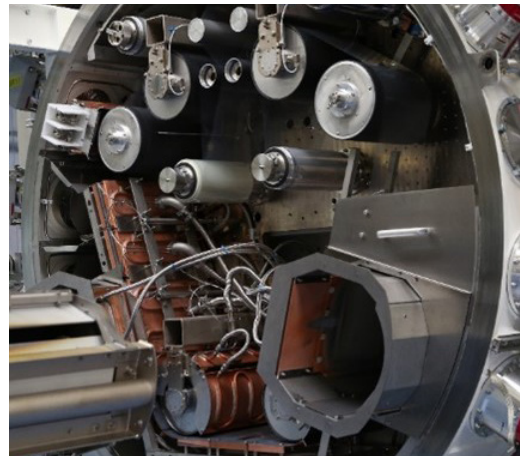
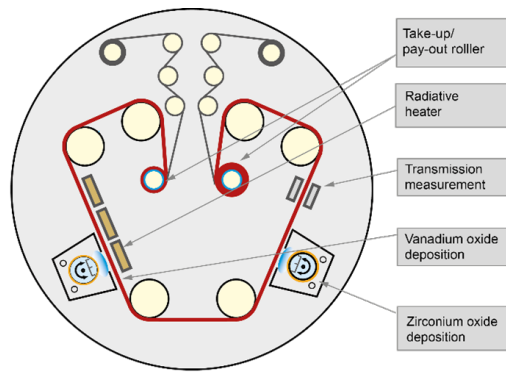
$$\int_{-20}^{\Theta_{tr}} \Delta T(\Theta) d\Theta = \frac{1}{2} \int_{-20}^{80} \Delta T(\Theta) d\Theta \quad (4)$$

For the example given in Figure 2 (left),  $\Theta_{tr} = 25^{\circ}\text{C}$  is obtained for the maximum approach, and  $\Theta_{tr} = 22^{\circ}\text{C}$  for the divided area approach. In the following, the divided area approach according to equation (4) will be applied if the authors refer to the transition temperature.

This choice takes all measurement points into consideration. Hence, it is less sensitive to deviations of single values. In the case of a symmetric hysteresis, both values are identical and equal to the value obtained by the acknowledged procedure described in (Houska et al., 2019).

A thermochromic three-layer system  $\text{ZrO}_2\text{-VO}_2\text{-ZrO}_2$  was deposited on ultra-thin flexible glass. The approach followed the concept outlined in (Vlcek et al., 2017).

The substrate was ultrathin glass (NEG) with a width of 300 mm and a thickness of 0.1 mm. The flexibility of the substrate allowed the application of a roll-to-roll coating approach. Therefore, the experimental work was carried out in the roll-to-roll sputtering equipment FOSA labX (VON ARDENNE) (Figure 3).



left

right

FIG. 3 Schematic drawing (left) and picture (right) of the roll-to-roll sputtering equipment FOSA labX for the deposition of the ZrO<sub>2</sub>-VO<sub>2</sub>-ZrO<sub>2</sub> layer stack on ultra-thin glass

A roll of this material with a length of 20 meters was installed in the position of the pay-out roller. The material was spliced between 10-meter-long polymer films as leader and follower, respectively. This ensured complete protection of the coated material inside the roll during the evacuation and venting of the vacuum chamber. The material can be conveyed back and forth between the pay-out and take-up rollers. On its way, it passes two deposition zones. The left and right deposition positions in the scheme shown in Figure 3 were used for the deposition of the thermochromic vanadium oxide and the zirconium oxide top and bottom layers, respectively. In this type of machine, at least two passes of the substrate through the machine were necessary to deposit the complete three-layer stack.

The zirconium oxide layer was sputtered using a rotatable magnetron with a zirconium oxide ceramic target (GfE FREMAT). The length of the target was 650 mm. The material was sputtered at 6 kW pulsed DC power ( $t_{on} = 16 \mu s$ ;  $t_{off} = 4 \mu s$ ). The dynamic deposition rate was 22 nm<sup>2</sup>/m/min. The argon gas flow of 250 sccm was regulated by a mass flow controller (MKS instruments). The oxygen flow of 8 sccm was regulated by a second mass flow controller (MKS instruments). This was the minimum amount of oxygen to obtain a zirconium oxide layer with an extinction coefficient  $k < 10^{-3}$ . The chamber pressure was 0.4 Pa.

The vanadium oxide layer was sputtered using a rotatable magnetron with a vanadium-tungsten alloy target (atomic percentage of W: 1.2 at%, GfE FREMAT). This vanadium-to-tungsten ratio is well-known for shifting the transition temperature from 68°C to ambient values [14]. The length of the target was 650 mm. The material was sputtered at 6 kW using a high-power impulse magnetron sputtering (HiPIMS) power supply (nano4Energy). The duty cycle was 5.25% ( $t_{on} = 70 ms$ ;  $t_{off} = 1263 ms$ ). The dynamic deposition rate was 11 nm<sup>2</sup>/m/min. The glass was pre-heated to 350°C by a radiation heater (Figure 3). The argon gas flow of 250 sccm was regulated by a mass flow controller (MKS instruments). The oxygen flow was regulated by a second mass flow controller (MKS instruments). The layer properties are very sensitive to the amount of oxygen introduced. Details about the interdependence of coating parameters and thermochromic properties were previously reported (Rezek et al., 2022). Metallic samples were sputtered for oxygen flow values below 22 sccm. Oxygen flow values higher than 26 sccm provided vanadium oxide targets without thermochromic properties. An inline monitoring system for the transmittance was used to determine the correct range of oxygen flow (Figure 3). The control scheme of the process is shown in Figure 4.

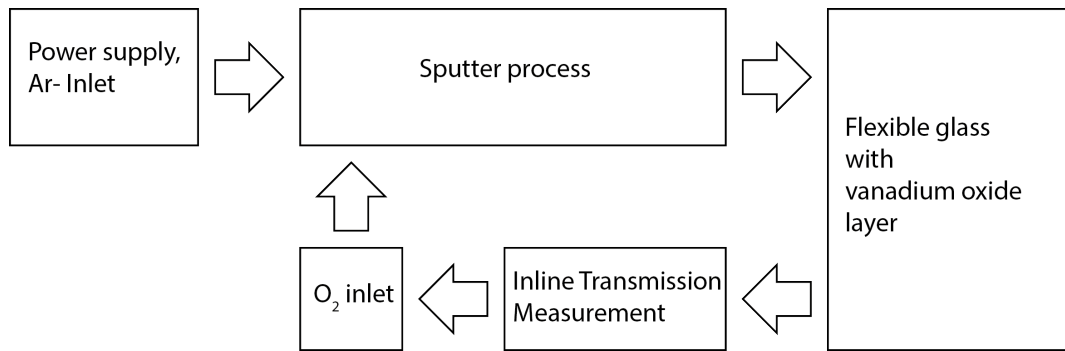


FIG. 4 Schematic drawing of the control setup for the reactive sputtering of vanadium oxide.

In the first pass, a zirconium oxide layer was sputtered onto the substrate. The thickness of this base layer was kept constant at 170 nm for all experiments. The vanadium oxide layer of 80 nm thickness was deposited in the second pass. The oxygen flow was adjusted to 25.4 sccm. This value was chosen based on the transmission inline monitoring value of 33% (at 550 nm) for the  $ZrO_2$ - $VO_2$  layer system. The deposition was completed by the top zirconium oxide layer of 170 nm thickness. The layer thickness for all three layers was kept constant. The choice is based on results reported in the literature (Houska et al., 2019). They found that this layer structure provided the highest values for both  $T_{lum}$  and  $\Delta T_{sol}$ .

Samples of the size 200 mm x 200 mm were cut out of the continuous roll for detailed investigation. The transmission and reflection spectra were measured by a spectrophotometer with integrating sphere (Perkin Elmer Lambda 1150).

### 3 RESULTS

Different thermochromic layer systems were investigated. They differ in both the optical properties and the transition temperature. The deposition method described in the previous section provided stable and reproducible properties of the layers. A comprehensive description of the coating process itself is beyond the scope of this paper. In the following, typical results will be presented, and possible application scenarios of such coatings will be discussed.

Figure 5 shows the transmission spectra of the sample with the highest  $\Delta T_{sol}$ .

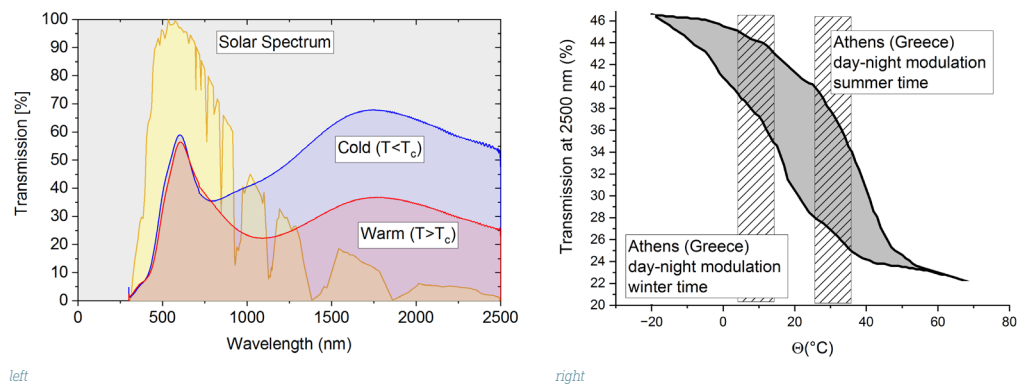


FIG. 5 Left: Transmission spectra of cold and warm states of a  $ZrO_2$ - $VO_2$ - $ZrO_2$  coating on flexible glass: Right: Thermal hysteresis of the optical properties, plotted for the transmission value at 2500 nm wavelength

The left-hand side of Figure 5 shows the transmission spectra of the sample in the low- and high-temperature modes. The solar spectrum AM1.5 is included in Figure 5 for reference. The spectra of the high- and low-temperature modes are nearly identical in the visible spectral range. However, starting from the wavelength of 1000 nm upwards, the transmittance in the low-temperature mode is higher, reaching a maximum of 65%. The change of the solar energy transmittance  $\Delta T_{sol}$  between the high- and low-temperature modes amounts to 9.6% for this sample. At the same time, the luminous transmittance  $T_{lum}$  of 50% remains unchanged during the phase transition. The right-hand side of Figure 5 shows the hysteresis in the switching behaviour between the high- and low-temperature modes. For reference, the approximate daily variation of the temperature in Athens is given for both summer and winter time. As shown, the sample is subject to seasonal and daily modulation effects under the climatic conditions of Greece. The coating shown in Figure 5 is the basis of all further investigations.

The thermochromic properties of the samples from this study are compared to the state-of-the-art values reported in review articles published in literature. An overview of the achievable properties is given in (Aburas et al., 2019) (Figure 6).

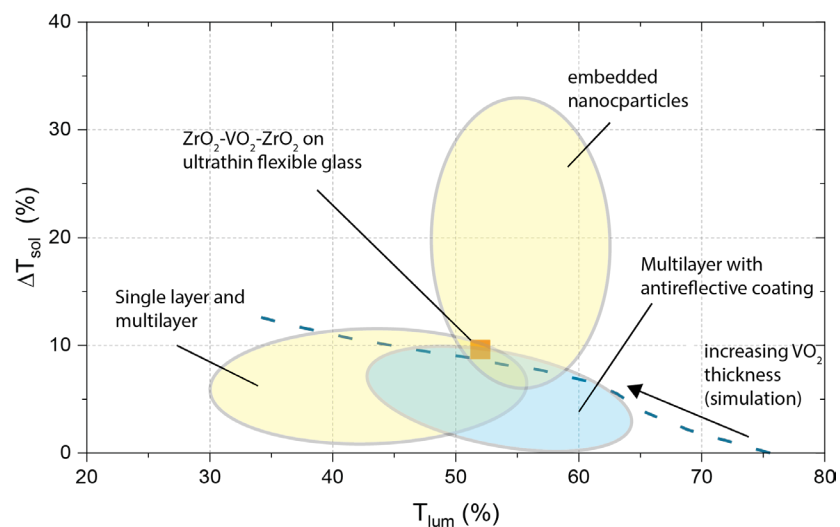


FIG. 6 Typical region for different kinds of vanadium oxide-based thermochromic coatings in the  $\Delta T_{sol}$ - $T_{lum}$  plane. The best obtained results reported in this paper are indicated by an orange square, and the blue area represents the expected performance range of the multilayer approach with an antireflection layer. The dashed blue line illustrates the range which can be covered by varying the  $VO_2$  thickness based on the present level of technology, and circled areas are adopted from (Aburas et al., 2019).

The multilayer approach with the antireflection layer is represented by the blue field in Figure 6. This corresponds to the type of coating investigated in this article. The results show that the performance values achieved on flexible glass are in the same range as those achieved by other research groups on sheet glass. The multilayer approach itself is only outperformed by the nanoparticle approach. A detailed analysis of this type of coating can be found in (Wang, 2021).

Based on the optical measurements, the temperature-dependent refractive index  $n$  and extinction coefficient  $k$  were determined. Using these values,  $\Delta T_{sol}$  and  $T_{lum}$  could be simulated (dashed blue line in Figure 6). Provided that the optical constants do not depend on the layer thickness, this gives an insight into potential performance improvements. The curve in Figure 6 indicates that an increase in  $\Delta T_{sol}$  can be achieved at the expense of the luminous transmittance. This result illustrates the applicability of the technology in scenarios with excessive availability of light.

As it was outlined in the introduction, the potential of smart coatings should be evaluated in combination with state-of-the-art solutions. Therefore, the data given in Figure 5 and Figure 6 were used to calculate the performance in various combinations of window coatings shown in Figure 7.

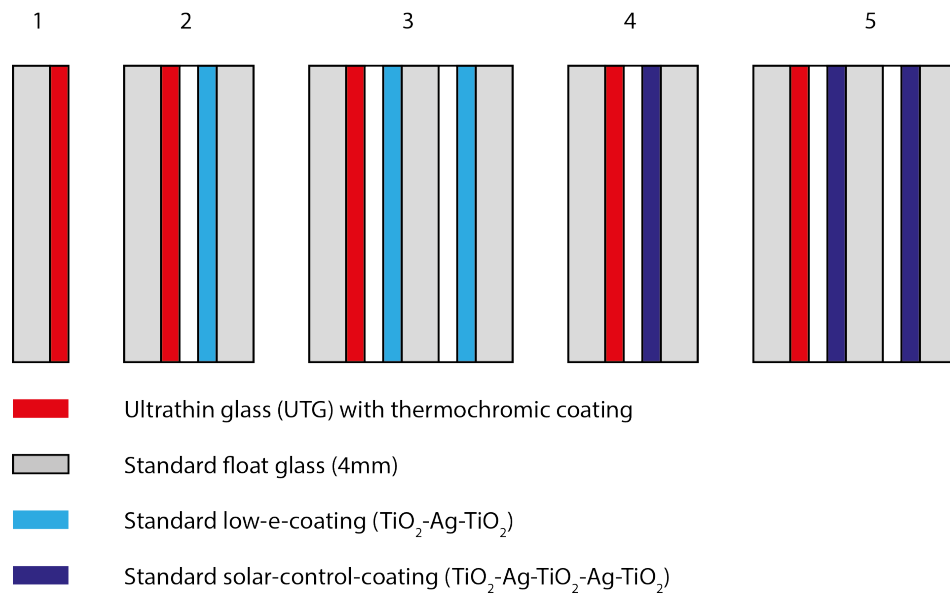


FIG. 7 Different configurations for calculating the performance of thermochromic windows.

The effect of the low-e and solar control coatings is simulated by introducing a typical layer stack (TiO<sub>2</sub> (30 nm)-Ag (10nm)-TiO<sub>2</sub>-(30nm))<sup>n</sup>, adopted from (Solovyev et al., 2015). A low-e coating corresponds to n = 1, and the solar control stack stands for n = 2. The solar control version has a sharper drop in transmittance in the near-infrared spectral range, thus preventing the thermal radiation of the sun from entering the building. Each of these coatings is combined with the thermochromic layer stack on one glass surface.

Figure 8 shows the calculated  $\Delta T_{sol}$  in these different combinations.

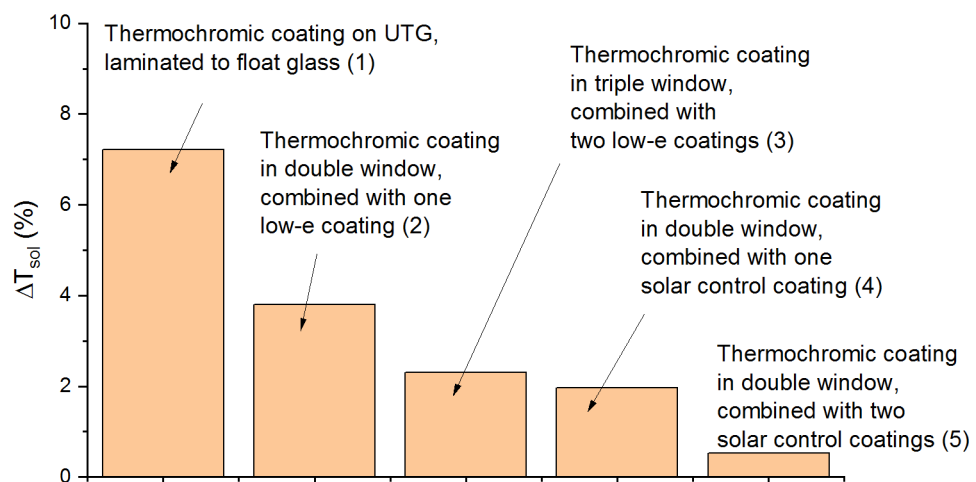


FIG. 8 Change of solar transmittance  $\Delta T_{sol}$  for a thermochromic coating in different window coating combinations.

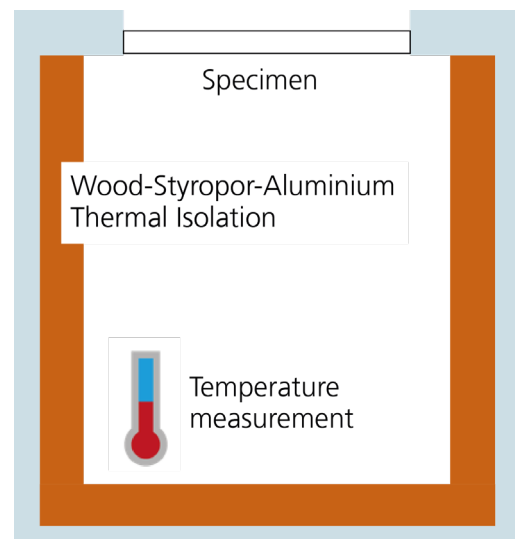
It is apparent that the combination of thermochromic coatings with state-of-the-art low-e coatings and solar control coatings does not offer any benefit to the overall optical properties of the window. Here, the change in the optical properties ( $\Delta T_{sol}$ ) of the entire window is remarkably suppressed and, in some cases, drops to negligible values of around 1%. The implementation of low-e-coatings is important and inevitable for the efficiency of heating systems in temperate and cold climates. Therefore, thermochromic coatings cannot improve the thermal insulation of such buildings efficiently.

In contrast to these examples, thermochromic coatings can be advantageous if applied in buildings that require permanent cooling. This coincides with findings presented in the literature (Tällberg et al., 2016). During the daytime, they are in a warm state and block solar radiation, similar to low-e coatings. In the nighttime, the thermochromic material switches to the cold state. Then, it outperforms the static low-e and solar control coatings. In its cold state, the thermochromic layer behaves like a non-conductive ceramic. It does not prevent the heat transport from the inside to the outside of the building. In the same way, it supports radiative cooling because the thermal radiation can escape the hot building to the colder outside in the same way as if the window glass of the building was completely uncoated. In contrast to that, state-of-the-art low-e coatings drastically reduce the possible energy exchange by thermal radiation.

The radiative heat exchange is especially effective for skylights. The sky is a heat sink for thermal radiation. In the mid-infrared spectral range between 3  $\mu\text{m}$  and 25  $\mu\text{m}$ , the optical properties of the sky are mainly determined by the water vapour content of the air. Thus, they are dependent on the local climatic conditions of the installation as well as on the weather. The emissivity of the sky is in the range of 0.9 (Algarni & Nutter, 2015). The effective temperature of the sky can vary considerably, but in most cases, it can be assumed to be at 0°C. In tropical conditions of high humidity, it can increase to 20°C. In contrast, in low-humidity desert-like conditions, it can be as low as -50°C (Algarni et al., 2015). If buildings in these areas need skylights for esthetical or other reasons, the application of thermochromic coatings is a viable option for decreasing the energy demand for cooling.



left



right

FIG. 9 Picture (left) and schematic design drawing (right) and mockup for the test of thermochromic coatings in transparent roof elements.

The effect of blocking the solar irradiation during the daytime and supporting radiative cooling during the night was tested with a set of mockups as shown in Figure 9.

The design of the mockups is shown on the right side of Figure 9. The mockups are identical, well-isolated boxes with a 22 cm x 30 cm base area and a height of 16 cm. Three identical mockups with different coatings on the transparent cover ("Specimen") were compared with respect to their inside temperature. Each of the mockups was covered with 4 mm float glass. The dimension of the transparent cover was 20 cm x 20 cm. For the first mockup, an ultra-thin glass layer with a thermochromic coating was laminated to the bottom side of the glass. For the second mockup, a PET film with a solar control coating was laminated, replicating the layer stack described in (Solovyev, 2015). For the third mockup, the glass was left uncoated. The properties of the thermochromic coating required a special adaptation to the low-temperature conditions in Dresden, Germany, at the time of the test. They were adapted to both the geographic location and the temperature conditions during the testing (between -2°C and 12°C). The hysteresis of the specially designed coating is shown in Figure 10 (right).

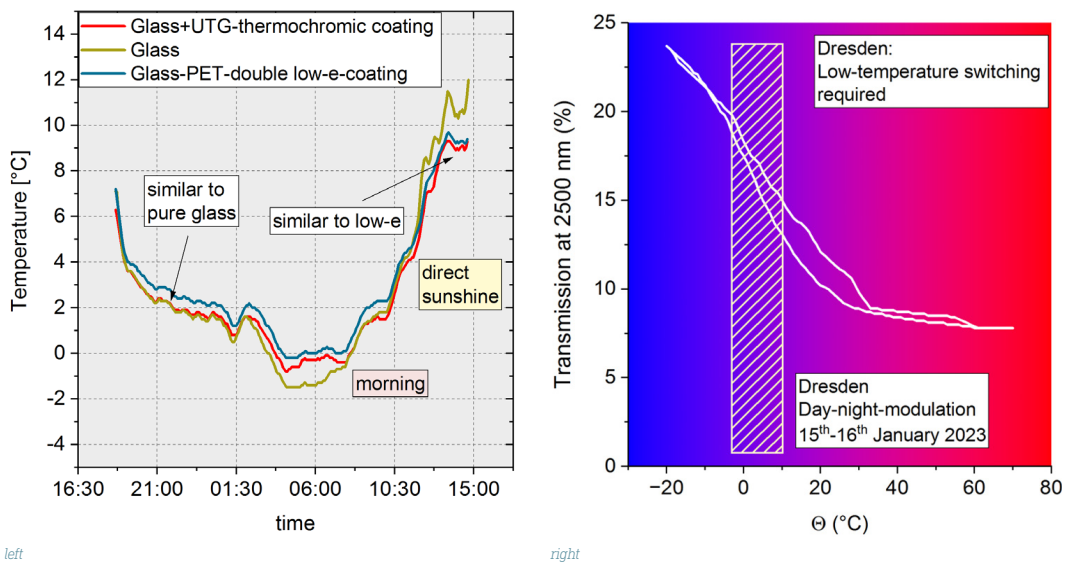


FIG. 10 Result of the mockup test in Dresden (left) and optical properties of the specially designed thermochromic coating (right)

The transition temperature of the coating was determined by the hysteresis data shown in Figure 10 (right). It was calculated according to the integral equation approach (see equation (4)) as  $\Theta_{tr} = 16^\circ\text{C}$ .

The temperature range during the 24h test is indicated by the crosshatched box in Figure 10 (right). It is slightly below the transition temperature, but the optical properties of the coating show enough modulation within the box.

The diagram on the left-hand side of Figure 10 shows three obtained temperature curves. During the cooling-down phase at night, the temperature in the box with the thermochromic coating followed the reference box with the uncoated glass. The cooling rate for these two mockups was higher than for the mockup with the solar control coating. Under sunshine conditions in the morning, the temperature increase of the mockup with the uncoated glass was excessive. On the other hand, the thermochromic coating as well as the standard static solar control coating significantly damped the increase in temperature.

Overall, the thermochromic coating showed a daily modulation that continuously ensured optimum cooling support for the mockup. This result coincides with the findings reported in literature (Tällberg et al., 2016), (Butt et al., 2021). A deviation from the expected behaviour was observed in the early morning hours around 6 am. An explanation of this phenomenon requires further investigation and longer observation time.

This first test has demonstrated the potential of skylights with thermochromic coatings. It featured results under ideal conditions of a clear sky and low air humidity. For a more profound evaluation, further investigations under various weather conditions over a longer time are necessary. In particular, it is useful to perform the test in a climatic area that primarily requires cooling buildings rather than heating. It is noteworthy how solar modulation, normally referred to as the crucial parameter for the evaluation of the thermochromic effect, loses its importance in the roof application scenario. The support of radiative cooling can be described more precisely by the relationship between daytime solar transmittance and nighttime emissivity. A deeper investigation of this interdependence will be the focus of further scientific work on thermochromic coatings.

## 4 CONCLUSIONS

VO<sub>2</sub> thermochromic coatings were sputter-deposited on ultra-thin glass in a roll-to-roll coating machine. The width of the continuous roll was 300 mm, and the areal weight of the thermochromic material was lower than 0.3 kg/m<sup>2</sup>. This makes it an attractive option for building retrofit. A modulation of the solar transmission between the high and low-temperature states of 9.6% was achieved. The luminous transmittance amounted to 50% in both states. The transition temperature of 22°C was in the comfortable ambient temperature range. These values correspond well with results reported for deposition processes on sheet glass. Various application scenarios were investigated. The combination with state-of-the-art low-e or solar control coatings drastically reduced the modulation of the solar transmittance. Therefore, thermochromic coatings were shown to be ineffective for heat insulation purposes in cold and temperate climates. For an alternative use case, an implementation in transparent roof elements of buildings which need permanent cooling was tested. Such a configuration reduces the solar transmittance during the daytime and supports radiative cooling during the night.

### Acknowledgement

---

The work presented in this article was funded by the Horizon Europe 2020 programme under the GA number 869929 (Project Acronym: Switch2Save).

The authors thank the colleagues of Jaroslav Vlcek's group at the University of West Bohemia (Plzen, Czech Republic) for their support and scientific input.

## References

---

- Algarni, S., Nutter, D. (2015). Survey of Sky Effective Temperature Models Applicable to Building Envelope Radiant Heat Transfer. DOI: 10/13140ORG.2.1.4212.5526
- Aburas, M., Soebarto, V., Wiliamson, T., Liang, R., Ebenhoff-Heidepriem, H., Wu, Y. (2019). Thermochromic smart window technologies for building application: a review. *Applied Energy*, 255, 113522
- Bahlawane, N., Lenoble, D. (2014). Vanadium oxide compounds: structure, properties, and growth from the gas phase. *Chem. Vap. Deposition*, 20, 299–311. DOI: 10.1002/cvde.201400057
- Baldassarri, C., Shehabi, A., Asdrubali, F., Masanet, E. (2016). Energy and emissions analysis of Next Generation Electrochromic Devices. *SOLAR ENERGY MATERIALS AND SOLAR CELLS* 156; p. 170-181. JRC95247
- Butt, A., de Vries, S., Loonen, R., Hensen, J., Stuijver, A., van den Ham, J., Erich, B. (2021). Investigating the energy saving potential of thermochromic coatings on building envelopes. *Applied Energy* Volume 291, 116788
- Chang, T., Coa, X., Bao, S., Ji, S., Luo, H., Jin, P. (2016). Review on thermochromic vanadium dioxide based smart coatings: from lab to commercial application. *Adv. Manuf.*, 6:1–19, doi.org/10.1007/s40436-017-0209-2
- Crosby, P., Netravali, A. (2023). Green Thermochromic Materials: A Brief Review. *Advances Sustainable Systems* (Vol. 6, Issue 9) 2022, 2200208 <https://doi.org/10.1002/adsu.202200208>
- D'Agostino, D., Mazzarella, L. (2019). What is a Nearly zero energy building? Overview, implementation and comparison of definitions. *Journal of Building Engineering*, Volume 21, Pages 200-212
- EN 673:2011, Glass in building - Determination of thermal transmittance (U value) - Calculation method
- Gudmundsson, J. T., Brenning, N., Lundin, D., Helmersson, U. (2012). High power impulse magnetron sputtering discharge. *Journal of Vacuum Science & Technology A* 30, 030801
- Houska, J., Kolenaty, D., Vlcek, J., Barta, T., Rezek, J., Cerstvy, R. (2019). Significant improvement of the performance of ZrO<sub>2</sub>/V<sub>1-x</sub>W<sub>x</sub>O<sub>2</sub>/ZrO<sub>2</sub> thermochromic coatings by utilizing a second-order interference. *Solar Energy Materials and Solar Cells* 191, 365–371
- Hu, P., Vu, T. D., Li, M., Wanh, S., Ke, Y., Zeng, X., Mai, L., Long, Y. (2023). Vanadium Oxide: Phase diagrams, Structures, Synthesis and Applications. *Chem. Rev.*, 123, 4353-4415
- ISO 9050, Glass in building – Determination of light transmittance, solar direct transmittance, total solar energy transmittance, ultraviolet transmittance and related glazing factors
- Jelle, B.P. (2013). Solar radiation glazing factors for window panes, glass structures and electrochromic windows in buildings— Measurement and calculation. *Solar Energy Materials and Solar Cells*, Volume 116, September 2013, Pages 291-323
- Jin, P., Nakao, S., Tanemura, S. (1998). Tungsten doping into vanadium dioxide thermochromic films by high-energy ion implantation and thermal annealing. *Thin Solid Films*, Volume 324, Issues 1–2, Pages 151-158
- Li, M., Magdassi, S., Gao, Y., Long, Y. (2017). Hydrothermal Synthesis of VO<sub>2</sub>: Advantages, Challenges and Prospects for the Application of Energy Efficient Smart Windows. *Small*, 13, 1701147
- Mohammad, A., Joshi, K., Rana, D., Ilhom, S., Wells, B., Wills, B., Sinkovic, B., Okyay, A., Biykli, N. (2023). Low-temperature synthesis of crystalline vanadium oxide films using oxygen plasmas. *J. Vac. Si. Technol.* A41, 032405
- Rezek, J., Szelwicka, J., Vlcek, J., Cerstvy, R., Houska, J., Fahland, M., Fahlteich, J. (2022). Transfer of the sputter technique for deposition of strongly thermochromic VO<sub>2</sub>-based coatings on ultrathin flexible glass to large-scale roll-to-roll device. *Surface and Coatings Technology*, Volume 442, 25, 128273
- Solovyev, A.A., Rabortkin, S.V., Kovsharov, N.F. (2015). Polymer films with multilayer low-E coatings. *Materials Science in Semiconductor Processing*, Volume 38, Pages 373-380
- Tällberg, R., Jelle, B., Loonen, R., Gao, T., Hamdy, M. (2016). Comparison of energy saving potential of adaptive and controllable smart windows: A state of the art review and simulation studies of thermochromic, photochromic and electrochromic technologies. *Solar Energy Materials and Solar Cells*, Volume 200, 109828

- Teixeira, H., Gomes, M., Rodrigues, A. Pereira, J. (2020). Thermal and visual comfort, energy use and environmental performance of glazing systems with solar control films. *Building and Environment*, Volume 168, 106474
- Vlcek, J., Koletany, D., Houska, J., Kozak, T., Cerstvy, R. (2017). Controlled reactive HiPIMS—effective technique for low-temperature (300 °C) synthesis of VO<sub>2</sub> films with semiconductor-to-metal transition. *J. Phys. D: Appl. Phys.* 50 38LT01
- Vu, T., Chen, Z., Zeng, X., Jiang, M., Liu, S., Gao, Y., Long, Y. (2019) Physical vapour deposition of vanadium dioxide for thermochromic smart window applications. *J. Mater. Chem. C*, 7, 2121-2145
- Wang, S., Jiang, T., Meng, Y., Yang, R., Tan, G., Long, Y. (2021). Scalable thermochromic smart windows with passive radiative cooling regulation. *Science* 374, 1501-1504
- Wang, X., Narayan, I. (2021). Thermochromic Materials for Smart Windows: A State-of-Art Review. S. *Front. Energy Res. Sec. Solar Energy* Volume 9, doi.org/10.3389/fenrg.2021.800382
- Yaşar, Y., Maçka Kalfa, S. (2012). The effects of window alternatives on energy efficiency and building economy in high-rise residential buildings in moderate to humid climates. *Energy Conversion and Management*, Volume 64, Pages 170-181

# JOURNAL OF FACADE DESIGN & ENGINEERING

VOLUME 11 / NUMBER 2 / 2023

**001 Definition and design of a prefabricated and modular façade system to incorporate solar harvesting technologies**

Izaskun Alvarez-Alava, Peru Elguezabal, Nuria Jorge, Tatiana Armijos-Moya, Thaleia Konstantinou

**029 SmartWall**

Emmanouil Katsigiannis, Petros Gerogiannis, Ioannis A. Atsonios, Aris Manolitsis, Maria Founti

**051 Plasmochromic Modules for Smart Windows: Design, Manufacturing and Solar Control Strategies**

Mirco Riganti, Julia Olive, Francesco Isaia, Michele Manca

**071 Implementation of a multifunctional Plug-and-Play façade using a set-based design approach**

David Masip Vilà, Grazia Marrone, Irene Rafols Ribas

**097 Off-site prefabricated hybrid façade systems**

Ioannis A. Atsonios, Emmanouil Katsigiannis, Andrianos Koklas, Dionysis Kolaitis, Maria Founti, Charalampos Mouzakis, Constantinos Tsoutis, Daniel Adamovský, Jaume Colom, Daniel Philippen, Alberto Diego

**123 Automation process in data collection for representing façades in building models as part of the renovation process**

Kepa Iturralde, Asier Mediavilla, Peru Elguezabal

**145 Comparative cost analysis of traditional and industrialised deep retrofit scenarios for a residential building**

Martino Gubert, Jamal Abdul Ngoyaro, Miren Juaristi Gutierrez, Riccardo Pinotti, Davide Brandolini, Stefano Avesani

**169 Assessing the circular re-design of prefabricated building envelope elements for carbon neutral renovation**

Ivar J.B. Bergmans, Silu Bhochhibhoya, Johannes A.W.H. Van Oorschot

**197 Energy-saving potential of thermochromic coatings in transparent building envelope components**

Matthias Fahland, Jolanta Szelwicka, Wiebke Langgemach

SOAP | STICHTING OPENACCESS PLATFORMS

ISSN PRINT 2213-302X

ISSN ONLINE 2213-3038